TABLE OF CONTENTS

CHAPTER 1 - GRANITES

MASTER

TABLE OF CONTENTS

CHAPTER 1 (CONT)

MASTER

LIST OF FIGURES

CHAPTER 1 - GRANITES

LIST OF FIGURES

LIST OF FIGURES

LIST OF FIGURES

vi

LIST OF TABLES

CHAPTER 1 - GRANITES

LIST OF TABLES

1.0 PREFACE

The Department of Energy has the responsibility for selecting and constructing Federal repositories for radioactive waste. The Nuclear Regulatory Commission must license such repositories prior to construction. The basic requirement in the geologic disposal of radioactive waste is stated as:

> Placement in a geologic host whereby the radio-active waste is not in mechanical, thermal or chemical equilibrium with the object of preventing physical or chemical migration of radionuclides into the biosphere or hydrosphere in hazardous concentration (USGS, 1977).

The object of this report is to document the known geologic parameters of large granite and basalt occurrences in the coterminous United States, for future evaluation in the selection and licensing of radioactive waste repositories.

The report is prepared by Willard Owens Associates, Inc., under subcontract to Lawrence Livermore Laboratories for incorporation in the Geoscience Parameter Data Base Handbook being prepared by Lawrence Livermore and the Nuclear Regulatory Commission.

The description of the characteristics of certain potential igneous hosts has been limited to existing data pertaining to the general geologic character, geomechanics, and hydrology of identified occurrences. A description of the geochemistry is the subject of a separate report.

GRANITES

1.1 INTRODUCTION TO THE GEOLOGIC CHARACTER OF GRANITIC ROCKS

"Granitic Rock" is defined as a term generally used to signify any coarse-grained, light-colored igneous rock containing essential quartz. In its broadest usage, it may even be loosely applied to certain metamorphic rocks and to quartz-free, light-colored igneous rocks.

Although its broad, undefined use can be confused with the very specific rock name granite, the term has attained a wide casual acceptance. Perhaps the reason for this acceptance of "granitic rock" is that it groups three important igneous rock types that have similar petrographic, tectonic, and genetic characteristics. These types are the granites, monzonites, and granodiorites. They are commonly found occurring as batholiths or huge rock bodies covering hundreds of square kilometers.

Together, granite, monzonite, and granodiorite comprise a major portion of the earth's igneous terrane. Although less common rocks are included in the definition of "granitic rock," this report and general usage will employ the term for the three major common rock types.

1.2 CLASSIFICATION

Granitic rocks and igneous rocks in general are classified
according to texture and mineralogy. Texture is the most
obvious and the least complicated. There are two divisions,
phaneritic and aphanitic, with one major modifier, porphy-
ritic. Granitic rocks are phaneritic, or coarse-grained.
They also may be porphyritic which simply means that there
are two distinct grain sizes present. However, with
phaneritic rocks, the relative differences in these sizes
are not great, and the physical properties of the rock are
not greatly affected.

Granitic rocks make up the acidic or high silica (SiO_2),
portion of the classification schemes. These schemes are
based on a changing ratio of potassium feldspar ($K_2AlSi_3O_8$)
to plagioclase feldspar ($[Ca,Na]Al[Al,Si]Si_2O_8$) (Figure 1-1).
As rock types become more silicious, potassium feldspars be-
come dominant. Also, the amount of quartz increases and the
calcium to sodium ratio of the plagioclases decreases.

1.3 COMPOSITION

By definition, the mineral composition of the granitic rock
series is constrained to certain ranges. These are outlined
in Figure 1-1. Total mineral compositions for example
granites, monzonites, and granodiorites are given in Table
1-1. From these it can be seen that even though variations
occur in the types and percentages of minor minerals pre-
sent, the real differences in the rocks occur with the
changing quantities of the potassium and plagioclase feld-
spars. In fact, all three rock types could have the same
minor minerals and still maintain their identity.

These major mineral differences have a distinct effect on
the physical properties of the different rock types. Since
all granitic rocks consist of about 80 percent feldspar with
quartz and the various feldspars have similar physical prop-
erties, all granitic rocks also have similar physical
properties.

The mineral changes that classify the granitic rocks have a
much greater effect on their chemistry. This effect is
apparent from the major oxide compositions shown in Figure 1-1
and the analyses for example granites, monzonites, and grano-
diorites given in Table 1-1.

	POTASSIUM FELDSPAR 2/3 TOTAL FELDSPAR			POTASSIUM FELDSIUM 1/3-2/3 TOTAL FELDSPAR			PLAGIOCLASE FELDSPAR 2/3 TOTAL FELDSPAR	
ESSENTIAL MINERALS	QUARTZ >10%	QUARTZ <10% FELDSPATHOID <10%	FELDSPATHOID >10%	QUARTZ >10%	QUARTZ <10% FELDSPATHOID <10%	FELDSPATHOID >10%	POTASSIUM FELDSPAR 10% TOTAL FELDSPAR QUARTZ 10%	POTASSIUM FELDSPAR 10% TOTAL FELDSPAR SODIC PLAGIOCLASE QUARTZ 10%
CHARACTERIZING ACCESSORY MINERALS	CHIEFLY: HORNBLEND, BIOTITE, PYROXENE, MUSCOVITE ALSO: SODIC, AMPHIBOLES, AEGIRENE, CANCRINITE SODALITE, TOURMALINE			CHIEFLY: HORNBLENDE, BIOTITE, PYROXENE ALSO: SODIC AMPHIBOLES, AEGIRINE			CHIEFLY: HORNBLENDE, BIOTITE, PYROXENE (IN ANDESITE) ALSO: PYROXENE FELDSPATHOID SODIC AMPHIBOLES	
AVERAGE CHEMICAL COMPOSITION % SiO_2 Al_2O_3 Fe_2O_3 FeO MgO CaO Na_2O K_2O	71.5 14.0 1.5 1.4 0.6 1.8 3.4 4.3	60.4 17.0 2.7 2.9 1.8 3.7 4.2 5.1	56.0 19.2 2.9 1.6 0.6 2.0 8.5 5.3	65.0 15.8 2.3 1.3 1.0 2.0 3.7 4.2	57.0 17.1 3.4 2.3 2.3 5.4 4.7 3.7	54.1 21.0 1.8 3.3 1.1 3.2 6.2 3.9	65.3 16.1 2.1 2.3 1.7 3.5 3.9 2.7	61.9 16.2 2.5 3.5 2.8 5.4 3.4 2.1
PHANERITIC — EQUIGRANULAR	GRANITE	SYENITE	NEPHELINE SYENITE	QUARTZ MONZONITE	MONZONITE	NEPHELINE MONZONITE	GRANODIORITE	QUARTZ DIORITE

FIGURE 1-1   Mineral Composition of Granitic Rocks
Source: Travis, 1965

		Quartz	
	Granite	Monzonite	Granodiorite
SiO_2	72.08	69.15	66.88
TiO_2	0.37	0.56	0.57
Al_2O_3	13.86	14.63	15.66
Fe_2O_3	0.86	1.22	1.33
FeO	1.67	2.27	2.59
MmO	0.06	0.06	0.07
MgO	0.52	0.99	1.57
CaO	1.33	2.45	3.56
Na_2O	3.08	3.35	3.84
K_2O	5.46	4.58	3.07
H_2O	0.53	0.54	0.65
P_2O_5	0.18	0.20	0.21
Quartz SiO_2	29.2	24.8	21.9
Orthoclase $KAlSi_2O_8$	32.2	27.2	18.3
Albite $NaAlSi_2O_8$	26.2	28.3	32.5
Anorthite $CaAl_2Si_2O_8$	5.6	11.1	16.4
C	0.8	--	--
$CaSiO_3$	--	--	--
$MgSiO_3$	1.3	2.5	3.9
$FeSiO_3$	1.7	2.2	2.9
Magnetite Fe_2O_4	1.4	1.9	1.9
Imenite $FeTiO_3$	0.8	1.1	1.1
Apatite $Ca_5(PO_4)_3(F,OH,Cl)$	0.4	0.5	0.5
No. of analyses	72	121	137

Table 1-1. Chemical analyses and mineral
norms for average compositions for granite,
quartz monzonite, and granodiorite
(from Huang, 1962)

As the rocks become more silicious progressing from the
diorites to the monzonites to granite, SiO_2, K_2O, and Na_2O
increase and Al_2O_3, CaO, MgO, and the iron oxides decrease.
The change in SiO_3 content is due to increasing quartz (SiO_2)
and the higher SiO_2 content of the potassium and sodium feld-
spars. K_2O, Na_2O, CaO, and Al_2Og_3 changes occur with increas-
ing potassium and sodium feldspars. MgO and iron oxide
decrease due to varying types and percentages of minor minerals.

Primary Structure of Granitic Rock Bodies

Granitic rocks have one other chemical characteristic that
sets them apart from all other groups of rocks. This is the
occurrence of a tremendously varied suite of trace elements.
The number and variety will be different with each rock body
but almost all bodies will contain at least some trace con-
centration of rare elements. Much of the world's mineral
wealth is associated with granitic rock bodies that concen-
trated rare metals during formation. The concentration
occurs because metals, other rare elements and a few compounds,
such as water, do not have the molecular properties necessary
to fit the structures of common minerals that form during
rock crystallization. This saves these elements and compounds
for the low temperature end of the igneous process. This
temperature range is also the range for crystallization of
the granitic rocks.

1.4 STRUCTURE OF GRANITIC ROCK BODIES

Granitic rock bodies can occur in any of the many forms
assumed by plutonic igneous rocks. Their coarse grain size
requires the slow cooling of a plutonic subsurface environ-
ment and precludes formation by any surface volcanic
mechanism. Although dikes, sills, stocks and other smaller
bodies are exceedingly common, by far the greatest volumes
of granitic rock now exposed at the earth's surface occur
as continental shield complex and orogenic belt batholiths.
These great rock bodies tend to be composed of granite,
monzonite and/or granodiorite. The less common granitic
rock types are only rarely found in large bodies.

Batholiths are igneous rock bodies with an exposed surface
area in excess of 100 square kilometers. They are roughly
equidimensional or they may have one long dimension. Their
vertical dimensions are so great that no lower boundaries
have been located. Technically, batholiths must be implaced
by the discordant (cutting other structures) intrusion of
magma.   However, this assumes a purely magmatic origin for
granitic rocks. Such an assumption may be misleading.

Granitic rock batholiths occur in the centers of orogenic
belts and over large areas of the earth's Precambrian con-
tinental shields. Overall they are not restricted to any
particular geologic time.

1.5 GENESIS

Generalizations concerning the genesis of the granitic rocks
run the risk of oversimplification. Carmichael (Carmichael
et al, 1974) states:

> "so wide is their (granitic rocks) extent, so
> varied their relations to crustal depth, thermal
> environments, metamorphism, tectonism, volcanism,
> and the flow of time, that generalization inevit-
> ably obscures with fictitous clarity one of the
> most complex of igneous phenomena."

However, a few statements can be made concerning present
thoughts on genesis of granitic rock batholiths.

Diapiric intrusion of melted, or at least partially melted,
crustal silicious material is thought to be the source of
most granitic rock bodies. This, along with local variations
in source material, can explain the similarities and differ-
ences between the specific rock types. The mechanism for
the melting is still argumentative. The orogenic, or mountain-
building, environment provides the necessary heat and pressure,
but how and why is still open to question.

Various methods for in-place granitization must also be able
to produce granitic rock batholiths. Melting without injec-
tion or granitic alteration by introduced or self-generated
fluids can explain many rock bodies with gradational boundaries.

1.6 WEATHERING OF GRANITIC ROCKS

Granitic rock minerals are relatively resistant to mechan-
ical abrasion. They have a moderate resistance to chemical
weathering.

Quartz is very resistant but the potassium feldspars, though
more stable than the plagioclases, alter quickly to clay
minerals. What ultimate effect weathering will have on a
given rock body is determined by the degree of structural
fracturing it has sustained. Highly fractured rocks allow
greater access for altering fluids.

1.7 DESCRIPTION OF OCCURRENCES

Introduction

Large, granitic rock occurrences are found in nine major
areas of the United States. The nine following areas sh wn
on Figure 1-2 were selected for analysis of their parameters
for the Data Base Handbook:

Front Range Uplift

Big Horn Uplift

Beartooth Uplift

Wolf River Batholith

Sierra Nevada Batholith

Southern California Batholith

Northern Washington Batholiths

Idaho Batholith

Boulder Batholith

It should be stated that certain specific geologic information
for areas of the size under consideration is lacking, because
consideration of the geology of an area the size of a batholith
requires generalization of a great many variables. These generali-
zations are unimportant when 100 plus square kilometers are
involved. But when 1 to 5 square kilometers are under study,
these generalizations may not be at all applicable.

FIGURE 1.2   Granitic occurrences chosen for inclusion in study

An example of this problem is the intensity and depth of
fracturing in a site area.

First, references on an entire batholith will generalize
with a statement such as: there are three "well defined"
joint trends. If the reference has been written during the
last 20 years, it may not mention minor fracturing at all.
Once a specific site is chosen within an occurrence, it may
be shown that locally this joint pattern is non-existent or
oriented differently; or a local structure may have caused
extremely fine granulation of the rock.

Depth of fracturing is even more difficult to determine. It
almost always requires drill hole data. Again, this data
may not apply over a large area.

The solution to this problem is simply to work with the gen-
eralizations and the more consistent properties of the rock.
Once local areas are chosen for study, specific data can be
gathered or, if necessary, generated.

Front Range Uplift

Location and Geology

The Front Range Uplift extends from southern Colorado to
southern Wyoming along the eastern slope of the Rocky

Mountains. Elevations range from 1,500 to over 4,000
meters. The rugged terrain is typical of youthful erosion
surfaces superimposed on recently uplifted igneous and meta-
morphic complexes.

An outline of the geologic history of the area begins with
the 1.7 billion year-old metamorphic complex. Sediments de-
posited prior to this time were metamorphosed into the Idaho
Springs series and intruded by the Boulder Creek granodio-
rite batholiths. Major intrusions and diastrophism occurred
again at 1.4 billion years (the Silver Plume granitic suite)
and at 1.1 billion years (the Pikes Peak granite). During
the Phanerozoic, uplift occurred during the Carboniferous,
the Cretaceous, and the Tertiary. Uplift is still in pro-
gress and the present elevations are due to this recent
period. Terrestrial and marine sedimentary rocks deposited
throughout the Phanerogenic are still found. The last period
of igneous intrusion, responsible for volcanism and many
small granitic rock bodies, began in the Cretaceous and
continued through the late Tertiary.

The various Precambrian intrusives are the major granitic
rocks of the Front Range Uplift. These occur in an almost
continuous series of batholiths along the length of the Up-
lift. Their total area is many million square kilometers.

The southern Tarryall region, which lies about 100 kilometers west of Colorado Springs, Colorado, is typical of the geology and petrology of the Front Range Uplift (Hawley and Wobus, 1977). This region is underlain by a large and varied suite of Precambrian intrusive igneous rocks locally covered by a recently-deposited veneer of sediments of the Tertiary and Quaternary periods. Most of the intrusive rocks are related to one of the three main granitic series of the Front Range: the Boulder Creek Granodiorite, the Silver Plume Quartz Monzonite, and the Pikes Peak Granite.

Petrology

The composition of the Boulder Creek Granodiorite varies widely from biotite-quartz diorite to granite. Three main lithology types can be distinguished: quartz diorite, granodiorite, and quartz monzonite.

The dominant unit of the Boulder Creek rocks is a quartz monzonite. Texturally, the rock may usually be classed as a gneiss because of the foliation that separates the light and dark minerals. The potassium feldspar present is microline; the major plagioclases are oligoclase and andesine; and quartz makes up roughly 30 percent of the rock. Biotite is the main ferromagnesian mineral and accessory zircon, apatite, magnetite, and sphene occur with it.

The Silver Plume Quartz Monzonite is a massive to flow-
foliated, plutonic igneous rock correlated with the Silver
Plume Granite of the central Front Range. It occurs in
igneous intrusions as large as 13 square kilometers and in
many dikes. Three varieties of the Silver Plume Quartz
Monzonite are recognized according to differences in grain
size and structure: (1) fine to medium-grained, (2) fine-
grained, and (3) medium to coarse-grained. All three are
found in the Front Range Plutons. The medium to coarse-
grained type forms separate plutons; the two finer grained
varieties commonly occur together in the same pluton. The
rock is generally red and porphyritic and contains micro-
clines, oligoclase, quartz biotite, muscovite with accessory
apatite, zircon, monazite and opaque oxides.

The Pikes Peak Granite forms massive, sharp-walled plutons.
The major Pikes Peak batholith covers at least 3,100 square
kilometers. A smaller batholith of Pikes Peak Granite, the
Tarryall Mountains mass, underlies a 245 square kilometer
area. Pikes Peak Granite consists of a coarse sub-equi-
granular granite, coarse porphyritic granite and a hetero-
geneous medium to coarse-grained granite. The batholiths
also contain small dikes of pegmatite or aplite and irregu-
lar masses of fine-grained granite. The granite averages
approximately 50 percent microcline, 30 percent quartz, 15
percent sodic plagioclase, and 5 percent biotite.

Only thin soils have developed since the last uplift. In areas where closely-spaced joints occur, there has been significant mechanical and chemical weathering. The granitic rocks were exposed to intense weathering during the late Paleozoic and mid-Tertiary. Paleosoils over 25 meters thick can be found where the old surface has been preserved.

Structure

The Front Range area has undergone at least three major Precambrian deformations and three Phanerozoic uplifts. The granite rocks and, to a great extent, the entire area is affected most by the Precambrian tectonics. Three major regional trends occur; northwest, northeast and east. Intense folding and fracturing follow all three, but the northwest is the major trend. The northeast is noted for its mineralization during the Tertiary. All trends have continued to be active into recent times.

Bighorn Uplift

Location and Geology

The exposure of granitic rocks in the Bighorn Uplift, located just west of Buffalo and Sheridan, Wyoming, occupies an area of about 3,100 square kilometers. Its shape is roughly elliptical, about 100 kilometers long and 48 kilo-

meters wide at its greatest width. The Precambrian granitic
rocks are in contact with the Cambrian Deadwood Formation on
all sides. In a few localities, its boundary is defined by
faults, along which it is brought into contact with various
formations.

The central portion of the uplift is comprised mainly of
older, Precambrian true gneiss (metamorphic). At the
northern and southern ends of the uplift the major rocks are
red to grey younger Precambrian, igneous granitics. These
range from granite to quartz diorite in composition and,
even though there has been some mobilization, they have
mostly been found in place through granitization of the
older rocks (Osterwald, 1955).

Petrology

Using color as a field criterion, the granitics consist
largely of two varieties, a moderately coarse-grained red
granitic rock and a medium to fine-grained gray granitic
rock. The boundary between the two rock types is grada-
tional, and both are believed to have originated from the
same magma. The feldspar in the red granite is mainly
orthoclase and microcline with some oligoclase. Quartz is
also a major constituent. The red color is caused by the
dissemination of small particles of iron minerals in the
orthoclase. In some areas, the gray rock contains a higher

proportion of more calcic plagioclase and grades into a
quartz monzonite or quartz diorite. Common accessory min-
erals in the gray granite are apatite, magnetite, titanite,
rutile, and zircon. Much of the gray granite shows evidence
of shearing. In weathered portions of the rock, biotite is
commonly altered to chlorite and some of the feldspar is
altered to kaolinite and sericite (Osterwald, 1955; Darton,
1906).

Texture of both rock types is typified by migmatization
and twin microshearing, gneissic foliation and various sizes
of inclusions. These are all common in granitic rocks that
have been granitized in place or formed from replacement by
metasomatic fluids.

Structure

A wide-spread joint system is prevalent throughout the
granitic outcrop area. This causes the granitics to weather
into rounded blocky boulders.

Dikes are common. These are either granitic, granite
aplites and pegmatites, or diabasic. No preferred pattern
has been recorded.

Major faulting and folding is generally confined to the margins of the granitic rocks. Thrust, normal and reverse faults occur with mainly dip movement. These and the simple folds of the overlying sediments reflect the movement of the uplift that produced the Bighorn Mountains.

Beartooth Uplift

Location and Geology

The Precambrian Beartooth Uplift is located in south central Montana, north and east of Yellowstone National Park. The felsic batholithic mass trends northwest and is approximately 97 kilometers long and 48 kilometers wide.

The granitic core of the Beartooth Uplift was formed by granitization of early Precambrian sediments about 2.7 billion years ago. The uplift that formed the present Beartooth Mountains started in the Cretaceous and continued into the Tertiary. The volcanism that is still evident in Yellowstone Park began with the later stages of the Uplift.

Petrology

The rocks of the granitic core consist mainly of granitic gneiss and granodioritic gneiss. The granitic gneiss consists of about equal amounts of quartz, microcline and sodic

plagioclase. Minor minerals are biotite, muscovite, magne-
tite, ilmenite, chlorite, apatite, zircon, and epidote. The
granodioritic gneiss is nearly half plagioclase with 43 per-
cent quartz. Microcline is almost totally absent. Minor
minerals are similar to the granitic gneiss. Both rocks are
foliated.

Structure

The major structural trend in the Beartooth Mountains is
northwest. The present mountains parallel it; there are
Precambrian dikes that follow it; and the prominent Cooke
City and Stillwater structures follow it. The only major
variation for this trend are the Cretaceous-Tertiary bound-
ing faults and folds at the ends of the elongated uplift.

Wolf River Batholith

Location and Geology

The Precambrian (1.5 billion years old) Wolf River Batholith
underlies an area of about 9,300 Km^2 in northeastern Wiscon-
sin. It is surrounded on three sides by older Precambrian
plutonic and volcanic rocks of the central and northeastern
Wisconsin complexes. The batholith is not apparently related
to an orogeny and it is epizonal, or formed near the surface.

Evidence for this includes widespread development of
porphyritic texture, local occurrences of chilled
margins, and sharp, discordant intrusive contacts with
country rocks. Adjacent metavolcanic and metasedimentary
rocks have been contact metamorphosed to hornblende-horn-
fels, pyroxene-hornfels facies (Van Schmus et al, 1975).

Petrology

The Wolf River Batholith contains mappable units of granite,
quartz monzonite, syenite, monzonite, quartz and feldspar
porphyry, and monzonite porphyry. Quartz monzonite is the
most common and the most extensively exposed rock type.

Although a porphyritic texture is the most extensively de-
veloped in certain rock types of the batholith, Rapakivi
texture is more spectacular. The Wolf River Batholith is
lithologically similar to the Rapakivi massifs of Finland and
the classic texture (ellipsoidal potassium feldspar mantled
by plagioclase) is well developed in the Wisconsin quartz
monozonites.

Perthitic alkali feldspar and quartz are the most abundant
minerals in the batholith, with smaller amounts of sodic
plagioclase, iron-rich biotite and amphibole, and locally,
olivine and pyroxene (Van Schmus et al, 1975). Typical
accessory minerals are fluorite, zircon, apatite, allanite,
ilmenite, and magnetite.

Joint and Fracturing

Although numerous and well-developed near the surface, fractures diminish in size and number with depth. Major fracture patterns in the batholith are oriented N.75°W., N.30°E. and N.30°W., N.85°E (Bell and Sherrill, 1974).

Sierra Nevada Batholith

Location and Geology

The Sierra Nevada Batholith is a group of many granitic plutons which, collectively, form the northwest trending Sierra Nevada mountain range in east central california. The batholith is approximately 644 kilometers long and 80 kilometers wide, and covers approximately 77,700 square kilometers. The Sierra Nevada Batholith was probably formed during the Mesozoic era when the upper layers of the earth's crust were depressed into deeper, more mafic regions. The more silicous rocks melted, migrated upward, and crystalized to form the batholith. For this reason, the base of the granitic batholith is gradational into ultramafic rocks at an approximate depth of 35 kilometers. The batholith has been block-faulted on the east and tilted westward so that sedimentary rocks lap onto the west side, forming gentle slopes while the east side is steep.

Petrology

At least two parent magmas formed the batholith. The eastern side of the batholith is 200 $\pm$20 million years old (Triassic Period). Individual plutons consist mainly of quartz monzonites and diorites (Bateman et al, 1963). Plutons on the western side are from the Jurassic period. They generally consist of quartz diorites and granodiorites. The mineralogy of this massive batholith is difficult to typify because the composition of the rocks will commonly vary from alaskite to quartz diorite within the same subsidary pluton. However, the rocks commonly have equigranular, prophyritic or seriate texture, and contain plagioclase, quartz, potassium feldspar, hornblende, biotite, and muscovite (in order of descending abundance).

Structural

The Sierra Nevada Batholith is thought to occupy the trough of a large synclinorium. The dominant trend within this structure is N.40W° or parallel with the Range itself. All the major strike, normal, and reverse faults follow this trend and all faults have a main strike-slip component.

Southern California Batholith

Location and Geology

The Southern California Batholith has been described as a
huge, composite injection dike (Larsen et al, 1958).
Formed during the Middle Cretaceous period, the batholith is
located in the southern part of California and northern
Mexico. The granitic mass is elongated in a northwesterly
direction and covers approximately 207,200 square kilometers.

Petrology

Both the Sierra Nevada Batholith and the Southern California
Batholith are composed of several individual plutons. The
batholith consists of what is thought to be a single magma
series with rocks ranging from gabbro to granite. The most
common rock composition of the batholith is quartz diorite.
The mineral percentages of a typical quartz diorite are
quartz - 18 percent; microcline - 7 percent; oligoclase - 58
percent; biotite - 7 percent; amphibole - 8 percent; and
magnetite - 1 percent. Grain size is irregular with oligo-
clase forming the larger grams and microcline and quartz
occurring as the small grain and interstitial material.

Structure

The main trend of the Southern California batholith is north-west. Excluding the Transverse Ranges in the same area, this is similar to the rest of Southern California. All the sediments and metamorphics that host the batholith, and most of the linear features within the batholith, strike parallel to this trend. Individual intrusives are elongate to the north-west as are inclusions, gneissic foliation and mineral zones within the intrusions.

References show that the few faults mapped within and adjacent to the granitics also trend northwest. No reference was found for jointing or minor fracture patterns. However, these certainly exist and no doubt also follow the regional trend (Larsen, 1948).

Northern Washington Batholiths

Location and Geology

The Colville, Chelan, Loon Lake, and Cathedral Batholiths cover about 181 square kilometers in a nearly circular area in northeastern Washington. The four comparably sized batholiths merge toward the south and are considered to be contemporaneous (Hutting et al, 1961). Age dating of the batholiths is difficult because few cross-cutting relationships

between the batholiths and surrounding strata are evident.
It is commonly believed that the four Mesozoic Batholiths
are from the Cretaceous period. Granitization produced the
Igneous as well as the gneiss rocks (Campbell, 1940; Krauskopf,
1941; Crowder, 1959; Hutting et al, 1961).

Petrology

In these four batholiths, rock composition ranges from
alaskite to granodiorite (Pardee, 1918; Waters and Krauskopf,
1941).

The centers of the batholiths commonly consist of light to
pinkish-grey, medium-grained, porphyritic granite. This
granite is composed of orthoclase phenocrysts, quartz,
plagioclase, and a smaller amount of biotite. Toward the
edges of each batholith, granodiorite and quartz diorite be-
come the most common rock types with hornblende increasing
to 30 percent of the total rock composition. Lamprophyre
and pegmatite dikes commonly intersect the edges of the
batholiths.

Quartz diorite gneisses display an unusual, but widespread,
swirled foliation in the Chelan and Colville Batholiths
(Waters, 1938; Waters and Krauskopf, 1941). The texture of
the rocks near the contacts of the batholiths varies. The

Cathedral Batholith border lacks the foliated and cataclastic structure of the Chelan Batholith. It is the only pluton with extensive contact metamorphism and a very unusual contact breccia (up to four miles thick) with hornblende schist as the xenoliths (Waters, 1938).

Jointing and Fracturing

Northwest trending faults which have had many episodic displacements are common. Joint patterns are less consistent than the fault patterns. Three sets of widely spaced joints (two vertical and one horizontal) are common throughout (Pardee, 1918).

Idaho Batholith

Location and Geology

The Idaho Batholith extends from central Idaho into western Montana. It underlies a roughly rectangular-shaped area of about 41,440 square kilometers (Larsen and Schmidt, 1958). The Idaho Batholith is relatively flat-topped and is about 836 kilometers long and 137 kilometers in maximum width. The middle Cretaceous age batholith is bounded on the north, east, and west by older rocks while the southern contact is with younger rocks, chiefly lavas of Tertiary age. The

Idaho Batholith is in an area of high, rugged mountains, yet
over large areas weathering is so deep that the geologic
character of the rock cannot be determined.

Petrology

The Idaho Batholith is made up of several individual rock
units. The extreme range in petrology of the rock units is
from quartz gabbro to granite, but many of these occur in
very small amounts. The range in petrography of the main
rock mass is from quartz diorite to quartz monzonite (Larsen
and Schmidt, 1958). The average composition is a granodiorite
with major quartz, potassium feldspar and plagioclase and
minor biotite. Muscovite hornblende or pyroxene, are rare
and sphene and apatite are accessories (Ross, 1963).
Generally, the rocks are coarse-grained. Some, especially
the quartz monzonites and some of the granodiorites, contain
phenocrysts of microcline and microperthite as much as 8
centimeters long. The large phenocrysts are unevenly dis-
tributed and are abundant in parts of some rock bodies and
absent in others. The principal dark minerals of the gabbro
are pyroxene and secondary hornblende, those of the tonalite
are hornblende with some biotite, and that of the quartz
monzonites is almost entirely biotite (Larsen and Schmidt,
1958).

The greater part of the Idaho Batholith was probably intruded as a unit or as a number of large, intimately related units. Changes in fabric and composition are common, but in many places the different varieties merge into each other without mappable boundaries. The changes record movement in the magma, differentiation and late-stage modifications during the long period required for so large a mass to move into position and consolidate.

Structure

Because of the size of the Idaho Batholith, the structure and interrelations of the various plutons are complex. Anderson (1952) divides it into two distinct age groups. The old rocks are related to the Sierra Nevada Orogeny granitics of Washington and Oregon. These cover the entire range of compositions from diorite to granite but granodiorite and quartz monzonite are most common. The younger plutons are also quartz monzonite and granodiorite, however, they are Cretaceous to Eocene.

Once in place, the Idaho Batholith played an important role in the crustal deformation that occurred in the western United States during the early Tertiary. Along the edges of the batholith, the compressional forces were transmitted to the surrounding rocks and produced great thrust faults and tight folds.

Within the batholith northwest trending thrusts were comple-
mented by northeast shear zones. These tend to have strike-
slip movement and are accompanied by normal faulting. Where
these shears are aligned with regional transverse zones, major
strike-slip shears developed. The Cour d'Alene's Osburn fault
is an example (Anderson, 1948).

Local fracturing intensities are related to the major struc-
tures. Where a major thrust or shear occurs, the rocks are
much more fractured and jointed.

Boulder Batholith

Location and Geology

The Boulder Batholith of southwestern Montana is an elonga-
ted mass 100 kilometers long and 50 kilometers wide, trend-
ing north-northeastward around Butte, Montana. This batho-
lith is of late Cretaceous Age and consists of plutons of
quartz monzonite, granodiorite, and other granitic rocks.
It is believed to be a relatively thin mesozonal batholith
that was injected into a shallow floor of premagmatic rocks
and then covered mainly by its own volcanic ejecta. Geologic
field relations and gravity data suggest that the average
thickness of the batholith is perhaps 5 kilometers (Hamilton
and Myers, 1974).

Petrology

The composition of igneous rocks in the Boulder Batholith
varies from syenogabbro to alaskite, but approximately 75
percent of the batholith is Butte quartz monzonite.

The Butte quartz monzonite contains the following mineral
percent ranges:

quartz	15-40%
plagioclase	20-48%
feldspar	15-45%
biotite	1-12%
accessories	1- 3%

Accessories include magnetite, sphene, zircon, apatite,
allanite, and rutile. Texture is generally equigranular;
however, porphyries with potassium feldspar phenocrysts up
to three centimeter long do occur (Beczaft, 1963).

Structure

The thin disk-like structure of the Boulder Batholith pre-
sented by Hamilton and Myers (1974) does not fit the classic
thick, no-bottom batholith shape. However, their theory is based
on inward dipping structures and floor-like features that

appear to lie beneath the batholith at its north and south edges. This shape makes at least this batholith the equivalent, on a much larger scale, of a lopolith.

The area of Montana underlain by the Boulder Batholith was caught up in the extensive eastward thrusting that took place in the Cretaceous and Tertiary.

In addition, smaller scale thrusting has occurred along the top of the batholith chamber in conjunction with intrusion. Hence, thrust faulting with accompanying strike-slip, shear zones and other union faulting is common.

On a smaller scale, individual areas will have well-developed joint and fracture patterns. A great number of dikes, veins, shear zones, and faults trend east, northeast and north. Yet, in the same area, no pattern for the well-developed joints could be identified.

1.8 REFERENCES

Anderson, A.L., 1952, Multiple unplacement of the Idaho Batholith: Jour. Geol., V. 60, p. 255-265.

Anderson, A.L., 1948, Role of the Idaho Batholith during the Laramide Orogeny: Econ. Geol. V. 43, p. 84-99.

Bateman, P.C., L.D. Clark, N.K. Huber, J.G. Moore and C.D. Rinehart, 1963, The Sierra Nevada Batholith - a synthesis of recent work across the central part: U.S. Geol. Survey Prof. Paper 414D, p. D1-D46.

Bayley and Muehlberger, 1968, Basement Rock Map of the United States: U.S. Geol. Survey, scale 1:2500,000.

Becraft, G.E., and others, 1962, Geology and mineral deposits of the Jefferson City quadrangle, Jefferson and Lewis and Clark Counties, Montana: U.S. Geol. Survey, Prof. Paper 428, p. 100.

Bell, E.A., and M.G. Sherrill, 1974, Water availability in Central Wisconsin, an area of near surface crystalline rock: U.S. Geol. Survey Water-Supply Paper 3033, p. 32.

Brown, S.G. and R.C. Newcomb, 1962, Ground water resources of Cow Valley, Malheur County, Oregon: U.S. Geol. Survey Water-Supply Paper, 1619-M, p. 35.

Campbell, C.D., 1940, Structural problems of the east border of the Colville Batholith: (abstract): Geol. Soc. America Bull., V. 51, p. 2019.

Carmichael, I.S.E., Turner, F.J., and Verhoogen, J., 1974, Igneous petrology: McGraw-Hill, New York, p. 740.

Crowder, D.F., 1959, Granitization, migmatization, and fusion in the northern Entiat Mountains, Washington: Geol. Soc. America Bull., V. 70, No. 7, p. 827-878.

Darton, N.H., 1906, Geology of the Bighorn Mountains; U.S. Geol. Survey Prof. Paper 51, p. 129.

Eckelmann, F.D. and Arie Poldervaart, 1956, Archean history of the Quad Creek area, Part 1. Geologic evolution of the Beartooth Mountains, Montana and Wyoming: Geol. Soc. America Bull., V. 68, p. 1225-1261.

Foose, R.M., 1961, Structural Geology of the Beartooth Mountains, Wyoming and Montana: Geol. Soc. Amer. Bull, V. 72, p. 1143-1172.

Gary, M., and others, eds., 1972, Glossary of Geology: Am. Geol. Inst., p. 805.

Hamilton, W. and W.B. Myers, 1974, Nature of the Boulder Batholith of Montana: Geol. Soc. America Bull, V. 85, p. 365-378.

Hawley, C.C. and R.A. Wobus, 1977, General geology and petrology of the Precambrian crystalline rocks, Park and Jefferson Counties, Colorado: U.S. Geol. Survey Prof. Paper 608-B, p. B1-B77.

Huang, W. T., 1962, Petrology, McGraw-Hill, New York, p. 480.

Hutting, M.T., W.A.G. Bennett, V.E. Livingston, Jr., and W.S. Moen, 1961, Geologic map of Washington, scale 1:500,000.

Hurr, R.T. and D.B. Richards, 1974, Hydrologic Investigations: Engineering geologic, geophysical, hydrologic, and rock mechanics investigations of the Straight Creek Tunnel Site and pilot bore, Colorado; in Robinson, C.S., et al; U.S. Geol. Survey Prof. Paper 815-E, p. 79-92.

Krauskopf, K., 1941, Intrusive rocks of the Okanogan Valley and the problem of their correlation: Jour. Geol., V. 49, p. 1-53.

Larsen, E.S. and R.G. Schmidt, 1958, A reconnaissance of the Idaho Batholith and comparison with the Southern California Batholith: U.S. Geol. Survey Bull. 1070-A, p. 33.

Larson, E.S., 1948, Batholith and associated rocks of Corona, Elainor, and San Luis Rey quadrangles, southern California: Geol. Survey Amer. Memoir 29, p. 182.

Nichols, T.C. and F.T. Lee, 1966, Preliminary appraisal of applied rock mechanics research on Silver Plume Granite, Colorado: U.S. Geol. Survey Prof. Paper 550-C, p. C34-C39.

Osterwald, F.W., 1955, Petrology of the Precambrian granitic in the northern Bighorn, Wyoming, Jour. Geol., V. 63, p. 310-327.

Pardee, J.T., 1918, Geology and mineral deposits of the Colville Indian Reservation, Washington: U.S. Geol. Survey Bull. 677, p. 11-34.

Piper, A.M., T.W. Robinson, Jr., and C.F. Park, Jr., 1939, Geology and ground water resources of the Harney Basin, Oregon, U.S. Geol. Survey Water-Supply Paper 841, p. 187.

Raguin, E., 1965, Geology of Granite: Interscience, London, p. 314.

Redden, J.A., 1968, Geology of the Berne Quadrangle, Black Hills, South Dakota: U.S. Geol. Survey Prof. Paper 297-F, p. 343-408.

Robinson, C.S., and F.T. Lee, 1974, Engineering geologic, geophysical, hydrologic, and rock-mechanics investigations of the Straight Creek Tunnel Site and pilot bore, Colorado gen. geology: U.S. Geol. Survey Prof. Paper 815-B, p. 7-25.

Ross, C., 1963, Model composition of the Idaho Batholith: U.S. Geol. Survey Prof. Paper 475C, p. 80-70.

Taylor, R.B., 1964, Geology of the Duluth Gabbro Complex near Duluth, Minnesota: Minnesota Geol. Survey Bull. 44, p. 63.

Tilling, R.I., 1974, Composition and time relations of plutonic and associated volcanic rocks, Boulder Batholith region, Montana: Geol. Soc. America Bull, V. 85, p. 1925, 1930.

Travis, R. L., 1956, Classification of Rocks: Colorado School of Mines Quart., V. 50, No. 1, p. 98.

U.S. Department of Energy, Technology for Commercial Radioactive Waste Management, Vol. IV.

Van Schmus, W.R., L.G. Medaris Jr., and P.O. Banks, 1975, Geology and age of the Wolf River Batholith, Wisconsin: Geol. Soc. America Bull, V. 86, No. 7, p. 907-914.

Waters, A.C., 1938, Petrology of the contact breccias of the Chelan Batholith: Geol. Soc. America Bull, V. 49. p. 763-794.

Waters, A.C., and K.B. Krauskopf, 1941, Protoclastic border of the Colville Batholith: Geol. Society America Bull, V. 52, No. 9, p. 1355-1417.

GEOMECHANICS OF GRANITES

1.9 INTRODUCTION TO GEOMECHANICS OF GRANITE

This section presents a review of the major rock mechanics
considerations which affect the evaluation of granite as a
potential nuclear waste disposal site. It is not the intent
to be exhaustive, rather to present the major effects and
trends of the principal parameters. Definitions of the
major terms used in this discussion may be found in Appendix
A.

The most important considerations in designing the excavations
for an underground repository for radioactive waste are
safety, stability, and longtime security of the excavations.
Ideally, one would like to take the results of laboratory
experiments performed on small samples of rocks and insert
these values into theoretical analyses, and on this basis
predict the stability of the openings created. Such an
approach, however, has not proven to be realistic for a
major underground structure. It is limited by the effects
of size and geologic structure on the strength of the rock.

Unfortunately, as will be discussed later, there is a great
lack of information regarding the effect of sample size on
the property measured. Because of the great expense associated
with large-scale insitu testing, the primary source of
information regarding the properties of rock are obtained
from laboratory measurements.

As will be shown in this report, there is a number of
properties which can be adequately described by such labora-
tory testing procedures. Unfortunately, there are many
which cannot. One of the major areas which will require
further work is on the procedures by which the input param-
eters for predictor models can be generated. It is clear
from a review of available data that all of the thermal,
thermoelastic and mechanical properties of rock are
functions of temperature.

Until just recently, most testing for determining rock
properties was done at room temperature. The consequences
of temperature on various properties are summarized in Table
1-2. with particular reference to the stability of an under-
ground opening (Tsui, 1979). Notice that both conductivity
and diffusivity decrease with increasing temperature.
Specific heat, on the other hand, increases with increasing
temperature. These have the effect of increasing the ther-
mal gradient and hence, increase thermal stress. The
coefficient of linear thermal expansion increases with
increasing temperature. This also has the effect of in-
creasing thermal stress and decreasing the stability of an
opening. Young's modulus and compressive strength decrease
with increasing temperature which combine to produce a
reduced structural stability for any opening placed in these
fields.

TABLE 1-2. Consequence of temperature dependence of
rock properties on cavern stability   (Tsui, 1979)

	PROPERTIES	TEMPERATURE DEPENDENCE	CONSEQUENCE ON CAVERN STABILITY
Thermal Properties	Conductivity (k) & Diffusivity (K)	Decrease with increasing temperature	1. Increases temperature gradient, hence increases thermal stress, therefore decreases stability. 2. Reduces the magnitude of temperature hence thermal stress, therefore, increases stability.
	Specific Heat (c)	Increases with increasing temperature	Same effect as decrease in diffusivity
	Density (ρ)	Negligible in non-porous rock	-
Thermoelastic Properties	Coefficient of Linear Thermal Expansion (α)	Increases with increasing temperature	Increases thermal stress and hence decreases stability
	Young's Modulus (E) & Poisson's Ratio (ν)	Decrease with increasing temperature	1. Decrease thermal stress, hence increase stability 2. Increase radial deformation
Mechanical Properties	Strength Parameters	Decrease with increasing	Decrease stability
	Stress-strain Behavior	Ductility and flow tendency increase with increasing temperature	Increase radial deformation

There has been an attempt to classify rocks generically and
discuss physical properties in the same way. One type of
strength classification is shown in Figure 1-3 for quite a
large number of rock types (Deere, 1966). As can be seen,
granite is indicated by group 6 (medium to high strength).
The variation, even for small laboratory samples, is of the
order of a factor of 3. The variation in going from intact
rock properties to rock mass properties is even greater.
The reader should keep these variability and scaling consid-
erations in mind when reviewing this report. This section
has been divided into the following six topics. They are:
Insitu Stresses, Mechanical Properties, Thermal Properties,
Thermoelastic Properties, Other Considerations, and Scaling
of Laboratory Results.

NOTE: E_t TANGENT MODULUS AT 50% ULTIMATE STRENGTH
CLASSIFY ROCK AS B, BH, BL, ETC.

E VERY LOW STRENGTH	D LOW STRENGTH	C MEDIUM STRENGTH	B HIGH STRENGTH	A VERY HIGH STRENGTH

YOUNG'S MODULUS E_t

H - high modulus ratio

average modulus ratio

L - low modulus ratio

UNIAXIAL COMPRESSIVE STRENGTH
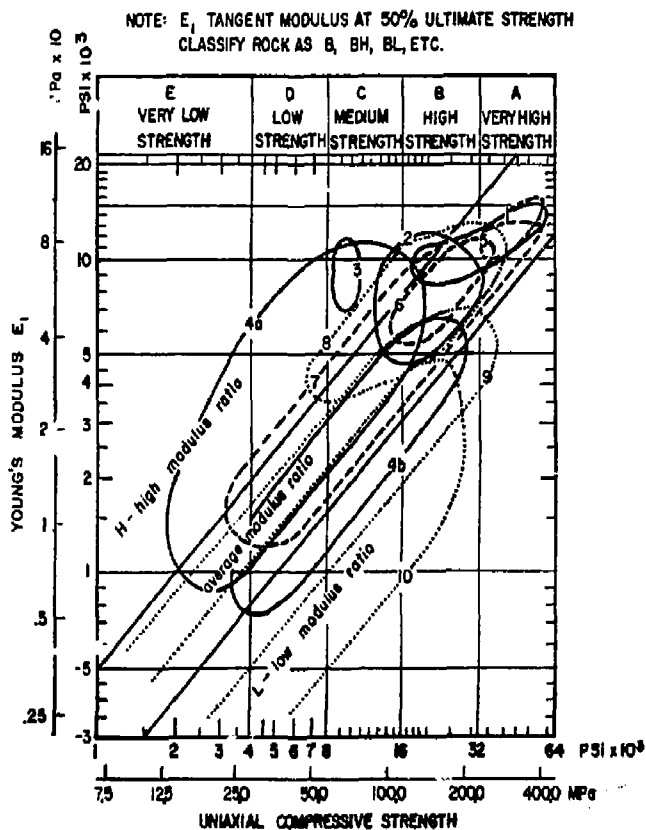
METAMORPHIC:—1—QUARTZITE, —2—GNEISS,—3—MARBLE,—4a—SCHIST, STEEP FOLIATION, ——4b—— SCHIST, FLAT FOLIATION.
IGNEOUS —--5---DIABASE, ---6 --GRANITE, ---7---BASALT AND OTHER FLOW ROCKS
SEDIMENTARY: —8—LIMESTONE AND DOLOMITE,—9—SANDSTONE,—10— SHALE.

FIGURE 1-3   Engineering classification of intact rock based on
uniaxial compressive strength and modulus ratio
Source: Deere and Miller, 1966.

1-44

1.10 INSITU STRESSES

The stability of any underground opening is determined by the strength of rock materials and by the stresses which are applied. These stresses are those existing in the ground prior to excavation, those induced during the excavation process, and those induced by activities after completion of the excavation. The latter category includes the effects of placement of radioactive waste.

In this section, the determination of the state of stress in the vicinity of a potential repository prior to excavation will be emphasized. In general, the vertical component of the insitu stress has a value close to that given by the weight of the overburden. It is, of course, influenced by variations in topography and the time which has passed since the rock was deposited.

A number of attempts to measure the stress field in place has revealed that the horizontal stresses can range from approximately 1/3 of the vertical up to several times the vertical stress. Compilation of these measurements has been done by Hoek and Brown, as shown in Figure 1-4. Note that the envelope at a 1,000 meter-depth, which might be typical for a repository, shows horizontal stress variation from about 0.5 up to 1.75 times the vertical stress. The exact

1-45

$$\bar{K} = \frac{\text{AVERAGE HORIZONTAL STRESS, } \sigma_{hav.}}{\text{VERTICAL STRESS, } \sigma_v}$$
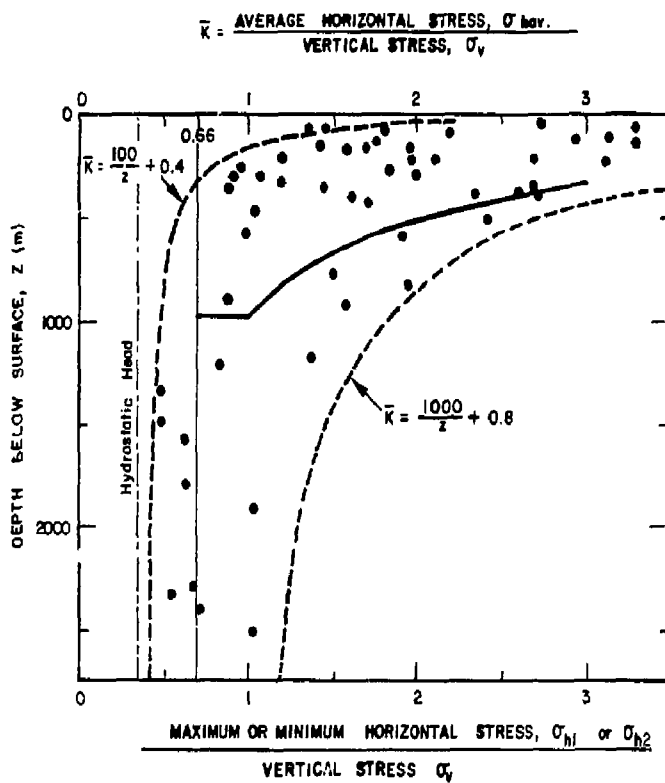
FIGURE 1-4   Compilation of measurements of the virgin
state of stress in the rock
Source: Hoek and Brown, 1977.

stress state is very site-dependent, and therefore, careful attention has to be placed upon the determination of the stress field at the location of interest.

It is obvious that the stability of an opening will vary considerably if the major principal stress is vertical or horizontal. The best design shape of the opening created will also change depending upon the stress field orientation. Table 1-3 (Lee, 1978; Tsui, 1979) shows the relationship of the stresses for various ages of rock in Ontario. Note that for Devonian age rocks, the horizontal stress is expected to be less than or equal to the vertical. For the older Silurian, Ordovician and Pre-Cambrian rocks, the horizontal stress is expected to be greater than the vertical stress.

A plot of stress variation with depth for Pre-Cambrian rocks is shown in Figure 1-5 (Lee, 1978; Tsui, 1979) for a number of different rock types and locations. There is quite a wide variation, but most of the sites and tests reveal a horizontal stress greater than the vertical. Figures 1-6 and 1-7 show the results of some stress measurement work which was done at the Stripa Mine in Sweden (Carlsson, 1978). The variation in principal stress magnitude is shown in Figure 1-6. The principal stress magnitude appears to vary by a factor of 3 over a hole length of about 5 meters.

1-47

TABLE 1-3. Stresses in Ontario rocks.

Geological Period		Probable Stress Conditions
Devonian		$\sigma_v \geq \sigma_h$ (?)
Uplift (20 m.y.)		
Silurian		$\sigma_h >> \sigma_v$
Ordovician	OR	$\sigma_h >> \sigma_v$
		$\sigma_h \simeq \sigma_v$
Uplift (500 m.y.)		
Precambrian		$\sigma_h > \sigma_v$

(m.y. = million year)

SOURCES: Tsui, 1979 and Lee, 1978.
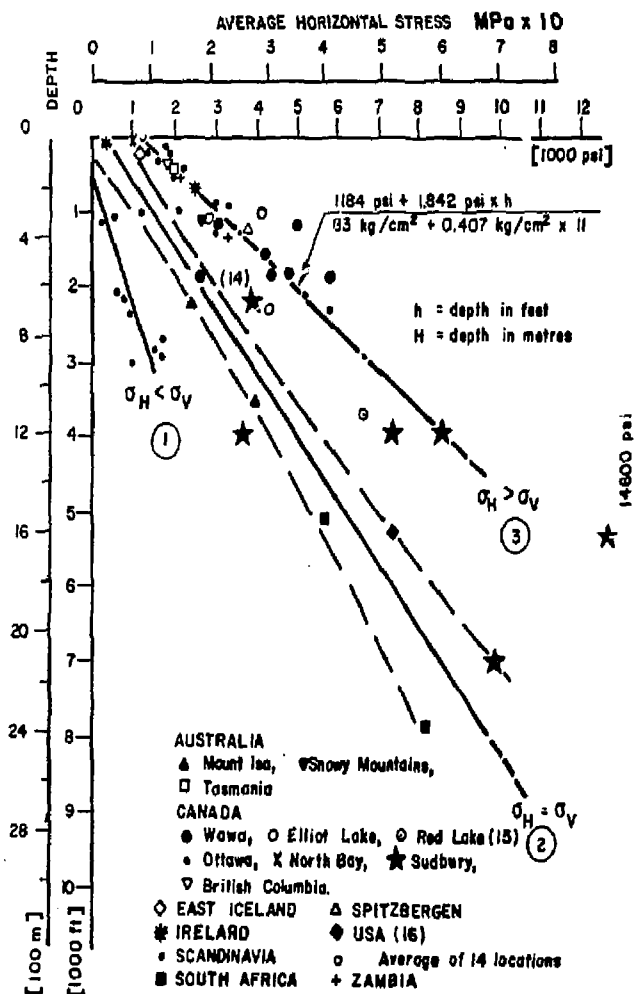
FIGURE 1-5   Increase of average horizontal stress with depth
in precambrian rocks Source: Herget et al, 1975.
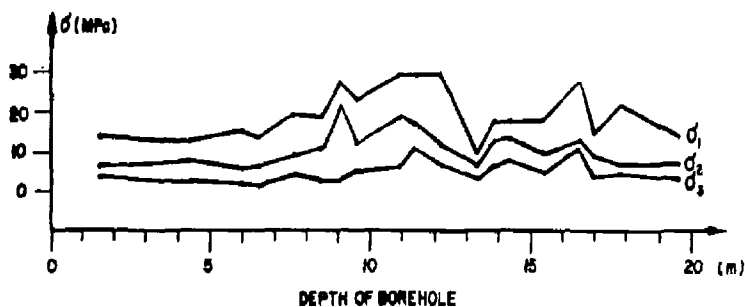
FIGURE 1-6   Variation of principal stresses in the borehole
             Source: Carlsson, 1978.
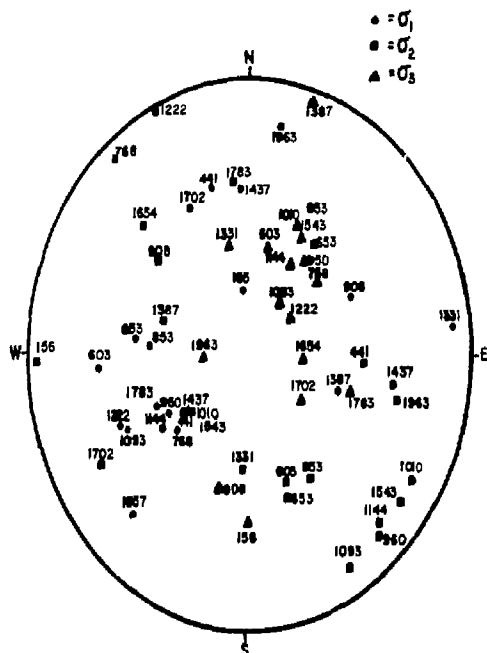
FIGURE 1-7   Direction of the principal stresses at each
             measure point plotted Source: Carlsson, 1978.

             Note: Depth of measurement in the borehole is
                    indicated on Wulff's net lower hemisphere.

1-50

Variability in principal stress direction is shown in Figure
1-5. Again, the variation is considerable. In general,
stress fields are found to be very site specific and may
vary significantly even within a specific rock mass.

1.11   MECHANICAL PROPERTIES

Mechanical properties which are normally consiered in any
description of a rock material are index properties (such as
unit weight or density), moisture content, porosity, stress-
strain relationships, which yield Young's modulus and
Poisson's ratio, and rock strength as measured by the com-
pressive and tensile strength.

A summary of properties for intact granite are given in
Table 1.4. These values have been collected during a
literature review (ONWI, 1978) of a large number
of published reports. Note that even properties such as
unit weight, which is normally considered relatively
constant for granite, varies from 2310 to 3040 kg/m^3. The
porosity varies from about 0.05% to 11%. Young's modulus
varies by a factor of 5 and Poisson's ratio by a factor of
9 or 10. The compressive strength varies from 34 to 350 MPa.
Although tensile strength is shown to vary from about 3.5
to 55 MPa, those samples which are already broken, of course,
are not tested, so the variation should actually be from
0 to 55 MPa.

A summary of properties for various types of granite are
shown in Tables 1.5 to 1.9.   All of the granites chosen are
from quarries. Therefore, they have some properties which

TABLE 1-4   Properties of Intact Granite

Type of Property	Parameter	Symbol	Mean*	Range	MKS Unit
Index	Unit Weight		2646.5	2306.9-3043.8	kg/m^3
	Natural moisture content (intact)		---	0.0.32	%
	Porosity (rock mass)		1.6	0.05-11.2	%
Stress-strain	Young's Modulus		50.3	15.9-83.4	GPa
	Poisson's Ratio		0.18	0.045-0.39	---
Strength	Uniaxial Compressive Strength		175.1	35.2-353.1	MPa
	Tensile Strength		6.3	3.4-55.9	MPa
Thermal	Coefficient of Linear Thermal Expansion		2.5×10^{-6}	$1.67 \times 10^{-6} - 3.34 \times 10^{-6}$	$^\circ C^{-1}$
	Heat Capacity		0.92	0.67-1.38	J/g-$^\circ$C
	Thermal Conductivity		TEMPERATURE	CONDUCTIVITY	
			0°C	2.86 w/m K	
			50°C	2.70	
			100°C	2.56	
			150°C	2.44	
			200°C	2.34	
			300°C	2.15	
			400°C	1.99	

*Number of tests used to derive mean.

SOURCE: Office of Waste Isolation, 1978.

TABLE 1-5   Intact properties of Barre Granite.

BASIC PARAMETERS

Type of Property	Parameter	MKS Units
Index	Unit Weight	2659.3 kg/m^3
	Natural moisture content (intact)	0.32%
	Porosity (rock mass)	0.4%
Stress-strain	Young's Modulus	72.4GPa
	Poisson's Ratio	0.22--
	Bulk Modulus	43.1GPa
	Shear Modulus	29.7Gpa
Strength	Cohesion. 10.3-24.1 Friction Angle MPa range	7.2MPa 45 degrees
	Uniaxial Compressive Strength	234.5MPa
	Tensile Strength	7.6MPa
Thermal	Coefficient of Linear Thermal Expansion	2.22x10^{-6} ^{o}C^{-1}
	Heat Capacity	0.9? J/g-^{o}c
	Thermal Conductivity	2.37 w/m^{o}K
Hydrological	Horizontal Permeability	less than 1x10^{-4} cm/sec

SOURCE: Office of Waste Isolation, 1978

1-54

TABLE 1-6. Intact properties of Colville Granite (unaltered).

BASIC PARAMETERS

Type of Property	Parameter	MKS Units
Index	Unit Weight	2627.3 kg/m^3
	Natural moisture content (intact)	0.6%
	Porosity (rock mass)	1.59%
Stress-strain	Young's Modulus	35.9GPa
	Poisson's Ratio	0.15--
	Bulk Modulus	17.2GPa
	Shear Modulus	15.9GPa
Strength	Cohesion 10.3-24.1 Friction Angle MPa range	22.4MPa 58 degrees
	Uniaxial Compressive Strength	144.8MPa
	Tensile Strength	7.4 (est.) MPa
Thermal	Coefficient of Linear Thermal Expansion	
	Heat Capacity	
	Thermal Conductivity	

Hydrological

*Linear stress-strain curve assumed.

SOURCE: Office of Waste Isolation, 1978

1-55

TABLE 1-7. Intact properties of Colville Granite (slightly altered)

BASIC PARAMETERS

Type of Property	Parameter	MKS Units
Index	Unit Weight	2609.7 kg/m^3
	Natural moisture content (intact)	1.0% (est.)
	Porosity (rock mass)	2.36%
Stress-strain	Young's Modulus	11.0GPa
	Poisson's Ratio	0.20--
	Bulk Modulus	6.2GPa
	Shear Modulus	4.8GPa
Strength	Cohesion 10.3-24.1 Friction Angle MPa range	9.8MPa 58 degrees
	Uniaxial Compressive Strength	64.8MPa
	Tensile Strength	3.2 (est.) MPa
Thermal	Coefficient of Linear Thermal Expansion	
	Heat Capacity	
	Thermal Conductivity	

Hydrological

*Linear stress-strain curve assumed.

SOURCE: Office of Waste Isolation, 1978

1-56

TABLE 1-8. Intact properties of Pikes Peak Granite.

BASIC PARAMETERS

Type of Property	Parameter	MKS Units
Index	Unit Weight	2636.9 kg/m^3
	Natural moisture content (intact)	.10%
	Porosity (rock mass)	
Stress-strain	Young's Modulus	70.6GPa
	Poisson's Ratio	.31--
	Bulk Modulus	62.0GPa
	Shear Modulus	26.96GPa
Strength	Cohesion 10.3~24.1 Friction Angle MPa range	
	Uniaxial Compressive Strength	226.2MPa
	Tensile Strength	11.9MPa
Thermal	Coefficient of Linear Thermal Expansion	
	Heat Capacity	
	Thermal Conductivity	
Hydrological		

SOURCE: Office of Waste Isolation, 1978

TABLE 1-9%. Intact properties of St. Cloud Gray Granodiorite.
(Precambrian Granite)

BASIC PARAMETERS

Type of Property	Parameter	MKS Units
Index	Unit Weight	2718.6 kg/m^3
	Natural moisture content (intact)	0.8%
	Porosity (rock mass)	1.5%
Stress-strain	Young's Modulus	71.0GPa
	Poisson's Ratio	0.25
	Bulk Modulus	46.5GPa
	Shear Modulus	28.6GPa
Strength	Cohesion 10.3-24.1 Friction Angle MPa range	
	Uniaxial Compressive Strength	282.1MPa
	Tensile Strength	6.97MPa
Thermal	Coefficient of Linear Thermal Expansion	
	Heat Capacity	
	Thermal Conductivity	
Hydrological	Permeability	Less than $1 \times 10^{-8} \text{cm/sec}$

SOUCE: Office of waste Isolation, 1978

would be the same as typical granites. On the other hand,
they have been specially selected because of their lack of
jointing, lack of weathering, homogeneous nature, uniform
coloring and texture and their proximity to the surface.
Some of these quarries exhibit very high insitu stress
fields. Table 1-10 (Ramspott, 1979) presents the comparison
of rock properties from Climax stock at the Nevada test site
and the Stripa Mine in Sweden. Notice that for any particu-
lar site, the variation in properties is much smaller than
the range established for a generic rock granite.

The most common test performed in rock mechanics work is the
uniaxial compression test from which one can obtain Young's
modulus (the ratio of stress to resultant strain) and Pois-
son's ratio (the ratio of lateral to longitudinal strain,
Appendix A). At the edge of an underground opening the
confining pressure is zero. As one progresses away from
the opening, the stress state becomes triaxial. The two
minor principal stresses may or may not be equal. Figure
1-8 shows the effect of confining pressure on the stress-
strain curve (Swan, 1978). Figure 1-9 depicts the variation
of Young's modulus and fracture stress with confining
pressure for Stripa granite (Swan, 1978). Notice that
as the confining pressure is changed from 0 to about 30
MPa, the modulus changes from approximately 70 to 80 GPa.
Thus the variation over this range is of the order of 15%.

TABLE 1-10. Comparison of rock properties.

Property	Climax stock quartz monzonite[a]	Stripa mine[b] Swedish granite
Dry density, g/cm^3 (lb/ft^3)	2.6-2.66 (163-166)	2.6 (163)
Porosity (%)	0.7-1.1	1.7
Compressive strength, MPa(psi)	210 (30,500)	217 (31,500)
Young's modulus, GPa(psi)	61.4-69.7 (8.9-10.1 x 10^6)	51.3 (7.4 x 10^6)
Poisson's ratio	0.21-0.22	0.23
Thermal conductivity, W/mK	3.0	3.5

[a]Data summarized from F. Maldonado, *Summary of the Geology and Physical Properties of the Climax Stock, Nevada Test Site*, U.S. Geological Survey, Open-file Rept. 77-356 (1977); L. Obert, *Shot Hard Hat, Static Stress Determinations*, U.S. Department of Defense (1963); F.H. Wright, *Shot Pile Driver, In-Situ Rock Stress*, U.S. Department of Energy (1967).

[b]Data from H. Pratt et al. *Thermal and Mechanical Properties - Stripa Sweden*, Terra Tek, Salt Lake City, Utah (1978).

[c]Data summarized from D.P. Krynine and W.R. Judd, *Principles of Engineering Geology & Geotechnics* (McGraw-Hill Book Co., New York, 1957); K. Szechy, *The Art of Tunneling*, Akademiai Kiado, Budapest (1966).

SOURCE: Ramspott, 1979.
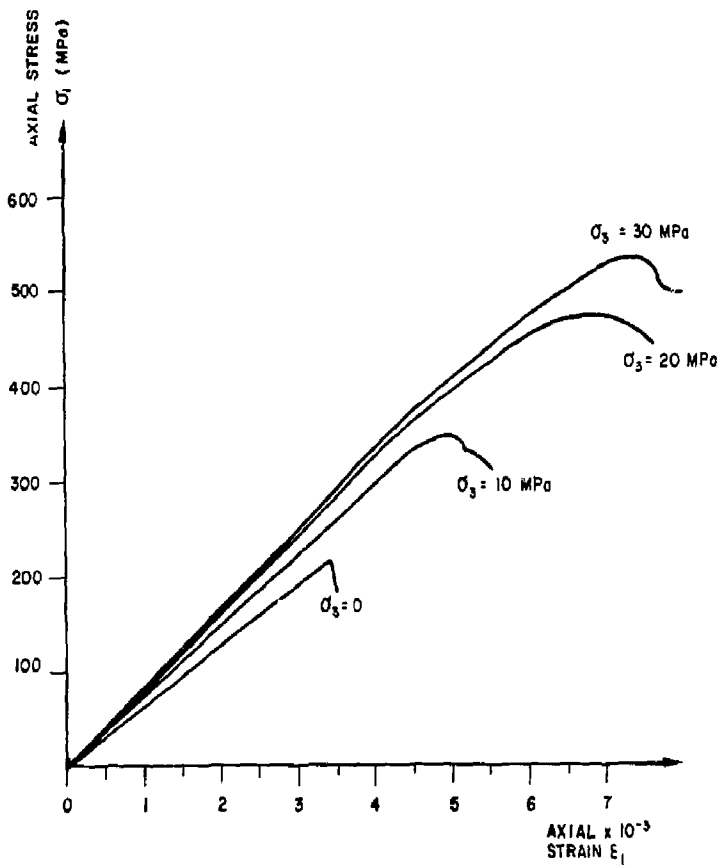
FIGURE 1-8   Axial stress versus strain plots for confining
              pressures of 0, 10, 20 and 30 MPa

Source: Swan, 1978.
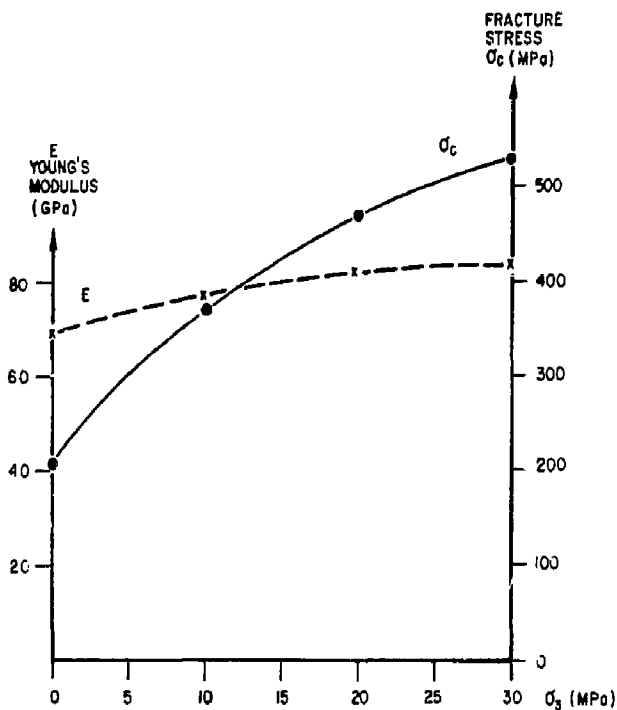
FIGURE 1-9   Graph showing variation of Young's modulus and
fracture stress σ_c with confining pressure
Source: Swan, 1978.

The compressive strength, on the other hand, varies from about 200 MPa at 0 confining pressure up to about 550 MPa at 30 MPa confining pressure. Therefore, although the modulus is relatively insensitive, the compressive strength is very dependent upon the confining pressure.

Tensile strength, as determined in the laboratory, is very dependent upon the sample selection, the sample size, and the method used. It is obvious that samples with pre-existing fractures, which would produce a tensile strength of 0, are discarded prior to testing. An indirect way of determining tensile strength is the Brazilian test. It is also the easiest technique and the one most often employed. The results one obtains are of the order of 2 times higher than one would obtain using a straight pull type of tension test. Yet both tests are supposedly measuring the same property.

1.12 THERMAL PROPERTIES

When the surface of an underground opening is exposed to a
heat source, transfer of heat will take place from the
source to the rock mass by conduction, and possibly by
radiation. Thermal transients, or a time-dependent temp-
erature distribution, will be generated across a heated zone
in the rock around the opening. The temperature distribu-
tion is dependent upon a combination of three thermal prop-
erties--conductivity, density and specific heat. These
properties can be characterized by a single thermal param-
eter known as diffusivity.

If an analytic solution to the temperature distribution is
sought, one must assume that the rock mass is a continuum
and that the thermal properties of the rock are independent
of temperature and spacial location. If the temperature
dependence is considered, the problem becomes nonlinear, so
numerical methods must be used. Such numerical techniques
are presently available, but the appropriate values of the
thermal properties are lacking. The thermal variation for
intact rock samples is generally rather high. In describing
rock mass properties, the problem can become even more
severe. If a piece of rock is free from constraint and
heated uniformly, the stresses generated are 0, even though

the rock changes size due to thermal expansion. However, in a rock mass which is subjected to a temperature gradient, the state of thermally induced stress is not 0. The change in stress is due both to geometric constraint and also to differences in the thermal expansion coefficients of the various constituents within the rock. These intergranular thermal stresses can develop independently of the existence of a thermal gradient or the geometric constraints described earlier. They can cause cracking along grain boundaries and also within the grains themselves. Such cracking can significantly affect both the mechanical and thermal properties of the rock. As noted earlier, rock strength decreases with temperature whereas, in this particular case the stresses would be increasing. When the thermally-induced stress field is imposed upon the existing stress field (that due to the insitu stresses, and the excavation-induced stresses), the total may exceed the strength of the rock.

Another type of thermally-induced failure is spalling. This is a progressive failure induced by thermal shock or a sudden application of heat. Thermal loading of rock using the jet piercing system has been used for many years as a technique for rock removal. Hence, for waste repository considerations, one must consider several types of thermal failure modes and have a very clear understanding of the thermal properties of the rock, on both a small and a large

scale. These properties can vary widely between crystalline
rock types, and even within the same rock type.

Thermal conductivity has been measured for many years. It
is dependent upon both rock temperature and pressure. At
present, there is very little data regarding the pressure
dependency. The variation of thermal conductivity with
temperature, however, is shown for various rocks in Figures
1-10 to 1-13 (Parsons et al, 1976; Thirumalai, 1970; Hasan,
1978; Mirkovich, 1968). Generally, a very rapid decrease in
thermal conductivity occurs between 0° and 250^oC. There-
after, the rate of decrease is considerably slower. This
lower temperature range is precisely that of most reposi-
tories, however. Note that there can be a rather large range
at any one particular temperature for a group of samples. This
is shown in Table 1-11. For any one rock the variation is
generally of the order of about 30%, but can be as high as
a factor of 2.

As mentioned earlier, one of the factors that must be con-
sidered is the spallability of the rock, since this affects
the conditions directly surrounding the bore hole. The
piercing rating or spallability index of a number of differ-
ent rocks is presented in Table ' 12. The spallability or
piercing index is based on a scale from 1-10, with 1
indicating the greatest degree of spallability. Granites
generally fall into the highest spallability category.
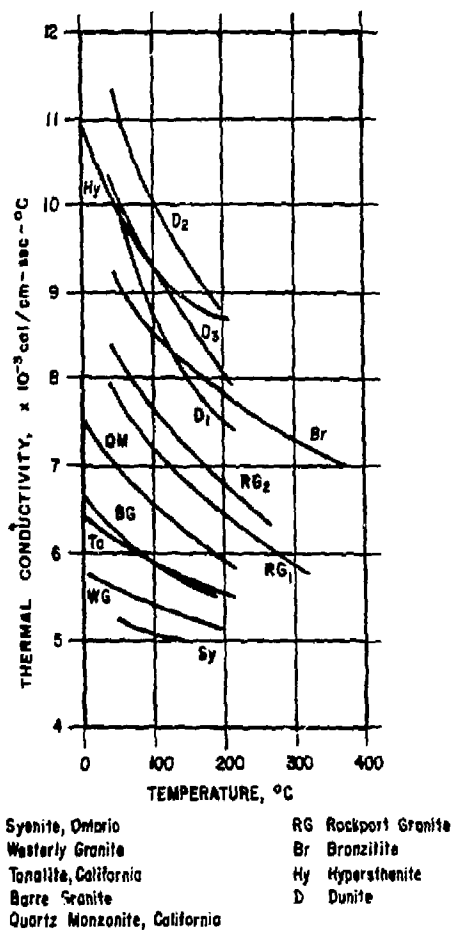
FIGURE 1-10 Variation of thermal conductivity with
temperature Source: PBQ&D, 1976.

Sy Syenite, Ontario
WG Westerly Granite
To Tonalite, California
BG Barre Granite
QM Quartz Monzonite, California

RG Rockport Granite
Br Bronzilite
Hy Hypersthenite
D Dunite
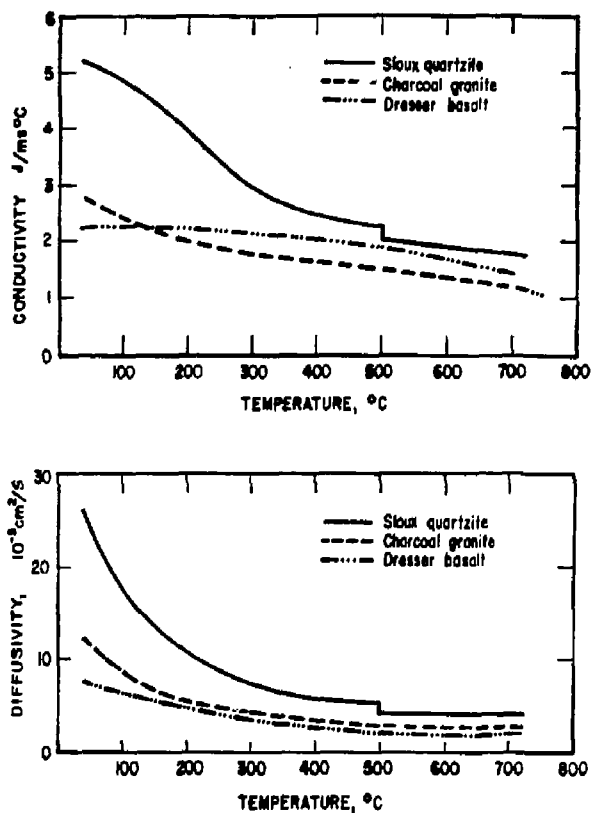
FIGURE 1-11 Variation of thermal conductivity and
diffusivity with temperature
Source: Thirumalai, 1970.
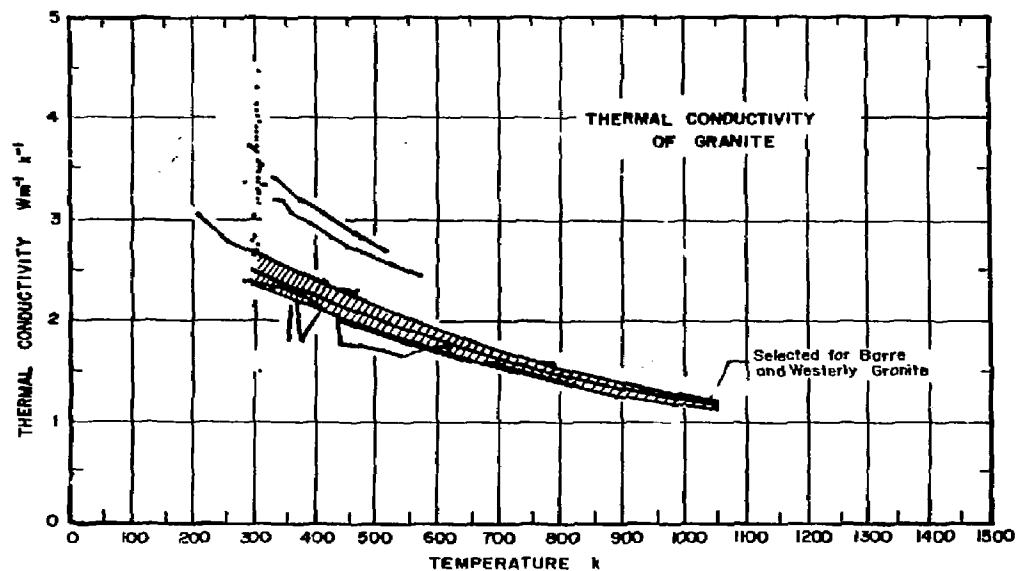
FIGURE 1-12 Variation of thermal conductivity with temperature
Source: Hasan, 1978.

178	———
188	··············
190	– – – –
191	∿∿∿∿
192	·· — ·· —
193	⊢⊣ ⊢⊣ ⊢⊣
194	— · — · —
208	⊣ ⊣ ⊣ ⊣
209	— ·· — ·· —
210	▆▆▆▆▆
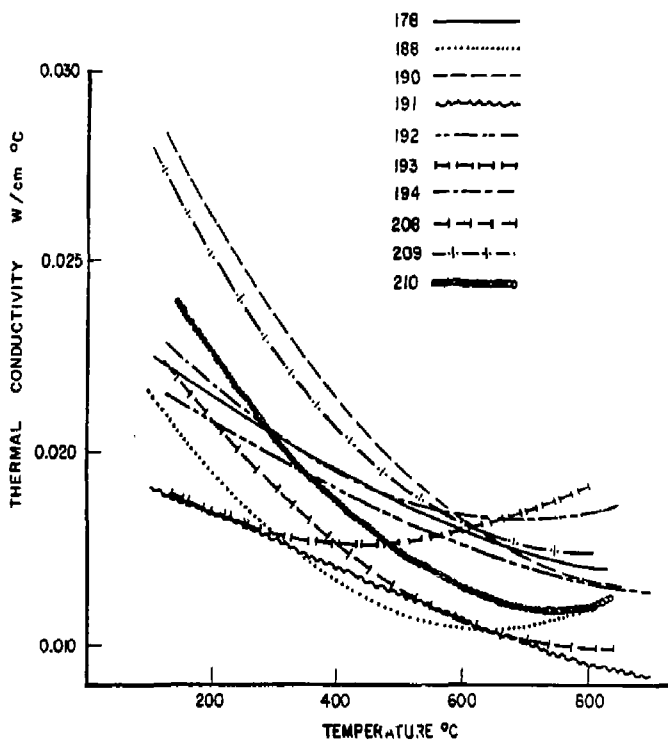
Sample No.	Rock Type	Sample No.	Rock Type
M-178	Gabbro (Diabase)	M-193	Anorthosite
-188	Nepheline Syenite	-194	Granite
-190	Rhyolite	-208	Granodiorite·
-191	Hbde Syenite	-209	Granite
-193	Nodmarkite	-210	Qtz Monzonite

Figure 1-13   Thermal conductivity of selected igneous rocks

Source: Mirkovich, 1968

1-70

TABLE 1-11. Conductivity of rocks (Source: Lee, 1978).

The measurements were made at a temperature of about 20° C unless other-wise noted. The values are the means of groups of measurements. Only cases in which there are five or more measurements from a single litho-logic unit are included. (σ = standard deviation.)

Rock Type and Locality	Number of determin-ations	Conductivity (10^{-3} cal/cm sec° C)	
		Mean	Range
Granite and Quartz Monzonite Adams Tunnel, Colorado	59	7.89	6.7- 8.6
Granite, Loetschberg Tunnel Switzerland	12	7.77	6.2- 9.0
Granodiorite, Steamboat Springs, Nevada	5	6.64	6.2- 6.9
Granodiorite, Grass Valley, California	14	7.61	7.0- 8.3
Quartz-Feldspar Porphyry, Jacoba Bore, Orange Free State, S. Africa (25° C)	5	8.0	7.6- 8.6
Syenite and Syenite Porphyry, Kirkland Lake, Ontario	37	7.66	6.3- 9.5
Altered Rhyolite, Timmins, Ontario	6	8.23	7.4- 8.8
Norite, Sudbury, Ontario	5	6.42	5.5- 7.3
Serpentinized Periodotite, Thetford Mines, Quebec	5	6.34	5.7- 7.0
Agglomerate, Roodepoort Bore, Transvaal, S. Africa	5	7.4	7.1- 8.0
Karoo Dolerite, Kestell Bore, Orange Free State (35° C)	9	4.3	4.0- 5.5
Ventersdorp Lava, Jacoba Bore, Orange Free State (25° C)	9	7.4	6.3- 8.6
Ventersdorp Lava, Roodepoort Bore, Transvaal	15	7.2	6.4- 8.3
Portage Lake Lava, Calumet, Mich., Dense Flows	27	5.01	4.1- 6.6
Amygdaloidal Tops	10	6.4	5.5- 9.0
Porphyrite and Diabase, Grass Valley, CA	21	7.14	6.2- 8.3
Quartz Diorite Gneiss, Adams Tunnel, CO	17	7.75	6.6- 8.5
Injection Gneiss and Schist, Adams Tunnel, Colorado	41	7.74	4.0-11.0
Gneiss, Gotthard Tunnel, Switzerland	15	5.63	5.1- 8.0
Gneiss, Simplon Tunnel, Switzerland, Perpendicular	22	6.34	4.6- 7.7
Parallel	8	8.90	6.0-11.4
Simplon Tunnel, Switzerland, Perpendicular	8	5.74	4.1- 6.8
Parallel	7	7.50	6.8- 8.9
Gneiss, Chester, Vermont, Perpendicular	9	6.24	4.9- 8.7
Parallel	9	8.33	6.1-10.4
Amphibolite, Homestake Mine, Lead, S.D.,	6	6.92	6.1- 9.1
Calcareous Mica Phyllite, Homestake Mine, Perpendicular	7	7.89	6.5- 9.0
Parallel	9	11.83	9.5-14.0
Quartzite, Homestake Mine	6	16.05	14.2-17.6
Witwatersrand Quartzite, Gerhardminnebron Bore, Transvaal (25° C)	17	14.3	8.7-19.2
	21	14.5	10.4-18.9
Witwatersrand Quartzite, Roodepoort Bore, Transvaal	7	10.1	7.4-12.7

Table 1-12 Classification, composition, texture, structure, piercing ratios, thermal expansion, specific heat and density of 19 Canadian rocks and minerals

Sample No.	Rock class	Quartz	K-Felds	Na-Felds	Mineral composition (%) Ca-Felds	Ferromagnesians and miscellaneous	Texture	Piercing	% Therm. exp. per °C	Sp. Heat (W/sec °C)	Density (g/cm³)
						1. Igneous Rocks					
M-175	Gabbro (Diabase)	--	12 (Graphic)	--	44 (An$_{60}$)	24 Aug; 11 Hnde. Biot; 7 Mag.	M.diabasic-hypidio-morphic	2	0.45	0.905	2.96
M-185	Nepheline Syenite	--	23	52	--	2 Mag; 23 Nepheline	M.hypidio-morphic	9	0.52	0.991	2.93
M-190	Rhyolite	20	52	51	--	3 Mag	F.allotrio-morphic	10	0.74	0.991	2.57
M-191	Rhde Syenite	--	73 (Perthite)	17	--	9 Hrnde; 2 Biot; 3 Mag	M.hypidio-morphic	6	0.63	0.955	2.62
M-192	Sned-arkite	9	89 (Perthite)	9	--	7 Hrnde; 2 Aug; 1 Mag; + Apatite	C.panidio-morphic	5	0.68	0.956	2.66
M-193	Anorthosite	--	1	--	67 (An$_{50}$)	7 Aug; 1 Mag	C.hypidio-morphic	2	0.45	0.970	2.63
M-194	Granite	34	31	31	--	3 Biot	M.hypidio-morphic	3	1.02	0.996	2.65
M-205	Granodiorite	21	4	--	51 (An$_{30}$)	12 Hnde; 9 Biot; 3 Epidote	M.hypidio-morphic	6	0.92	0.991	2.77
M-209	Granite	33	29	25	--	10 Biot; + Sphene	M.hypidio-morphic	9	0.82	0.991	2.66
M-210	Qtz Monzonite	27	20	--	42	10 Biot; 1 Muscovite	C.panidio-morphic	7	0.84	0.004	2.65

NOTE: All homogeneous structure except 209 granite, coarsely gneissic.

Source: Clark, 1969

Specific heats of rocks are determined by heating specimens
of known weights to a given temperature and then measuring
the heat content of the rock by calorimetric methods.
Figure 1-14 shows the variation of specific heat with temp-
erature for a number of different rock types. The rather
strange behavior of quartz in the vicinity of 573° C is due
to the transformation of quartz from the alpha to beta form.
Note that over the temperature range shown in Figure 1-14,
the variation in specific heat is approximately 25%. Some
additional values for mean specific heat values for the
range of 25° up to 625° C are given in Table 1-13.

The effect of temperature on density for relatively non-
porous rocks such as granites, is negligible. For other
rocks, however, the density may decrease with increasing
temperature as a result of moisture changes.

Thermal diffusivity is considered a derived quantity which
includes thermal conductivity, specific heat, and density.
The results presented in Figures 1-15, 1-16 and 1-17 reveal
that the thermal diffusivity decreases with increasing
temperature to at least 600° C. Above this temperature, as
shown in Figure 1-17, the diffusivity may increase slightly.

The fusion temperatures of the rock, which may or may not be
appropriate for consideration in nuclear waste disposal, are
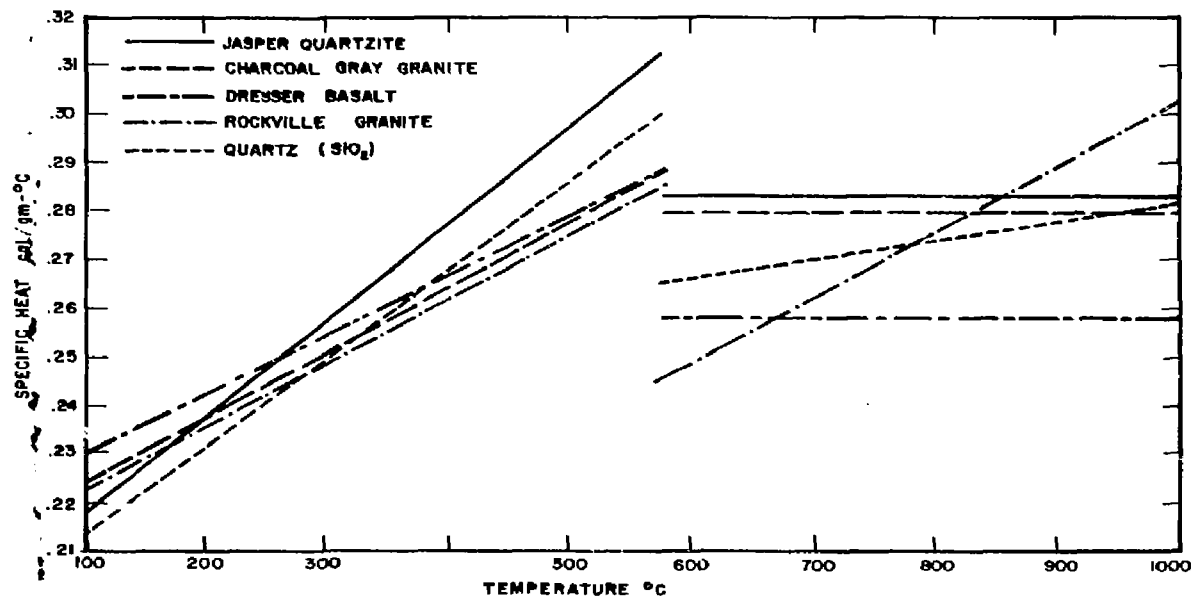
FIGURE 1-14 Variation of specific heat with temperature
Source: PBQ&D, 1976 and Lindroth and Krawza, 1971.

TABLE 1-13. Specific heat determinations of various samples

Common Designation	Lab. No.	No. of Runs	Sample weight g	Sample temperature °C	Water temperature in calorimeter °C Initial	Water temperature in calorimeter °C Final	Total rise in temperature of water in calorimeter, °C	Mean specific heat between 25°C and 625°C cal/g/°C	
Granite	M-195	1	438.30	625	25.007	26.774	1.767	0.241	
		2	464.60	625	25.586	27.453	1.867	0.240	0.241
Anorthosite (Péribonka Black)	M-193	1	474.54	625	25.595	27.457	1.862	0.235	
		2	421.06	625	25.546	27.189	1.643	0.233	0.234
"Nepean sandstone"	M-176	1	344.47	625	25.411	26.826	1.415	0.245	
		2	345.40	625	25.411	26.831	1.420	0.246	0.246
"Diabase"	N-179	1	445.49	625	25.407	27.078	1.671	0.224	
		2	439.89	625	25.387	27.064	1.677	0.228	0.226
Nepheline syenite	M-188	1	367.90	625	25.397	26.859	1.462	0.237	
		2	376.50	625	25.453	26.948	1.495	0.237	0.237
"Basalt"	M-	1	475.91	625	25.445	27.304	1.859	0.234	
		2	501.72	625	25.532	27.517	1.985	0.237	0.236
"Rhyolite"	M-190	1	367.50	625	25.418	26.878	1.460	0.237	
		2	321.91	625	25.340	26.617	1.277	0.237	0.237
Syenite (Sienna Red)	M-191	1	442.46	625	25.452	27.116	1.664	0.230	
		2	447.41	625	25.526	27.237	1.711	0.228	0.229
Nordmarkite (Scots Green)	M-192	1	419.50	625	25.351	26.968	1.617	0.230	
		2	413.10	625	25.500	27.123	1.623	0.232	0.231

Source: Clark, 1969
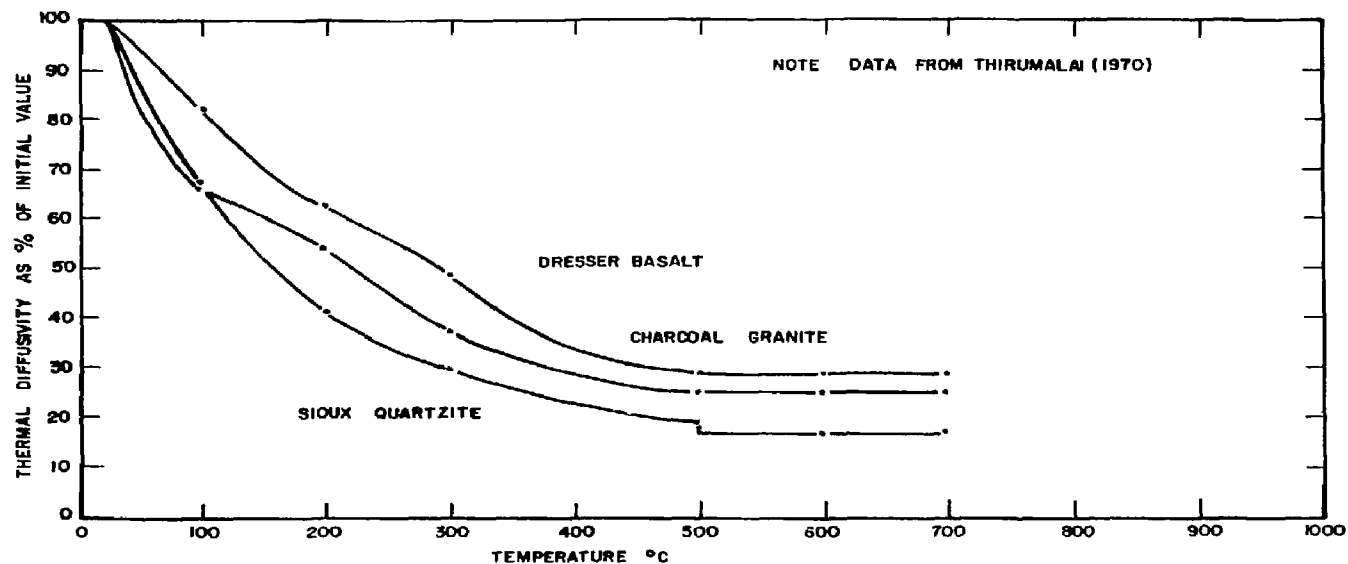
FIGURE 1-15 Variation of normalized thermal diffusivity with temperature
Source: Thirumalai, 1970.
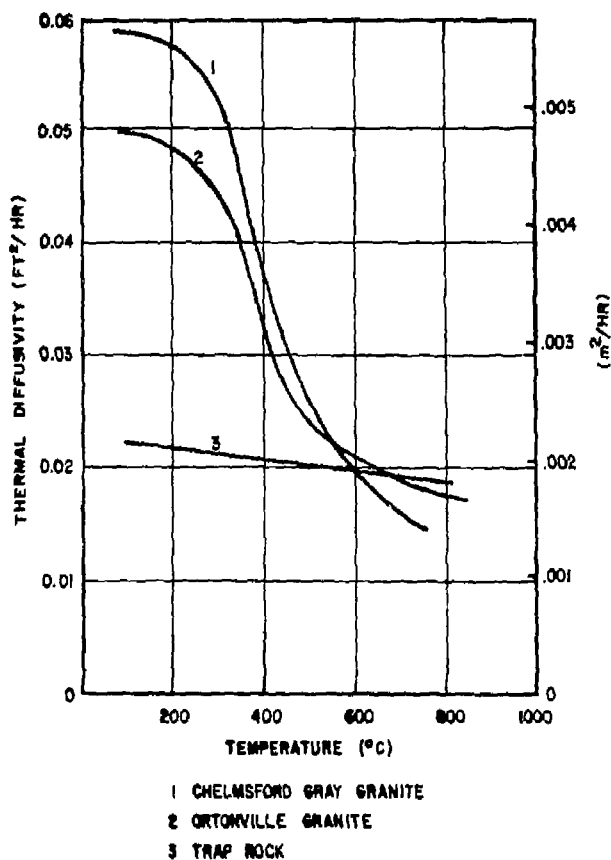
FIGURE 1-16 Variation of thermal diffusivity
with temperature
Source: Freeman et al, 1963.
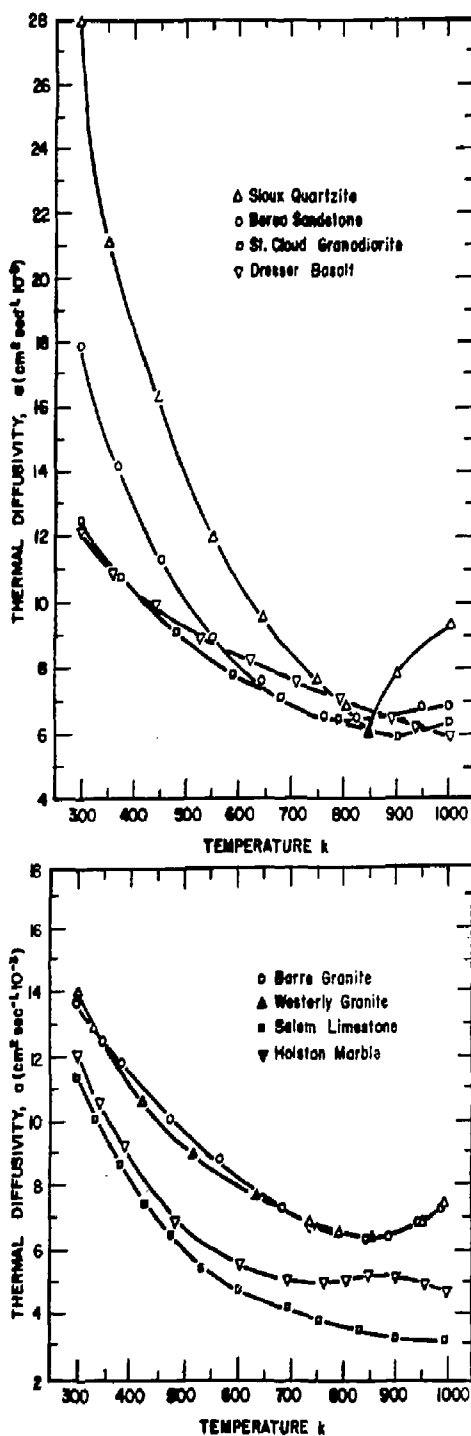
FIGURE 1-17 Thermal diffusivity of eight air-dried
rocks as a function of temperature
Source: Hanley,

1-78

shown in Tables 1-14 and 1-15. Notice that they are in the

range of about 1,100° to 1,300° C, or well above the pro-

posed operating temperatures for repositories.

TABLE **1-14**. Fusion temperatures of series "A" rocks

Lab. No.	Rock Common Designation	Origin	Fusion Temp., °C	Pyrometric Cone Equivalent (P.C.E.) No.
a. **Crystalline Igneous Rocks**				
M-143	Basalt (traprock)	New Jersey	1152-1168	C-3
M-137	Diabase traprock ("Black Granite")	French Creek Granite Co.	1168-1186	C-4
M-135	Medium red granite	Leeds County, Ontario	1168-1186	C-4
M-149	White granite (high mica content)	Chelmsford, Massachusetts	1168-1186	C-4
M-155	Opalescent granite	Cold Springs, Minnesota	1201-1222	C-6
M-136	Grey granite	Norway	1215-1240	C-7
M-138	Grey granite	Salisbury, N.C.	1236-1263	C-8
M-140	Collins pink granite	Salisbury, N.C.	1236-1263	C-8
M-151	"Syenite"	Lake Asbestos, Quebec	1236-1263	C-8
M-152	Red granite	Wausau, Wisconsin	1236-1263	C-8
M-154	Melrose pink granite	Guenette, Quebec	1236-1263	C-8
M-157	Granite gneiss	Mount Wright, Quebec	1236-1263	C-8
M-153	Grey granite	Chelmsford, Massachusetts	1285-1305	C-10

Source: Clark, 1969

TABLE 1-15. Fusion temperatures of series "B" rocks

Lab. No.	Rock Common Designation	Origin	Fusion Temp., °C	Pyrometric Cone Equivalent (P.C.E.) No.
a. Crystalline Igneous Rocks				
1. Quartz rich (more than 10% quartz)				
M-195	Granite	Stanstead, Quebec	1198-1221	C-5 1/3
M-208	"Granite" (blue)	Riviere-a-Pierre, Quebec	No results. All of the test cones broke off.	
M-210	"Granite" (Stanstead Grey)	Stanstead, Quebec	1201-1222	C-6
M-209	Granite (Saguenay Red)	Lake St. John, Quebec	1177-1196	C-5
M-194	Granite (Vermilion Pink)	Vermilion Bay, Ontario	1207-1232	C-6 1/2
M-190	"Rhyolite"	Havelock, Ontario	1215-1240	C-7
a. Crystalline Igneous Rocks				
2. Quartz poor (less than 10% quartz)				
M-189	"Basalt"	Havelock, Ontario	1149-1165	C-2 2/3
M-178	"Diabase"	Bell's Corners, Ontario	1164-1179	C-3 2/3
M-193	Anorthosite (Peribonca Black)	Peribonca River, Quebec	1297-1319	C-11 1/3
M-191	Syenite (Sienna Red)	Rawcliffe, Quebec	1168-1186	C-4
M-192	Nordmarkite (Scots Green)	Mount Megantic, Quebec	1167-1184	C-3 4/5
M-188	Nepheline syenite	Methen Township, Ontario	1168-1186	C-4

Source: Clark, 1969

1.13 THERMOELASTIC PROPERTIES

The thermoelastic properties which will be discussed include
the effect of temperature on strength, Young's modulus and
Poisson's ratio, and on the linear coefficient of thermal
expansion. Figure 1-18 shows a typical stress-strain plot
for an uniaxial compression test conducted at 150° C on
Stripa granite (Swan, 1978). Even at this elevated temperature,
the relationship between stress and strain is still fairly
linear. Figure 1-19 shows the change in ultimate compressive
strength with temperatures for a number of different rock
types including four granites. The very severe decrease
which occurs at about $1,100^\circ$ C is due to reaching fusion
temperature for these rocks. Otherwise, over the temperature
range of principal interest (from 20° to 400° C) the decrease
in strength varies depending on the rock, from 0% to approximately
50%.

Figures 1-20 and 1-21 show the change in compressive strength
with temperature and confining pressure. These tests have
all been done with a confine pressure of 5 kilobars. Note
that for the granite shown in Figure 1-20, the decrease
over the temperature range of 0° to 400° C is relatively
small. In Figure 1-21, the deviatoric stress ($\sigma_1 - \sigma_3$) is
plotted as a function of strain. With increasing
temperatures at this pressure of 5 kilobars, the rocks
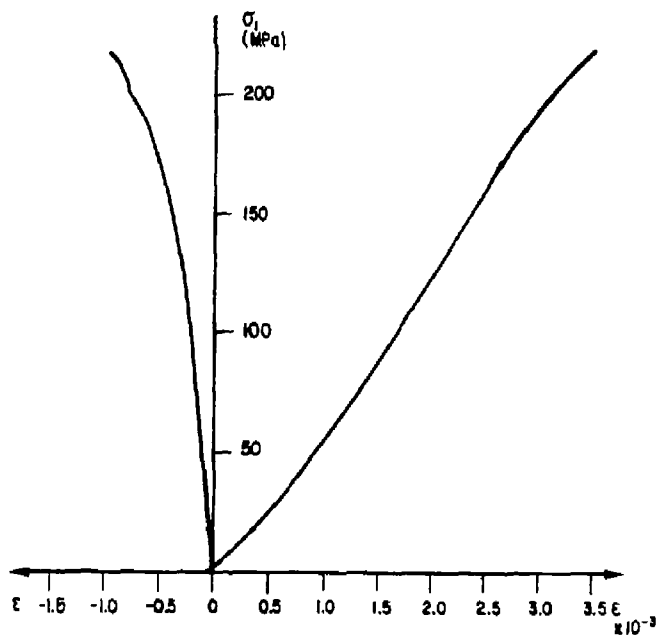
FIGURE 1-18 Typical stress vs strain plot from uniaxial test at
150° C. Source: Swan and Graham, 1978.
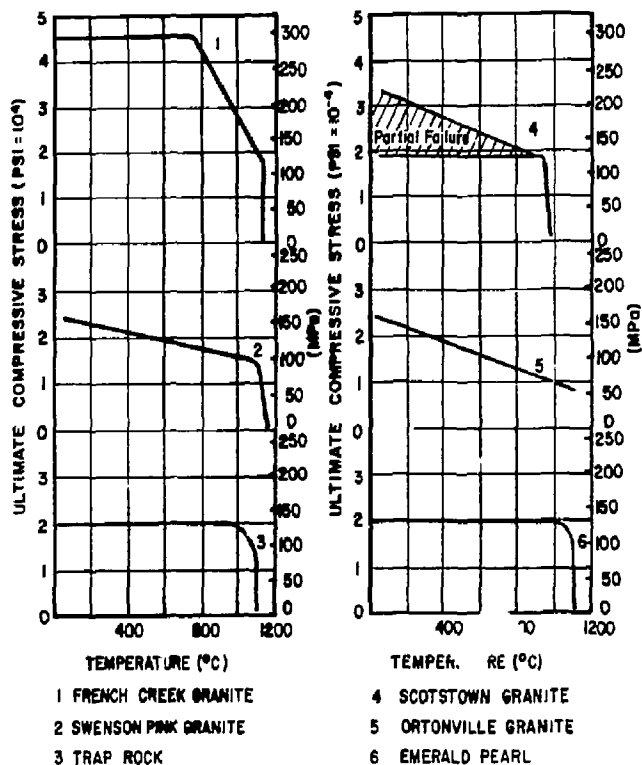
FIGURE 1-19 Variation of ultimate compressive
             stress with temperature
             Source: Freeman et al, 1963.
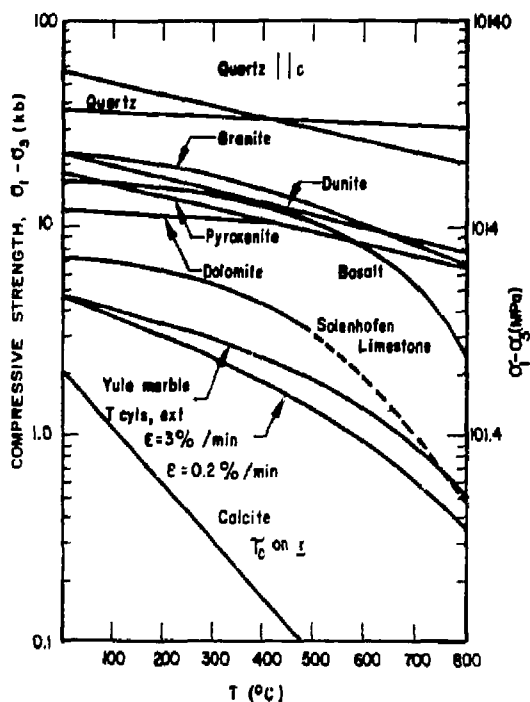
FIGURE 1-20 Strength of rocks and minerals at 5kb
Source: Griggs et al, 1960.
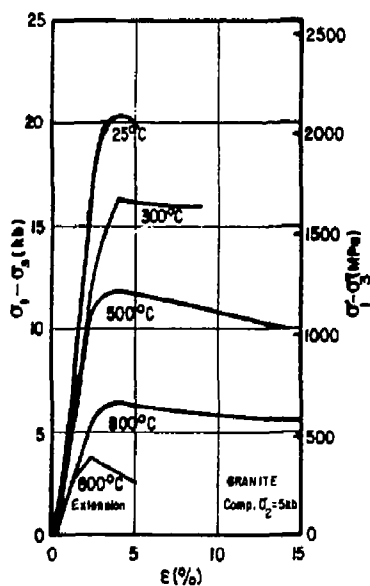
FIGURE 1-21 Effect of temperature on stress-strain curves for rocks
Source: Griggs et al, 1960.

become much more plastic and the deviatoric stress required
to cause extension is much smaller.

Figures 1-22 and 1-23 show Young's modulus and Poisson's
ratio as a function of temperature for Stripa granite.
The error bars indicate 90% confidence limits for these
laboratory tests. Notice that over the temperature range of
0° to 200° C, Young's modulus has decreased by approximately
30%. For the same temperature range, Poisson's ratio has
decreased to about half. The variation of Young's modulus,
Shear modulus, and Poisson's ratio with temperature is shown
for four rock types in Figure 1-24. Note that Young's
modulus for charcoal granite is reduced by about a factor of
2, when going from room temperature to 400° C. Poisson's
ratio would appear to change from positive to negative,
which is rather unusual. It is clear that on-going work
will help to clarify some of these relationships. In gener-
al, both the uniaxial and triaxial compressive strengths of
granite decrease markedly with increased temperature. Both
the elastic modulus and Poisson's ratio are reduced.

The coefficient of linear thermal expansion is very impor-
tant for the calculation of both the displacements and the
stresses that will result from the thermal field. The
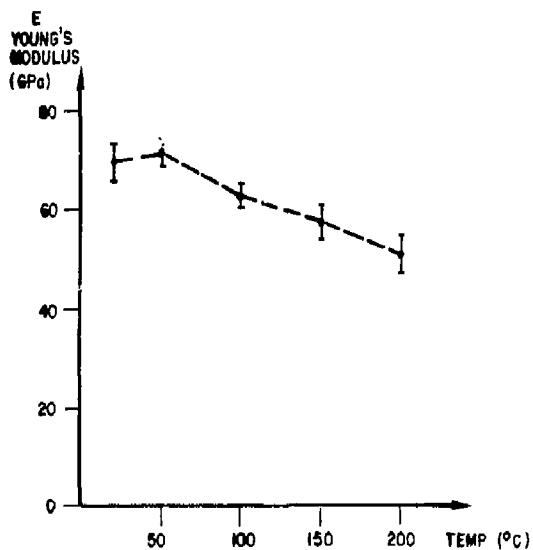
FIGURE 1-22 Young's modulus versus temperature showing
90% confidence limits Source: Swan, 1978.
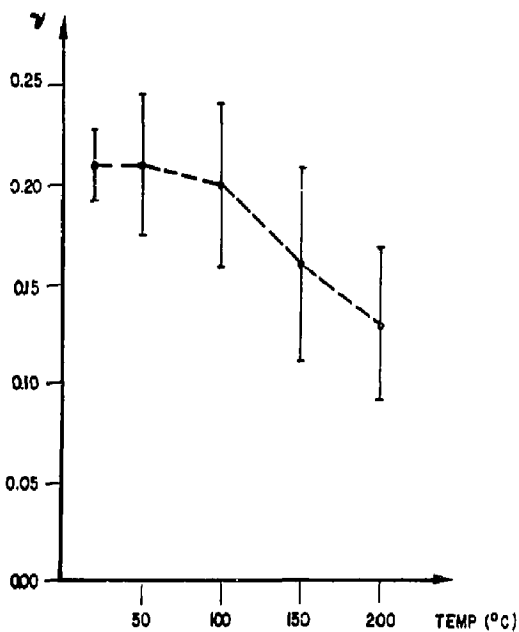
FIGURE 1-23 Poisson's ratio versus temperature showing
90% confidence limits Source: Swan, 1978.
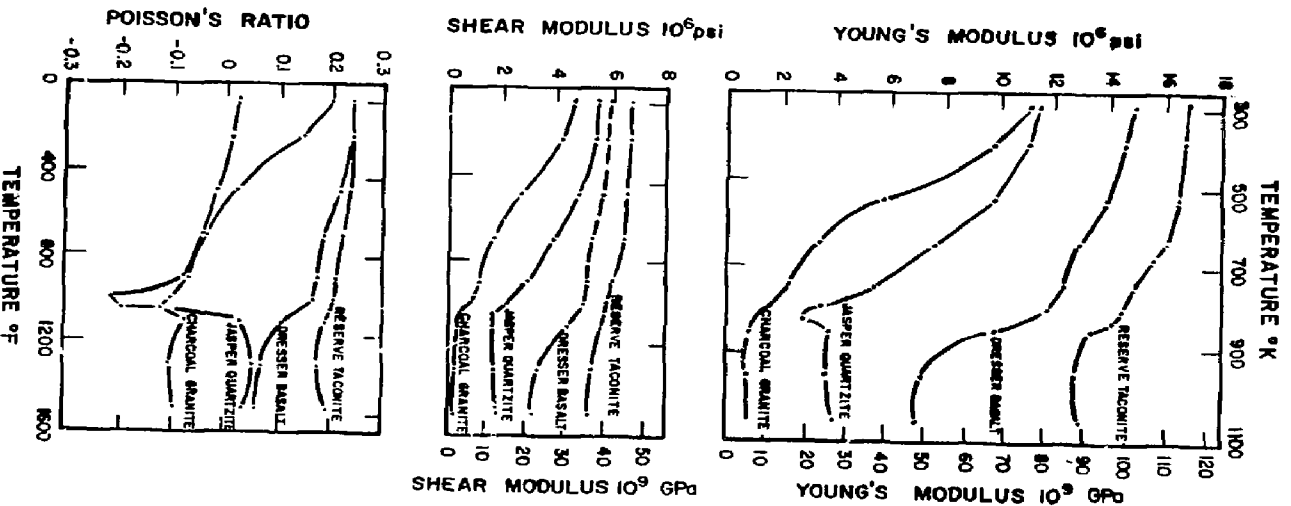
FIGURE 1-24 Variation of Young's modulus, shear modulus,
and Poisson's ratio with temperature.
Source: Wingquist, 1970.

degree of temperature dependence of thermal expansion varies widely among different rocks as shown in Figures 1-25, 1-26 and in Table 1-16. For example, the coefficient of linear expansion for charcoal granite is about 8 times that at 200° C as it is at 424° C. This parameter is also affected by the alpha-beta inversion temperature (573° C) of quartz, illustrated in Figure 1-26.

It is interesting to note from Table 1-16 that the values for most granites or granite-type rocks are relatively similar over a wide temperature range.

The variation in percent volume expansion for some common igneous minerals shown in Figure 1-27 illustrates why quartz is so effective in causing thermal stresses in high quartz content rocks, such as igneous rocks. This difference in volume expansion is exploited in thermal types of rock removal processes. The average linear expansion of rocks (Table 1-17) having excellent and very good spallability is shown in Figures 1-28 and 1-29, as a function of temperature. Most granitic rocks have a very good spallability and, therefore, would be expected to spall under high thermal gradients.

Table 1-18 shows the effect of the combination of heat and moisture on the strength of granite. Note that when granite
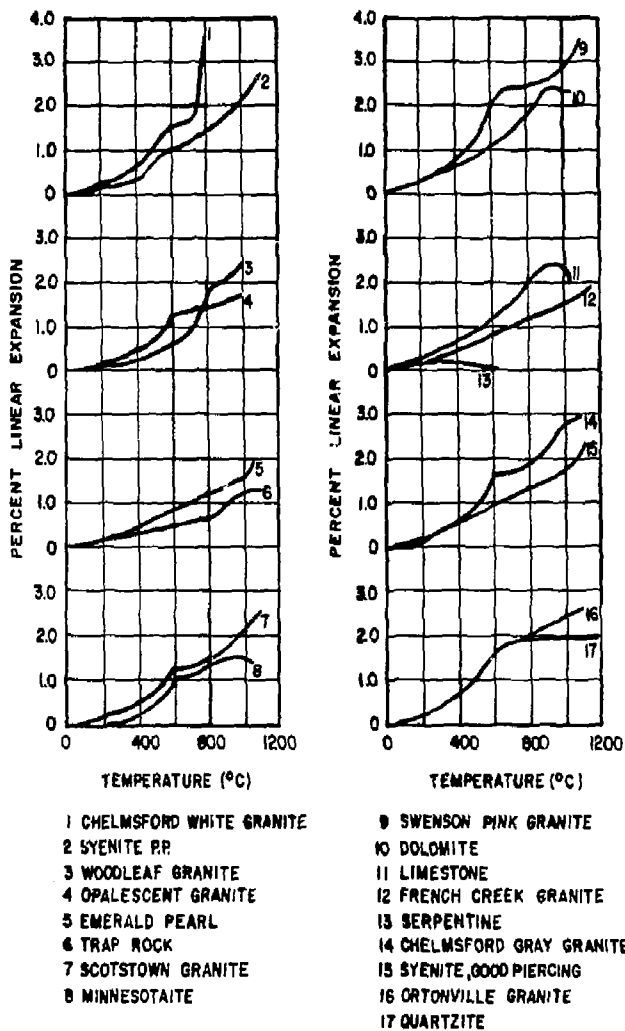
FIGURE 1-25 Variation of linear thermal expansion with
            temperature Source: Freeman et al, 1963.

1 CHELMSFORD WHITE GRANITE	9 SWENSON PINK GRANITE
2 SYENITE P.P.	10 DOLOMITE
3 WOODLEAF GRANITE	11 LIMESTONE
4 OPALESCENT GRANITE	12 FRENCH CREEK GRANITE
5 EMERALD PEARL	13 SERPENTINE
6 TRAP ROCK	14 CHELMSFORD GRAY GRANITE
7 SCOTSTOWN GRANITE	15 SYENITE, GOOD PIERCING
8 MINNESOTAITE	16 ORTONVILLE GRANITE
	17 QUARTZITE
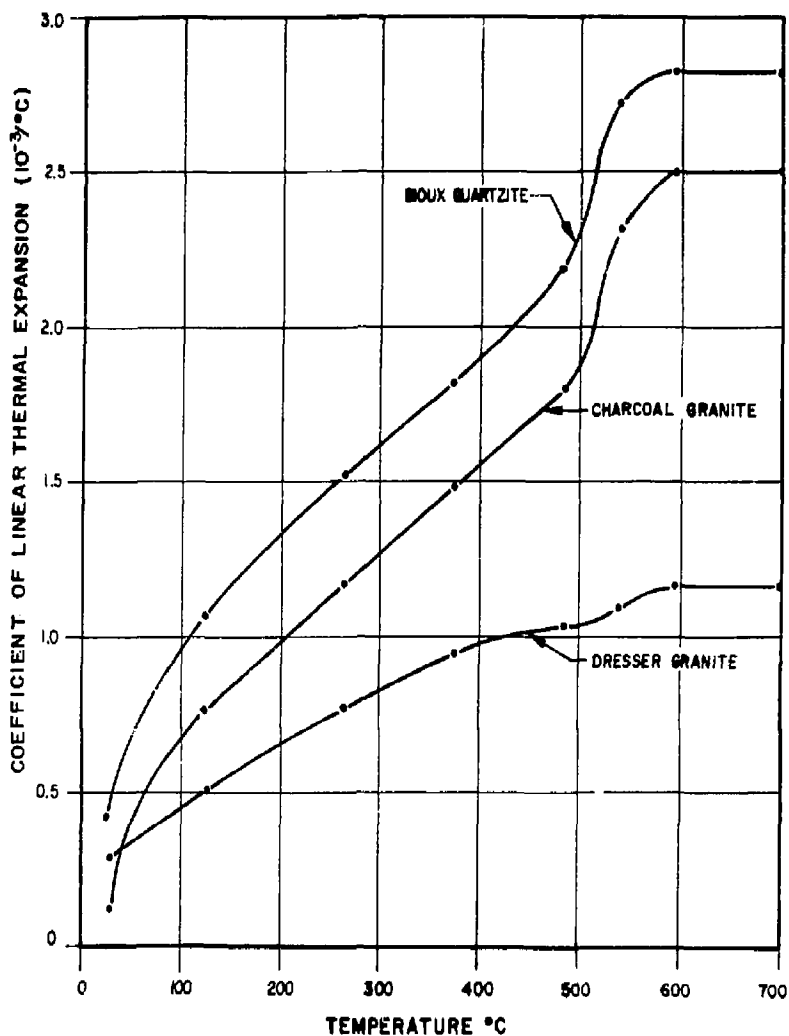
FIGURE 1-26 Variation of coefficient of linear thermal expansion with temperature. Source: Lehnhoff and Scheller, 1975.

TABLE 1-16. Measured coefficients of thermal expansion.

Rock type	Specimen No	$\alpha_v (25°C) \times 10^{-6}$	$\alpha_v (400°C) \times 10^{-6}$
		Experiment Ref. [1]	Experiment Ref. [1]
Chelmsford granite	A757	21.5	73.3
Westerly granite	1134	24.8	67.0
Wausau granite	1343	19.9	71.5
Graniteville granite	1410	25.1	76.8
Red River Quartzmon	1370	21.1	75.0

SOURCE: Swan, 1978.
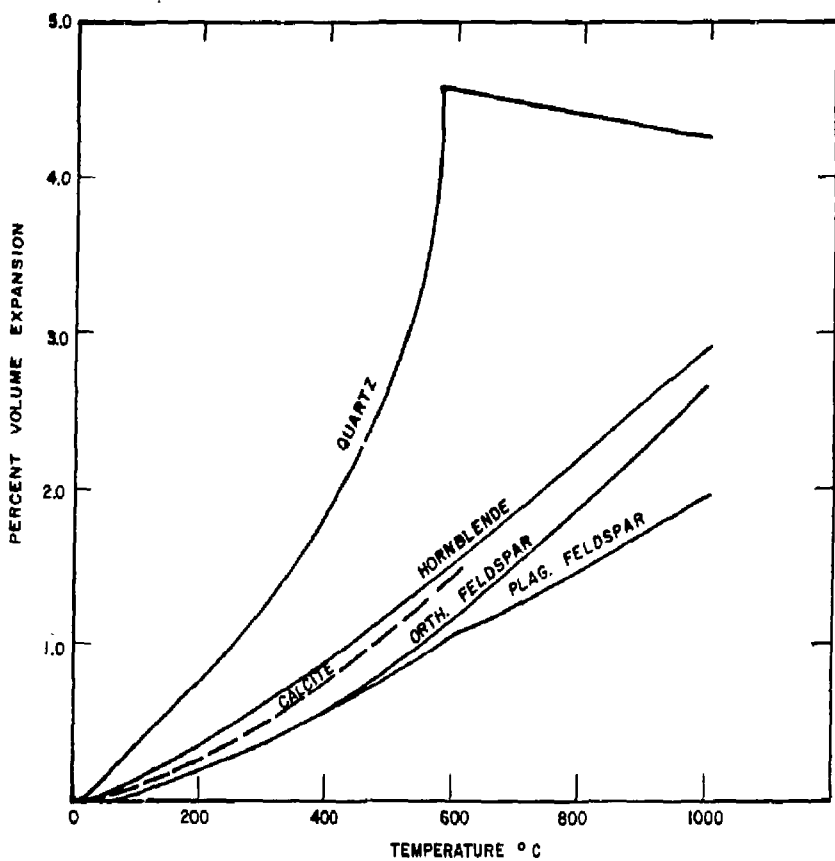
FIGURE 1-27 Volume thermal expansion of some common minerals
Source: Skinner, 1966.

TABLE 1-17.   Mineralogical composition of rocks vs. rock-removal rate and percent elongation at 600° C

A. CRYSTALLINE IGNEOUS ROCKS

1. Quartz-rich Rocks-(10% Quartz)

Rock Class. Rock Sample	Granite M-195	Granodiorite M-208	Quartz Monzonite M-210	Granite M-209	Granite M-194	Graphic Granite M-190
K-Feldspar[1]	21.2	3.8	19.5	28.6	31.1	51.5
Plagioclase[2]	44.8	50.5	41.4	23.0	31.3	20.5
Perthite	-	-	-	2.4	0.9	(70%)
Quartz	29.3	20.6	27.4	33.5	32.8	23.2
Amphibole	0.1	12.0	-	-	-	0.1
Other Mafics	-	2.0	0.3	-	-	0.6
Biotite	2.9	9.4	9.9	0.6	0.4	0.6
Muscovite	1.7	-	1.1	9.8	2.9	1.0
Magnetite	-	-	0.3	0.3	0.1	0.6
Carbonate	-	-	0.1	0.3	0.3	2.5
Others	-	1.7	-	1.5	0.2	-
Rock-removal Rate (cu in./ cu ft O_2)	1.0	1.5	2.4	3.1	3.1	3.4
% Elongation at 600°C	1.4	2.0	1.4	1.5	1.6	1.5

2. Quartz-poor Rocks (10% Quartz)

Rock Class. Rock Sample	Basalt (Saussurite) M-189	Gabbro (Diabase) M-178	Anorthosite M-193	Syenite M-191	Nord-markite M-192	Neph. Syenite M-183
K-Feldspar[1]	-	6.0	0.5	-	-	23.0
Plagioclase[2]	17.8	46.2	98.0	17.4	7.6	52.3
Perthite	-	-	-	69.2	73.3	-
Nepheline	-	-	-	-	-	23.0
Quartz	5(?)	6.2	-	-	-	-
Pyroxene	19.7	23.8	-	-	9.4	-
Amphibole	-	5.0	1.0	-	1.8	-
Other Mafics	52.1	4.9	0.3	8.8	6.7	-
Biotite	-	1.0	-	-	-	-
Muscovite	-	-	0.2	2.3	0.1	-
Magnetite, Hem.	5.2	6.9	0.2	-	-	0.2
Carbonate	0.2	-	-	2.3	1.1	1.5
Rock-removal Rate (cu in./ cu ft O_2)	0.4	0.6	1.0	1.5	2.0	3.9
% Elongation at 600°C	0.5	0.75	0.55	0.82	1.0	1.15

NOTES: [1] Includes both orthoclase and microcline.
[2] Intergrown plagioclase and potassic feldspar.

SOURCES: Clark, et al, 1970. Geller, et al, 1962.

1-95
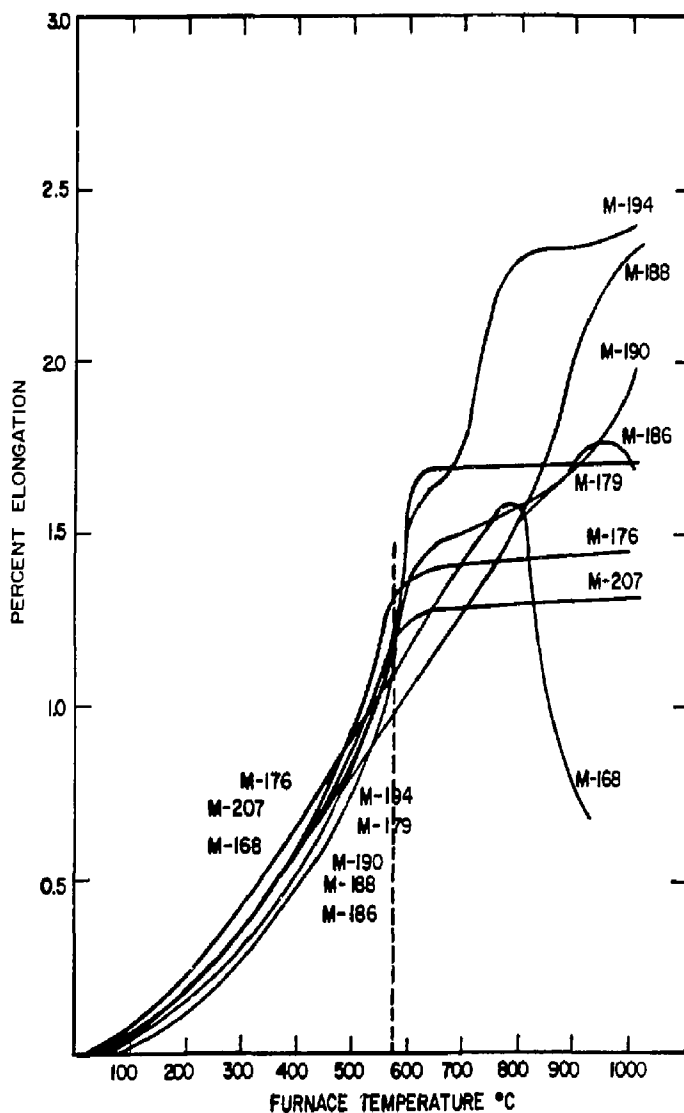
FIGURE 1-28 Average linear expansion of rocks of excellent
and very good pierceability
Source: Clark et al, 1969 and Geller et al, 1962.
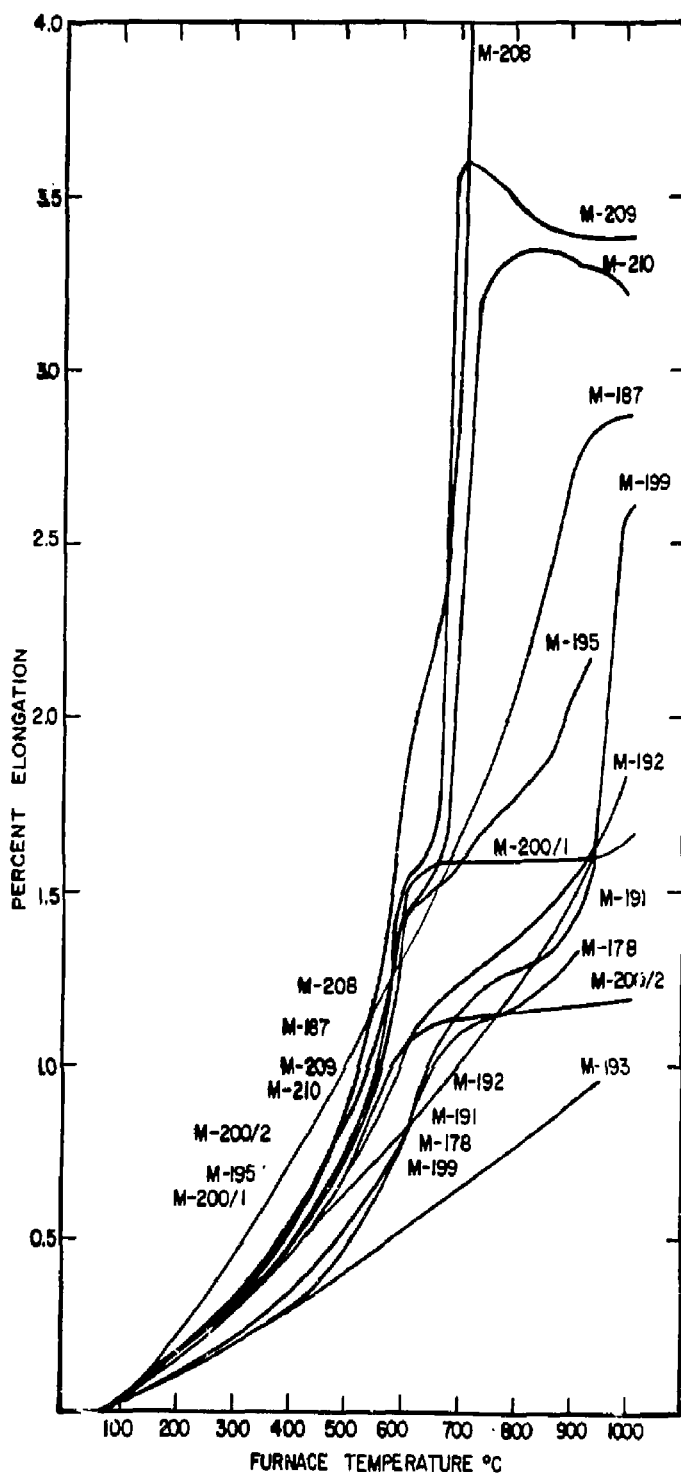
FIGURE 1-29 Average linear expansion of rocks of good
and fair pierceability
Source: Clark et al, 1969 and Geller et al, 1962.

1-97

was tested at 240° C in a dry nitrogen atmosphere, the
compressive strength was about 20,000 psi. If the atmos-
phere is now changed to a saturated water vapor and the
tests redone, the strength drops to about 6,000 psi. Unfor-
tunately, at present there is relatively little test data
available on the effect of environmental conditions on the
strength of various rocks. This, however, can be an
extremely important consideration in evaluating the long-term
competence of a repository.

TABLE 1-18. Compression tests on granite.

(Machine loading rate - 5 mils/min)

Prior Treatment	Test Temperature	Test Atmosphere	Average Failure Stress, MPa
60 hours in saturated steam (240°C, 345MPa)	25°C	saturated water vapor	151.7
None	240°C	dry nitrogen	135.9
None	240°C	saturated water vapor	41.4
None	25°C	saturated water vapor	162.1
None	-195°C	liquid nitrogen	257.9

SOURCE: Charles, 1959.

1.14 OTHER CONSIDERATIONS

To date, most of the studies have been performed using rock
types which are considered to be "homogeneous and isotropic."
The assumption is made that average properties do not vary
markedly from point-to-point within the rock mass, and that
they do not vary substantially with respect to orientation.
This is borne out by a number of experimental investigations
carried out in the laboratory. Table 1-19 shows the results
of tests made on a number of samples taken at various orienta-
tions from a block of Stripa granite., It is noted that
Young's modulus, wave velocity, compressive strength, and
density are relatively insensitive to orientation. Table
1-20, however, presents the results of another set of ex-
periments that were done on a gneissose granite. Therefore,
there are some rock masses for which directional properties
must be considered.

Because of the very long time frame that one must be con-
cerned about repository behavior, it is important to con-
sider the effect of creep on rock strength and rock behavior.
Although there has been a considerable amount of information
collected on the behavior of salt and salt-like materials,
relatively little work has been done on the creep relationship

TABLE 1-19. Small-scale anisotropy test results.

Specimen number	Density	C_1 Wave velocity		Youngs modulus		C_c
			mean		mean	
	(kg/m^3)	(m/s)	s.d.	(GPa)	s.d.	(MPa)
B1.1	2616.9	5164.2	5180.3	66.8	64.9	227.4
B1.2	2616.9	5196.3	±16.1	63.0	±2.0	81.2
B2.1	2614.4	5268.8	5240.9	65.8	65.8	237.2
B2.2	2609.8	5213.0	±27.9	64.6	±0.6	227.4
B3.1	2613.8	5310.1	5311.1	64.4	65.5	207.6
B3.2	2616.3	5312.1	±1.0	66.6	±1.2	233.9
B4.1	2617.8	5353.5	5831.6	64.4	65.7	131.2
B4.2	2619.7	5409.7	±28.1	67.0	±1.4	234.3

SOURCE: Swan, 1978

Table 1-20 Summary of Anistropic Properties of Granite

Site	Gallery	Fig. No.	Moduli of elasticity, GPa				Ultimate strength, MPa				Ratio $r=\dfrac{e}{e_1}$	Value of determinant 10^{-9} $|D|$
			Semi-axes			maximum anisotropy	Semi-axes			maximum anisotropy		
			A	B	C	e	A_1	B_1	C_1	e_1		
Alvarenga	G 4L	2	76.9	42.9	30.3	2.54	126.8	132.6	99.8	1.33	.1.91	16.4
	G 6L	3	37.8	17.5	24.3	2.16	46.4	84.2	56.7.	1.82	1.19	15.6
Alto Lindoso	G 1R	4	37.4	48.3	30.4	1.59	112.5	108.8	123 ⌐	1.14	1.39	27.1
	G 2L	5	49.9	36.2	28.5	1.75	125	117.7	125.6	1.07	1.64	35.2
	G 4R	6	26.5	34.2	41.3	1.56	74.6	110.2	99.0	1.48	1.05	21.5
Vilarinho	G12R	7	48.1	42.3	38.3	1.25	132.7	123.8	109.8	1.21	1.03	23.5
	G14L	8	48.6	34.6	36.3	1.41	134.6	101.5	96.8	1.39	1.01 ...	21.9
			average maximum anisotropy			1.75	average maximum anisotropy			1.35	1.31	

Source: Rodrigues (1970)

for hard rocks, such as granite. Stress-time and strain-time relationships for westerly granite are presented in Figures 1-30 and 1-31. In Figure 1-30, it is observed that over a period of from 25 to 250 hours the strength of westerly granite decreased from about 31,000 psi to 27,000 psi. From the data, it is not clear whether the strength will continue to decrease, or if it will reach some plateau. This is extremely important when evaluating long-term behavior. For westerly granite samples under a constant load of 26,630 psi, (Figure 1-31) the strain increased rather rapidly, then increased at a constant rate which changed into tertiary creep, and the sample finally failed. Table 1-21 is a summary of creep data collected at room temperature for two granites and one granite diorite. Note that the strain is related to the stress raised to an exponent varying between 1 and 1.3. Although important, the collection of good creep data is extremely difficult, due to the very long time frames involved and the sophistication of equipment necessary to provide the control of loading. Present data are insufficient to incorporate creep into predictive models for hard rock repositories.

There are some other factors which should be considered in evaluating geomechanical aspects of repositories in granite. One factor is the behavior of rock under cyclic loading conditions. The rock mass itself will undergo a heating and
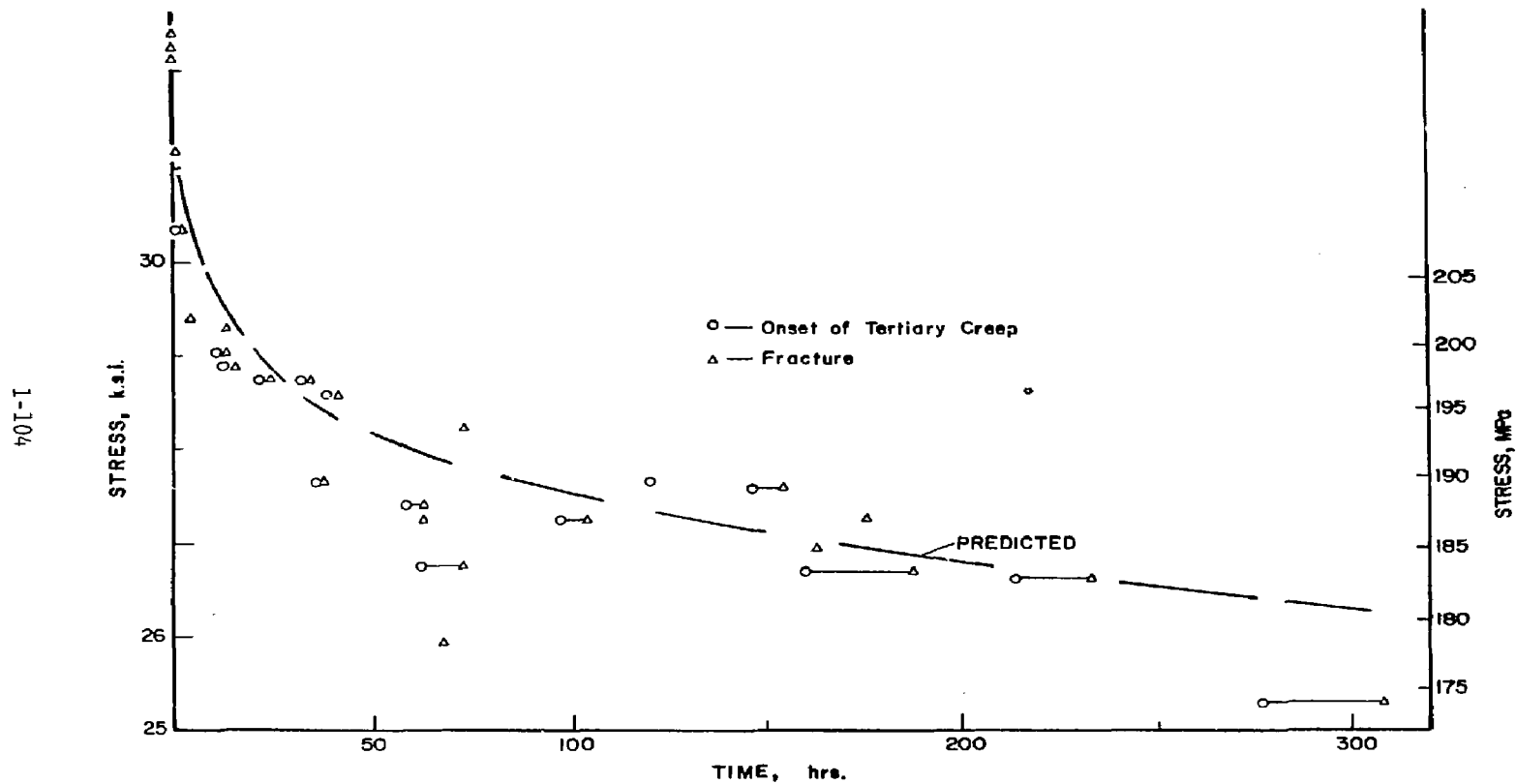
FIGURE 1-30 Strength-time relationship for Westerly granite
Source: Wawersik, 1974.
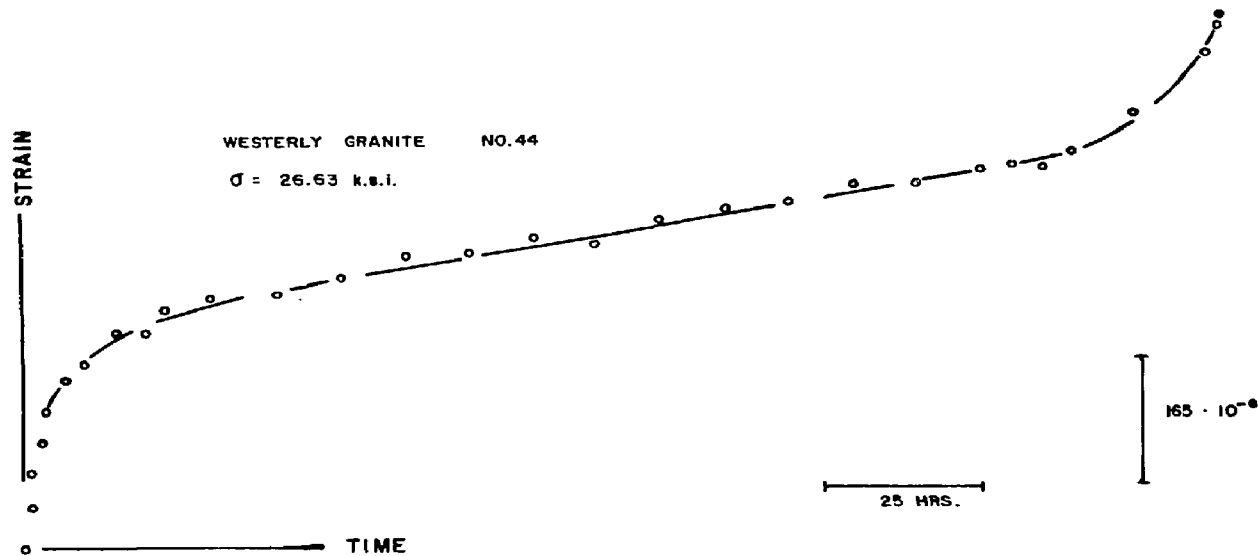
FIGURE 1-31   Typical creep curve of water-saturated Westerly granite
Source: Wawersik, 1974.

TABLE 1-21. Values of the exponent n in the equation $\varepsilon = A\sigma n$ in the creep of granites and a granodiorite at room temperature (Robertson, 1964)

Rock Type	Maximum Strain $(10^{-3}cm/cm)$	Maximum Stress MPa	Hydrostatic Pressure MPa	Exponent n	Reference
Granite	1	355	0	3.3	
Granite	0.08	101	0	2.1	Matsushima (Ref. 29)
Granodiorite	0.2	10.1	0	1.0	

SOURCE: Office of Waste Isolation, 1978

then a cooling phenomenon and the effects of this cycling
are not necessarily reversible. Very little information
exists at present regarding this phenomenon. Rock materials
may also weaken due to radiological or chemical effects.

The discussion to this point has focused primarily on intact rock samples. It is well known, however, that in underground excavations it is not the intact rock that causes problems, but rather the discontinuities, such as jointing, faulting, dikes, etc. There are many ways of trying to incorporate such discontinuities into a design. One method is to model individual features and to describe them in terms of joint stiffnesses, both normal and shear. Another approach is to treat the entire rock mass as a continuum, but to reduce the modulus, strength and other properties obtained in the laboratory for intact rock. The most common approach is to take laboratory properties and apply some sort of scale factor to them to obtain a first estimate of the field properties.

Table 1-22 (ONWI, 1978) is a comparison of rock properties for generic granite. One column is for intact rock, and the adjacent one is for the rock mass. In comparing these two columns, one will notice differences between the intact rock and the rock mass in only three properties. They are the Young's modulus, uniaxial compressive strength, and tensile strength. All the other values are assumed to be the same between the intact rock and the rock mass. Note that Young's modulus has been reduced by a factor of 3, the

TABLE 1-22 Rock properties for a generic granite

Type of Property	Parameter	Intact Rock	Rock Mass	MKS Units
Index	Unit Weight	2643.3	2643.3	kg/m^3
	Natural moisture content	---	---	%
	Porosity	0.4	0.4	%
Stress-strain	Young's Modulus	50.3	17.2	GPa
	Poisson's Ratio	0.18	0.18	---
Strength	Strength Parameters			
	A	4.5	4.5	
	k	0.75	0.75	
	Uniaxial Compressive Strength	182.8	131	MPa
	Tensile Strength	6.90	0	MPa
Thermal	Coefficient of Linear Thermal Expansion	31.0	31.0	GPa

Heat Capacity

TEMPERATURE	HEAT CAPACITY
0°C	0.88 J/g-°C
100°C	0.92
200°C	0.96
300°C	1.05
400°C	1.09

Thermal Conductivity

TEMPERATURE	HEAT CAPACITY
0°C	2.86 w/m°K
50°C	2.70
150°C	2.56
100°C	2.44
200°C	2.34
300°C	2.15
400°C	1.99

Type of Property	Parameter	Rock Mass	MKS Units
Hydrological	Horizontal permeability	3.05x10^{-8}	m/min.
	Vertical permeability	3.05x10^{-8}	m/min.

SOURCE: Office of Waste Isolation, 1978

compressive strength by about 30%, and the tensile strength reduced from 6.9 MPa to 0. These figures are considered to be extremely misleading and should not be used for modeling purposes.

The apparent modulus of a rock mass can be very low under small loads since it is determined primarily by the closing of joints, etc. (Very large deformations are possible under rather low stresses.) With internal boundaries, discontinuities tend to absorb the displacement, and Poisson's ratio may actually be close to 0. The uniaxial compressive strength of cubes, for example, for some materials has been shown to vary as the inverse of the square root of the length of the side. For samples of other shapes, the strength is dependent upon the width-heighth ratio. Assuming that the values for intact rock given in the table are for samples of the order of 5 cm in diameter and 10 cm long, on this basis, the rock mass values correspond to relatively small sample sizes. The tensile strength of intact rock, as has been noted earlier, varies from 0 to some fraction, generally 1/10 to 1/20 of the compressive strength of the rock. If the tensile strength of the rock mass were really 0, it would be extremely difficult to support openings such as are created underground every day in granitic rocks.

An example cf variation in strength with size has been
provided by (Pratt et al, 1979), as shown in Figure 1-32.
Note that it would appear that there is a characteristic
length of 1/2 to 1 meter, at which strength becomes rela-
tively constant. The variation in strength with sample
size, as shown in the figure, suggests that for large samples
the strength would be,perhaps, an order of magnitude lower
than for smaller samples. The 0.5 meter characteristic
length may not be at all appropriate, when large openings
are considered, since some other characteristic discontinuity
would then be the determining factor for rock mass strength.

The modulus would be expected to follow a similar trend, as
it is closely related to compressive strength. Figure 1-33
shows the relationship between the insitu modulus and the
number of fractures which were observed in the core. As can
be seen, there is a rather strong correlation between the
number of fractures and the modulus, with the modulus
decreasing as the fracture number increases. Figure 1-34
shows insitu modulus results for Stripa. These tests were
conducted in 3.8 cm diameter holes drilled into +he rock
mass. The volume of rock influenced by the test was rela-
tively small, although much greater than what would be
experienced in testing the core taken from the same hole.
Note that the average insitu modulus for the relatively
small volume was on the order of 1/2 of the laboratory
value.
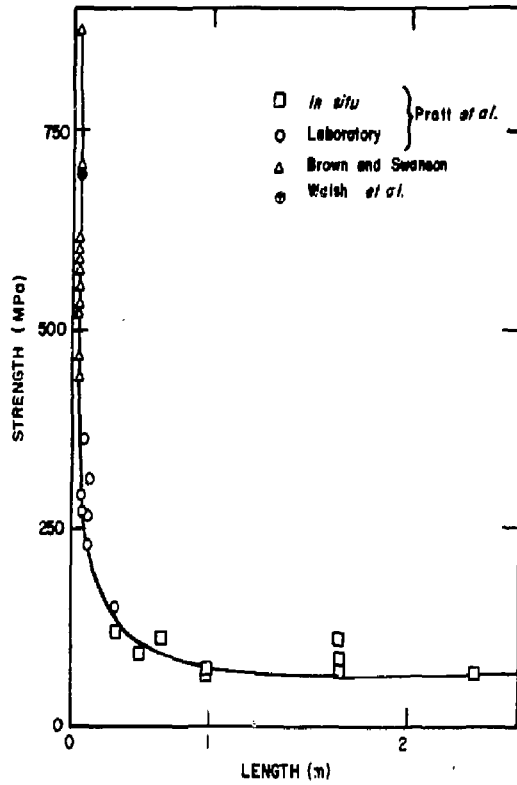
FIGURE 1-32 A diagram illustrating the effect of size on the
uniaxial compressive strength of quartz diorite
Source: Pratt et al, 1972.
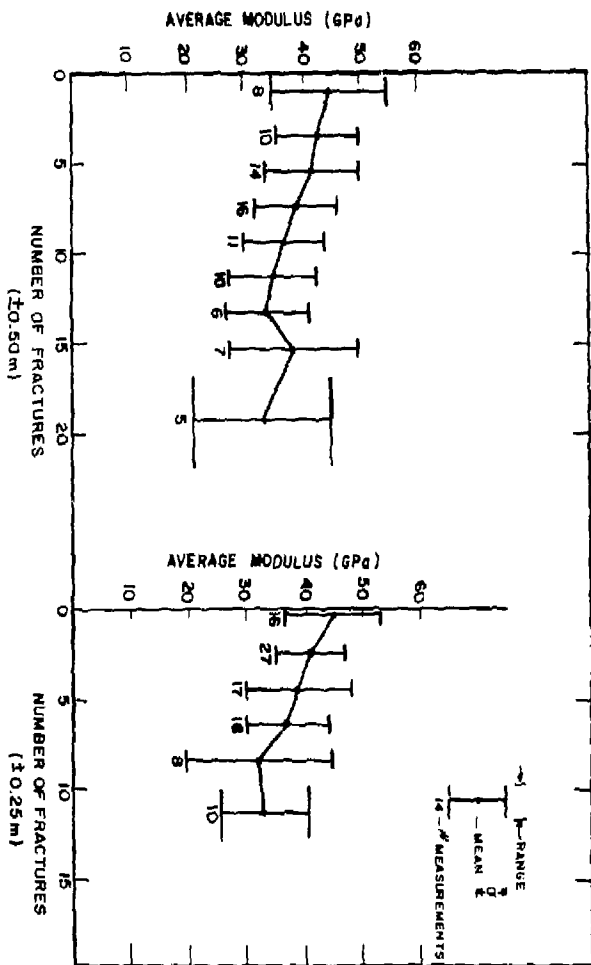
FIGURE 1-33 Insitu Young's modulus determinations versus
fracture density from visual inspection of core
Source: Nelson et al, 1979.

1-113

CSM CELL-MODULUS MEASUREMENT DISTRIBUTION
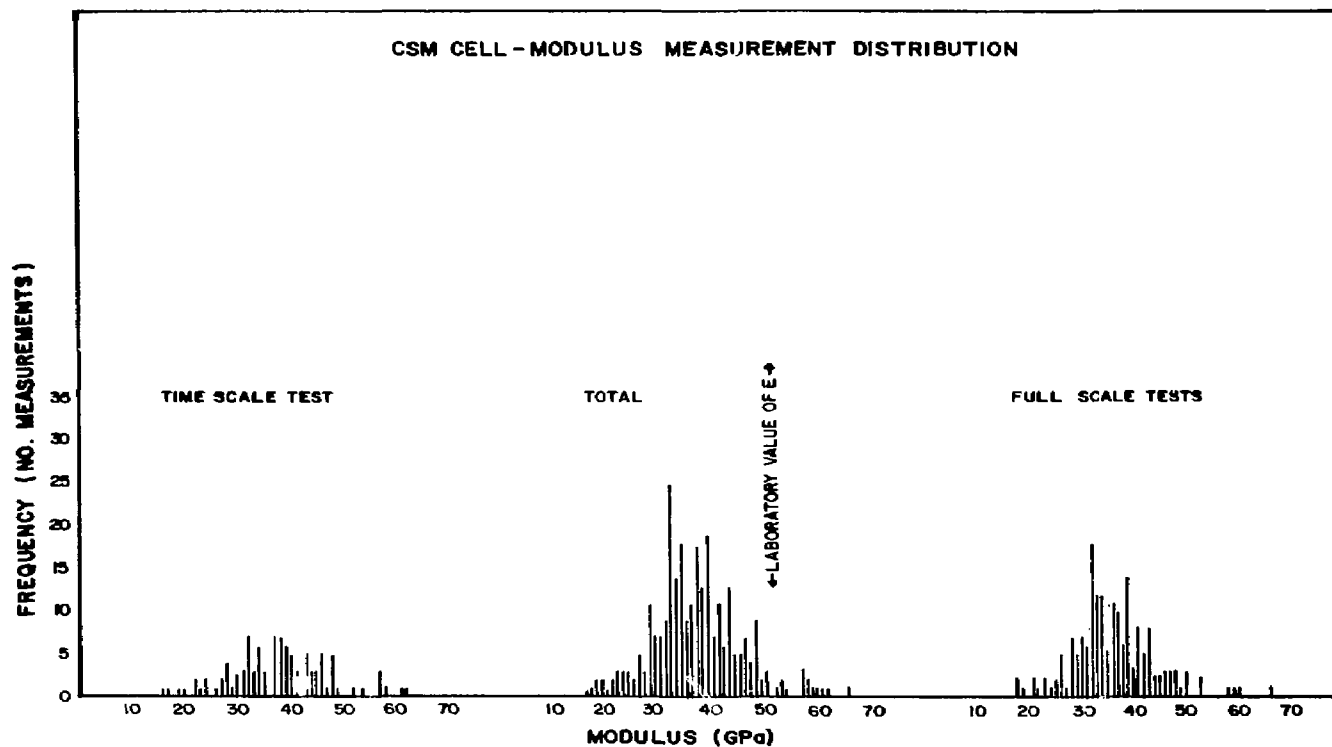
FIGURE 1-34   Histograms of CSM-cell determinations of Young's modulus
Source: Nelson et al, 1979.

Due to this problem of not being able, at the present time, to assess insitu properties from tests performed on small samples of rock, a number of insitu test experiments are either underway or planned at Stripa. The purpose of such experiments is to gather thermal and mechanical data appropriate for loading conditions similar to those which would be expected in an actual repository. Models are being prepared for predicting the field behavior. Of crucial importance is how well the input parameters describe the actual field situation.

The initial predictions will be made using laboratory values for thermal conductivities, specific heat, density, thermal diffusivity, coefficient of linear expansion, Poisson's ratio, and Young's modulus such as those given in Table 1-23. which were applied at Stripa, or some modified scaled laboratory values might be appropriate. The problem in the latter case is justifying the scaling values which are used for the initial approximation. The procedure is to compare predicted values with those actually measured and then to (a) revise the estimate of the input parameters so that agreement is reached between predicted and experimental and/or (b) reevaluate the form of the model which is used. If the initially predicted and actual field results do not agree, the input parameters are then scaled to those required to achieve agreement. Model verification and validation can then only be evaluated by

TABLE 1- 23   Laboratory values for stripa granite
used in the simulations

Thermal conductivity   =   3.2 (W/m°C);
Specific heal   =   837 (J/kg°C);
Density   =   2600 kg/m^3;
Thermal diffusivity   =   1.47 x 10^{-6}(m^2/s);
Coefficient of linear
  thermal expansion   =   11,1 x 10^{-6}(/°C);
Poisson's ratio   =   0,23;
Youngs modulus   =   51,3 (GPa)

applying the revised model "input data" to a new loading

situation. A comparison of the theoretical predictions made

using properties collected from small intact samples and the

actual field measurements from preliminary measurements of

the Stripa Mine are shown in Figures 1-35 through 1-41. It

is observed that predicted temperatures and actual tempera-

tures based upon laboratory values for thermal conductivity,

density, diffusivity, and specific heat are very good,

suggesting that size effects on such thermal parameters may

be relatively small. As seen in Figures 1-39, 1-40 and

1-41, however, the predicted and actual displacements are

quite different, with the actual values being considerably

less than those projected.

These predictions are based upon single "average" laboratory

values for Young's modulus and the linear thermal expansion

coefficient. The initial portions of the displacement curves

differ the most with the actual curves showing essentially no

displacement for a considerable period of time. Eventually,

they follow a slope, not too unlike that predicted from

theory. This can be easily explained by the presence of

joints or other discontinuities between the measurement points

which absorb internally any displacement. They could also be

explained by non-linear Modulus-temperature and/or expansion

coefficient-temperature curves. There could, of course, be

a number of other reasons for this disparity.
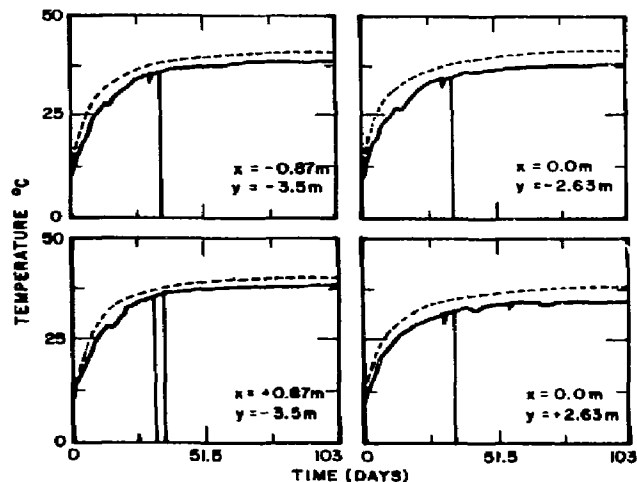
FIGURE 1-35 Curves showing the predicted and
measured temperatures as a function
of time at a radius of 0.87m from
the mid-points of the two inner-
most heaters on the y-axis
Source: Cook and Hood, 1978.

Note: The near vertical excursions
of the measured values reflect
malfunctions in the data
collection system.

■HEATER HOLES   □THERMOCOUPLE HOLES
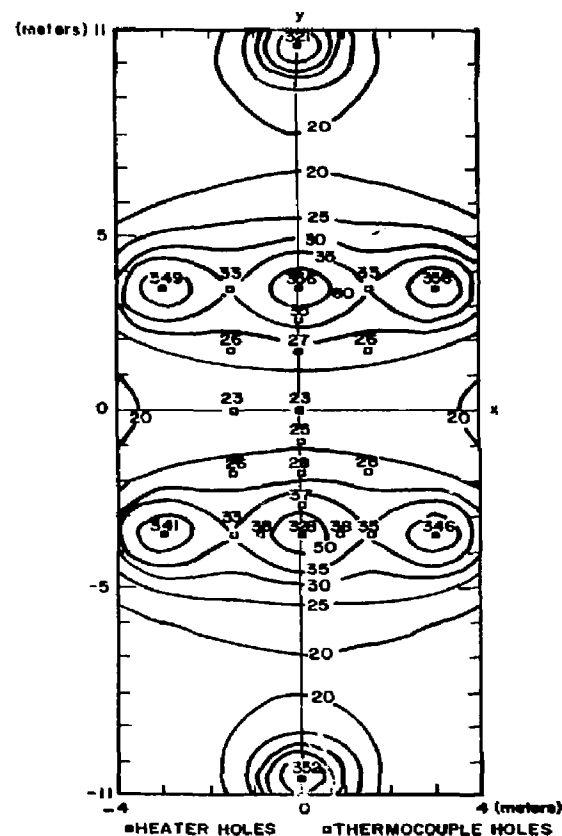
FIGURE 1-36 Predicted isotherms and measured
temperatures in a horizontal plane
through the middle of the time-scale
experiment 90 days after heating had
started Source: Cook and Hood, 1978.
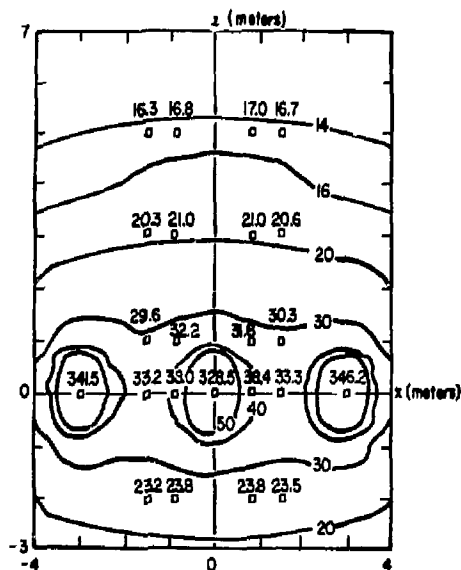
FIGURE 1-37 Predicted isotherms and measured
temperatures in a vertical plane
(y=-3.5m) containing three of the
time-scale heaters, 90 days after
heating had started
Source: Cook and Hood, 1978.
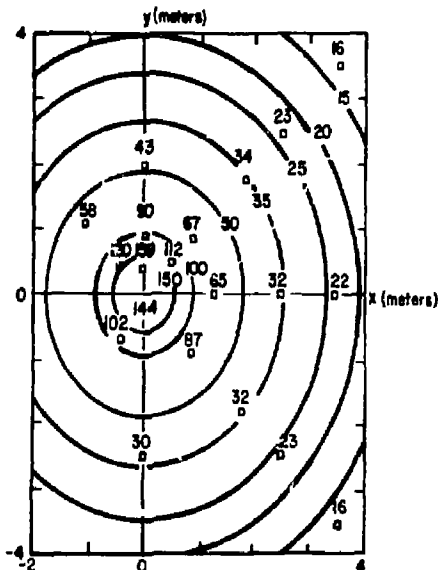
FIGURE 1-38 Predicted isotherms and measured
temperatures in a horizontal plane
through the middle of the 5 kw full-
scale heater, 65 days after heating
had started
Source: Cook and Hook, 1978.
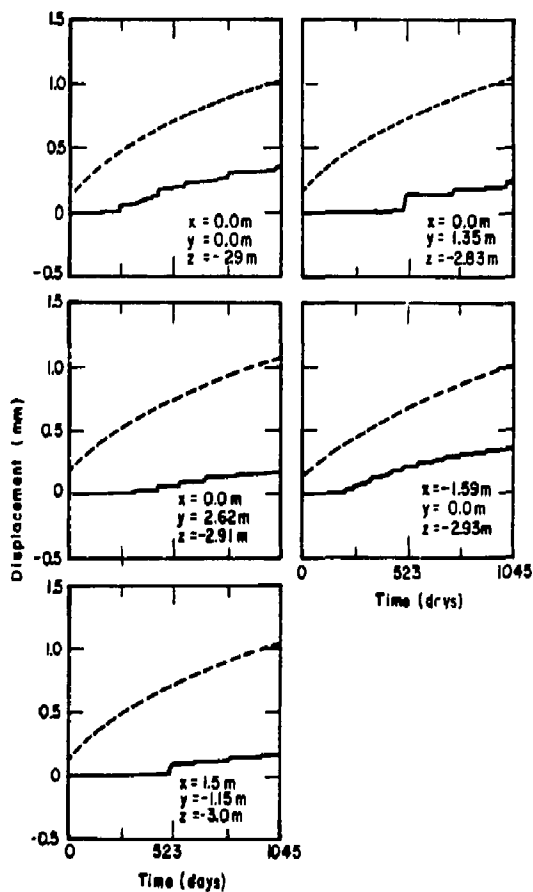
FIGURE 1-39 Predicted (dashed) and measured (solid) relative
displacements between anchor points 3m below the
heater mid-plane and the hole collars in the floor
of the time-scale drift, plotted as a function of
time Source: Cook and Hood, 1978.
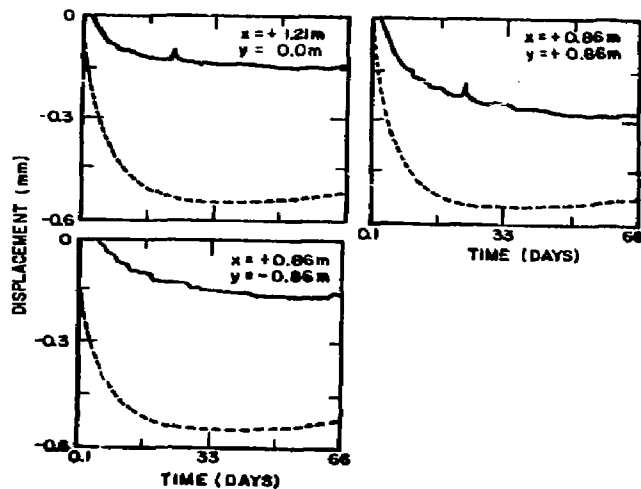
IGURE 1-40 Predicted and measured horizontal displacements of
the rock in the mid-plane of the 5 kW full-scale
heater taken along different directions.
Source: Cook and Hood, 1978.

Note: These curves show relative displacements
between anchor points at a radial distance of
1.2m from the heater and the collar of the hole
on the wall of the extensometer drift.
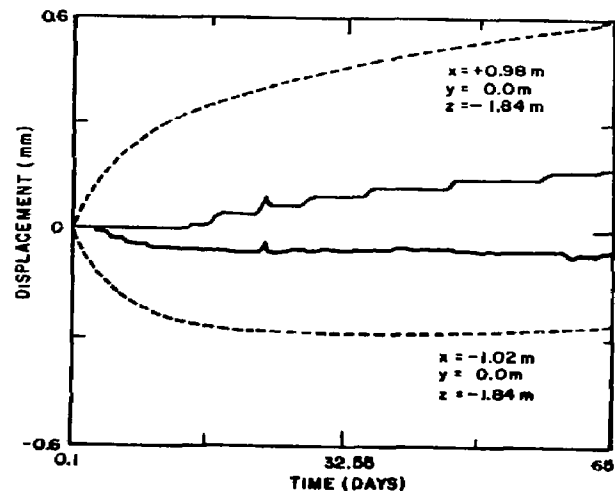
FIGURE 1-41 Predicted and measured horizontal displacements
below the 5kW full-scale heater at anchor points
symetrically positioned on each side of the
heater. Source: Cook and Hood, 1978.

Note: Both of these displacements are measured
relative tot he collar of the hole on the wall
of the extensometer drift.

The important point is that this should not be concluded as a failure of the theory to adequately predict the results. It is, rather, the inability of researchers to insert into models the appropriate rock mass parameters, whether they be mechanical paramters such as strength, density, etc.; thermal parameters, or thermoelastic parameters.

The major emphasis in the near future will be on the gathering and evaluating insitu rock mass characteristics which can be used in presently-existing models for adequately defining and explaining full-scale experiments and projected repository behavior.

1.16 REFERENCES

Abou-Sayed, A.S., and E.E. Brechtel, "Experimental Investigation
    of the Effects of Size on the Uniaxial Compressive Strength
    of Cedar City Quartz Diorite", 17th U.S. Symposium on Rock
    Mechanics, 1976.

Advani, S.H., and K.Y. Lee, "Thermo-Mechanical Failure Criteria
    for Rock Media", 20th Symposium on Rock Mechanics, Austin,
    Texas 1979.

Anderson, B., and P.A. Halen, "Mining Methods Used in the Under-
    ground Tunnels and Test Rooms at Stripa", LBL 7081, August,
    1978.

Apps, J.A., Cook, N.G.W., and P.A. Witherspoon, "An Appraisal of
    Underground Radioactive Waste Disposal in Argillaceous and
    Crystalline Rocks: Some Geochemical, Geomechanical, and
    Hydrogeological Questions", LBL 7047, June, 1978.

Balmer, G.G., "Physical Properties of Some Typical Foundation
    Rocks", U.S. Bureau of Reclamation, Concrete Laboratory
    Report Sp-39, August 13, 1953.

Barbish, A.B., and G.H.F. Gardner, "The Effect of Heat on Some
    Mechanical Properties of Igneous Rocks," Journal of Society
    of Petroleum Engineers, December, 1969.

Barton, N., "The Shear Strength of Rock and Rock Joints", IJRM,
    Sept., 1976.

Bauer, S.J., and B. Johnson, "Effects of Slow Uniform Heating on
    the Physical Properties of the Westerly and Charcoal Granites"
    20th Symposium on Rock Mechanics, Austin, Texas, 1979, pp. 7-18.

Bieniawski, Z.T., and W. L. Van Heerden, "The Significance of
    Insitu Tests on Large Rock Specimens", IJRM, April, 1975.

Birch, F., Compressibility: Elastic Constants, p. 98, in Handbook
    of Physical Constants, S. Clark, ed., Geological Society of
    American Mem. 97, 1966, 587 p.

Brace, W.F., Walsh, J.B., and Frangos, W.T., Permeability of
    Granite Under High Pressure. Jour. Geophy. Res. 73 2225 1968.

Byerlee, J.D., "Static and Kinetic Friction of Granite at High
    Normal Stress", IJRM, Nov. 1970 (international Journal of
    Rock Mechanics & Mining Sciences).

Carlsson, H., "Stress Measurements in the Stripa Granite", LBL
    7078, August, 1978.

Chappell, B.A., "Component Characteristics of Jointed Rock
    Masses", IJRM, April, 1975.

Charles, R.J., "The Strength of Silicate Glasses and Some Crystalline Oxides", Conf. on Fracture, Swampscott, Mass., April, 1959.

Charlwood, R.G., and P.F. Gnirk, "Conceptual Design Studies for a High Level Waste Repository in Igneous Rock", Storage in Excavated Rock Caverns (Proceedings of Rock Store 77), Stockholm, Sweeden, 1977, Vol. 3.

Clark, G.B., et al, "Rock Properties Related to Rapid Excavation", Final Report To Office of High Speed Ground Transportation (Contract 3-0143), March, 1969.

Cook, N.G.W., "An Appraisal of Hard Rock For Potential Underground Repositories of Radioactive Wastes", LBL Report 7004, October, 1977.

Cook, N.G.W. and P.A. Witherspoon, "Mechanical and Thermal Design Considerations For Radioactive Waste Repositories in Hard Rock", LBL 7073, October, 1978.

Cooper, H.W., and Simmons, Gene, The Effect of Cracks on the Thermal Expansion of Rocks. Earth and Planetary Science Letters 36 404, 1977.

Deere, D.U., and Miller, R.P., "Engineering Classification and Index Properties for Intact Rock", Air Force Weapons Lab Tech. Report, AFWL-TR-65-116, Dec. 1966.

Freeman, D. C., Sawdye, J.A., and F.A. Mumpton, "Mechanism of Thermal Spalling in Rocks", 11th Symposium on Rock Mechanics; Quarterly CSM, V58, N4, Oct. 1963.

Friedman, M. and b. Johnson, "Thermal Cracks in Unconfined Sioux Quartzite", 19th Symposium on Rock Mechanics, Lake Tahoe, Nevada, 1978.

Friedman, M., Handin, J., Higgs, N.G., and J.R. Lantz, "Strength and Ductility of Four Dry Igneous Rocks at Low Pressures and Temperatures to Partial Melting", 20th Symposium on Rock Mechanics, Austin, Texas, 1979.

Geller, L.B., et al, "Jet Piercing Research Project", Dept. of Mines & Mineral Survey, Mines Branch, IR 62-27, 1962.

Goetze, C., "High Temperature Rheology of Westerly Granite", J. of Geophysical Research, Vol. 76, 1971.

Goldsmith, W., Sackman, J.L., and C. Ewert, "Static and Dynamic Fracture Strength of Barre Granite", IJRM, Nov. 1976.

Griggs, D.T., Turner, F.J., and H. C. Heard, "Deformation of Rocks at 500° to 800°C", Rock Deformation, Griggs and Handin, GSA Memoir 79, 1960.

Handin, John, Strength and Ductility in Handbook of Physical Constants, S. Clark ed. Geol. Soc. America Mem. 97, 1966, 587 p.

Hanley, E.J., Dewitt, D.P., and R.F. Roy, "The Thermal Diffusivity of Eight Well-Characterized Rocks for the Temperature Range 300-1000°K", Engineering Geology, 12, 1978, pp. 31-47.

Hasan, S.E., "Thermophysical Properties of Rocks", 19th U.S. Rock Mechanics Symposium, 1978.

Herget, G., Pahl, A., and Oliver, P., "Ground Stresses below 3000 feet", Proc. 9th Can Rock Mechanics Symp., Kingston, Ontario, 1975, pp. 281-307.

Herget, G., and K. Unrug, "Insitu Rock Strength From Triaxial Testing", IJRM, Nov. 1976.

Hoek, E., and E.T. Brown, Underground Excavation Engineering, The Institution of Mining and Metallurgy, London, In Press.

Jamison, D.B., and N.G.W. Cook, "An Analysis of Measured Values for the State of Stress in the Earth's Crust", LBL 7071, Aug. 1978.

Johnson, B., Gangi, A.F., and J. Handin, "Thermal Cracking of Rock Subjected to Slow, Uniform Temperature Changes", 19th Symposium on Rock Mechanics, Lake Tahoe, Nev. 1978.

Lee, C.F., "Design of Hydraulic Tunnels in Rock For Generating Stations", Ontario Hydro (Geotechnical Engineering Dept.), Feb. 1978.

Lehnhoff, T.F., and J.D. Scheller, "The Influence of Temperature Dependent Properties on Thermal Rock Fragmentation", IJRM, 1975.

Lindner, E.N., and J.A. Halpern, "Insitu Stress: An Analysis", 18th U.S. Symposium on Rock Mechanics, 1977.

Lindroth, D.P., and W.G. Krawza, "Heat Content and Specific Heat of Six Rock Types at Temperature to 1000°C", USBM RI7503, 1971.

Lundborg, N. "The Strength - Size Relation of Granite", IJRM, July, 1967.

Mahtab, M.A., Ratigan, J.L., D.R. McCreath, "Stability of Radio-active Waste Repository in the Canadian Shield", 18th U.S. Symposium on Rock Mechanics, 1977.

Mirkovich, V.V., "Experimental Study Relating Thermal Conductivity to Thermal Piercing of Rocks", IJRM, May, 1968.

Nelson, P., et al, "Preliminary Report on Geophysical and Mechanical Borehole Measurements at Stripa", LBL 8280, May 1979.

Office of Nuclear Waste Isolation (ONWI), "Technical Support for GEIS: Radioactive Waste Isolation in Geologic Formations - Volume 5, Baseline Rock Properties, Granite", Y/OWI/TM-36/5, April, 1978.

Parson, Brinckerhoff, Quade and Douglas, Inc., "Thermal Guidelines for a Repository in Bedrock", Y/OWI/SUB-76/16504, Sept. 1976.

Perami, R., "The Formation of Microcracks in Rocks as a Result of Temperature Variations-(In French)", Proceedings Int. Symp. on Rock Fracture Nancy, France, 1971.

Pratt, H.R., et al, "Elastic and Transport Properties of an Insitu Jointed Granite", IJRM Jan, 1977.

Pratt, H.R., et al, "The Effect of Specimen Size on the Mechanical Properties of Unjointed Diorite", IJRM, July, 1972.

Pratt, H.R., Black, A.D., and W.F. Brace, "Friction and Deformation of Jointed Quartz Diorite", Proceedings Third Int. Cong. on Rock Mechanics, Denver, Colo. 1974.

Ramspott, L.D., et al, "Technical Concept for a Test of Geologic Storage of Spent Reactor Fuel in the Climax Granite, Nevada Test Site", UCRL-52796, June 15, 1979.

Richter, D., and G. Simmons, "Thermal Expansion Behavior of Igneous Rocks", Int. Journal of Rock Mechanics and Mining Science, VII, p. 403-411, 1974.

Robertson, E.C., "Viscoelasticity of Rocks", State of Stress in Earth's Crust (Santa Monica Conference), Elsevier, New York, 1964.

Rodrigues, F.P., "Anisotropy of Granites", 2nd Int. Congress on Rock Mechanics, Belgrade, 1970.

Schock, R.N., and H.C. Heard, "Static Mechanical Properties and Shock Loading Response of Granite", JGR, V. 79, n11, pp. 1662-1666, 1974.

Schock, R.N., Heard, H.C., and D.R. Stephens, "Stress-Strain Behavior of a Granodiorite and Two Graywackes on Compression to 20 kilobars", JGR, V78, n26, pp. 5922-5941, 1973.

Simmons, G. and H.W. Cooper, "Thermal Cycling Cracks in Three Igneous Rocks", Int. Journal of Rock Mechanics and Mining Science, V. 15, 1978.

Skinner, B. J., "Thermal Expansion", Handbook of Physical Constants, Memoir 97, GSA, 1966.

Swan, Graham, "The Mechanical Properties of Stripa Granite", LBL 7074, August, 1978.

Thirumalai, K., "Rock Fragmentation by Creating a Thermal Inclusion with Dielectric Heating", USBM RI7424, 1970.

Touloukian, Y.S., Thermophysical Properties of Matter, V12: Thermal Expansion 1975.

Tsui, K.K., "A Study on the Thermomechanical Stability of Rock Caverns", Report No. 78239, Ontario Hydro (Geotechnical Engineering Dept.), 1979.

Tullis, J., and R.A. Yund, "Experimental Deformation of Dry Westerly granite", JGR, Vol. 82, n 36, pp. 5705-5718, 1977.

Van der Molen, I., A Note on the Thermal Expansion of Granite at High Pressure and on the Associated Shift in the A-B Transition of Quartz, Ph.D. Diss., Australian Nat. Univer., Canberra, 1979.

Wawersik, W. R., "Time - Dependent Behavior of Rock in Compression", Proceedings Third Int. Cong. on Rock Mechanics, Denver, Colo., 1974.

Wingquist, C.F., "Elastic Moduli of Rock at Elevated Temperatures", USBM RI7269, 1970.

Witherspoon, P.A., et al, "Rock Mass Characterization For Storage of Nuclear Waste in Granite", LBL 8570, Feb. 1979.

Wong, T.F., and Brace, W.F., Thermal Expansion of Rocks: Some Measurements at High Pressure, Tectonophysics (in press), 1979.

Wu, F.T., and L. Thomsen, "Microfracturing and Deformation of Westerly Granite Under Creep Condition", IJRM, June, 1975.

HYDROLOGY OF GRANITES

1.17 INTRODUCTION TO HYDROLOGY OF GRANITES

Contact of radioactive waste with ground waters and subsequent
transport by ground waters is thought to be one of the few ways
radioactive materials in a repository may communicate with the
biosphere. Consequently, accurate identification of those para-
meters controlling ground water flux and velocity coupled with
representative modeling and field testing of the ground water
environment is critical to the identification of appropriate
repository sites. A summary of measured values for various hydrologic
parameters may be found in Appendix A.

This section begins with a discussion of the fundamentals of ground-
water flow through porous media. Presented is a discussion of ground-
water flow through single fractures, fracture networks, and regional
flow systems. The section is concluded with a summary of the effects
of temperature on the hydraulic characteristics of a rock mass and
a discussion on hydraulic dispersivity.

1.18 FUNDAMENTALS OF GROUND WATER FLOW

Ground water flow through both intergranular and fractured media
is based upon the same fundamental concepts. To understand flow
in either medium, it is necessary to be familiar with Darcy's law,
the various methods of presenting permeability and porosity and
the equations leading up to the general equation of flow in
isotropic homogeneous materials.

Darcy's Law and Permeability

The fundamental relationship describing flow through a porous media
is Darcy's law. This law is an empirical relationship which describes
laminar flow through an isotropic and homogeneous medium. In its
simplest form, Darcy's law describes ground-water flow as follows:

$$Q = KA \frac{dh}{dl}$$

where:

Q is rate of flow (m^3/sec)

A is the cross sectional area of the medium (m^2)

K is hydraulic conductivity (m/sec)

$\frac{dh}{dl}$ is hydraulic gradient (non-dimensional)

Hydraulic conductivity is a measure of the ability of a fluid at a
specific temperature to pass through a medium. It is a function of
properties of the medium as well as of the viscosity and specific
weight of the fluid. Many ground water texts utilize hydraulic
conductivity with the assumption that the fluid is water at a

temperature of $20^{\circ}C$. In applications where fluid parameters are not constant, some authors prefer to utilize intrinsic permeability (k), expressed in units of m^2. Intrinsic permeability is a function of medium properties and is independent of properties of the fluid. Intrinsic permeability is related to hydraulic conductivity by the following relationship:

$$K = \frac{kg}{\nu}$$

where:

g is acceleration of gravity (m/s^2)

ν is kinematic viscosity (μ/ρ in cm^2/sec)

ρ is fluid density (g/cc at specific temp)

μ is absolute viscosity (g/cm. sec.)

Another related parameter, transmissivity, is often utilized in discussions of ground water movement. Transmissivity, expressed in units of area per unit time (l^2/t) is defined as the rate at which water of a prevailing kinematic viscosity is transmitted through a unit width of the entire aquifer under unit hydraulic gradient. Transmissivity (T) is related to hydraulic conductivity as follows:

$$T = Kl \qquad (1-3)$$

where:

l is aquifer thickness

Porosity and Storativity

Total porosity is defined as the ratio of the aggregate volume of interstices in a rock to its total volume. Included in the determination of true porosity are isolated vugs, microfractures and discontinuous voids which do not contribute to ground water flow.

1-131

Effective porosity is defined as the ratio of the volume of water which can be put in motion under the effect of gravity forces to the total volume of rock (Battelle, 1979). Effective porosity is that portion of the void which actively contributes to ground water flow, and consequently it is of more significance in hydrologic evaluations than is total porosity.

Closely related to porosity is aquifer storativity, which is the ability of an aquifer to retain and release waters. Specific yield (Sy) is a dimensionless measure of storativity expressed as the ratio of the volume of water which an aquifer, after being saturated, will yield by gravity to its own volume. Storage coefficient (S) is defined as "the volume of water an aquifer releases from or takes into storage per unit surface area of the aquifer per unit change in the component head normal to the surface" (Todd, 1967).

For an unconfined aquifer, the storage coefficient is equivalent to its specific yield. In a confined aquifer, water is not released by gravity drainage, but rather, storage releases are derived from the small expansion of water as the head declines and from compaction of the aquifer itself. Storage coefficients for unconfined aquifers are related to porosity and will have decimal values slightly less than porosity. Storage coefficients of confined aquifers are not directly related to porosity and may range from 10^{-3} to 10^{-6}.

Ground Water Velocity

Although hydraulic conductivity bears units of velocity (l/t), this does not represent the true rate of particle movement. Many authors utilize "Darcian velocity" in their discussions. This represents the product of the hydraulic conductivity and ground water gradient. For a material of less than unit porosity, this again is not representative of particle velocity. Darcy velocity may be obtained by dividing both sides of the Darcy relationship, $Q = KA \frac{dh}{dl}$ by area, . However, flow comes only from that portion of the area which is pore space, or $A\theta$ where θ is effective porosity. The average particle velocity is consequently the Darcy velocity divided by effective porosity:

$$V = \quad (K \frac{dh}{dl}) / \theta \qquad (1-4)$$

where:

> V is average particle velocity
>
> θ is effective porosity

The "seepage" velocity derived from this equation is a vector average velocity. It does not represent the range of particle velocities in the rock mass. Consequently, "seepage" velocity should be used only with appropriate assumptions when describing particle migration.

General Flow Equation

In order to model three dimensional flow in a homogeneous, isotropic system, a general equation describing ground water movment was developed. This equation can be derived directly from Darcy's equation

$$Q = KA \frac{dh}{dl} \qquad (1-1)$$

the equation defining storage coefficient

$$S = \frac{1}{A} \frac{dv}{dh}$$ (1-5)

where v is volume and the equation of continuity (conservation of mass)

$$\text{inflow} - \text{outflow} = \text{storage}$$ (1-6)

The general equation for unsteady state flow in a confined aquifer is:

$$\frac{\partial^2 h}{\partial x^2} + \frac{\partial^2 h}{\partial y^2} + \frac{\partial^2 h}{\partial z^2} = \frac{S}{T} \frac{\partial h}{\partial t}$$ (1-7)

or

$$\nabla^2 h = \frac{S}{T} \frac{\partial t}{\partial t}$$ (1-8)

For steady state flow or for unconfined unsteady state flow, the term $\frac{S}{T} \frac{\partial h}{\partial t}$ may be neglected (Davis and DeWiest, 1970) and the general equation becomes:

$$\nabla^2 h = 0$$ (1-9)

or Laplace's equation.

This equation, or modifications of it, serve as the basis for many of the finite element models of ground water systems currently being utilized.

1.19 GROUND WATER FLOW THROUGH SINGLE FRACTURES

A granite chosen as a host rock for a nuclear waste storage facility
will have a groundmass with negligible permeability. The only
significant method of ground water transport through such a rock
mass will be by means of flow through unfilled fractures. Although
Darcy's law was developed from observations made on materials
with intergranular porosity, the relationship may be extended to
describe flow in a fracture in an effectively nonpermeable rock mass.
This extension of Darcy's law was first proposed in a thesis by Snow
(1965). Snow concluded that laminar flow through fractures is analogous
to flow between smooth parallel plates. Based upon this parallel plate
model, he determined that hydraulic conductivity may be expressed by:

$$K = \frac{\rho g \ (2b)^2}{12 \ \mu} \qquad (1\text{-}10)$$

where:

$2b$ is fracture aperture.

Intrinsic permeability can consequently be expressed:

$$k = \frac{g \ (2b)^2}{12 \ \nu} \qquad (1\text{-}11)$$

Now relating this back to Darcy's law, an equation describing the
flow rate per unit width in a single fracture q , can be written:

$$q = \frac{g \ (2b)^3 \ \frac{dh}{dI}}{12\nu} \qquad (1\text{-}12)$$

(Apps et al, 1979)

This relationship, demonstrating discharge to be proportioned to the
cube of fracture aperture, is known as the cube law. This law
confirms that only slight changes in aperture can cause large changes
in flow and is a key to modeling flow in a fractured aquifer.
Correspondingly, average velocity may be expressed:

$$V = \frac{g \ (2b)^2 \ \frac{dh}{dI}}{12\mu} = k \frac{dh}{dI} \qquad (1\text{-}13)$$

The area considered in determining velocity of flow is the cross
sectional area of the fracture, and the porosity of the open fracture
is unity. Table 1-24 illustrates the hydraulic conductivities and the
average velocities that result from equations 1-10 and 1-13 for a
range of apertures and assuming water at ambient conditions under a
hydraulic gradient of .001.

As flow velocities increase, roughness of the fractures will cause
turbulence and non-uniform flow within the fracture plane. Louis
and Maini (1970), Sharp and Maini (1972) and Gale (1975) have
investigated nonlinear, non-Darcian flow through an "equivalent"
aperture. The equivalent aperture will be that of a parallel plate
model having the same hydraulic behavior as the natural fracture.

Gale ran double set packer tests on single fractures in a borehole.
Utilizing a constant head, he was able to measure the rate at which
a single fracture would take water. With this information, he
utilized a form of the cube law to calculate equivalent aperture.
A summary of Gale's work, Table 1-25, shows the calculated, equiva-
lent apertures to differ with the true (measured) apertures by at
least an order of magnitude, the true aperture being larger. Because
roughness of fracture walls and non-uniform flow within the fracture
plane are very difficult to evaluate directly, the concept of equiva-
lent apertures is very significant in current approaches to modeling.

Table 1-24. Hydraulic conductivity and velocity for
water flowing through a single fracture

Aperture b microns	Hydraulic Conductivity, K $m.sec^{-1}$	Effective velocity, v	
		$m.sec^{-1}$	$km.year^{-1}$
0.1	8.2×10^{-9}	8.2×10^{-12}	2.6×10^{-7}
1.0	8.2×10^{-7}	8.2×10^{-10}	2.6×10^{-5}
10.0	8.2×10^{-5}	8.2×10^{-8}	2.6×10^{-3}

Source: Apps et al, 1968

TABLE 1-25. Fracture data and equivalent fracture apertures
for selected fractures at Sambro, Nova Scotia.

Fracture Depth		Aperture estimated from Borehole periscope log (m)	Excess Hydraulic Head (m)	Flow Rate (cfs)x10^{+3}	Calculated Equivalent Apertures (m)
Model (m)	Borehole (m)				
3.05	2.85	.030 - .024	.14	4.46	.0011
3.96	·..020	.0030 - .0061	3.8	.98	.00021
			5.28	1.12	.000207
5.03	5.063	.0015	15.7	.027	.00004
			22.9	.45	.00009
6.10	6.117	.0015 - .0030	1 77	.67	.00026
			4.02	1.29	.00024
			7.59	1.56	.00021
8.53	8.806	.0015 - .0030	6.05	1.29	.000207
			12.7	1.87	.00019
10.2	7.315	.0015	3.097	.003	.000034
			7.251	.005	.000030
12.2	12.50		7.102	0.001	.000046

SOURCE: Gale, 1975

1.20 FRACTURE NETWORKS

Many parameters have a bearing on the rate of ground water flow
through a fracture network. Fracture spacing, aperture sizes,
orientation, and continuity are among the most significant factors.
Also of importance is the roughness of fracture walls, wall coatings,
fracture fillings and the degree of uniformity of apertures.

Joint & Fracture Systems

Early research in granitic tectonics conducted by Hans Cloos
(Kendorski and Mahtab, 1976) identified an orthogonal system of
joints which is characteristic of nearly all granitic plutons.
Cloos identified this orthogonal joint system as consisting of
Q, S, and L fracture systems.

Q-fractures or cross-joints were determined to result from
extensive fracturing parallel to the principal direction of
stress in the rock mass.

S-joints or longitudinal fractures formed parallel to the
flow lines or crystal orientation and result from failure
along the anisotrophy resulting from the flow.

L-joints are flat-lying joints resulting from variations
in vertical loading or rebound.

Although later tectonic activity may superimpose additional fracture systems on a granitic mass, nearly all possess the primary set of orthogonal joints identified by Cloos. Subsequent authors (Price, 1966), confirm the basic concepts of Cloos; however, Price proceeds to conclude that joints have little hydraulic significance. Price proposes that brittle fractures resulting from unloading and uplift are of the most significance to ground water flow.

Variation In Aperture and Fracture Spacing

Snow (1965, 1968, 197), Lewis and Burgy (1964), Uhl and Sharma (1978) and others concur that the permeability and fracture porosity of crystalline rocks decrease with depth and that the rock type is of less importance in describing these parameters than is fracture geometry. Fracture spacings are found to generally increase with depth, while fracture openings generally decrease. Snow (1968), in studies of crystalline rock at four dam sites in Colorado, found fracture spacings at the weathered surface to range from .15 to 1.2 meters and found spacings to increase to 1.5 to 4.6 meters immediately beneath this surface. Fracture spacings were found to further increase to 5 to 11 meters at depths of 61 meters. Effective apertures inferred from packer tests were observed to range from 75 to 400 microns in the upper 9 meters of the rock mass and to decline to 50 to 100 microns at depths of 15 to 61 meters as shown on Figure 1-42.
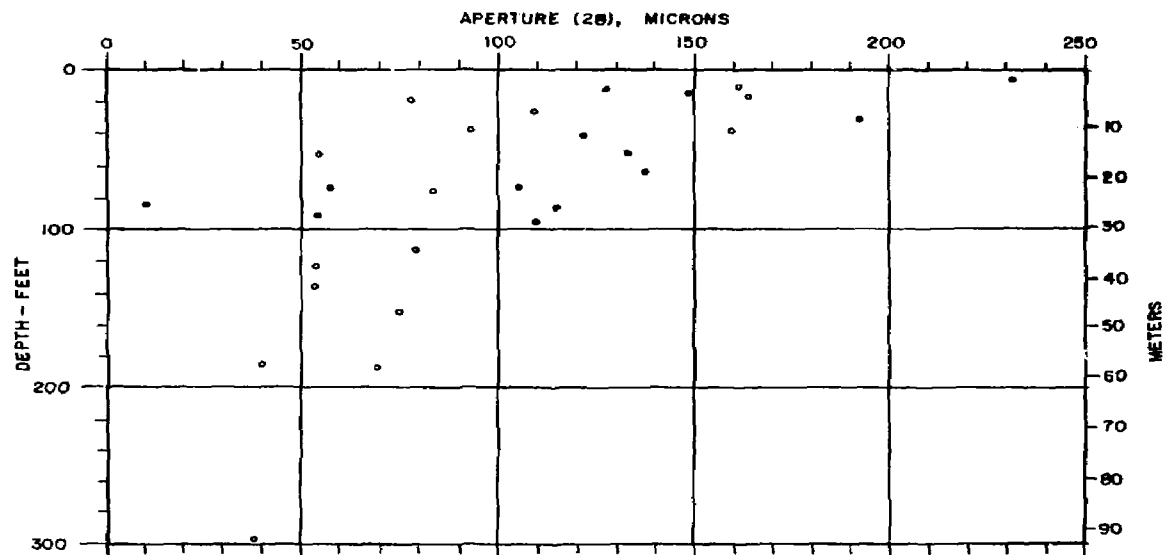
FIGURE 1-42 Fracture openings in the gneisses of
the Front Range, Colorado, computed
from injection tests
Source: Snow, 1968b.

Corresponding to the observed changes of fracture spacing and
aperture sizes with depth in Dr. Snow's studies is a decline in
both fracture porosity and permeability. Fracture porosity is
found to decline from .05% near the surface to approximately .0005%
at 122 meters, and it is generalized that fracture porosity decreases
at a rate of approximately an order of magnitude per 61 meters of
depth (Snow, 1968a). Permeability measured at equivalent depths at
the four dam sites varied; however, all followed a logarithmically
declining trend with depth.

Utilizing data from the four dam sites, Snow (1971) suggests a
technique for estimating the permeability of a fractured crystalline
rock mass. By plotting the mean permeability of each depth zone
against mean depth, Figure 1-43, and constructing a line through
these points by means of a least-square fit, Snow concludes that
permeability varies with depth relative to the following equation:

$$\text{Log } k = -8.9 - 1.67 \log d$$

where:

k is intrinsic permeability (Ft^2)

d is depth below the surface of the rock mass measured in feet

Research conducted in Sweden concludes that permeability declines
somewhat more rapidly with depth along an exponential curve (ONWI,
1978b). Laboratory work with fractured granite in artificial stress
fields (Pratt et al, 1971) correlates somewhat more closely with the
conclusions of Snow; however, this research considers only declining

1-142

10^{-14}	10^{-13}	10^{-12}	10^{-11}	10^{-10}	10^{-9}	10^{-8} Ft^2

DEPTH BELOW OVERBURDEN, FEET

METERS

KEY

1 Upper Crystal Damsite

2 Two Forks Damsite

3 Morrow Point Damsite

4 Blue Mesa Damsite

FRACTURE PERMEABILITY
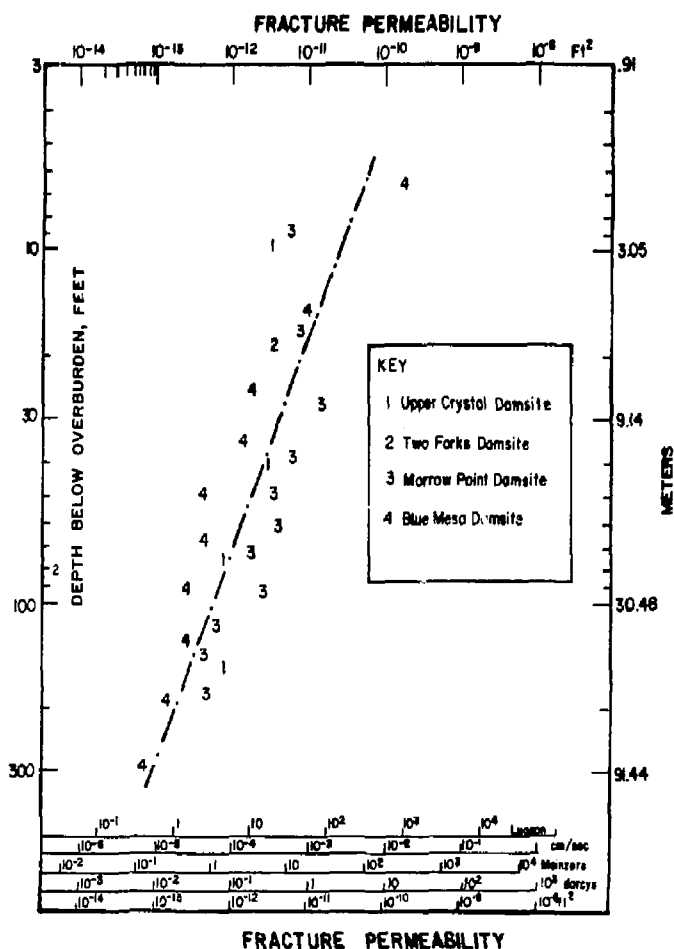
FIGURE 1-43   The mean permeability in each depth zone at 4
damsites vs the mean depth of mid-points of
test sections.   Source: Snow, 1968b.

fracture density with depth. At depths exceeding 450 meters, the validity of either relationship is uncertain. Pratt suggests that
fracture permeability asymtotically approaches a value approximately one order of magnitude greater than the permeability of the rock matrix as normal stress increases.

The fracture porosity of a rock mass with a specific permeability is dependent upon the fracture geometry and fracture aperture. Snow concludes from his work on the four Colorado dam sites that an orthogonally fractured rock mass at a specific depth with uniform fracture openings will have a porosity which is related to fracture spacing by the following relation:

$$\theta = 3(3k/2)^{1/3} (2/\Delta)^{2/3} = 5.45 (k/\Delta^2)^{1/3} \qquad (1\text{-}15)$$

where:

θ = effective porosity

k = permeability (ft^2)

Δ = fracture spacing (ft)

The apparent spacings of individual fractures within each of three assumed orthogonal sets of water bearing fractures as observed at the Colorado dam sites is summarized on Figure 1-44. In the work by Snow, it is assumed that fracture spacings are normally distributed. More recent work by Priest and Hudson (1976) suggests spacing is exponentially distributed. The effect these differences in distribution will have on resultant permeability and porosity has not been specifically evaluated.
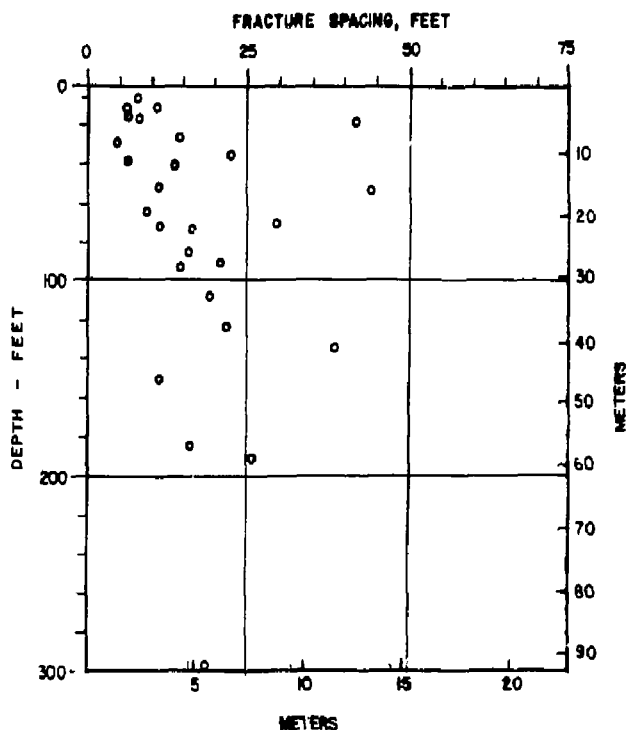
FIGURE 1-44 Apparent spacing of individuals of each
of three assumed orthogonal sets of water-
bearing fractures at four dam sites in
gneisses of the Front Range, Colorado,
computed from injection tests
Source: Snow, 1968.

Effects Of Stress On Fracture Permeability

It is generally accepted that stress can have a large effect on the permeability of rock. A decrease in permeability with depth as demonstrated by Davis and Turk (1964) and Show (1968) is often considered to be stress related. There has, however, in recent years, developed some disagreement among authors as to whether decreasing permeability with depth is due in greater degree to decreasing aperture size or increasing fracture spacing. Raven and Gale (1976) and Kendorski and Mahtol (1976) indicate aperture decreases with depth while fracture geometry remains constant. Conversely, Swedish investigators on the Stripa project conclude that fractures with significant apertures persist to depth but that spacing increases (Battelle, 1978).

Work by Iwai (1976) on man-made fractures in basalt, granite and marble generally supports the concept of decreasing aperture. Under normal stresses ranging from 0 to 20 MPa, Iwai found both aperture and hydraulic conductivity to decrease with increased stress. However, a minimum hydraulic conductivity was found to be approached asymptotically as stress was increased. Imperfect matching of opposing surfaces caused apertures to approach 15 microns as normal pressures approached 20 MPa.

Recent work by Brace (1979) to some degree contradicts the accepted concepts of declining permeability with depth. Brace assembled laboratory and in situ permeability measurements from a number of

locations and presented this data in the form of a histogram, see
Figure 1-45. Utilizing this data, Brace makes the following observations:

a) The average k of the more permeable crystalline rocks
   is about 10^3 greater than corresponding laboratory
   measurements. This variance is due in part to the
   dependence of permeability measurements on sample
   size in laboratory determinations.

b) There is a hint of decrease of permeability with depth
   but hardly enough to justify the exponential relation-
   ships suggested in the literature.

c) At nearly every site some portion of the rock sampled
   by the drill holes has a permeability of 1 to 100 md.
   This relatively permeable zone may be as deep as 3.3 km.

Given the square relationship between flow velocity and aperture size,
it is particularly critical to define, at least on a site specific
basis, the relationship between aperture size and depth.

Orientation And Continuity Of Fractures

In many fractured crystalline bodies, a variation in average aperture
with fracture orientation is observed. Given the cube relationship
between aperture and flow, it can be seen that the orientation of
large fractures with respect to the potential gradient makes a major
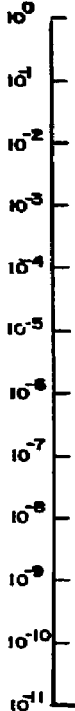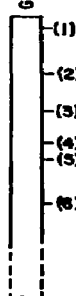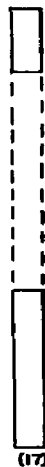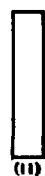
FIGURE 1-45   Summary of laboratory and insitu measurements
of permeability in crystalline rocks.
Source: Brace, 1979.

Determination No.	Rock Type
1	Laramie Granite
2	Quincy Garnite
3.	Westerly Granite
4.	Samples from Los Alamos, New Mexico
5.	Barre Granite
6.	Ontario Granites
7.	Front Range Gneiss
8.	Front Range Schist
9.	Quartzite
10.	White Lake Gneiss
11.	Metamorphics - Colorado Front Range (well tests)
12.	Crystalline rock at 38 western damsites
13.	Laramie Granite - well test
14.	Crystalline basement rock - pump test from Aiken, S.C.
15.	Stripa Granite - pumping tests
16.	Granites and Gneiss - 500 pumping tests - Sweden
17.	Lac du Bonnet batholith - pumping tests, Pinawa, Manitoba
18.	Granodiorite - pumping tests - Los Alamos, New Mexico
19.	Crystalline basement - injection tests - Rocky Mt. Arsenal, Denver
20.	Climax granitic stock - pressure decay tests
21.	Quartzite

FIGURE 45 (Cont.) Key to Rock Types

difference in ground water flow velocity and direction. The defini-
tion of orientations of fractures is critical to the determination
of anisotropic permeability.

The results of fracture mapping in many geologic environments have
shown that fractures cannot be assumed to be continuous within their
own planes (Apps et al, 1979). Continuity is the most difficult of
the fracture parameters to measure in situ. However, defining the
continuity of fractures is of prime importance in describing ground
water movement. Long duration well tests that affect large volumes
of rock and single fracture cross-hole tests are currently most widely
utilized for determinations of fracture continutiy.

Fracture Network Flow

Equations describing flow through a fracture network can be developed
from the flow equation for a single fracture:

$$V = k \frac{dh}{dI} \qquad (1-13)$$

For anisotropic conditions in a rockmass, the equation can be
modified:

$$\{V\} = [kp]\{i\} \qquad (1-16)$$

where:

    $\{V\}$ is the velocity vector

    $\{i\}$ is the potential gradient vector

    $[kp]$ is a second order tensor formed from the permeability
        terms of each fracture set.

The derivation is continued by Apps et al (1979) by defining area
permeability (kp) in terms of gradient and flow rate per unit area
(§A):

$$qA = kpi \qquad (1\text{-}17)$$

For a set of fractures with a frequency λ , the single fracture
permeability, k, can then be related to area permeability, kp, by:

$$[Kp] = 2b\nu \ [k] \qquad (1\text{-}18)$$

Assuming a uniform set of fractures oriented in the x-y plane with
aperture $2b$,

$$[Kp] = 2b\lambda \begin{bmatrix} \frac{g(2b)^2}{12\nu} & 0 & 0 \\ 0 & \frac{g(2b)^2}{12\nu} & 0 \\ 0 & 0 & \frac{g(2b)^2}{12\nu} \end{bmatrix} = \begin{bmatrix} \frac{\lambda g(2b)^3}{2\nu} & 0 & 0 \\ 0 & \frac{\lambda g(2b)^3}{2\nu} & 0 \\ 0 & 0 & \frac{\lambda g(2b)^3}{2\nu} \end{bmatrix}$$

The principal permeabilities and their orientations are the eigen-
values and eigenvectors of the permeability tensor formed from the
combination of the tensors of the individual fractures (Apps et al
1979). A detailed summary of the derivation of permeability tensors
from single fracture data may be found in Bianchi and Snow (1969).
Although k almost certainly varies with direction in rocks, principal
values of the permeability tensor are rarely given (Brace, 1979).
Network flow studies utilizing the permeability tensor are, to date,
principally theoretical and have little field conformation.

1.21 REGIONAL GROUND WATER FLOW

While fluid flow through individual fractures is well understood
and flow through fracture networks has been theoretically proposed,
ground water flow on a regional scale is only beginning to be
investigated.

Fundamental Regional Flow Characteristics

In a granite drainage basin, ground water movements will vary
laterally and vertically in the various fracture networks that
interface to allow ground water flow through the region. In general,
water will be recharged into the country rock in topographically
lower areas. In the recharge area, the direction of water movement
is principally downward, the depth of penetration depending upon
fracture geometry, continuity and numerous other geologic parameters.
Ground water flow eventually becomes roughly horizontal until a zone
of discharge is reached where the flow lines turn upward. The
distance between recharge and discharge points in a granite drainage
basin may range from only a few tens of meters to many kilometers.

In many granite drainages, the water table roughly parallels surface
topography. Water table configuration, and hence topography, often
controls the locations of recharge and discharge zones. As demonstrated
on the flow nets of Figure 1-46, the size of recharge and discharge
zones will vary depending on their position and the degree of topo-
graphic relief in the basin (Apps et al, 1978).
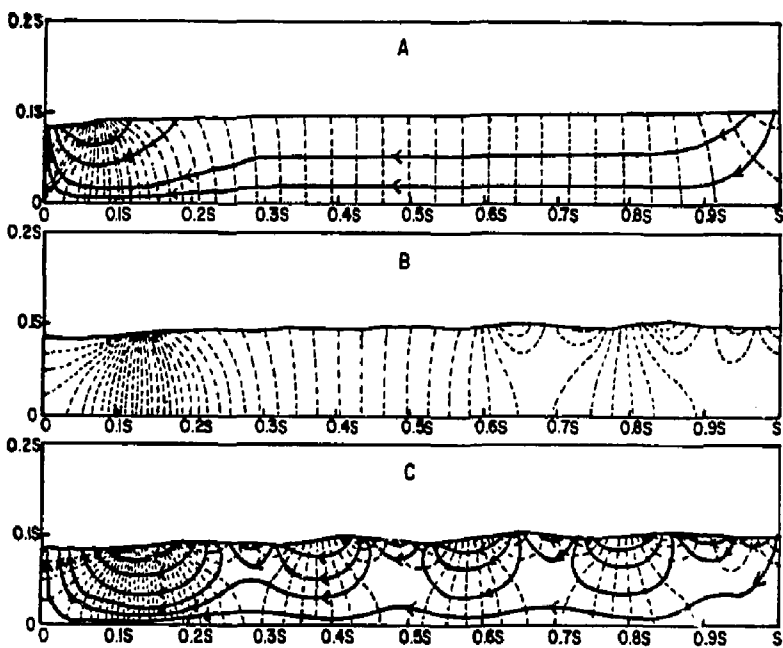
FIGURE 1-46 Effect of water-table configuration on regional
groundwater flow through homogeneous isotropic
media. Source: Freeze and Witherspoon, 1967.

1-153

Regional ground water flow may also be interrupted by geologic anomalies such as faults or shear zones. These features occur on scales from a few meters in length to tens of kilometers. If the fractures associated with these features are open, they may channelize ground waters and control the movements of both surface and ground waters within a basin. Such features have been observed carrying significant ground water flows at depths in excess of 3.5 km.(Brace, 1979) (Robinson, 1978). Often, however, faults and shear zones are filled with rubble which has undergone extensive chemical or mechanical alteration producing a clay rich material of very low permeability known as fault gouge. In areas where fractures and voids associated with faults or shear zones are filled with gouge, or other fines or precipitates, the feature may act as a barrier to ground water flow.

It is anticipated that a repository would not be sited in a granite body at a location significantly dissected by faults or shears. Rather, a repository would probably be sited in a recharge zone of a deep geologic structure with a low fracture permeability. The site should be chosen to maximize ground water flow paths to the surface and thus maximize the underground residence time of waters leaving the repository.

Layer Models Of Regional Systems

Various authors have attempted to identify different horizons in the crystalline aquifer to simplify descriptions of ground water flow. Hurr and Richards (1974) broke the aquifer down into an active zone

and a passive zone. The active zone is defined as that near-surface, weathered zone in which the water table is subject to seasonal fluctuation, and significant flows may be observed. The passive zone is defined as an underlying zone of lower permeability in which water may be stored for tens to thousands of years. In research at the Straight Creek Tunnel in Colorado, the contact between the active and passive zones was found to fluctuate in depth; however, it was identified as the point at which the seismic velocity increased from 3780 m/sec. to approximately 5400 m/sec.

In modeling studies for the Office of Nuclear Waste Isolation (1978b), three zones of saturation were considered. The upper zone was identified as that of the highest permeability, holding young waters containing both Carbon 14 and tritium. The intermediate zone was identified as that bearing water of intermediate age containing Carbon 14, but lacking tritium. The deepest and least permeable zone was identified as containing the oldest water which bears no measurable tritium or Carbon 14.

Either technique for identifying specific horizons in the crystalline aquifer can be a simplification of some assistance in modeling. However, the boundaries between these horizons are often quite gradational and difficult to specifically define in the field.

Representative Elementary Volume

Regional evaluation of ground water systems is currently often
approached by continuum modeling. This technique requires that
representative values be assigned to parameters for a finite volume
element. Consequently, some technique must be developed for
establishing representative values from field data. Bear (1972) has
proposed the concept of representative elementary volume (REV).
As illustrated on Figure 1-47, the representative elementary volume
(u_0) is that volume at which small additional increased in volume
will have no significant effect on the value of the parameter
measured.

For volumes smaller than the REV, discrete fracture effects will
influence the value of the parameter as the test volume is increased
by small increments. However, for a volume equivalent to or larger
than the REV, we move into the domain of porous media effects
(Battelle, 1979). A list and summary of some of the models currently
being utilized for regional flow analysis are presented in Battelle (1979).

Figure showing Physical parameter, n (vertical axis) versus Volume, u (horizontal axis). Labels: n_{max}, n_1, n_0 on vertical axis; u_0, u_1 on horizontal axis. "Domain of Discrete Fracture Effects" and "Domain of Porous Media" at top. "Inhomogeneous media" and "Homogeneous media" curves labeled.
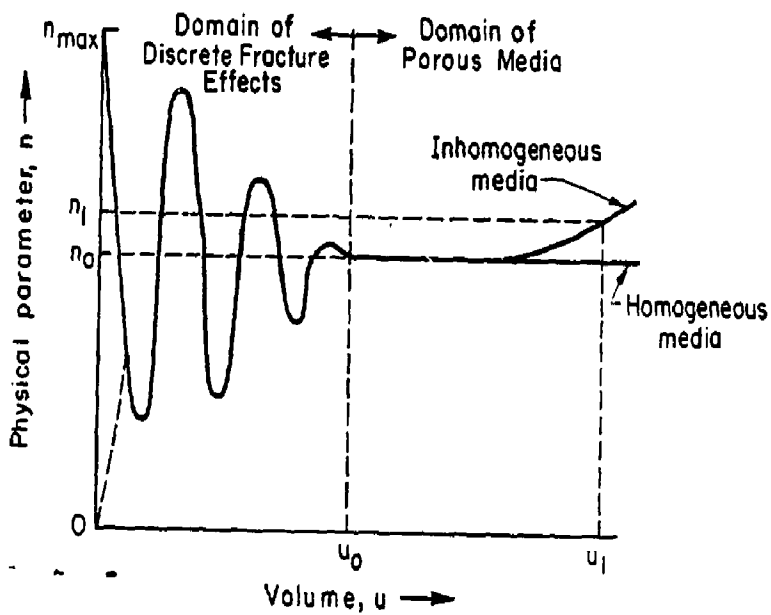
XBL 7811-6115

FIGURE 1-47   Definition of a representative elementary volume
Source: Bear, 1972

1.22 EFFECTS OF TEMPERATURE ON FRACTURE FLOW SYSTEMS

During the initial stages of repository construction and loading,
ground water movement can adequately be defined by the approach
outlined in previous sections. However, as the repository becomes
heated in later stages of its life, the rate and direction of ground
water flow may be altered. Large scale permeability tests at the
Stripa Mine Project (Lundstrom and Stille, 1978) confirmed that
permeability of the rock mass was reduced 50% as temperature was
increased from $10^{o}C$ to $35^{o}C$. This decline in permeability can
probably be attributed principally to a decrease in aperture along
fractures resulting from thermal expansion of the rock mass.

Thermal convection may also alter ground water movements in a
crystalline rock mass. In model studies conducted for the Office
of Nuclear Waste Isolation (1978), large convection cells were
predicted to develop in the country rock surrounding a repository.
However, Apps et al (1978) suggest that in fractured rocks of very
small aperture, the Rayleigh number is so large that a local heat
source is unlikely to cause natural circulatory convection. To
establish throughflow due to a buoyancy unbalance requires recharge
from a surrounding rock mass that is filled with cold ground water.
If the repository is sited in nearly impermeable rock, then the low
velocities of the regional system will restrict cold water inflow
and control overall fluid movement.

It should be noted that few, if any, large scale field studies have been undertaken to evaluate the effects of thermal convection in a granite rock mass. Most information now available is purely theoretical or is drawn from modeling studies which incorporate assumed hydraulic and thermal parameters.

1.22 REFERENCES

Apps, J.A., N.G.W. Cook, and P.A. Witherspoon, 1978, Lawrence
     Berkeley Laboratory, GAIN, "An Appraisal of Underground
     Radioactive Waste Disposal in Argillaceous and Crystalline
     Rocks: Some Geochemical, Geomechanical, and Hydrogeological
     Questions".

Apps, J., T. Doe, B. Doty, S. Doty, R. Galbraith, A. Kearns, ...
     B. Kohrt, J. Long, A. Monroe, T.N. Narasimhan, P. Nelson,
     C.R. Wilson, and P.A. Witherspoon., 1979, "Geohydrological
     Studies for Nuclear Waste Isolation at the Hanford Reservation,
     Volume II: Final Report, July, 1979.

Bear, J. 1972, Dynamics of Fluids in Porous Media, Americal Elsevier,
     New York, pp. 764.

Bear, J. and Todd, P.K., 1960, The Transition Zone Between Fresh and
     Salt Waters in Coastal Aquifers, University of California, Water
     Resources Center Contribution, No. 29.

Beissel, D.R., 1971, Geophysical studies in fractured rock. M.S.
     Theisis, Colorado State University, Ft. Collins, Colorado.

Biachi, L. and D.T. Snow, 1969. Permeability of crystalline rock
     interpreted from measured orientations and aperatures of
     fractures: Annals of Arid Zone, 8:221-245.

Brace, W.F., 1979, Permeability of Crystalline and Argillaceous.
     Rocks., Preprint Submitted to Mt. Journal of Rock Mech. and
     Min. Sci.

Bredehoeft, J.D. and G.F. Pinder, 1973, Mass Transport in Flowing
     Ground water, Water Resources Research, 9, 1.

Crosby, W.O., 1881, On the absence of joint-structure at great
     depths, and its relations to the forms of coarsely crystalline
     eruptive masses. Geol. Mag. (Decade 2). 8.

Davis, S.N., 1969, "Porosity, Permeability of Natural Materials",
     Chapter 2 of Flow Through Porous Media, Edited by R.J.M.
     DeWiest. New York: Academic Press, pp. 54-88.

Davis, S.N., and L.J. Turk, 1964, Optimum depth of wells in
     crystalline rocks. Ground Water. V. 2, No. 2, pp. 6-11.

Davis, S.N., and R.J.M. DeWiest, 1966, Hydrogeology, New York:
     J. Wiley and Sons, Inc.

DeWiest, R.J.M., 1970, Geohydrology, New York: J. Wiley and
     Sons, p. 366.

Duguid, J.O., and P.C. Lee, 1971, "Flow in Fractured Porous
     Media", Water Resources Research.

Einstein, H.H., and R.C. Hirschfeld, 1973, Model studies on
     mechanics of jointed rock, J. Soil Mech. Found Div. Amer.
     Soc. Civil Eng., V. 99, pp. 229-248.

Freeze, R. A. and P.A. Witherspoon, "Theoretical analysis of
     regional groundwater flow. 2. Effect of water-table
     configuration and subsurface permeability variation",
     Water Resources Research, Vol. 3, No. 2, pp. 623-634, 1967.

Fritz, P., J.F. Barker, and J.E. Gale,"Geochemistry and Isotope
     Hydrology of Groundwaters in the Stripa Granite", April, 1979.

Gale, J., 1975. A numerical, field, and laboratory study of
     flow in rocks with deformable fractures: Ph.D. Thesis,
     University of California, Berkeley.

Gale, J.E., and P.A. Witherspoon,"An Approach to the Fracture
     Hydrology at Stripa": Preliminary Results, May, 1979.

Gringarten,A. and P.A. Witherspoon, 1972. A method of analyzing
     pump test data from fractured aquifers: Proc. Symp. on
     percolation through fissured rocks, International Society
     for Rock Mechanics, Stuttgart.

Grove, D.D., and W.A. Beetem, 1971, "Porosity and Dispersion
     Constant Calculations for a Fractured Carbonate Aquifer
     Using the Two-Well Tracer Method", Water Resources
     Research, V. 7, No. 1.

Hurr, R.T., and D.B. Richards, 1974, "Hydrologic Investigations" in
     Robinson, C.S. et al "Engineering Geologic, Geophysical,
     Hydrologic and Rock Mechanics Investigations of the
     Straight Creek Tunnel Site and Pilot Bore, Colorado",
     U.S. Geol. Surv. Prof. Paper 815, pp. 79-88.

Iwai, K., 1976. Fundamental studies of fluid flow through a
     single fracture: PhD. Thesis, University of California,
     Berkeley.

Johnson Division, Universal Oil Products, 1972, Ground
     Water and Wells, St. Paul, Minn.

Jouanna, P., 1972, Seepage tests under stress in situ, Proceedings
     of the Percolation Through Fissured Rock, Pap. T2-G, Inter-
     national Society of Rock Mechanics, Stuttgart, Germany.

Kendorski, Francis S., and M. Ashraf Mahtab, 1976, "Fracture
     Patterns and Anistrophy of San Manuel Quartz Monzonite",
     Assoc Eng. Geo. Bull. V. XIII, No. 1.

Kendorski, F.S. and Mahtab, M. (1976) Fracture patterns and
    anisotropy of San Manuel quartz monzonite. Assoc. Eng.
    Geologists 13.

Kranz, R.L., A.D. Frankel, T. Engelder, C. H. Scholz,"The
    Permeability of Whole and Jointed Barre Granite,"Pergamon
    Press Ltd., 1979, Printed in Great Britain.

Lachenbruch, A.H., 1961, Depth and spacing of tension cracks.
    Jour. Geophys. Research, 66.

Lewis, D.C. and R.H. Burgh, 1964, Hydraulic characteristics
    of fractured and jointed rock. Ground Water, Vol. 2,
    No. 3, pp.4-9

Lohman, S.W., 1972, "Ground-water Hydraulics", USGS PRof Paper
    708, Gov. Printing Office.

Louis, C. and M. Pernot, 1972. Three dimensional investigation
    of flow conditions of Grand Maison damsite: Symp. on
    Percolation through fissured rocks, International Society
    for Rock Mechanics, Stuttgart.

Louis, C. and T. Maini, 1970. Determination of in situ hydraulic
    parameters in jointed rock: Congress International Society
    for Rock Mechanics, Belgrade, Vol. 1.

Lundstrom L. and Stille H, 1978, Large scale permeability
    test of the granite in the stripa mine and thermal
    conductivity test, Lawrence Berkley Laboratory, Berkley,
    California.

Maini, T. and G. Hocking, 1978. An examination of the feasibility
    of hydrologic isolation of a high level waste repository
    in crystalline rock: International Journal of Rock
    Mechanics and Mineral Engineering, in press.

Maini, Y.N.T., 1971, In situ hydraulic parameters in jointed
    rock: Their measurement and interpretation, Ph.D
    thesis, Imperial College, London.

Marine, I.W., 1965, Correlation and water-transmitting properties
    of fractures. AIME, Soc. Petrol. Engrs. Preprint paper
    no. SPE 1280, 7 pp.

McWhorter, David B. and Daniel K. Sunada, 1977, Ground-water
    Hydrology and Hydraulics, Fort Collins, Co. Water Resources Pub.

Office of Nuclear Waste Isolation (ONWI),1978, Technical
    Support For GEIS: Radioactive Waste Isolation In
    Geologic Formation, Vol. 5, Baseline Rock Properties
    Granite, Y/ONWT/TM-36/5.
——1978, Vol. 21, Ground Water Movement and Nuclide Transport,
    Y/ONWI/TM-36/21.
——1979, Geotechnical Assessment and Instrumentation
    Needs for Nuclear Waste Isolation in Crystalline
    and Angillaceous Rocks, Symposium Proceedings,
    July 16-20, 1978

Pinder, G.F., 1973, A Gelerkin Finite-Element Simulation of
    Ground Water Contamination on Long Island, New York,
    Water Resources Research, 9, 6.

Pratt, H.R., and H.S. Swolfs, W.F. Brace, A.D. Black, and J.W.
    Handin, 1977, Elastic and transport properties of insitu
    jointed granite, Int. J. Rock Mech. Mining Sci., 14, 35-45,
    ——1971, Insitu and Laboratory Measurements of Velocity and
    Permeability.

Price, N. Fault and Joint Development in Brittle Rock, Pergamon,
    1966.

Priest and Hudson, Discontinuity Spacings in Rock, Int. Journ.
    of Rock Mechanics and Min. Sci., V. 13, pg. 135 (1976).

Proctor, J.F., and I.W. Marine, 1965, Geologic, hydrologic, and
    safety considerations on the storage of radioactive wastes
    in a vault excavated in crystalline rock. Nuclear Science
    and Engineerin. vol. 22, pp. 350-365.

Rasmussen, W.F., 1963, permeability and Storage of Heterogeneous
    Aquifiers in the U.S., International Association of Sci.
    Hydrology, Publication 674, pp. 317-325.

Raven, 3., and Gale, J. (1976) Evaluation of structural and
    groundwater conditions in underground mines and excavations
    in Subsurface containment of solid radioactive wastes.
    Progress report EMR/GSC-RW Int. Rept. No. 1/76. Library
    Geological Survey of Canada, Ottawa, Canada.

Robinson, Charles S, 1978, Hydrology of Fractured Crystalline
    Rocks, Henderson Mine; Colorado, Soc. of Min. Eng. T.P.

Scheidegger, A.E., 1961, General Theory of Dispersion in Porous
    Media. Journal of Geophysical Research, Vol. 66, No. 10

Sharp, J. C., 1970. Fluid flow through fissured media: Ph.D.
    dissertation, Imperial College, London.

Snow, David, T. 1965, A parallel plate model of permeable
    fractured media. Unpubl. PhD Thesis, Univ. of California,
    Berkely, 331 pp.
    ——1968a, Rock fracture spacings, openings, and porosities.
    ASCE, Soil Mechanics and Foundations Div. Jour. v. 94,
    no. 5MI, proc. paper 5736, pp. 73-91.
    ——1968b, Hydraulic characteristics of fractured metamorphic
    rocks of the Front Range and implications to the Rocky
    Mountain arsenal well. Colo. Sch. Mines Quarterly, v.63,
    no. 1, pp. 167-199.
    ——1968c, Fracture deformation and changes of permeability and
    storage upon changes of fluid pressure. Colo. Sch. Mines
    Quarterly, v. 63, no. 1. pp. 201-244.

————1968d, Rock Fracture Spacings, Openings and Porosities, *Journal Soil, Mec. Foundation Div.*, Proc. ASCE, 94, 3-91.
————1969, Anisotropic permeability of fractured media. Water Resources Res. v.5, no. 6, pp. 1273-1289.
————1970, The frequency and apertures of fractures in rock. Jour. Rod. Mech. Min. Sci. v.7, pp. 23-40.
————1971, Fracture Deformation and Changes in Permeability and Storage Upon Changes of Fluid Pressure, Colorado School of Mines Quarterly.
Stewart, J.W. 1962b. Relation of permeability and jointing in crystalline metamorphic rocks near Jonesboro, Geogia. (Article 69 in Geological Survey Research, 1962) U.S. Geol. Survey Prof. Paper 450D, pp. D168-D170.
————1962a, Water yielding potential of weathered crystalline rocks at the Georgia Nuclear Laboratory. (Article 43 in Geological Survey Research, 1962). U.S. Geol. Survey Prof. Paper 450B, pp. B106-B107.
————1964, Infiltration and permeability of weathered crystalline rocks, *Georgia Nuclear Laboratory, Dawson County, Georgia*, U.S. Geol. Survey Bull. 1133-D, 59pp.

Streltsova, I.D., 1976, Hydrodynamics of Groundwater Flow in a Fractured Formation, Water Resources Research, Vol. 12, No. 3, pp. 405-414.

Swolfs, H. H.R. Pratt, A.D. Black. W.F. Brace, A.S. Orange and K.A. Granseth, 1974, In situ propertoes of a jointed granite (Abs) Trans. Am. Geophys. Union, 55, 432.

Taylor, G.I., 1953, Dispersion of soluble matter in solvent flowing slowly through a tube, Proc. Roy, Soc. A, No. 1137, 219, 186-203.

Todd, D.K., 1959, 1967; Groundwater Hydrology, John Wiley & Sons, Inc.

Towndrow, R.G.P., Information Office, Atomic Energy Research Est., Harwell, Symposium Proceedings, July 16-20, 1978., GAIN, "Geotechnical Assessment and Instrumentation Needs for Nuclear Waste Isolation in Crystalline and Argillaceous Rocks,"Prepared for the U.S. Dept. of Energy under Contract No. W-7405-ENG-48.

Uhl, Vincent W. Jr. and G.K. Sharma, 1978, Results of Pumping Tests in Crystalline-Rock Aquifers, Groundwater, V.16 No.3.

U.S.G.S., 1977, U.S. Geol. Survey Yearbook. Role of Earth Sciences in the Disposal of Radioactive Waste

Wahlstrom, E.E. and V.Q. Hornback, 1962, Geology fc the Harold D. Roberts Tunnel, Colorado: west portal to station 468 & 49. Geol. Soc. America Bull. 73

Witherspoon, P.A.,"Movement of Fluids in Largely Impermeable
    Rocks,"Report from seminars held January 27-29, 1977,
    University of Texas at Austin, Y/OWI/SUB-77/14223, April,
    1977.

Witherspoon, P.A., P. Nelson, T. Doe, R. Thorpe, B. Paulsson,
    J. Gale, C. Forster,"Rock Mass Characterization for Storage
    of Nuclear Waste in Granite,"Swedish-American Cooperative
    Program on Radioactive Waste Storage in Mined Caverns in
    Crystalline Rock, February, 1979.

TABLE OF CONTENTS

CHAPTER 1 - GRANITES

TABLE 1-20 TO FOLLOW UNDER SEPARATE COVER

TABLE OF CONTENTS

CHAPTER 1 (CONT)

LIST OF FIGURES

CHAPTER 1 - GRANITES

iii

LIST OF FIGURES

LIST OF FIGURES

v

LIST OF FIGURES

LIST OF TABLES

CHAPTER 1 - GRANITES

TABLE OF CONTENTS

Chapter 2

LIST OF TABLES

LIST OF TABLES (CONTINUED)

LIST OF FIGURES

GEOLOGIC CHARACTER OF BASALT

2.1 INTRODUCTION TO GEOLOGIC CHARACTER OF BASALT

Basalt is a dark-colored, mafic igneous rock composed of calcium plagioclase and clinopyroxene. It is generally extrusive or volcanic in origin causing a glassy or fine-grained texture. Basalt is one of the major rock types exposed at the earth's surface. The ocean basins are composed of it and extensive basaltic terranes occur on all continents.

In recent years, as more sophisticated physical-chemical data have been gathered, the basalts, their tectonic frameworks, and their compositions, have become a major source of support and argument for plate tectonic and other planetary development theory. As such, basalt has commanded an interest far beyond its already major importance as a common terrane at the earth's surface.

2.2 CLASSIFICATION

All igneous rocks, including basalts, are classified on the
basis of texture and mineralogy. By definition basalts are
all fine-grained, calcium plagioclase-clinopyroxene rocks.
Within this framework there are numbers of textures and
mineral subclasses that specify different genetic types of
basalt.

There are two main mineralogical subgroups of basalts (Figure
2-1). Each of these is derived from a distinct type of parent
magma. The tholeiitic magma is saturated with SiO2 and pro-
duces basalts consisting of calcium-poor augite, (Ca,Na)
$(Mg,Fe,Al,Ti)(Si,Al)_2O_6$, labradorite plagioclase, $(Ca,Na)Al(Si,Al)$
Si_2O_8, and iron oxides. Olivine, $(Mg,Fe)_2SiO_4$, may be absent
or, as in olivine tholeiite, present in accessory amounts.

The alkali basaltic magma is undersaturated with respect to
SiO_2 and produces nepheline, $(NaK)AlSiO_4$, bearing calcium-
rich augite. In the resulting rocks, alkali feldspars often
occur with the calcium plagioclases and, in general, alkali
basalts contain much more complex assemblages of feldspars.
As with the tholeiites, olivine may be absent or occur as an
accessory; however, it is more common in the alkalis. Also,
alkali-basaltic olivine occurs in the groundmass and it
tends to be zoned from magnesium-rich to iron-rich. This is
unusual for tholeiite olivine.

FIGURE 2-1

Mineralogical Subgroups of Basalts
Exploded view of generalized simple basalt system
illustrated in upper right inset. Entered are names
of rocks whose major normative phases are contained
in the tetrahedra. Names underlined are within the
tetrahedra. Names in faces are written parallel to
base. Lherzolite is in Ol-Cpx-Opx face. An additional
inset, Ol-Cpx-An, gives alternative nomenclature when
plagioclase is rich in An. After Yoder and Tilley (1962).

ALKALI BASALT GROUP   OLIVINE THOLEIITE GROUP   THOLEIITE GROUP
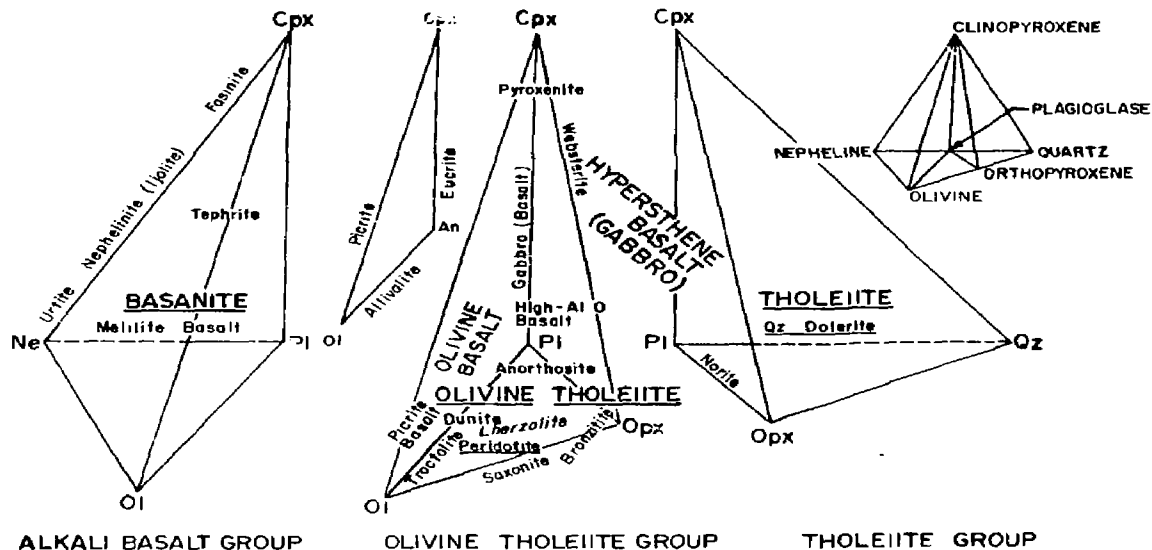
Two lesser suites of basalts are the calc-alkali series and the high alumina series. The genesis of both are controversial. The calc-alkalis are thought to be high alkali differentiates of the tholeiitic magmas. The high alumina basalts contain in excess of 17 percent Al_2O_3 and are also thought to be derivatives of the tholeiites.

Basaltic textures and their causes are almost as prolific as the various basalt rock names. For practical purposes, particularly if the physical properties of the rock are of concern, only a few are important. Basalts tend to be porphyritic (larger crystals set in a fine-grained groundmass). The large crystals or phenocrysts are often aligned, creating anisotropy. The ground-mass may be vitreous or glassy. Although basalt glasses, or obsidians, are rare, matrices can contain high proportions of glass. Basalt flows commonly contain frothy or vesicular layers where gasses were trapped during extrusion. Also, flows usually have some type of jointing that occurred during cooling. This weakens the rock body and allows more rapid weathering.

2.3 COMPOSITION

The major mineral groups that make basalts (plagioclases,
pyroxenes and olivine) produce a dark-colored heavy rock that
is relatively low in silica and high in iron, magnesium and
calcium. The mineral and chemical analyses for examples of
a tholeiite, an alkali and a high alumina basalt are given
in Table 2-1. The rather exacting compositional requirements
discussed under Classification are evident. The tholeiite
is high in SiO_2 and the alkali basalt is undersaturated in
SiO_2 and high in sodium and potassium. The high alumina
basalt is high in Al_2O_3.

	Olivine Tholeiite	High Alumina	Olivine Alkali Basalt
SiO_2	49.18	48.27	41.60
TiO_2	2.29	0.89	2.64
Al_2O_3	13.33	18.28	10.38
Fe_2O_3	1.31	1.04	3.58
FeO	9.71	8.31	9.07
MmO	0.16	0.17	0.20
MgO	10.41	8.96	14.38
CaO	10.93	11.32	10.90
Na_2O	2.15	2.80	4.32
K_2O	0.51	0.14	1.02
H_2O	0.09	0.22	1.46
P_2O_5	0.16	0.07	0.38
Quartz (SiO_2)	-	-	-
Orthoclase $KAlSi_3O_8$	2.78	0.56	0.56
Albite $NaAlSi_3O_8$	17.82	23.58	-
Anorthite $CaAl_2Si_2O_8$	25.30	39.97	5.84
Diopside $(CaMgSi_2O_6)$	22.93	15.23	36.54
Hypersthene $(Mg,Fe)_2Si_2O_6$	15.35	-	-
Olivine $(Mg,Fe)SiO_4$	9.14	20.55	20.37
Magnetite Fe_3O_4	2.09	1.39	5.10
Ilmenite $FeTiO_3$	4.41	1.67	5.02
Apatite $Ca_5(PO_4)_3(F,OH,Cl)$	0.34	0.17	1.01
Nepheline $(Na,K)AlSiO_4$	-	-	19.88
Leucite $(KAlSi_2O_6)$	-	-	4.36

Table 2-1   Chemical Composition and Mineralogy in percent of some basaltic rocks (1. Kilawea Caldera, Hawaii; 2. Medicine Lake Highlands, California; 3. Ponape Island)   Source: Hess and Poldervaart, 1967

2.4 PRIMARY STRUCTURE OF BASALTIC BODIES

Most basalts occur in flows. Small near-surface intrusions
have produced basalt but the volume is very minor. The
majority of the great flow sequences underlie the oceans.
These have spread from centers along the earth's surface
plate boundaries and represent the formation of the new
crust required to fill in as the plates shift.

There are also major periods of basalt flow deposition on
the continents. These flow sequences, known as flood or
plateau basalts, spread to great thicknesses over various
areas of all the continents during the Permian, Triassic and
mid-Tertiary periods. Because of their accessibility these
continental flood basalts have, until recently, received
more attention than the oceanic basalts. For the purposes
of this report, they certainly are the most important type
of occurrence.

2.5 GENESIS

Genetic theory for the basaltic rocks is extremely detailed and complicated. Basaltic magmas are now conceded to develop directly from the earth's mantle material (Carmichael et al, 1974; Hess and Poldervaart, 1967). Controversies are still heated, however, over where in the mantle this occurs, what materials are involved, and how many primary basaltic magmas are developed.

The major type of basalt in both oceanic and continental occurrences is tholeiitic. The magma producing this basalt is thought to be a primary magma generated from a garnet-peridotite, or eclogite, in the upper mantle. Continental and oceanic tholeiites are slightly different in some respects, particularly in their trace element suites. However, these differences are believed to be due to contamination as the magmas pass up through either the continental or oceanic crusts (Carmichael et al, 1974; Hess and Poldervaart, 1967).

Alkali, calc-alkali, and high alumina basaltic magmas hypothetically all develop from tholeiite magma. For calc-alkali and high alumina magmas, the hypothesis is subjective simply because the data are insufficient and inconclusive. For alkali basaltic magma, the problem is more substantial.

Alkali magma can be differentiated from tholeiitic but an
enormous volume of tholeiitic magma is required. Proponents
of the relationship have devised a partial melting of
tholeiites with subsequent filter pressing of alkali magma
to solve this problem. Opponents believe this is fortuitous.
They prefer a separate primary alkalic magma (Hess and
Poldervaart, 1967). This would mean that the concept of a
relatively homogenous mantle is suspect. Hence, the problem
of the alkali basaltic magma source still awaits solution.

2.6 WEATHERING OF BASALT

Basalts are composed of high temperature, igneous rock minerals. These are as much out-of-equilibrium with the surface environment as any group of rock-forming minerals can be. Hence, basalt will rapidly deteriorate once it is exposed. Physically, it is compact and resistant. However, most bodies are severely fractured during post-depositional cooling. This accelerates chemical and physical deterioration.

2.7 DESCRIPTION OF OCCURRENCES

Extensive areas of flood basalts occur in the northwestern
United States. This region, known as the Columbia Plateau,
is the largest area of basalt in the United States. All of
the flows of this region are of the continental tholeiitic
type.

The Columbia Plateau flood basalt region consists of three
distinct, smaller areas of basalt flows (Figure 2-2). The
Columbia River Basalt covers a large area in central and
southern Washington. The Modoc Plateau is a smaller area
mainly in northern California. The Snake River Plain extends
across most of southern Idaho. Each area has basalts of
slightly different stratigraphic and water-bearing properties.

The following discussions of these three areas will concen-
trate on general features that are consistent with the entire
area. When dealing with such large areas, it is not possible
to provide certain types of geologic data that may only be
important for given locales. Small-scale fracturing or joint-
ing is an example. Trends, intensities, and depths of occur-
rence for such features can only be measured, and their
importance to rock properties judged, for a specific site.

COLUMBIA
RIVER
BASALT

MODOC
PLATEAU

SNAKE
RIVER
PLAIN
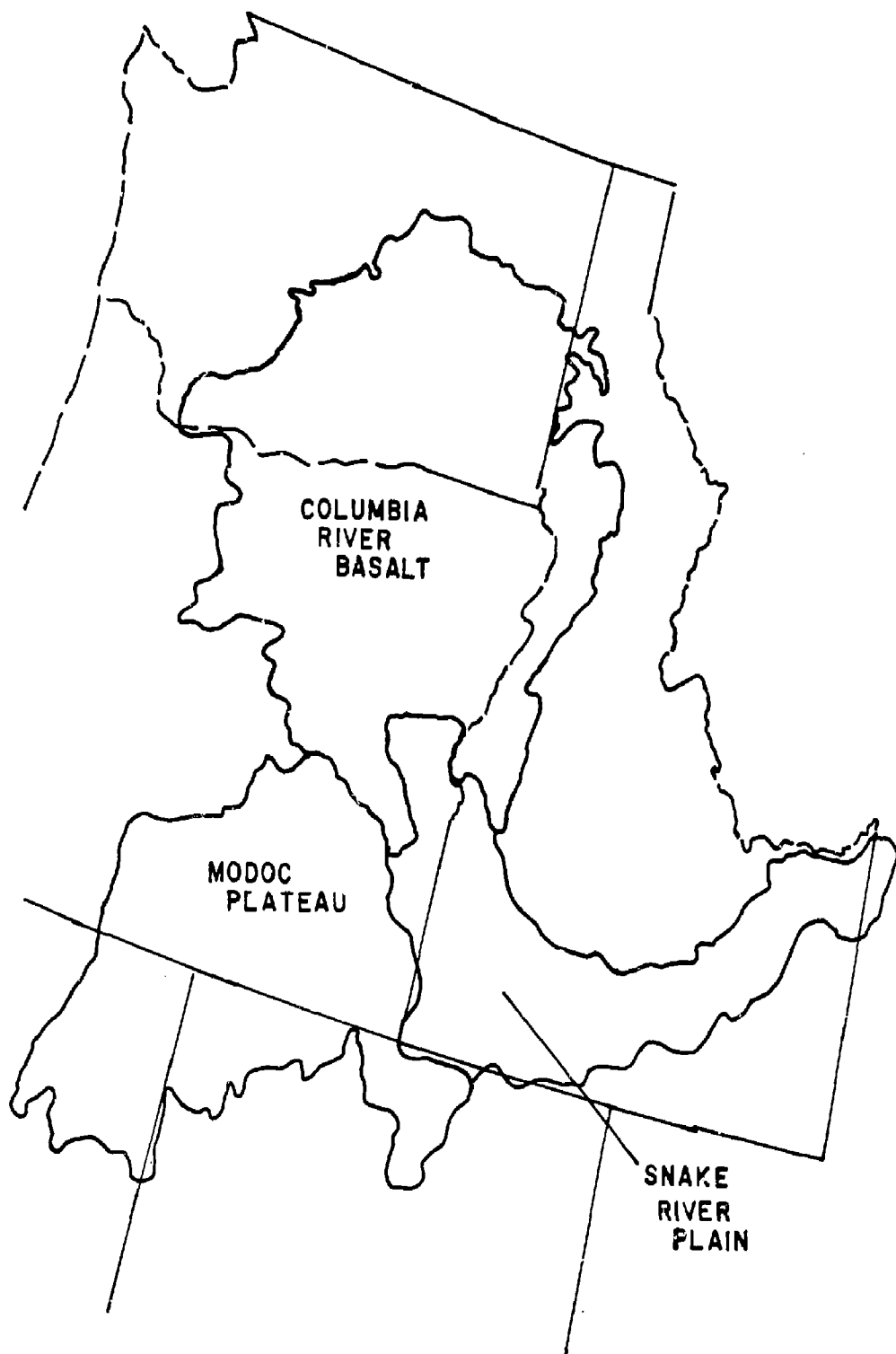
FIGURE 2-2   Flood basalt occurrences chosen for study

Columbia River Basalt

The Columbia River flows cover an area in excess of 150,000
square kilometers in southeast Washington, northeast Oregon,
and adjacent Idaho with a volume of more than 300,000 cubic
kilometers. The thickness of individual basalt flows generally
ranges from 1.5 meters to about 61 meters, averaging 24 meters
(Newcomb, 1969).

The average thickness of the basalt sequence underlying the
Columbia Plateau is greater than 500 meters, and the greatest
known thickness is 3,200 meters (Deju, 1977). It consists
of a thick sequence of accordantly-layered lava flows and
interbedded sediments (Newcomb, 1969). The flows are Miocene
to Pliocene in age, and are tholeiitic. Repeated eruptions
of enormous volumes of basaltic lava filled a slowly sub-
siding planoconvex basin. Between each eruption, the surfaces
of many flows were exposed to erosion.

The Columbia River Basalt is a black to dark-gray, dense,
fine-grained rock composed mostly of microscopic crystals
with some intercrystalline glassy groundmass. The average
composition of this basalt is labradorite - 55 percent;
augite - 15 percent; magnetite - 15 percent; and brown glass
and microlites - 25 percent. Most of the basalt has an even,
microgranular texture, but in a few places the crystals are

so small that the texture is flinty or nearly glassy. The textural fabric of the rock indicates that most of the crystallization occurred after the highly fluid lava had come to rest (Newcomb, 1969).

The two most distinctive petrologic structures in the Columbia River Basalt are layers and joints. The layering resulted from the accumulation of successive flows of highly fluid lava of the same general chemical and mineral type. The individual flows are generally separated by: 1) a difference in jointing, texture, or color; 2) a difference in susceptibility to alteration; 3) interbedded sedimentary material, and/or 4) a vesiculated top and a flinty basal section.

Joints, actual and potential fractures or partings, traverse the basalt. The main sets of fractures were caused by shrinkage of the solidified rock during cooling. The cooling of the lava induced joints that are arranged in: 1) vertical columnar joints, 2) flat or sheeting joints, and 3) unsystematic miscellaneous partings. These joints separate some parts of flows into angular, irregular blocks of all sizes and shapes (Newcomb, 1969). Columnar jointing systems are present in almost every flow.

In addition to the shrinkage joints, the basalt is traversed
by regional joints. These long, straight sets of parallel
vertical cracks trend in various patterns across most of the
basalt. They are believed to be extension fractures (Newcomb,
1969).

The basalt has a thin, oxidation skin on all but newly-exposed
surfaces. Where basalt has been exposed, it may be weathered
to depths of up to 50 and 60 meters (Newcomb, 1969).

Snake River Plain Basalt

The Snake River Group extends over an area of more than
20,720 square kilometers in central and southern Idaho
(Walker, 1964). It consists mainly of an accumulation of
basalt flows with intercalated lacustrine and alluvial
sediments. The basalt fills a huge graben and is known to
be more than 1,500 feet thick (Walker, 1964; Nace et al, 1972).

The eruptions that emplaced the basalt were intermittent.
The sheet of lava that spread out during each event usually
solidified before the next overlying sheet was laid down.
Each sheet has an upper and lower chilled zone. Commonly,
the surface of a flow was exposed to erosion or deposition
of sediments between the lava flows (Walker, 1964). The
molten basalt was fluid enough to spread many miles on rela-
tively low gradients.

The structure, chemistry and minerology of the Snake River
Basalt is similar to the Columbia River Basalt. The major,
regional fractures in the basalt are vertical and trend
north-south, east-west.

The Modoc Plateau

The Modoc Plateau is the area east of the Cascade Mountains
in southern Oregon and northern California and west of the
Basin and Range Provinces. The area contains extensive
volcanic flows and is a "transition zone" between the
Cascade Mountains and the Basin and Range Provinces. The
rocks of the plateau are mainly from lava flows that range
in composition from rhyolite to basalt (MacDonald, 1966).
Tuff, ignimbrite, agglomerate, diatomite, shale, siltstone,
sandstone, and gravel are interstratified within the lava
flows in varying degrees while many recent cinder cones rest
on their surfaces. Lassen Crater, the sight of the last
eruption in the contiguous United States (1914), is located
on the Modoc Plateau.

The oldest flows are Miocene or Oligocene in age while the
youngest are recent (MacDonald, 1966). The major basalt
flows are the Warner Basalt (Miocene', Steens Basalt
(Miocene), Picture Rock Basalt (Pliocene), and Hayes Butte
Basalt (Pliocene). Every flow does not underlie the entire

area. Individual flows commonly fill grabens and their sur-
faces are distinguished by pahoehoe or ropy lava structures.

These Tertiary basalts are usually composed of dark-gray
olivine basalts. Commonly, the texture of the basalt is
porphyritic with phenocrysts of olivine or labradorite
(Hampton, 1961).

Faults trending north to northwest are common and usually
delineate horsts and grabens. These normal high-angle
faults show considerable displacement, up to 305 meters, and
some strike-slip displacement (MacDonald, 1966). The fault
surfaces can be undulating or angular. Minor faulting can
be seen perpendicular to these faults.

Vertical shrinkage joints are very common, especially in the
tops or bottoms of each individual flow. Individual flows
range from 3 to 15 meters thick. The thickness of the major
basalt flows vary from a few tens of meters to over 300
meters, and generally thin toward the south and east (Piper,
1939; MacDonald, 1966; Brown et al, 1962).

2.8 REFERENCES

Brown, S.G. et al, 1962, Ground Water Resources of Cow Valley, Malheur County, Oregon, USGS, WSP., 1619-M, p. M1-M35.

Carmichael, I.S.E., Turner, F.J., and Verhoogen, J., 1974, Igneous petrology: McGraw-Hill, New York, p. 740.

Deju, R.A., P.A. Eddy, M.W. Grutzeck, and C.W. Myers, 1977, Environmental factors needed to establish the geotechnical feasibility of storing radioactive waste in Columbia River Basalt: U.S. Dept. Energy RHO-ST-8, p. 114.

Diery, H.D. and B. McKee, 1969, Stratigraphy of the Yakima Basalt in the Type Area, ini Northwest Science. V. 43, No. 2.

Gary, M., and others, eds., 1972, Glossary of geology: Am. Geol. Inst., p. 805.

Greeley, R., and J. King, 1975, Geologic field guide to the quarternary probes of S-C, Snake River Plain, Idaho; Geo. Soc. of America, Rocky Mountain Section.

Hampton, E.R., 1961, Geologic factors that control the occurrence and availability of ground water in the Fort Rock Basin, Lake County, Oregon: U.S. Geol. Survey Prof. Paper 383-B, p. 29.

Hess, H. H., and Poldervaart, A., 1967, Basalts: Interscience, Londo.., V. 1&2, p. 862.

Leet, L.D. and Sheldon Judson, 1971, Physical Geology, 4th Ed., Prentice Hall, Inc., New Jersey.

MacDonald, G.A., 1966, Geology of the Cascade Range and Modoc Plateau, in Geol. of Northern California: California Division of Mines, Geol. Bull, No. 190, Bailey, E.H., ed., p. 65-96.

Meinzer, O.E., 1942, Hydrology, McGraw Hill, New York, p. 712.

Nace, R.L., M. Deutsch, and P.T. Voegeli, 1972, Physical environment of the Nation Reactor Testing Station, Idaho - a summary: U.S. Geol. Survey Prof. Paper 725-A, p. 38.

Newcomb, R.C., 1969, Effect of tectonic structure on the occurrence of ground water in the basalt of the Columbia River Group of the Dallas Area Oregon and Washington: U.S. Geol. Survey Prof. Paper 383-C, p. 33.

Piper, A.M. et al, 1939, Geology and Ground Water Resources of the Harney Basin, Oregon, USGS, WSP, 841, p. 1-187.

_____, 1975, Hypothetical prototype sites of repositories for radioactive wastes: flood basalt, USERDA Y/OWI/SUB-3745/6.

Spock, L.E., 1961, Guide to the Study of Rocks, 2nd Ed., Harper and Row, New York, p. 298.

Stearns, H.T., L. Crandall, and W.G. Steward, 1938, Geology and ground-water resources of the Snake River Plain in southeastern Idaho: U.S. Geol. Survey Water-Supply Paper 774, p. 268.

Travis, R. L., 1956, Classification of rocks: Colorado School of Mines Quart., V. 50, No. 1, p. 98.

Walker, E.H., 1964, Subsurface geology of the National Reactor Testing Station, Idaho: U.S. Geol. Survey Bull., 1133-E, p. 22.

Yoder, H.S., Jr., 1976, Generation of basaltic magma: National Acad. Sci., Washington, D.C., p. 265.

GEOMECHANICS OF BASALTS

2.9 INTRODUCTION TO GEOMECHANICS OF BASALT

Basalt is described as a fine-grained, sometimes glassy, basic igneous rock with essential minerals of calcic plagioclase in pyroxene with a silica content generally less than 50%. Sometimes gabbro, norite, diabase, dolerite and basaltic glass are included in a general discussion of basalt. These rock types are all of similar chemical and mineralogical composition with the grain size being the main distinguishing feature (Agapito and Hardy, 1977).

The engineering behavior of basaltic flows is expected to vary widely due to their unique depositional and cooling characteristics. Variations within a flow are largely a function of the flow thickness which determines the rate of cooling throughout the mass. Normally, thick flows have dense basalt in their lower portions and are jointed. The jointing forms 5- or 6-sided columns with individual columns averaging 0.6 to 0.9 meters across. Cross joints either inclined or normal to the column may also be present (Office of Nuclear Waste Isolation, 1978).

In the Columbia River basalt, columnar joints are the most common internal structures within individual flows. Although the pattern of columnar jointing exhibits variability, both within and between flows, a typical flow usually has a lower zone, which is generally 1/3 to 1/2 of the entire thickness

of the flow and consists of nearly symmetrical columnar
joints, and an upper zone, which is generally 1/2 to 2/3 of
the entire thickness of the flow, consisting of an irregular
jointing pattern. The jointing pattern variations include
fan-like columnar joints, plating joints, swirling joints,
brick-bat joints, cross joints, and others. Abr t lateral
changes in joint patterns can occur. dep h, most joints
and fractures are filled with secondary minerals such as
zeolite, amorphous iron-rich silicates, and ferro-magnesium
clays. The top of the flow may be a slaggy, ropy, or clinker-
type basalt (Office of Nuclear Waste Isolation, 1978).

Hence, the geomechanical behavior of the basalt flows depends
upon the zone being studied. Potential repository sites
would logically be located in the most massive part of the
flow, where the joints are the most widely spaced, and the
streng h is the greatest. The behavior of the joints will
certainly be a major consideration. The types of geomechani-
cal factors which will be included in any study of basalt as
a potential repository rock are indicated in Table 2-2.
Note that it includes defining the major structural properties
of the rock-mass as well as characteristics of the rock on a
much smaller scale.

The geotechnical factors that influence design have been
summarized very well in the report prepared by Parsons,

TABLE 2-2   Geomechanical factors to be considered

I.   TECTONICS AND SEISMOLOGY   Source: R.A. Deju et al, 1977

1. Assess the tectonic stability of   Regional geology; field studies; evalua-
   the region.   tion of seismic records; seismic moni-
                                          toring; literature survey; geophysical
                                          surveys.

2. Define major faults, fractures,   Field studies in outcrops, trenches,
   and fissures.   and boreholes; remote sensing; litera-
                                          ture survey; geophysical surveys.

3. Document the seismic record.   Examination and documentation of the
                                          seismic record, including microearth-
                                          quake studies.

4. Assess the structural integrity   Field analyses; laboratory and insitu
   of the basalt mass.   tests; geophysical surveys.

5. Define the frequency, orientation,   Remote sensing.
   and character of major lineaments

6. Define the frequency and   Core analysis, supplemented by borehole
   orientation of fractures in basalt.   geophysics.

7. Define the extent of folding and   Integration of geologic and geophysical
   the forces that led to its present   data.
   state.

II. ROCK PROPERTIES AND STRATIGRAPHY

1. Define the petrographic, mineral-   Petrographic, mineralogic, and chemical
   ogic, and chemical characteristics   analyses of selected basalt flows;
   of the basalts.   literature survey.

2. Assess the stratigraphy and define   Stratigraphic correlation using petro-
   variations.   graphic, mineralogic, chemical,
                                          paleomagnetic, and geophysical techniques.

3. Define erosional stability over   Regional geology, interpretation of
   geologic time.   observations; geologic history;
                                          geomorphological studies.

4. Define the thermal properties of   Laboratory tests on cores under simulated
   basalt (expansion, conductivity,   conditions.
   and fracture potential).

5. Assess the effect of thermal stress   Same as for II-4.
   gradients on fractures and basalt
   properties.

6. Assess the effect of fractures on   Same as II-4.
   the heat transfer properties of
   the basalt mass.

7. Examine the effect of radiation on   Same as for II-4.
   structural integrity of the basalts.

2- 24

Blinckerhof et al, 1978 (PBQ6D). Their discussion is included

in its entirety below as it sets the basis for the more

detailed discussions of the individual factors that follow:

"Geotechnical Factors That Influence Design

Because of the geological characteristics and general
stratigraphic setting of insitu basalt, the choice
of basalt for a repository will influence many of
the design and layout features of the surface and
subsurface facilities as well as the amount of waste
that can be stored.

The basis for design decisions in basalt are underlain
by the objective to keep the total of all stress
components significantly below the threshold value
required for the occurrence of an initial failure
mechanism. The characteristics that would signifi-
cantly impact the design of the waste storage facility
include:

  . Effects of heat on rock strength
  . Rock movement and faulting
  . Room and pillar stability
  . Ground-water movement
  . Rock hardness

Effects of Heat on Rock Strength

At high temperatures, the strength of rock is dimin-
ished as the rock crystalline structures begin to
break down. In basalt, major losses of strength are
expected to occur at around 400°C to 500°C. To
prevent weakening of the rock adjacent to the waste
packages and the concomitant problems it would pose
to retrievability, the thermal loading should be
adjusted so that temperatures do not exceed critical
values in large volumes of rock in the immediate
vicinity of the canisters.

To maintain room safety and to reduce the possibility
of progressive spalling failures, the temperature of
the rock surfaces 'n the room walls and roof should
also be held below the values that cause excessive
strength loss.

Rock Movement

The rock surrounding and overlying the repository
would react or move in response to the stresses imposed
by the mined excavation and by thermal loading from
the implanted waste materials. Mining activities would
cause the surrounding rock to subside or move into and
towards the mined opening. In contrast, the thermal
loading would expand the rock and cause heaving to occur.

The repository layout and geometry and the allowable
thermal loading should be designed to minimize rock
movements so that the safety or integrity of the
shafts is not adversely affected. Movements at the
ground surface should be less than that which would
cause distress in any structure. In addition, rock
movement should not cause disruption or shearing of
any aquifers in the vicinity of the repository.

Room and Pillar Stability

When basalt is overstres ed, it will fail quickly
with comparatively little warning. Accordingly, the
main philosophy used in establishing design guide-
lines for waste facilities was to limit stresses to
a value well below the level required for initial
failure.

Room Stability

The repository layout and geometry and thermal load-
ing limits are chosen such that the ratio of rock
strength to rock stress within any rock cube with
one face exposed in the wall of the room and with
dimensions equal to 20% of the mean tunnel diameter
was two or greater. Rock strength is defined as the
mean compressive strength of the rock mass, considering
the confining pressures, the offsets of fractures and
joints, and temperatures. Rock stress is the mean
compressive stress including a combination of the
virgin stresses, stresses developed by the opening, and
thermal stresses.

Analytical studies indicate that the room stability
guidelines were met for the generic repository in
basalt at the proposed 2,000 ft. (660m) depth.
Therefore, additional support (rock bolting) would
be necessary only in localized areas where loose
rock is observed.

Pillar Stability

> The repository layout is designed such that the ratio
> of pillar strength to pillar stress remains greater
> than two. This ratio is defined as the mean com-
> pressive strength of the pillar at mid-height. To
> protect against blast damage, the pillars were designed
> with a minimum width of 20 ft. In all cases, the
> pillar width was designed to be at least equal to the
> height of the room." (PBQ&D, 1978)

Please note that within the section on "Room Stability",

definiti s of rock strength and stress are given in the

first paragraph. It must be stated that, at the present

time, there is no universally accepted way of estimating

rock-mass strength nor is there agreement as to how the

stress around an opening should be calculated. Furthermore,

the 20% criteria which has been used is not one found widely

in the literature. Little field data is available to pro-

vide the required substantiation. This will be discussed

in more detail later.

Based on analytic studies done by Hardy and Hocking, 1977,

PBQ&D arrived at three hypothetical designs shown in Figure 2-3,

which are to meet the canister criteria recommendations

indicated in Table 2-3. The local areal thermal loading,

which would apply from the theoretical calculations, are

shown on Table 2-4. These are compared with "allowable

areal thermal loading." The designs were based on thermal

modeling of the type that will be discussed later in this

report. The basis for selecting "allowable level guidelines"

is not given in the report. Factual data on the thermal-

mechanical properties of various basalt flows and formations

BASALT

CYCLE I
HLW: Extraction Ratio = 25%
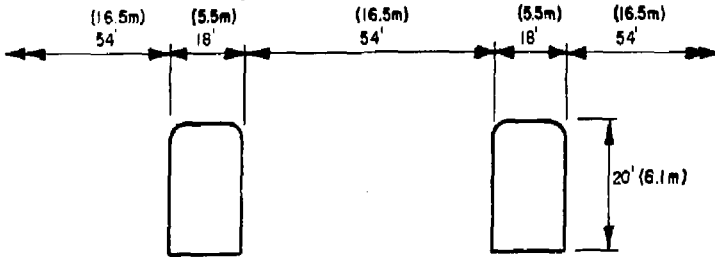
ILW & CW: Extraction Ratio = 40%
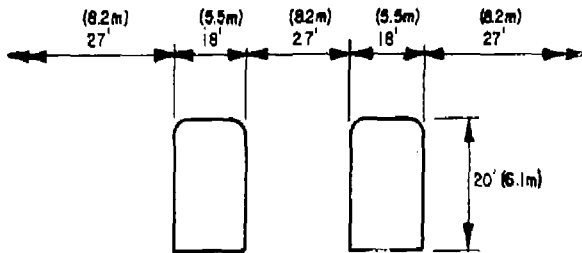
CYCLE II
PWP/BWR: Extraction Ratio = 40%
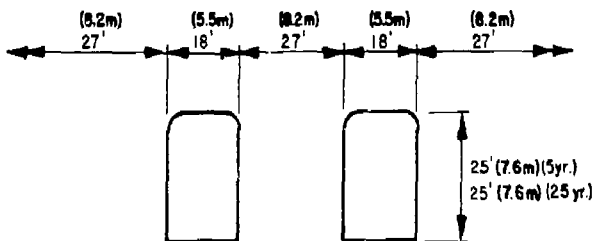
CYCLE III: Same as CYCLE I

FIGURE 2-3   Extraction Ratio Chart
Source: PBQ&D, 1978.

TABLE 2-3   Canister receipt criteria recommendations.

Contents	Canister Outside Diameter m	Canister Overall Length m	Overpack Outside Diameter m	Overpack Overall Length m	Age (Years)	Maximum Radiation Level (rem/hr) At Surface gamma dose rate	At Surface neutron dose rate	3.05m from Ctr. Line gamma dose rate	3.05m from Ctr. Line neutron dose rate
HLW in Glass	.324	3.048	.356	3.35	10	2.0×10^5	1.0×10^2	1.0×10^4	1.0×10^1
HLW in Calcine	.219	3.048	.273	3.35	10	5.0×10^5	1.0×10^2	5.0×10^4	1.0×10^1
IL-TRU	.324	3.048	.356	3.35	5	1.0×10^2	1.0×10^{-1}	1.0×10^1	5.0×10^{-3}
Cladding	.324	3.048	.356	3.35	5	1.0×10^3	1.0×10^{-1}	1.0×10^1	5.0×10^{-3}
PWR	.356	4.877	.406	5.03	10	7.0×10^4	1.0×10^1	3.5×10^3	5.8×10^{-1}
BWR	.273	4.877	.324	5.03	10	5.0×10^4	1.0×10^1	2.5×10^3	5.8×10^{-1}

ADDITIONAL RECEIPT CRITERIA
(For All Canisters)

Max. Weight (incl. overpack) = 6,613.8 kg.
Max. outer surface contamination
with transferable radioisotopes:
   beta-gamma radiation emitting nuclides: 10,000 dis/min/dm^2 (disintegration/minute/100 centimeters^2)
   alpha emitting nuclides: 300 dis/min/dm^2

Source: PBQ&D, 1978

TABLE 2-4   Local areal thermal loading basalt.

Cycle	Waste Type	Average KW/can	Allow. Areal Thermal Loading	Design Areal Thermal Loading
I	HLW	1.2	190 w/m^2	189 w/m^3
II	PWR	0.55	190	627*
	BWR	0.18	190	142*
II (25-Yr.)	PWR	0.55	80	79
	BWR	0.18	80	78
III	HLW + Pu (glass)	1.2	190	189

*Design areal thermal loading could not be brought up to allowable due to physical restrictions on spacing.

Source: P3Q&D, 1978, v. 14

is scarce. Developing such data and guidelines is the purpose of the present heater experiments being conducted in the Hanford Basalt.

This report discusses the geomechanical characteristics of basalts in general, providing information about the specific rock types as appropriate. It has been divided into six major sections. These are insitu stress, mechanical properties, thermal properties, thermoelastic properties, other characteristics, and scaling of laboratory results. A great deal of research is underway (with particular reference to the Hanford Operation) for evaluating the properties of basalt. These include both laboratory and field studies as well as a large amount of modeling using analytic, finite element, finite difference and other types of models. Because of these activities, progress in evaluating and measuring important geomechanical characteristics should be rapid.

2.10 STRESS STATE

In analyzing the stability of an underground excavation,
one must consider the stresses that are applied and the
strength of the materials involved. The stresses can be
divided into three categories. The first is insitu stresses,
those that exist prior to excavation. The second is stresses
induced by the excavation process itself and the third
category includes the stresses that are induced by the
materials which are placed within the excavation. Prior to
discussing each of these categories in some detail, it is
perhaps worthwhile to consider the methods by which stresses
are evaluated.

Stresses are generally* not measured directly but rather are
calculated by introducing strain (or displacement) measure-
ments and suitable elastic constants, into equations devel-
oped from elastic theory. The most common and widely
accepted means of obtaining insitu stress fields in the U.S.
is through the use of the U.S.B.M. borehole deformation
gauge. Here a 38 mm diameter hole is drilled, a gauge which
measures changes in borehole diameter in three directions is
inserted, and the hole overcored with a 150 mm diameter bit.
By measuring the borehole deformations, knowing the elastic

---

*The possible exceptions are hydraulic fracturing and
 flatjack type determinations.

modulus and Poisson's ratio of the rock, and using the
equations for a thick walled cylinder, one can calculate
stress magnitudes and directions. Three holes are required
to determine the complete stress tension at any point. Due
to the overcoring requirement, this technique is generally
limited to use in relatively short holes (<30 m). Hence,
measurements at depth would be obtained from underground
openings. Of the other techniques available, many suffer
from both operational and calculational difficulties.
Results obtained using several techniques at the same loca-
tion have generally shown wide variations. This may be due
to real variations; however, it is more likely due to the
instruments/procedures/evaluation techniques employed. Most
techniques assume that the rock is linearly elastic and
isotropic. This is a good approximation for some rocks, but
not good for others. The determination of absolute stress
or stress changes is compounded by moisture and temperature.
For nuclear waste applications, a great deal of development
will be required in this area.

In Situ Stress

As was stated by Hardy and Hocking, "no stress measurements
have been recorded in the basalt flows to our knowledge,
but in other parts of the U.S. stress measurements have
shown a trend toward lithostatic case at depths of around
a thousand meters." (Hardy and Hocking, 1977) The stress
measurements referred to by Hardy and Hocking were those
compiled by Lindner shown in Figures 2-4 and 2-5. Note that
no definite "trend" towards a lithostatic stress field at
depth is observed. Rather, there are few data points, and
those exhibit a wide degree of scatter. A wide scatter is
also noted in Figures 2-6 and 2-7. Lindner and Halpern
have fit equations to the data for North America. They
found that:

$$\sigma_V = (9.42\underline{+}13.1)kg/cm^2 + (0.339\underline{+}0.67)Kg/cm^2 \text{ per m-depth}$$

$$= (135\underline{+}185)psi + (1.469\underline{+}0.289)psi \text{ per foot-depth}$$

$$\sigma_H = (620\underline{+}116)psi + (1.690\underline{+}0.311)psi \text{ per foot-depth}$$

$$= (43.6\underline{+}8.15)kg/cm^2 + (0.390\underline{+}0.072)kg/cm^2 \text{ per m-depth}$$

where

σ_V = vertical stress

σ_H = horizontal stress

For the horizontal stress, Lindner comments, "This curve
fit is a poor one. The horizontal stress data indicate
considerable scatter. Data vary from three to four times
the least-square average, to less than lithostatic. Hence,
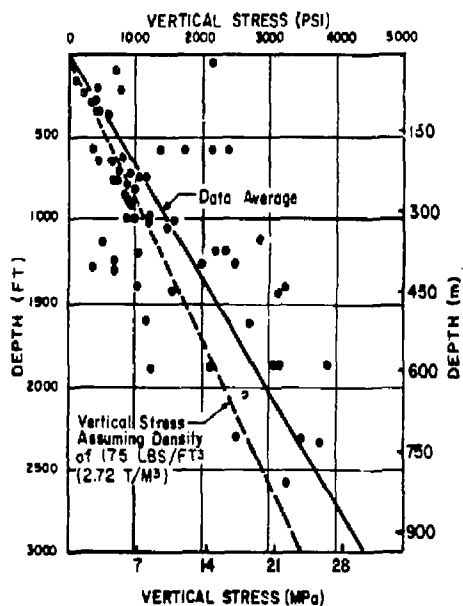
FIGURE 2-4   Vertical stress with depth
             Source: Lindner and Halpern, 1977.
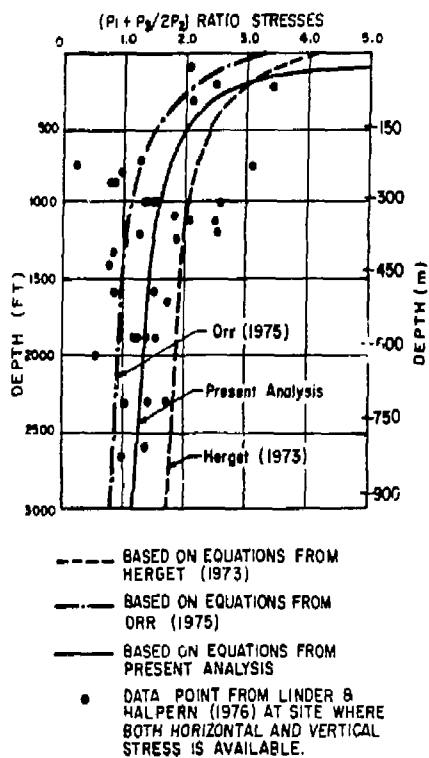
FIGURE 2-5   Ratio of the average horizontal stress to
              vertical stress
              Source: Lindner and Halpern, 1976.
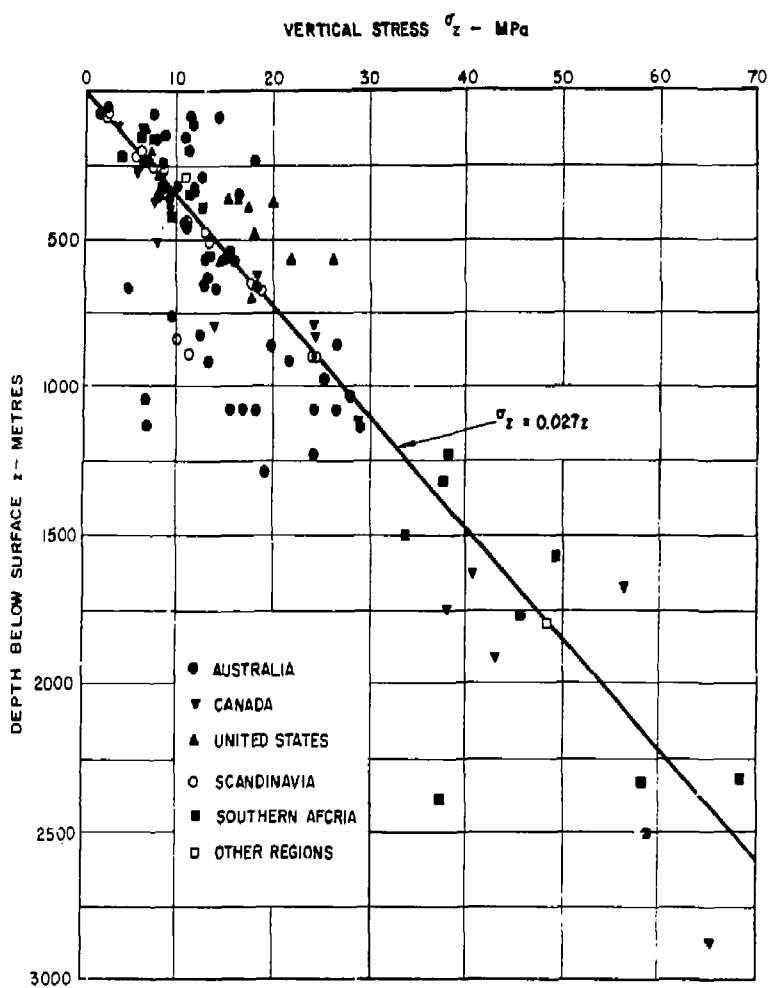
FIGURE 2-6   Plot of vertical stresses against depth below surface
              Source: Hoek and Brown, in press.
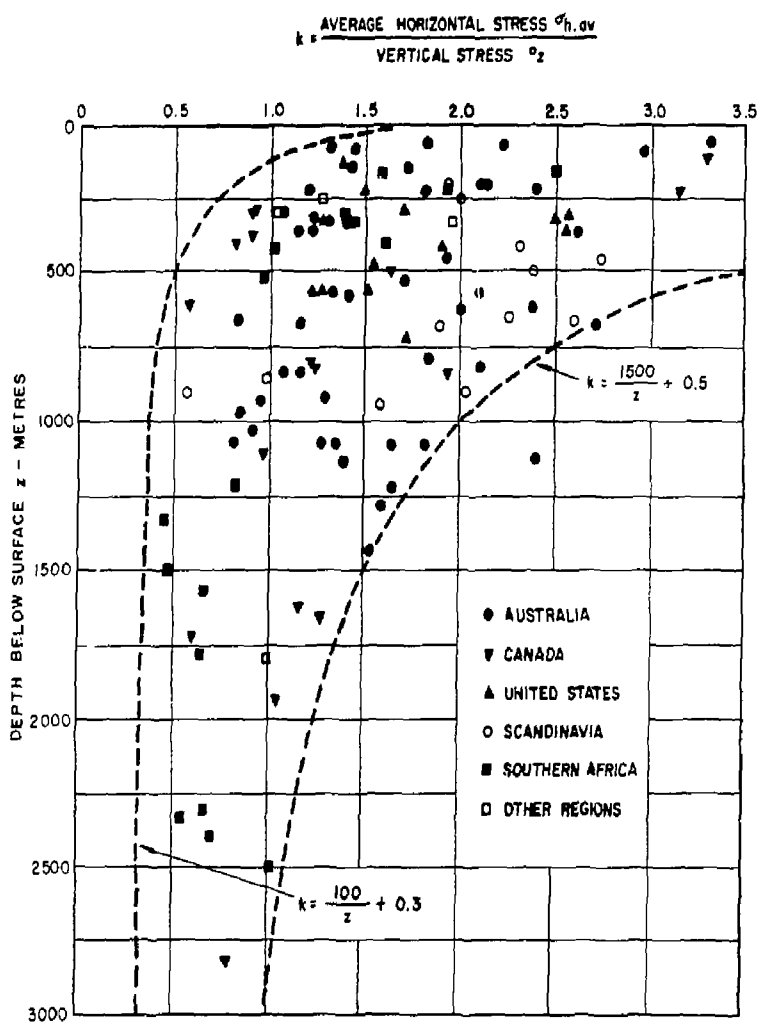
FIGURE 2-7 Variation of ratio of average horizontal stress
to vertical stress with depth below surface
Source: Hoek and Brown, 1976.

the curve fit is at best a trend rather than an average
that could be utilized in design."

The presence of the basalts themselves is evidence of
previous tectonic activity in the area in which they are
found. Therefore, one might expect to find significant
deviations from a stress state calculated based on the
weight of overburden. However, in the case of lithostatic
conditions, the three stresses would be equal to each other
and equal to the weight of the overburden. The presence of
faults, dikes or other major structures would also affect
the insitu stress field in the vicinity of such a feature.

Stresses Induced By Excavation

Hardy and Hocking made a two-dimensional analysis of the
effect of various in situ stress fields on the stresses
around a typical waste repository room, shown in Figures
2-8 and 2-9 using the values given in Table 2-5. For
the base case, it has been assumed that the initial in situ
field stresses were 25 megapascals at a depth of 1,000 meters
(the horizontal stress field was assumed to be equal to the
vertical). In Figure 2-9, the effect of areal thermal
loading on the tangential boundary stresses for the base
case is shown for three points around the periphery of the
room. The boundary stresses and temperatures for the central
room with other in situ stress fields are shown in Figure 2-10.
When the horizontal insitu stress is equal to one-half the
vertical, the most significant difference between this case
and the base case is that the boundary stresses in the roof
and floor are very much reduced. Tensile stresses are actually
present in the roof. When the in situ horizontal stress is
one and one-half times the vertical, the boundary stresses
are shown to be much higher in the roof and floor of the
rooms when compared to the base case. The boundary stresses
in the side walls are lower than the base case.

In summary, the boundary stresses in both the roof and
floor of the room decrease with decreasing horizontal to

CORRIDOORS EXTEND
⬅— OUTWARD

CORRIDOORS EXTEND
OUTWARD —➡

CORRIDOOR

24 m   6 m

7.5 m

8 m   5 m

RADIOACTIVE WASTE
CANISTER
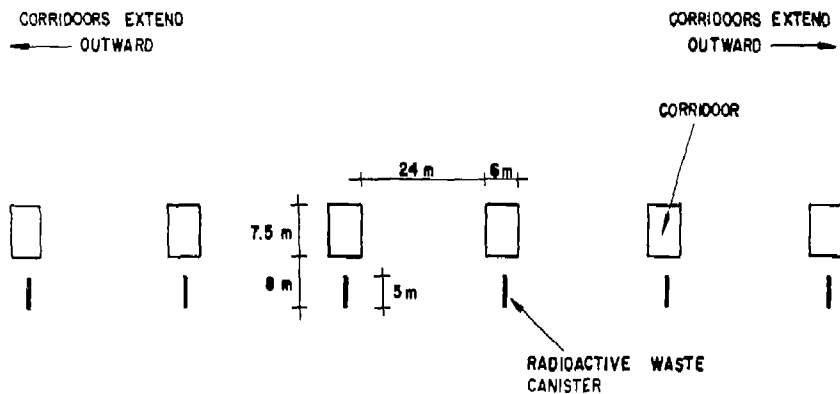
FIGURE 2-8   Base case for excavation and canister location geometry
             Source: Hardy and Hocking, 1977.
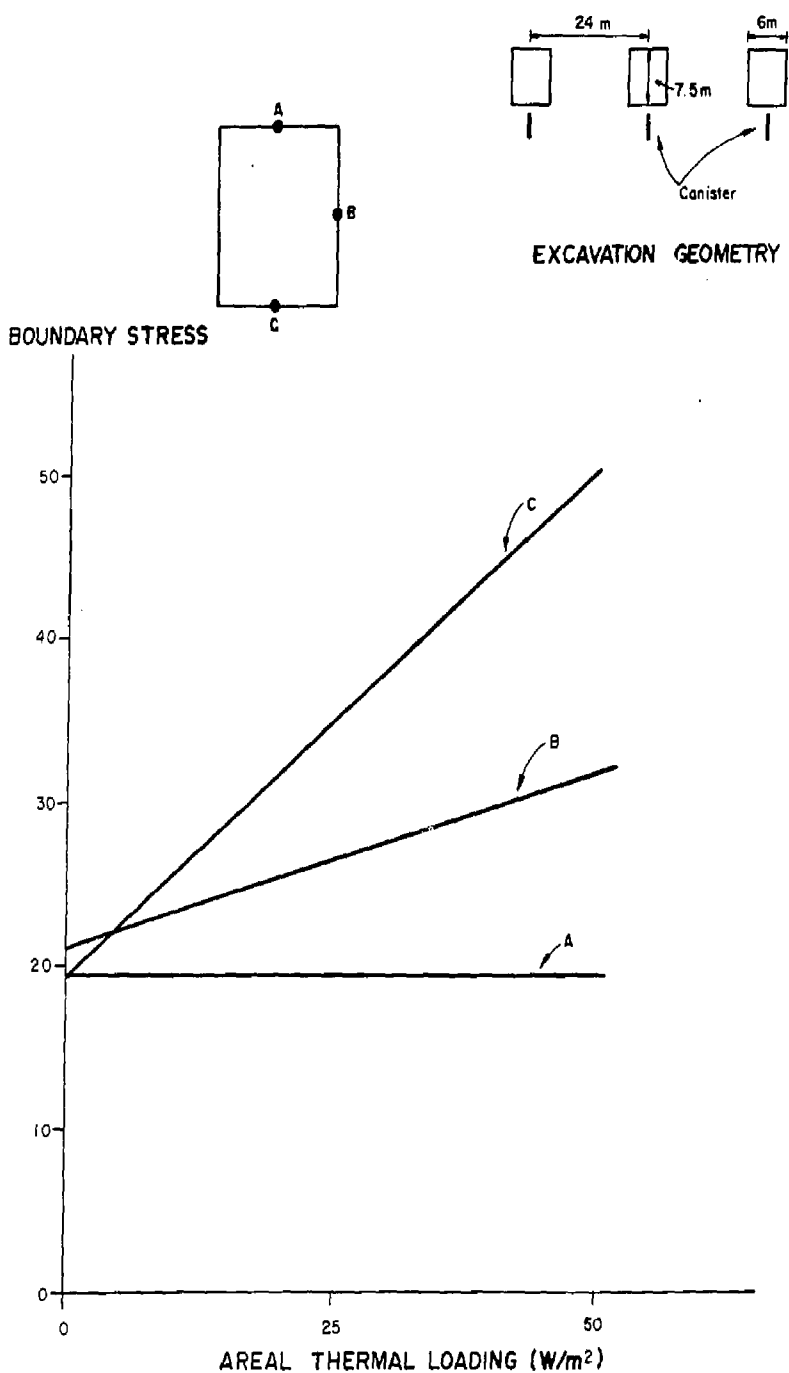
FIGURE 2-9   Effect of areal thermal loading on boundary
stresses for the base case
Source: Hardy and Hocking, 1977.

TABLE 2-5 Basalt properties.

Property	Basalt
Thermal Conductivity W/m° C	1.86
Specific Heat J/kg° C	1030
Density kg/m^3	2900
Diffusity (m^3/sec)	6.5×10^{-7}
Heat capacity (J/m^3° C)	3.0×10^6
Elastic modulus (Pa)	0.48×10^{11}
Poisson's ratio	0.2

Source: Hardy and Hocking, 1977
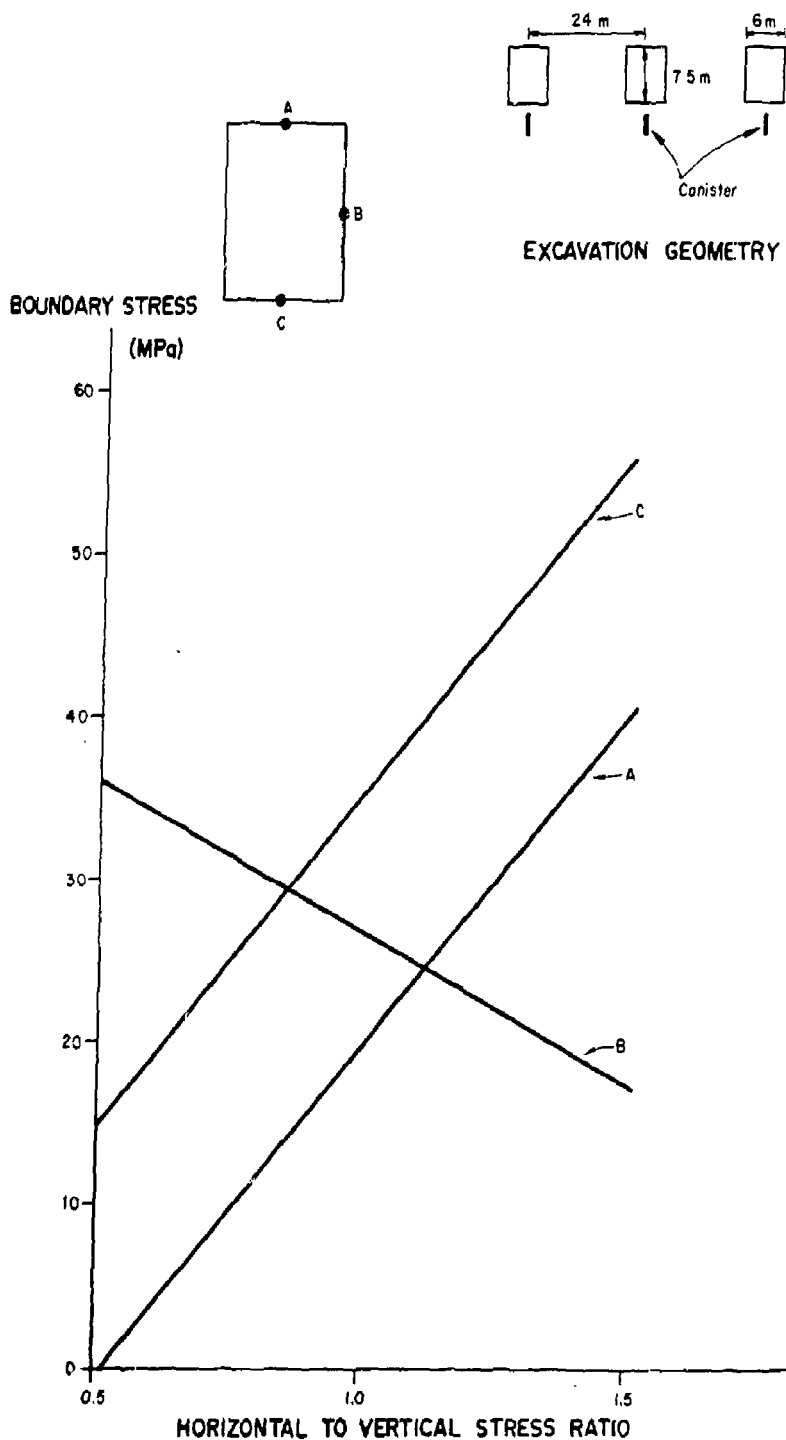
FIGURE 2-10 Effect of insitu field stress ratio on boundary
stresses for base case
Source: Hardy and Hocking, 1977.

vertical in situ stress field ratio, whereas, the boundary
stress in the sidewall increases with a decreasing stress
ratio.   Hence, it is very important to know at least the
ratios of the major principal stresses, and their direction.
At the present time, this information is not available.

Thermally Induced Stresses

It is possible, using a thermal-mechanical analysis, to perform a series of parametric studies in order to determine optimum size, shape, support of the rooms, canister location, and placement sequence. At this point, such studies are useful primarily from a scoping viewpoint; that is, to reveal the relative effect of changing one parameter while keeping all others constant. Such a study was done by Hardy and Hocking (1977), and it is felt worthwhile to discuss some of the results. These parametric studies have all been conducted on the base case, shown in Figure 2-8. Note that this is the same geometry, essentially, as was assumed in the PBQ&D Study. The temperature distribution around the room for an elapsed time of five years is illustrated as contours in Figure 2-11. Note that the contours should be perpendicular to the opening. The fact that they are not is due to the modeling procedure used. The areal thermal loading in this case was 25 watts per square meter, and the air in the room was analyzed as if it was stagnant and no convection or radiation heat-transfer mechanisms were modeled. The thermal stresses at various points in the basalt around the room are illustrated in magnitude and direction in Figure 2-12. The magnitude of the stresses are measured between the ends of the crosses; tensile stresses being denoted by arrowheads. Only thermal stresses are presented with no account being taken of in situ stress fields.

TEMPERATURE FIXED AT SURFACE
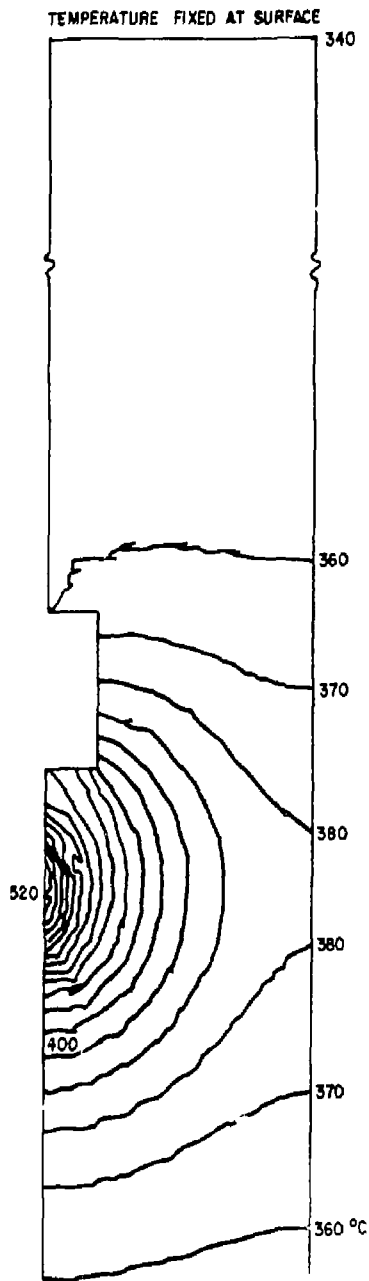
FIGURE 2-11   Temperature contours for elapsed time of 5 years
               areal thermal loading of 25W/M2
               Source: Hardy and Hocking, 1977.
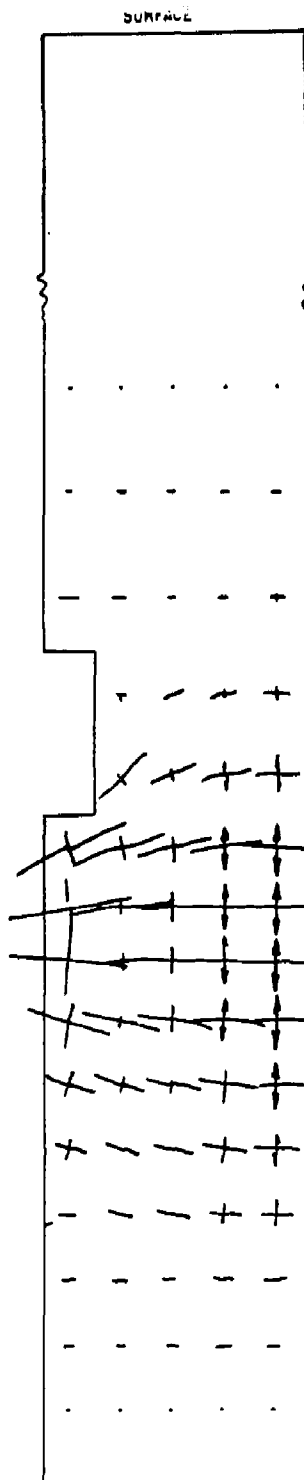
FIGURE 2-12 Stresses for elapsed time of 5 years-areal
thermal loading of 25W/M2
Source: Hardy and Hocking, 1977.

As can be seen in Figure 2-13, rather high stresses occur in the corners of the room. It must be kept in mind, however, that no reduction in modulus or change of thermal properties has been introduced to take into account the blasting damage around the room.

The variation in boundary stresses for the three points a, b, and c, described earlier, are shown in Figure 2-14 as a function of basalt properties (Poisson's ratio, Young's modulus, and coefficient of linear thermal expansion). A reduction of Poisson's ratio from 0.3 to 0.1 results in a maximum reduction (point c) of thermal stress by about 11%. The thermal stresses vary linearly, with both Young's modulus and the coefficient of linear thermal expansion. This suggests that a good knowledge of Poisson's ratio is not necessary, whereas it is of great importance to know the appropriate coefficient of linear expansion and Young's modulus.

Using this approach, one can also examine the influence of room shape and the influence of room spacing. Various shapes can significantly affect the boundary stresses in the roof and floor of the room. The effect is somewhat less on the side. A summary showing a comparison of boundary stresses at selected points for various configurations and loading is shown in Table 2-6. These numbers should all be compared with the base case shown in the first row.
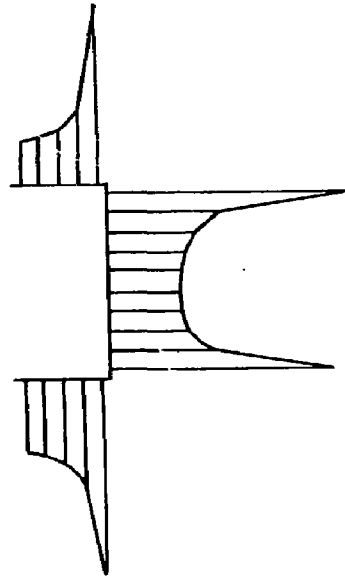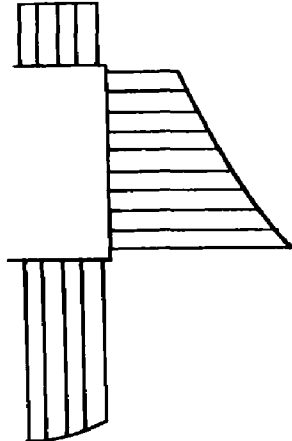
BOUNDARY STRESSES INITIAL   BOUNDARY TEMPERATURES   BOUNDARY STRESSES TOTAL
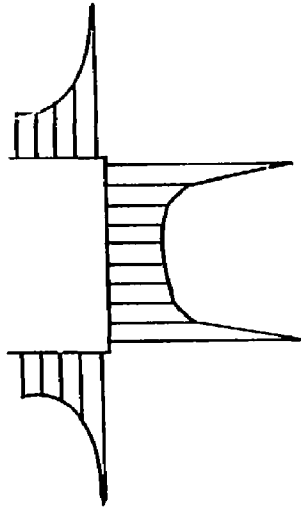
Scale: 1 Cm Represents 2.0 Meters,   1 Cm Represents 25. MPA,   1 Cm Represents 50 Degs. Celsius

FIGURE 2-13 Boundary stresses and temperatures for central excavation at an elapsed time of 5 years-25 W/M2 at 1000m depth
Source: Hardy and Hocking, 1977.

2-50
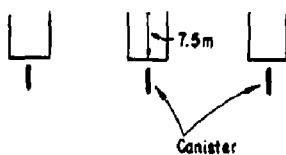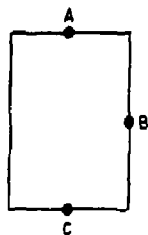
EXCAVATION GEOMETRY

BOUNDARY STRESS (MPa)

POISSON'S RATIO

BOUNDARY STRESS (MPa)

COEFFICIENT OF LINEAR
THERMAL EXPANSION
$(\times 10^{-6}/°K)$

YOUNG'S MODULUS
$(\times 10^{4} \text{ MPa})$
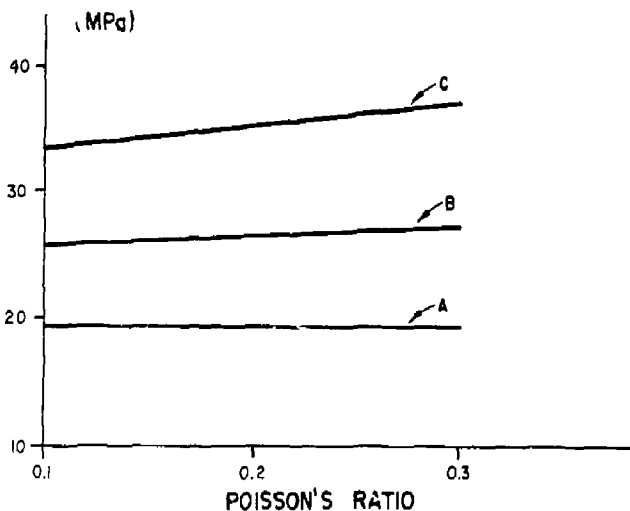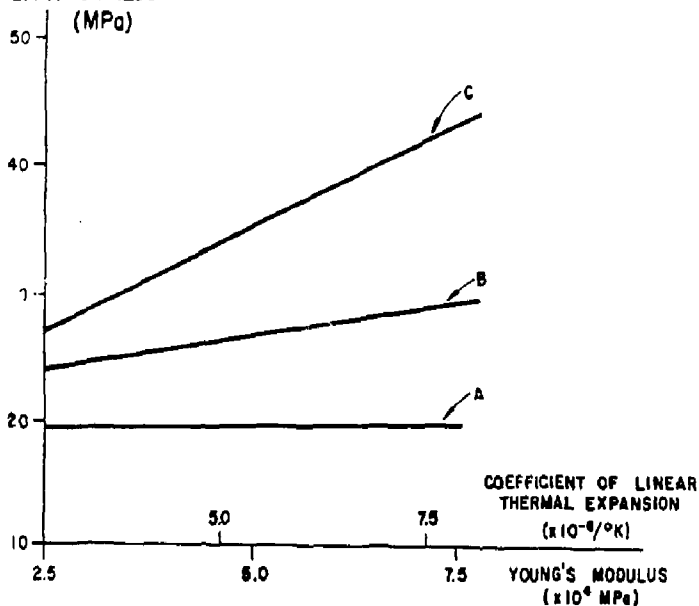
FIGURE 2-14   Effect of basalt thermomechanical properties
on stresses for the base case.
Source: Hardy and Hocking, 1977.

TABLE 2-6   Comparison of Boundary Stresses at Selected Points
for Various Configurations and Loadings

Location
Tangential room stress (MPa)**

Condition	A*	B	C
Base case	19.5	26.6	34.9
Thermal loading 50 W/m^2	19.5	32.0	50.3
Depth 1400 M	27.3	35.1	42.6
E = Twice base case	19.8	32.0	51.4
Poisson's ratio 0.3	19.7	27.0	36.8
Poisson's ratio 0.1	19.5	25.9	33.2
Insitu horizontal 0.5 vertical	- 0.7	36.0	14.7
Insitu horizontal 1.5 vertical	39.7	17.3	55.1
Canister relocation	24.8	19.9	31.0
Room shape	64.2	30.0	34.1
Canister placement sequence	23.8	26.3	41.2
At end of retrieval period (25 years)	45.9	20.4	66.4

*From Figure 2-13
**1 MPa = 145 lbs/in^2

SOURCE: Hardy and Hocking, 1977

In conclusion, one can presently perform scoping studies such as have been described by Hardy and Hocking to provide an indication of the importance of various variables on the stress distribution around an underground excavation. One can investigate in situ stress, the induced stress due to the excavation, and thermal stress. They should be considered at this point as strictly qualitative results and not appropriate for detailed design due to lack of appropriate input data. However, they suggest which parameters need to be measured accurately.

2.11 MECHANICAL PROPERTIES OF INTACT ROCK

This section describes the mechanical properties (rock strength, Young's modulus, and Poisson's ratio) of basalt. Rather little information is available for these properties whether for intact rock or the rock mass.

The available data, however, is for intact rock samples. As shown in Figure 2-15, the rocks which are classified as basalts have a very wide range of compressive strengths and moduli and, therefore, it is not possible to generalize or use a generic basis for any analysis.

Tables 2-7, 2-8, 2-9 and 2-10 are summary sheets compiled by the Office of Nuclear Waste Isolation, 1978. It was noted that the information base is rather small and that there was a wide variation in properties within the generic term "basalt." The modulus varies between 5 and 16 x 10^6 psi (34.5-110GPa), for example. More detailed values for Dresser basalt are given in Tables 2-11 and 2-12 for tests conducted under atmospheric temperature and pressure conditions. As might be expected, the strength increases with the confining pressure. Engineering data for basalts tested from Amchitka Island are given in Tables 2-13 and 2-14. It is noted that these data are for dry rocks. Figure 2-16 shows the significant effect of moisture on the compressive and tensile
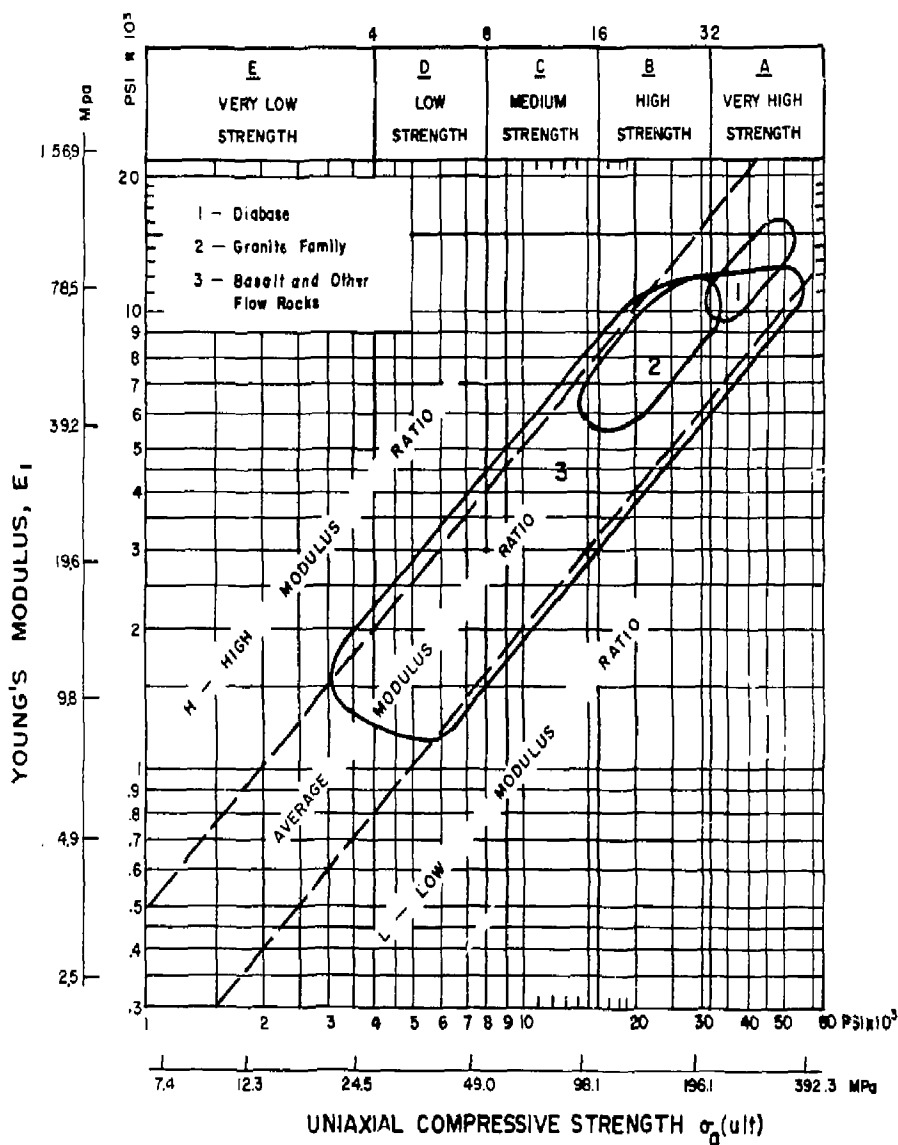
FIGURE 2-15   Engineering classification for intact rock—
summary plot igneous rocks, 176 specimens
Source: Deere et al, 1966.

TABLE 2-7   Intact properties of Dresser basalt.

BASIC PARAMETERS

Type of Property	Parameter	MKS Units
Index	Unit Weight	3010.2 kg/m^3
	Natural moisture content (intact)	--%
	Porosity (rock mass)	0.19%
Stress-strain	Young's Modulus	93.1GPa
	Poisson's Ratio	0.264
	Bulk Modulus	
	Shear Modulus	4.15GPa
Strength	Cohesion 10.34-24.14 Friction Angle MPa range	
	Uniaxial Compressive Strength	440.7MPa
	Tensile Strength	22.1MPa
Thermal	Coefficient of Linear Thermal Expansion	8.9x10^{-7}/°C
	Heat Capacity	.96 J/g/°C
	Thermal Conductivity	1.30 w/m°K
Hydrological	Horizontal Permeability	
	Vertical Permeability	

SOURCE: Office of Nuclear Waste Isolation, 1978

Table 2-8   Intact properties of Amchitka Island dense basalt.

BASIC PARAMETERS

Type of Property	Parameter	MKS Units
Index	Unit Weight	2729.8 kg/m^3
	Natural moisture content (intact)	--%
	Porosity (rock mass)	2.8%
Stress-strain	Young's Modulus	61.1GPa
	Poisson's Ratio	0.19
	Bulk Modulus	32.8GPa
	Shear Modulus	25.7GPa
Strength	Cohesion 10.34-24.14 Friction Angle MPa range	60 degrees
	Uniaxial Compressive Strength	250MPa
	Tensile Strength	15.5MPa
Thermal	Coefficient of Linear Thermal Expansion	$8.90 \times 10^{-7}/°C$
	Heat Capacity	.96 J/g/$°C$
	Thermal Conductivity	1.30 w/m°K
Hydrological	Permeability	.0205 m/day

TABLE 2-9   Intact properties of Nevada test site basalt.

BASIC PARAMETERS

Type of Property	Parameter	MKS Units
Index	Unit Weight	2689.8 kg/m^3
	Natural moisture content (intact)	
	Porosity (rock mass)	4.6%
Stress-strain	Young's Modulus	34.9GPa
	Poisson's Ratio	0.32 --
	Bulk Modulus	
	Shear Modulus	
Strength	Cohesion 10.34-24.14 Friction Angle MPa range	
	Uniaxial Compressive Strength	148MPa
	Tensile Strength	13.1MPa
Thermal	Coefficient of Linear Thermal Expansion	
	Heat Capacity	
	Thermal Conductivity	
Hydrological	Horizontal Permeability	
	Vertical Permeability	

SOURCE: Office of Nuclear Waste Isolation, 1978

TABLE 2-10 Intact properties of Columbia River group basalt.

BASIC PARAMETERS

Type of Property	Parameter	MKS Units
Index	Unit Weight	2403-3085 kg/m^3
	Natural moisture content (intact)	
	Porosity (rock mass)	
Stress-strain	Young's Modulus	55.2-110GPa
	Poisson's Ratio	0.22-0.30
	Bulk Modulus	
	Shear Modulus	
Strength	Cohesion 10.34-24.14 Friction Angle MPa range	14.5-38.6MPa 45°-60°
	Uniaxial Compressive Strength	193.1-400.0MPa
	Tensile Strength	12.41-24.14MPa
Thermal	Coefficient of Linear Thermal Expansion	1.67×10^{-6} °C^{-1}
	Heat Capacity	.72-.96 J/g/°C
	Thermal Conductivity	1.00-1.35 w/m°K
Hydrological	Permeability	9.67×10^{-6}-3.87×10^{-5} μ m/sec

SOURCE: Office of Nuclear Waste Isolation, 1978

TABLE 2-11 Dresser Basalt test results
(Kreck et al, 1964)

Property[1]		Block No. 17		Block No. 28		Block No. 68		Composite	
		Mean	CV[2]	Mean	CV[2]	Mean	CV[2]	Mean	CV[2]
Porosity. . . . . pct . .		0.16	9.0	0.15	0.05	0.25	12.7	0.19	57.3
Permeability. . . . . .um/sec . .		([3])	−	([3])	−	([3])	−	([3])	−
Density . . . . g/cm^3 . .		3.02	0.1	3.01	0.7	3.01	0.1	3.01	0.5
Shore hardness.		95.0	3.1	93.2	2.5	94.2	1.9	94.1	2.6
Compressive strength. . . . . .MN/m^2. . .		479	7.91	413	10.7	429	9.16	440	11.0
Do . . . . 10^3 psi . .		69.5	7.91	59.9	10.7	62.2	9.16	63.9	11.0
Compressive Young's Modulus . . GN/m^2 . .		88.5	2.43	82.1	2.18	87.5	2.42	86.1	4.1
Do . . . . 10^6 psi . .		12.8	2.43	11.9	2.18	12.7	2.42	12.5	4.1
Tensile strength. . . . . . . .MN/m^2. . .		22.9	24	24.0	38.0	17.6	57.0	22.1	39.7
Do . . . . 10^3 psi . .		3.33	24	3.48	38.0	2.56	57.0	3.20	39.7
Tensile Young's modulus . . . .GN/m^2. . .		133	9	121	21	105	23	119	20.2
Do . . . . 10^6 psi . .		19.2	9	17.6	21	15.3	23	17.3	20.2
Pulse velocity. . . . . .km/sec . .		6.77	0.3	6.67	0.3	6.72	0.3	6.72	0.7
Bar velocity. . . . . .km/sec . .		6.12	0.2	5.99	0.4	6.04	0.5	6.05	1.0
Torsional velocity. . . . . . .km/sec . .		3.86	0.2	3.76	0.4	3.80	0.6	3.80	1.2
Dynamic Young's modulus[4] . . .GN/m^2. . .		113	0.5	108	1.5	109	1.1	110	2.5
Dynamic shear modulus[1] . . . .GN/m^2. . .		44.9	0.4	42.5	1.5	43.4	1.3	43.6	2.6
Poisson's ratio[4].		0.261	1.4	0.266	1.1	0.266	1.5	0.264	1.6

[1]Specimen prepared with the long axis perpendicular to the top face (along Z-axis)

[2]Coefficient of variation, percent.

[3]Less than 1×10^{-4} um/sec.

[4]Calculation is based on the assumption of isotropy.

TABLE 2-12 Properties of Dresser basalt
(Morrell and Larson, 1974) and (Avco, 1972)

Commercial Name. . . . . .DRESSER BASALT

Rock Type. . . . . .Basalt

Locality . . . . .Dresser, Wisconsin

Compressive Strength, MPa.   439

Tensile Strength, MPa.   14

Shore Hardness, Scleroscope units. 85.8

Apparent Density, g/cm^3. . . . .   3.029

Static Young's Modulus, GPa. 98.3

Longitudinal Velocity, mps 6,669

Bar Velocity, mps. 5,949

Shear Velocity, mps. 3,739

Dynamic Young's Modulus, GPa 107.2

Poisson's Ratio.   0.2725

Shear Modulus, GPa 42.3

Tensile Fracture Stress, n/m^2. . . . . 1.45×10^7

Thermal Conductivity Coefficient A . . . . 1.45×10^{-5}

Thermal Conductivity Coefficient B . . . .   -.15

Coefficient of Thermal Expansion, $°C^{-1}$ . . . . 3×10^{-6}

TABLE 2-13 Average engineering properties of water saturated
Amchitka Island rocks by major rock types in the recognized formations
(Sharp, 1972)

(2) LEGEND (See Notes)	(3) INCREASED MOISTURE (vol. pct.)	(4) COMPRESSIVE STRENGTH (MPa)	(5) TENSILE STRENGTH (MPa)	(6) YOUNG'S MODULUS GPa	(7) VIOLENCE OF RUPTURE
CHITKA POINT FORMATION: HORNBLENDE PYROXENE ANDESITE - Tcpl-1					
AVG:	3.5	108.69	10.61	22.90	3.1
MAX:	15.6	198.25	17.57	56.21	8
MIN:	1.2	9.34	.66	2.00	1
N:	26	.14	.06	137.93	23
S:	4.0	62.05	5.03	14.76	2.0
V:	115.9	.40	.33	445.51	58.3
CHITKA POINT FORMATION: DENSE FLOW BRECCIA - Tcpl-11					
AVG:	6.4	73.95	11.86	17.79	2.8
MAX:	10.4	104.72	18.37	31.72	4
MIN:	2.4	47.23	5.35	10.21	2
N:	10	.03	.01	34.48	5
S:	2.9	22.86	9.20	8.34	0.8
V:	46.3	.21	.54	324.14	29.9
CHITKA POINT FORMATION: HORNBLENDE ANDESITE BRECCIA - Tcp - 1					
AVG:	7.7	48.42	3.01	14.62	2.0
MAX:	17.9	117.92	6.01	25.24	3
MIN:	3.2	13.32	1.47	4.00	1
N:	9	.06	.02	55.17	7
S:	4.5	32.57	2.59	8.21	1.0
V:	57.9	.46	.59	388.27	50.2
CHITKA POINT FORMATION: TUFF BRECCIA - Tcp-11					
AVG:	14.6	49.83	3.06	9.03	2.8
MAX:	31.4	116.05	2.12	20.97	7
MIN:	6.7	4.49	.70	1.45	1
N:	26	.15	.06	151.72	23
S:	7.3	32.42	1.74	5.59	1.6
V:	50.1	.45	.39	424.13	57.2
BANJO POINT FORMATION: BRECCIA - Tcp					
AVG:	16.6	34.44	6.49	6.76	1.6
MAX:	29.2	157.96	17.11	19.03	4
MIN:	3.7	9.33	.92	1.79	1
N:	18	.08	.05	68.97	11
S:	7.2	42.58	7.38	5.66	1.1
V:	43.2	.85	.78	580.00	68.5
DENSE BASALTS - Tb					
AVG:	2.8	123.21	15.17	30.14	5.1
MAX:	7.7	196.72	17.54	77.31	9
MIN:	1.1	75.48	12.79	14.34	3
N:	10	.07	.01	68.97	10
S:	2.2	38.22	3.36	18.76	.0

TABLE 2-13   (Continued)

(2) LEGEND (See Notes)	(3) INCREASED MOISTURE (vol. pct.)	(4) COMPRESSIVE STRENGTH (MPa)	(5) TENSILE STRENGTH (MPa)	(6) YOUNG'S MODULUS (GPa)	(7) VIOLENCE OF RUPTURE
AMCHITKA FORMATION:		KIRILOF POINT GLASSY BRECCIAS - TAkb-1			
AVG:	8.1	19.99	2.72	6.90	1.1
MAX:	10.7	33.24	14.03	16.00	2
MIN:	2.7	12.95	1.86	2.28	1
N:	14	.05	.04	48.28	7
S:	2.8	8.06	.69	6.07	0.4
V:	34.4	.28	.18	606.90	33.2
AMCHITKA FORMATION:		KIRILOF POINT PILLOW LAVAS - TAkb-11			
AVG:	9.2	111.90	--	16.28	3.7
MAX:	10.5	130.34	--	26.97	4
MIN:	7.6	95.67	--	16.97	3
N:	5	.02	--	20.69	3
S:	1.1	18.34	--	2.28	0.6
V:	11.9	.11	--	192.41	15.6
AMCHITKA FORMATION:		DENSE OLDER BRECCIAS - TAb			
AVG:	3.3	196.56	18.15	44.90	6.7
MAX:	6.9	304.87	23.65	98.48	6
MIN:	0.4	37.90	13.32	11.79	3
N:	17	.08	.03	75.86	11
S:	1.8	84.08	4.66	24.90	1.6
V:	56.0	.30	.18	382.07	29.5
EAST CAPE QUARTZ DIORITE:		Tcc			
AVG:	1.7	168.62	12.34	36.28	5.7
MAX:	3.0	264.36	15.86	99.17	9
MIN:	0.8	41.34	8.07	11.17	3
N:	37	.21	.04	213.79	31
S:	0.5	62.43	3.13	17.52	1.3
V:	23.0	.26	.17	345.51	24.7

NOTES: The average (AVG), maximum (MAX), and minimum (MIN) values
determined from the number (N) of specimens in each group,
with the standard deviation (S) and percentage variation (V),
are given in acsending order for each group property across
the table. Values in Column 5 represent the increased moisture
in the saturated state (after 7 days submersion) over that air
dried (14 days) in volume percent.

TABLE 2-14 Average engineering properties of air dried Amchitka Island rock types within the various recognized formations

(1) NO.	(2) LEGEND (See Notes)	(3) SOIL'S HARDNESS	(4) APPARENT SPECIFIC GRAVITY	(5) AIR DRIED PORE SPACE (vol.pct.)	(6) COMPRESSIVE STRENGTH (MPa)	(7) TENSILE STRENGTH (MPa)	(8) YOUNG'S MODULUS (GPa)	(9) POISSON'S RATIO	(10) RIGIDITY MODULUS (GPa)	(11) BULK MODULUS (GPa)	(12) LONGITUDINAL VELOCITY (mps)	(13) SHEAR VELOCITY (fps)	(14) VIOLENCE OF RUPTURE	(15) STRAIN ENERGY (MPa)	(16) INTERNAL FRICTION (deg)	(17) MAGNETIC SUSCEPTIBILITY (emsu/cc)
	CHITKA POINT FORMATION: HORNBLENDE PYROXENE ANDESITE - Tcp-1															
1	AVG:	6.0	2.67	3.5	-288.66	14.86	47.72	0.23	19.38	29.45	4974.95	2683.46	6.3	.48	58	2,662
	MAX:	7.0	2.91	15.6	300.22	23.17	91.79	0.34	36.90	109.31	6908.60	3257.09	9	.93	85	3,385
	MIN:	3.5	2.34	1.2	61.65	4.91	11.03	0.17	4.14	10.83	2468.88	1767.23	1	.15	20	1,298
	N:	36	105	26	.17	.37	172.41	18	124.14	124.14	7.92	3.05	85	.17	25	12
	S:	1.2	0.13	4.0	74.97	5.13	19.31	0.06	8.97	21.93	1152.14	579.73	2.3	.22	15.0	595.0
	V:	20.4	4.9	115.9	.25	.24	279.31	27.40	295.86	477.24	7.07	6.58	36.1	.31	25.6	22.5
	CHITKA POINT FORMATION: DENSE FLOW BRECCIA-Tcp1-11															
2	AVG:	5.2	2.57	6.4	126.67	15.03	30.83	0.18	13.03	16.07	4479.95	2298.50	5.5	.30	62	1,904
	MAX:	7.5	2.76	10.4	185.16	21.61	54.00	0.22	23.10	27.24	5446.78	2910.54	9	.56	70	3,274
	MIN:	2.5	2.38	2.4	81.57	8.12	21.24	0.14	9.03	11.03	3712.16	1948.90	1	.15	54	542
	N:	18	38	10	.06	.17	55.17	7	48.28	48.28	3.05	1.52	33	.05	8	6
	S:	1.2	0.11	2.9	36.37	4.32	10.69	0.03	4.76	5.86	693.72	384.05	2.6	.14	6.5	1,102.8
	V:	23.0	4.2	46.3	.20	.20	239.58	15.50	231.65	245.65	4.72	5.09	47.3	.32	10.5	57.8
	CHITKA POINT FORMATION: HORNBLENDE ANDESITE BRECCIA - Tcp-1															
3	AVG:	4.8	2.47	7.7	91.37	10.35	34.28	0.17	14.62	17.31	3798.11	2754.78	3.7	.15	61	1,953
	MAX:	6.5	2.59	17.9	138.80	13.77	56.90	0.19	23.93	30.62	4180.03	3335.73	8	.26	82	2,820
	MIN:	3.5	2.07	3.2	21.41	4.35	8.14	0.15	12.14	13.31	3410.71	2457.90	1	.004	40	534
	N:	10	37	9	.05	.15	48.28	6	41.38	41.38	1.22	.91	29	.05	6	4
	S:	0.8	0.13	4.5	45.22	2.49	14.76	0.02	4.21	5.86	387.10	502.92	2.4	.09	14.1	326.3
	V:	17.2	5.1	57.9	.34	.17	297.52	11.16	174.96	208.27	3.11	5.58	64.1	.41	23.2	16.7
	CHITKA POINT FORMATION: TUFF BRECCIA - Tcp-11															
4	AVG:	4.2	2.24	14.6	82.30	6.02	23.17	0.22	9.52	13.79	3181.50	1937.31	3.1	.18	58	2,353
	MAX:	7.5	2.55	31.4	134.00	14.28	60.28	0.43	16.48	61.72	4351.32	2444.19	8	.46	80	2,930
	MIN:	3.5	1.73	6.7	17.05	1.06	4.07	0.11	3.10	3.24	1828.80	1380.13	1	.003	30	1,487
	N:	40	128	26	.17	.48	172.41	21	144.83	144.83	6.40	2.44	99	.17	25	11
	S:	1.7	.19	7.3	48.17	3.64	11.52	0.10	3.93	12.90	701.95	388.62	2.4	.16	12.9	404.1
	V:	40.6	8.7	50.1	.40	.42	343.17	44.05	338.20	553.44	6.71	6.04	77.5	.59	22.2	17.2
	BANJO POINT FORMATION: BRECCIA - Tbp															
5	AVG:	4.0	2.27	16.6	118.83	6.81	29.38	0.22	12.07	17.59	3218.69	2155.85	2.5	.28	60	2,554
	MAX:	7.5	3.09	29.2	339.49	29.54	81.03	0.37	34.48	66.00	5651.60	3141.88	8	.92	70	3,565
	MIN:	1.5	1.93	3.7	9.18	1.43	3.31	0.11	3.03	3.24	1177.14	1254.56	1	.003	40	787
	N:	35	82	18	.10	.34	96.55	8	57.17	55.17	6.40	1.22	68	.09	15	10
	S:	1.4	0.29	7.2	125.96	7.00	28.76	0.10	13.03	31.86	1255.47	818.39	2.4	.33	16.3	♦ 907.4
	V:	35.4	12.8	43.2	.73	.71	396.07	43.90	566.20	2548.19	11.89	11.58	96.6	.79	23.7	35.5

TABLE 2-14 (Continued)

(1) NO.	(2) LEGEND (See Notes)	(3) SOIL'S HARD-NESS	(4) APPARENT SPECIFIC GRAVITY	(5) ...TED ...SPACE (...pct.)	(6) COMPRESSIVE STRENGTH (MPa)	(7) TENSILE STRENGTH (MPa)	(8) YOUNG'S MODULUS (MPa)	(9) POISSON'S RATIO	(10) RIGIDITY MODULUS (GPa)	(11) BULK MODULUS (GPa)	(12) LONGITUDINAL VELOCITY (mps)	(13) SHEAR VELOCITY (mps)	(14) VIOLENCE OF RUPTURE	(15) STRAIN ENERGY (MPa)	(16) INTERNAL FRICTION (deg)	(17) MAGNETIC SUSCEPTIBILITY (emu/cc)
							DENSE BASALTS - Yb									
6	AVG:	5.4	2.73	2.8	249.91	15.51	61.10	9.19	25.65	32.83	4415.33	3234.84	5.9	.56	60	2,730
	MAX:	7.5	2.93	7.7	356.35	25.43	91.93	0.31	27.65	51.93	5860.39	3630.17	9	.99	80	6,020
	MIN:	2	2.17	1.1	124.45	6.56	32.21	0.17	21.52	27.38	3229.05	2920.60	1	.12	30	1,088
	N:	28	63	10	.06	.30	62.07	7	48.28	48.28	4.27	1.22	53	.06	70	5
	S:	2.1	0.21	2.2	73.20	5.18	16.90	0.01	5.66	8.34	884.22	293.83	2.8	.28	15.3	1,587.2
	V:	38.7	7.9	80.3	.20	.23	190.34	5.26	167.03	170.00	6.10	2.77	47.7	.34	25.6	72.3
						ANCHITKA FORMAT. ...: KIRILOF POINT GLASSY BRECCIA - TALb-1											
7	AVG:	4.7	2.24	8.1	38.03	3.43	12.76	0.27	5.03	9.24	3317.14	1726.39	1.4	.11	63	907
	MAX:	7.5	2.34	10.7	55.65	5.12	30.00	0.40	11.93	20.76	4421.12	2315.87		.50	70	2,539
	MIN:	3.5	2.15	2.7	18.79	2.15	4.41	0.20	4.21	6.28	2396.64	1404.04	1	.02	48	401
	N:	25	63	14	.07	.36	68.97	6	41.38	41.38	4.57	1.22	60	.07	10	6
	S:	0.9	0.04	2.8	10.79	.70	6.76	0.07	2.83	5.38	699.82	404.77	0.8	.14	8.7	8,232
	V:	20.1	1.8	34.6	.20	.14	383.86	26.60	304.89	367.72	6.41	7.16	51.0	.88	23.77	90.5
						ANCHITKA FORMATION: KIRILOF POINT PILLOW LAVAS - TALb-11											
8	AVG:	5.8	2.42	9.2	161.76	13.89	30.76	0.18	13.03	16.00	3930.70	2433.22	6.8	.46	60	2,976
	MAX:	7.0	2.54	10.5	186.52	23.90	39.03	0.38	16.69	19.72	4621.07	---	9	.77	70	3,078
	MIN:	4.5	2.32	7.6	148.90	6.63	24.55	0.17	12.14	14.90	3331.77	---	3	.29	40	2,875
	N:	10	25	5	.02	.13	20.69	1	13.79	13.79	1.22	.3048	22	.02	3	2
	S:	1.3	0.07	1.1	21.44	4.66	7.45	0.01	3.24	3.43	461.11	0	1.8	.22	17.3	---
	V:	22.9	3.0	11.9	.09	.22	167.45	5.56	134.00	136.00	5.12	0	23.6	.33	28.9	---
						ANCHITKA FORMATION: DENSE OLDER BRECCIA - TAb											
9	AVG:	6.7	2.77	3.3	258.85	20.01	46.64	0.25	18.69	31.10	4960.01	2700.22	6.9	.76	67	3,165
	MAX:	7.3	2.95	8.9	373.38	36.00	69.72	0.38	29.31	42.97	8096.00	3088.54	9	1.39	75	7,247
	MIN:	2.5	2.36	0.4	65.71	8.01	18.00	0.19	12.69	29.03	3219.60	2200.05	1	.12	44	727
	N:	29	72	17	.11	.28	110.34	10	68.97	68.97	5.49	2.13	58	.11	17	8
	S:	0.9	0.08	1.8	93.67	7.22	15.72	0.06	5.59	5.93	833.32	316.99	2.2	.37	7.3	2,481.9
	V:	13.8	3.0	36.0	.25	.25	232.07	23.76	176.83	108.83	5.12	3.57	31.8	.34	10.9	78.4
						EAST CAPE QUARTZ DIORITE - Tqd											
10	AVG:	7.0	2.71	1.7	289.52	16.40	49.31	0.28	19.24	37.38	5040.59	2897.73	6.2	.59	64	2,646
	MAX:	7.0	2.86	3.0	332.39	27.69	76.76	0.40	45.80	131.03	6226.74	3450.03	9	1.04	70	3,607
	MIN:	6.5	2.58	0.8	49.42	7.87	19.66	0.11	13.38	15.24	3484.05	2441.45	1	.05	40	8,787
	N:	55	174	37	.23	.62	227.58	22	151.72	151.72	8.23	3.46	134	.23	34	16
	S:	0.2	0.05	0.6	49.49	4.29	12.49	0.07	6.48	28.07	534.31	252.07	2.3	.24	16.1	406.7
	V:	2.1	3.7	19.0	.21	.18	177.45	26.65	195.31	424.13	3.08	2.65	38.7	.28	25.2	18.7

NOTES: The average (AVG), maximum (MAX), and minimum (MIN) values determined from the number (N) of specimens in each group, with the standard deviation (s) and percentage variation (V), are given in descending order for each group property across the table. Values in Column 5 represent increased moisture in the saturated state (after 7 days submersion) over that air dried (14 days), in volume percent.

All samples air dried 14 days or submerged in water one week

WET COMPRESSIVE STRENGTH −10³ PSI

1:1.0
1:1.2
1:1.4
1:1.6
1:1.8
1:2.0
1:3.0

FOR ROCK TYPE OF VARIOUS GROUPS
SEE LEGEND BELOW

DRY COMPRESSIVE STRENGTH −10³ PSI
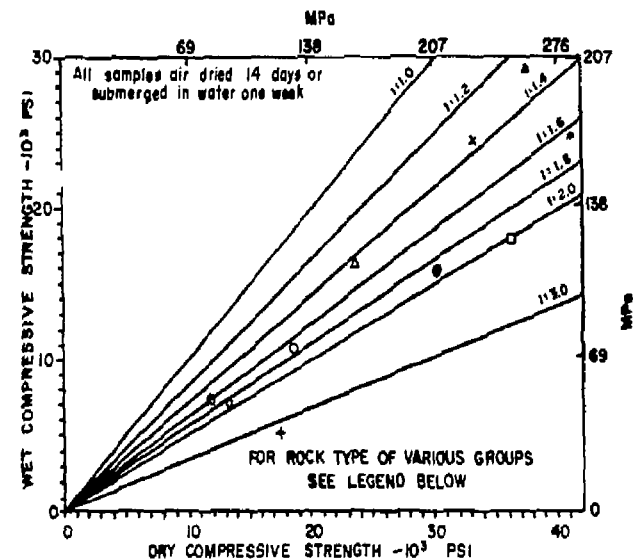
WET ·VS· DRY COMPRESSIVE STRENGTHS OF LOCAL ROCK

AVERAGE VALUES OF MAJOR FORMATIONAL AND LITHOLOGIC GROUPS

LEGEND

● −Tcp:: N−P ANDESITE   + −Tbp BANJO PT. BRECCIA   ▲ −TAbs: DENSE OLD BRECCIAS
○ −Tcp:: DENSE FLOW BRECCIA   ⊘ −Tb: DENSE BASALTS   X −TRd: QUARTZ DIORITE
□ −Tcp: N ANDESITE BRECCIA   ⊕ −TAbs: GLASSY BRECCIAS   ✴ −TAn: HORNFELS
◙ −Tcp: TUFF BRECCIA   ▲ −TAbs: PILLOW LAVAS

All samples air dried 14 days or submerged in water one week

WET TENSILE STRENGTH −10³ PSI

△ } NO DATA FOR THESE
◉ }   ROCK TYPES

1:1.0
1:1.2
1:1.4
1:1.6
1:1.8
1:2.0
1:3.4

FOR ROCK TYPE OF VARIOUS GROUPS
SEE LEGEND ABOVE

DRY TENSILE STRENGTH −10³ PSI

MPa
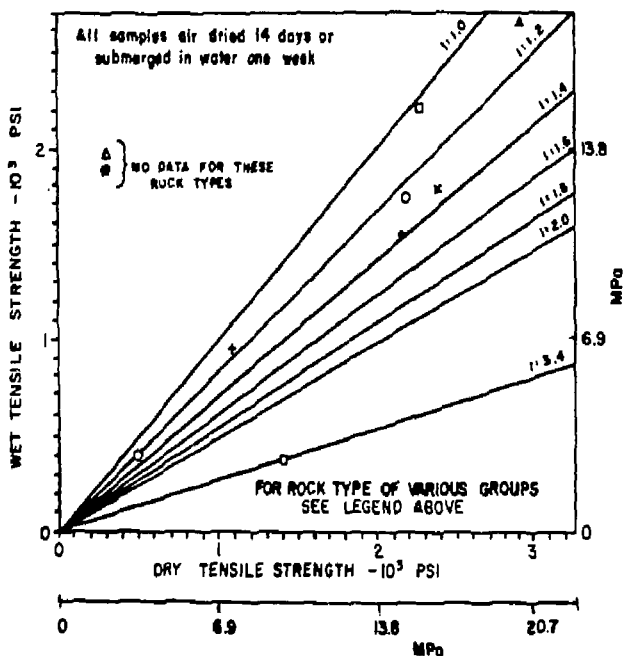
FIGURE 2-16 Wet vs. dry tensile strengths of local rock average
values of major formational and lithologic groups.
Source: Sharp, 1972.

strengths of Amchitka basalt. Data for basalt tested from the Nevada test site are shown in Figures 2-17 to 2-19. Figure 2-18 shows the relationship between strength and confining pressure for basaltic rocks of different porosities. A very high dependence of strength on the porosity is observed. Figure 2-19 shows variation of Poisson's ratio with confining pressure for NTS basalt. Notice that for a relatively large change in confining pressure, Poisson's ratio varies rather little. As suggested earlier from the scoping studies, this variation is probably not significant. Values for the strength for samples from the Hanford reservation are shown in Table 2-15. Of particular interest are the results from rock zone RM4 which illustrate the large effect of jointing on strength. Tables 2-16 and 2-17 and Figures 2-20 and 2-21 are for physical properties of Columbia Plateau basalts. As seen in Figures 2-20 and 2-21 there are very large variations in strength with porosity and density. Both of these values would depend very much on the position within the flow. The same type of behavior for test site basalt is shown in Figure 2-22. Because of this great variation, one must be very careful when attempting to determine and assign property values. Tables 2-18 and 2-19 summarize some values for elastic and strength properties of basaltic rock samples (Agapito et al, 1977, Rodriquez, 1970).
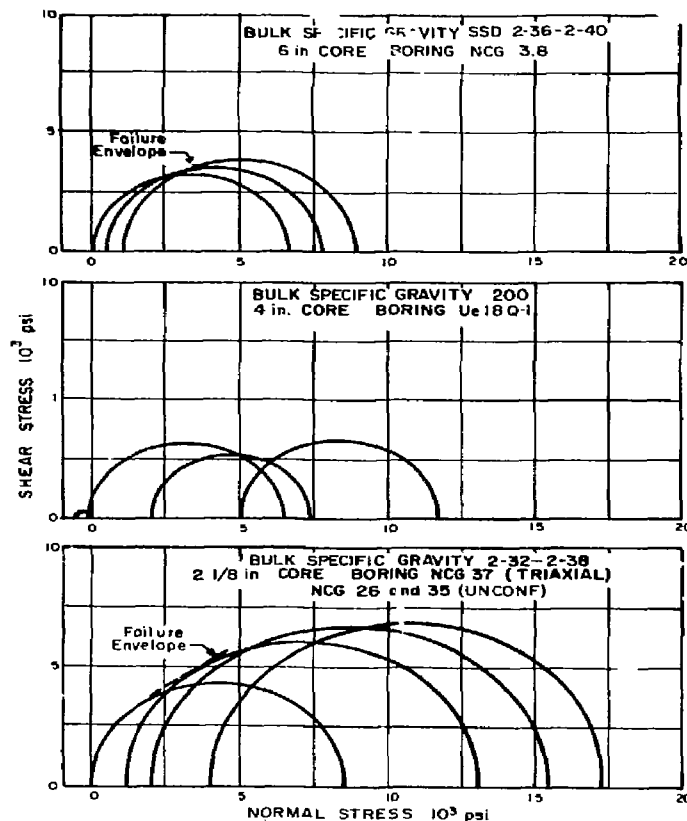
MOHR CIRCLES and FAILURE ENVELOPES
FOR HIGHLY VESICULAR BASALT
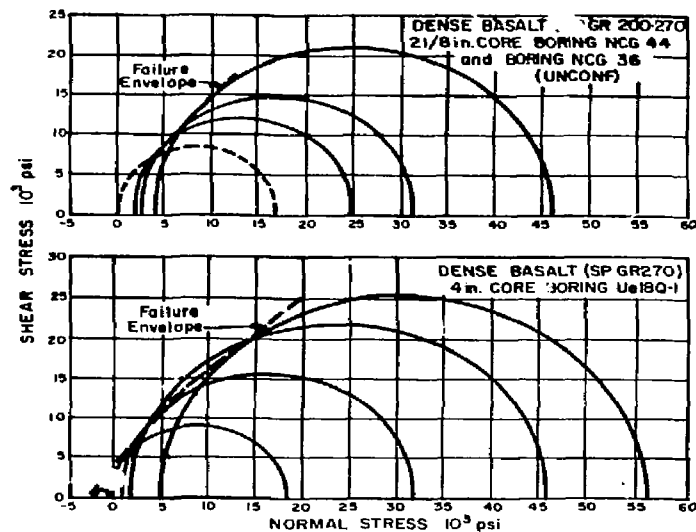
MOHR CIRCLES and FAILURE ENVELOPES
FOR DENSE BASALT

FIGURE 2-17   Mohr circles for dense and vesicular basalt
Source: Lutton, 1968.
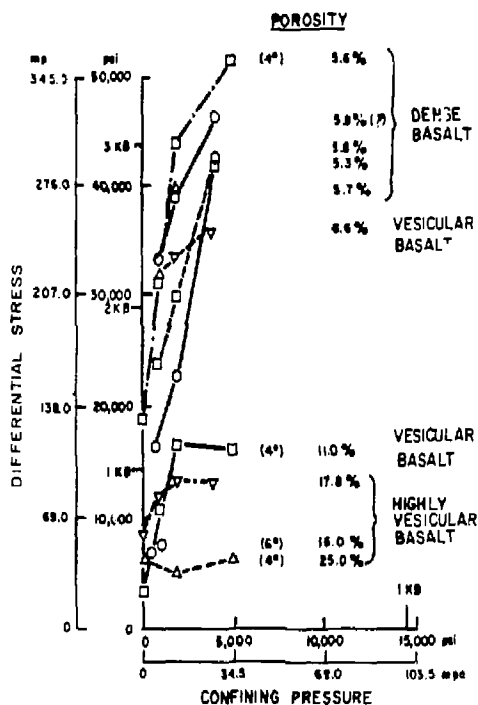
FIGURE 2-18 Relationship between strength and confined
pressure for basaltic rocks of different porosity.
Source: Lutton, 1968.
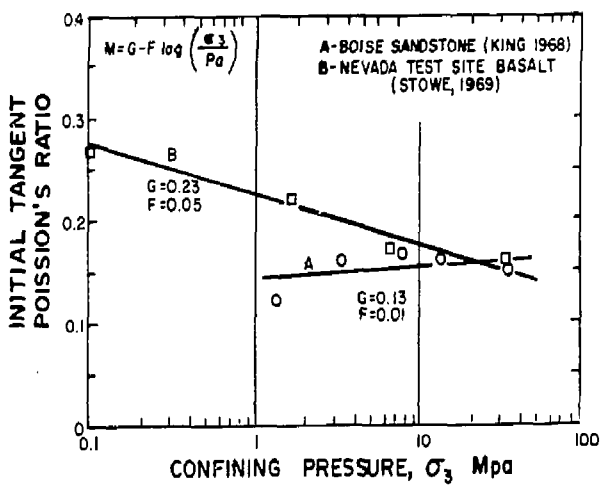
FIGURE 2-19   Variation of initial tangent Poisson's ratio
with confining pressure
Source: Stowe, 1969.

TABLE 2-15 Summary of triaxial compression strength tests
on core from the Hanford Reservation, DDH-1 tests
by Teledyne Terrametrics
(Agapito, Hardy and St. Laurent, 1977)

Rock Zone	Number of Tests	Confining Pressure MPa	Average Strength MPa
RM 1	3	0	212
	3	3.5	287
	3	7.0	305
	3	14.0	350
	3	21.0	400
RM 2 (Solid)	2	0	266
	2	7.0	361
	2	14.0	481
	1	21.0	562
	1	28.0	638
RM 1 (With Slip Planes)	1	0	143
	1	7.0	179
	1	14.0	252
	2	21.0	331
	2	28.0	390
RM 3 (All Specimens Contained	3	0	69
Many Open Vugs and Pores)	2	7.0	93
	3	14.0	145
	3	21.0	172
	3	28.0	152
RM 4 (Solid)	2	0	216
	2	7.0	307
	1	14.0	434
RM 4 (With Joints)	1	0	16
	1	7.0	168
	2	14.0	281
	3	21.0	310
	2	28.0	333

TABLE 2-16   Summary of rock properties
Bacon Siphon and Tunnel - second unit
DH-100 series samples
Columbia Basin Project
Source: Agapito et al, 1977

Specimen No. DH	Depth	Rock Type	Secant 1/ Elasticity GPa	Compressive Strength MPa	Fracture 2/ Mode	Absorption, Percent by Weight	Specific Gravity	Petrographic Laboratory No.
100	88.3	Basalt	43	81	Across matrix and structure	3.9	2.57	P-8527
100	101.9	Basalt	53	98	Across matrix and structure	3.7	2.61	P-8528
101	120.9	Basalt	23	216	Across matrix and structure	2.1	2.74	P-8529
100	148.7	Basalt	22	83	Across matrix and structure	3.9	2.58	P-8530
100	152.8	Basalt	22	137	Across matrix and structure	3.7	2.62	P-8531
100	181.6	Basalt	30	194	Across matrix and structure	2.5	2.65	P-8532

Notes:
   1/E is given at first cycle of loading, 7MPa stress.

   2/Pertains to samples failed in compression tests.

TABLE 2-17   Summary of rock properties
Bacon Siphon and Tunnel — second unit —
DH-200 series samples
Columbia Basin Project
Source: Agapito et al, 1977

Specimen No. D.H.	Depth 1/	Rock Type	E 2/ GPa	Poisson's Ratio 2/	Compressive Strength, MPa	Absorption by Weight	Specific Gravity	Porosity
200	133.21	basalt	45	0.09	176	1.6	2.76	4.4
200	135.58	basalt	74	0.16	204	0.8	2.78	2.2
200	148.75	basalt	59	0.05	109	4.1	2.56	10.4
200	149.55	basalt	49	0.31	39	5.3	2.46	12.9
200	166.06	basalt	54	0.10	125	1.5	2.73	4.2
200	166.42	basalt	55	0.14	104	1.5	2.73	4.0
205	232.69	basalt	58	0.14	180	1.5	2.68	4.2
205	233.50	basalt	66	0.22	192	1.1	2.70	3.1
205	235.54	basalt	36	0.10	179	2.3	2.65	6.0
205	239.53	basalt	3/	3/	139	3.1	2.58	8.0
205	239.31	basalt	3/	3/	125	3.7	2.54	9.4
207*	120.33	basalt	77	0.18	293	0.2	2.86	0.6
207*	133.60	basalt	72	0.26	229	0.3	2.88	0.9
207*	147.98	basalt	80	0.23	241	0.2	2.90	0.6

Notes:

1/Depth, in feet, is measured to the center of the test specimen.
2/Elasticity and Poisson's Ratio are given for first cycle loading at 7MPa.
3/No elasticity run on these test specimens due to large vesicles.
*No Petrographic analysis requested for Drill Hole 207.
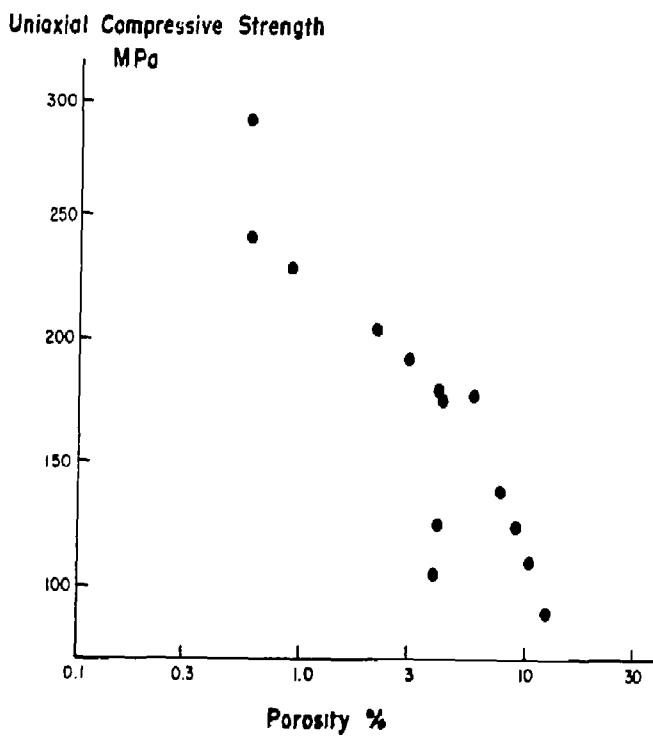
FIGURE 2-20 Compressive strength versus porosity Columbia
Plateau basalt Source: Agapito et al, 1977.
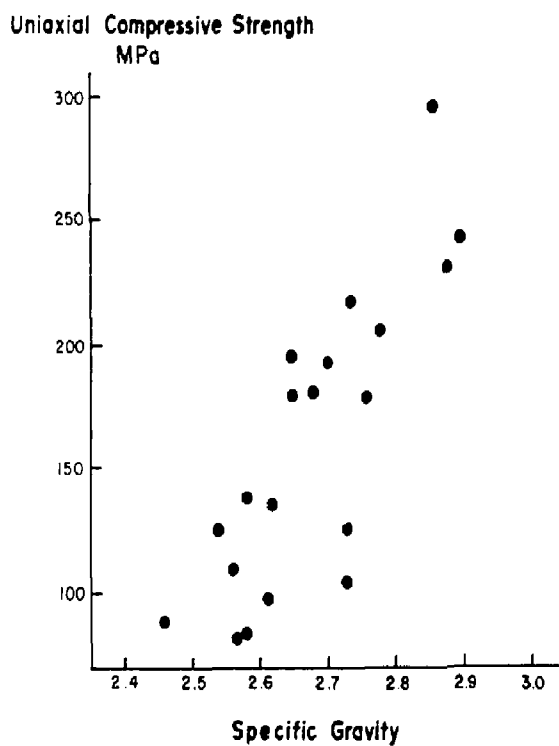
FIGURE 2-21 Compressive strength versus specific
gravity Columbia Plateau basalt
Source: Agapito et al, 1977.
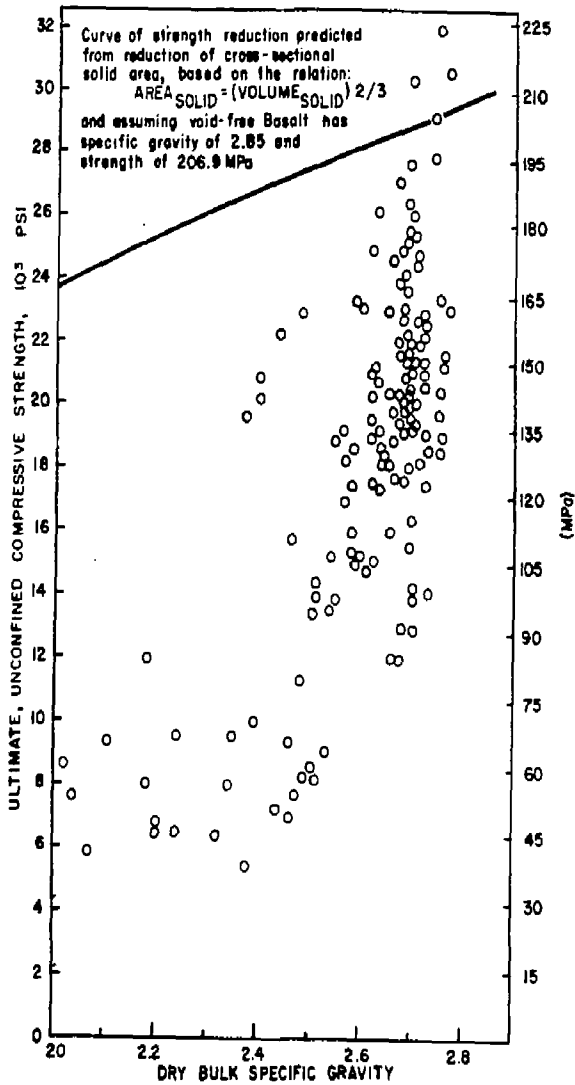
FIGURE 2-22 Relation of compressive strengths and
specific gravity.
Source: Sandia, 1962.

TABLE 2-18   Strength data on basalts

Rock Type	Crushing Strength MPa	Cohesive Strength MPa	Tan $\emptyset$	Reference
Basalt, Miocene, Oregon	169	32	1.2	8
Basalt, Miocene, Oregon	219	44	1.1	8
Hyperstene, Andesite	133	29	1.0	8
Hyperstene, Andesite	129	28	1.0	8
Basalt, Dresser	440	NA	NA	11
Basalt, Dresser	363	NA	NA	19
Basalt, Knippa	262	NA	NA	17

Source: Agapito et al, 1977

TABLE 2-19 Elastic Properties of Basaltic Rock

Rock Type	Young's Modulus GPa	Poisson's Ratio
Basalt, Ostritz,Germany	111.5	NA
Basalt, Champion Mine, Michigan	61	NA
Basalt, Champion Mine, Michigan	85	NA
Basalt, Dresser, Wisconsin	83.5	0.26
Diabase, Frederick	99	NA
Dolerite, Karroo	84	NA
Gabbro, Norites, Diabases	78 - 99	0.11 - 0.31

Source: Agapito et al, 1977

In summary, the amount of data presently available regarding
the mechanical properties of basalt is sparse. Available
data from tests would suggest a high variability of compres-
sive strength and modulus, with a lesser variation of Poisson's
ratio. All vary with porosity and density.

2.12 THERMAL PROPERTIES

Data concerning thermal properties of the rock are required
for the calculation of thermal distributions around the
excavation due to the introduction of the waste. There are
a number of numerical techniques which can be used to calcu-
late such thermal distributions. In general, they require
as input the density, specific heat, thermal conductivity,
and/or the thermal diffusivity of the basalt surrounding the
caverns. These induced thermal fields are superimposed upon
the geothermal gradient at the point of interest. Such a
geothermal gradient from a hole at the Hanford facility is
shown in Figure 2-23.

A knowledge of the density is required, since it controls
the initial stress gradient and is needed to estimate thermal
diffusivity. Table 2-20 summarizes the values obtained for
the density of some 'asalts. There is a considerable varia-
tion in density, as one might expect from the characteristics
of basalt, and the tabulated values should not be used
without extreme caution.

A number of tests have been performed to determine thermal
constants for basalt as a function of temperature. Thermal
properties for Hanford basalt are shown as a function of
temperature in Tables 2-21 and 2-22. Values for thermal
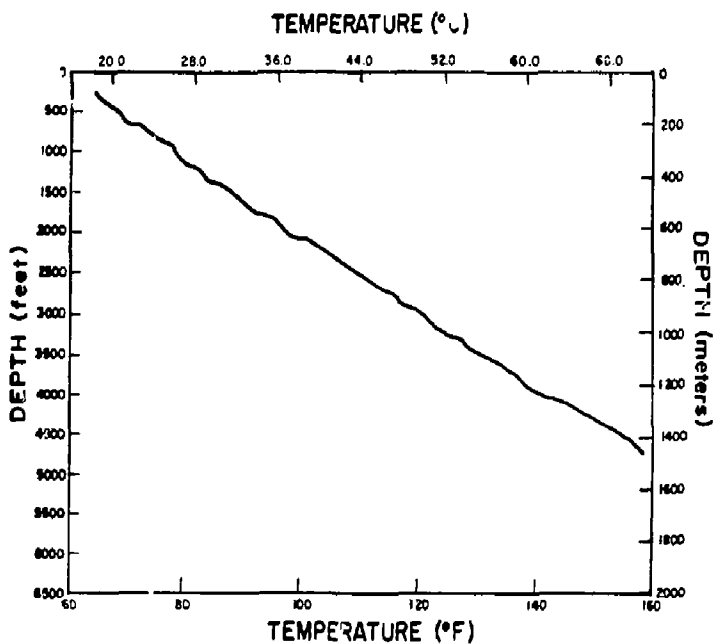
FIGURE 2-23 Subsurface temperature as a function of depth
in DC-1 drill hole (geothermal gradient)
Source: Atlantic Richfield Hanford, 1976, v 1.

TABLE 2-20 Density of some basalts.

ROCK TYPE	DENSITY (g/cm^3)
Basalt	2.4-3.1
Basalt	2.9
Average of General Basalt	2.8-2.9
Basalt	2.8
Gabbros, Norites, Diabase	3.0
Basalt, Dresser	3.02

SOURCE: Agapito et al, 1977

TABLE 2-21 Thermal properties of basalt
as a function of temperature
(Atlantic Richfield Hanford Co., 1977)

Sample 1005   Depth = 306 m (1005 ft)

Temperature, T		Density,	Heat Capacity, Cp
°F	°C	Kg/m^3	J/g/°C
100	37.8	2941.3	0.728
200	93.3	2944.5	0.779
300	149	2947.7	0.829
400	204	2949.3	0.879
500	260	2952.5	0.929
600	316	2955.7	0.980

Temperature, T		Thermal Diffusivity,	Thermal Conductivity, k
°F	°C	m^2/hr	w/m°k
100	37.8	.00191	1.12
200	93.3	.00187	1.19
300	149	.00182	1.24
400	204	.00177	1.28
500	260	.00173	1.32
600	316	.00168	1.30

Sample 1084   Depth = 330 m (1084 ft)

Temperature, T		Density,	Heat Capacity, Cp
°F	°C	Kg/m^3	J/g/°C
100	37.8	2660.9	.737
200	93.3	2662.5	.783
300	149	2665.7	.825
400	204	2667.3	.867
500	260	2670.5	.908
600	316	2672.1	.950

Temperature, T		Thermal Diffusivity,	Thermal Conductivity, k
°F	°C	m^2/hr	w/m°k
100	37.8	.00186	1.02
200	93.3	.00181	1.04
300	149	.00176	1.07
400	204	.00170	1.09
500	260	.00164	1.11
600	316	.00150	1.12

TABLE 2-22 Heat capacity.

CONDUCTIVITY w/m°K	TEST CONDITIONS	REFERENCE
0.623	---	Ratigan, 1976
0.346	20 - 100°C	LANGE'S Handbook of Chemistry, 1956
0.398	100° C	Parsons 1976
0.415	200° C	"
0.433	300° C	"
0.301	37.8° C	ARH-ST-137, 1976
0.322	93.3° C	"
0.343	148.8° C	"
0.363	204.4°C	"
0.384	260° C	"
0.405	315.6° C	"
0.305	37.8° C	"
0.324	93.3° C	"
0.341	148.8° C	"
0.358	204.4° C	"
0.376	260° C	"
0.393	315.6° C	"

SOURCE: Office of Nuclear Waste Isolation, 1978

conductivity of basaltic rocks, as collected by Agapito et al, are shown in Table 2-23. Similarly, thermal diffusivity is shown in Table 2-24.

An equation for the inverse thermal conductivity as a function of temperature for Dresser basalt is given in Figure 2-24. Note that the curve fits the data for three of the five blocks tested quite well. Values for specific heat for several rock types as a function of temperature are given in Figure 2-25. Both thermal conductivity and specific heat are strongly dependent on the chemical composition of the rock.

It is possible, using such models, to show the effect of uncertainty in one of the properties on the thermal distribution. The effect of thermal conductivity of the basalt layer on the cavern temperature is shown in Figure 2-26. Note that increasing the thermal conductivity causes a large reduction in the maximum cavern temperature.

In summary, relat. 'el" .ttle information regarding the thermal properties   basalt is presently available. At least one study (Hanford basalt is underway (Colorado School of Miner and the results should be available soon.

Table 2-26 lists a summary of average physical properties for basalt from Deere et al (1966).

TABLE 2-23 Thermal conductivity of basaltic rocks

	Temperature °K	Thermal Conductivity w/m°K
Basalt	NA*	1.8 - 2.2
Basalt (Japan)	NA	1.4
Gabbro, Norites, Diabase	273 - 373	1.7 - 2.6
Basalt, Columbia Plateau	373	1.53
Basalt, Dresser	373	3.0
Basalt, Diabasic	303	1.69
Basalt, Diabasic	348	1.73
Average		2.2

NOTE:

*Not Available

Source:
Açapito et al, 1977

TABLE 2-24   Thermal diffusivity

Rock Type	Thermal Diffusivity $m^2/s \times 10^{-7}$
Gabbro	5.2
Fine-Grained Diabase	5.8
Silicified Diabase	8.1
Basalt (Japan)	7.0
Gabbro (Japan)	8.0
Basalt, Dresser	10.0
Basalt, Columbia Plateau	6.5
Average	7.0

Source: Agapito et al, 1977
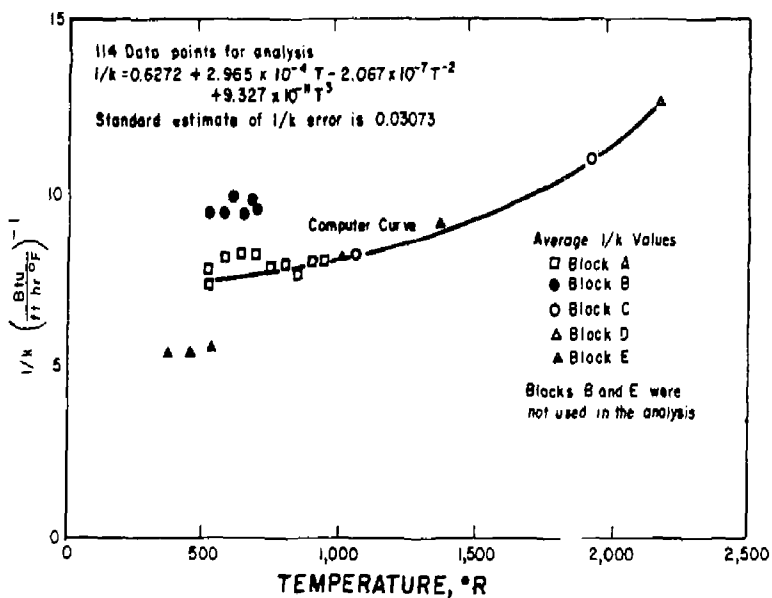
FIGURE 2-24   Inverse thermal conductivity versus
temperature, Dresser basalt
Source: Marovelli and Veith, 1965.
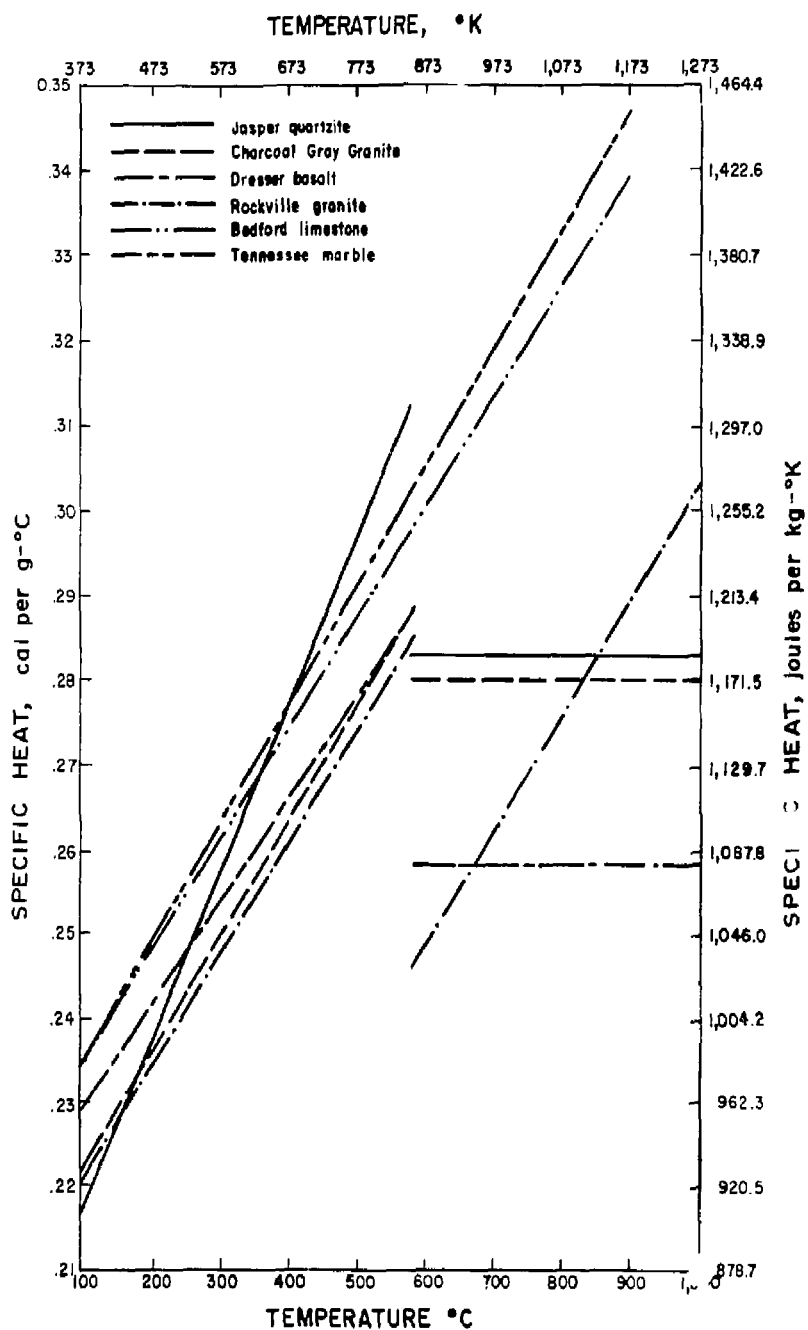
FIGURE 2-25 Comparison of the specific heats for the six rock types
Source: Lindroth and Krawza, 1971.
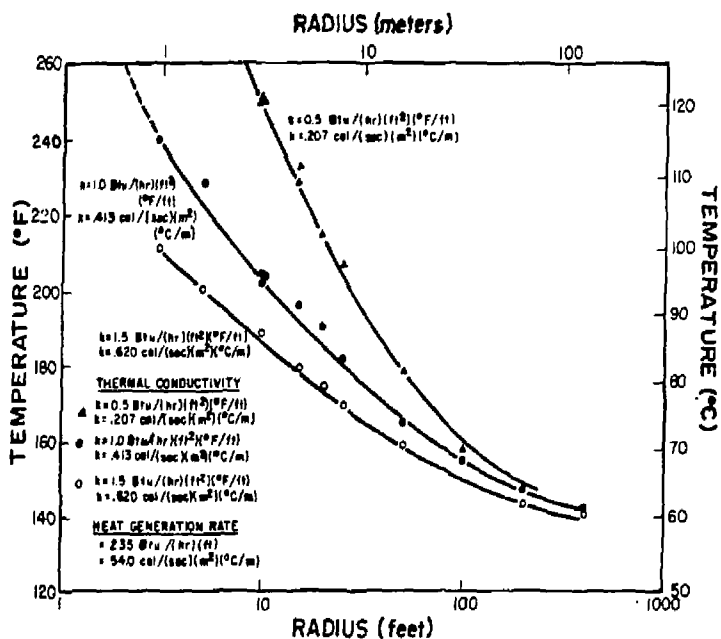
FIGURE 2-26   Cavern temperature versus cavern radius for
                various thermal conductivity values
                Source: Atlantic Richfield Hanford, 1976, v.1

Table 2-25 Summary of average physical properties for basalt

Group No.	Rock Type and Location		Unit Weight, gms/cm³ (lbs/ft³)			Compressive Strength		Shore Hardness, S_h		Schmidt Hardness, R		Abrasion Hardness A_h	Absorption % of dry weight	Tensile Strength Point Load MPa
					L/D	qa (ult) MPa	Load Rate MPa/sec	Sides	Ends	All Rdgs.	High 50%	1/Area (m²)		
1.1	Basalt (Lower Granite) Pullman, Washington	No. Tests 12	2.73	(170.2)	2.08	230	.25	79	86	53	57	.078	1.92	~2.9
				12	12	55	.06	960	480	144	72	.0026	1	13.8
		VZ	1.0			76.6		7.6	6.9	9.3	5.1	.0035		2.1
1.2	Basalt (Little Goose) Walla Walla, Washington	No. Tests 6	2.82	(175.8)	2.12	297	.41	70	67	54	58	.114	.44	10.4
				6	6	21	.01	480	240	72	36	.0026	1	6.9
		VZ	.4			40		6.5	4.8	9.0	5.3	.0048		
1.3	Basalt (John Day) Arlington, Oregon	No. Tests 6	2.87	(179.1)	2.08	355	.46	82	91	55	58	.145	.75	14.5
				6	6	21	.01	480	240	72	36	.0052	1	6.9
		VZ	.5			14		6.3	4.6	7.3	6.1	.0057		

NOTE: VZ = Coefficient of variation

SOURCE: Deere et al, 1966

2.13   THERMOELASTIC PROPERTIES

The influence of temperature and pressure on the elastic
properties of basaltic rocks will be discussed in this
section.   These elastic properties include Poisson's ratio,
Young's modulus, and the coefficient of linear thermal
expansion.   Tables 2-26 - 2-29 and Figure 2-27 show the
effect of temperature on the elastic modulus and Poisson's
ratio of various basalts and basalt like rocks.   It is noted
that for Dresser basalt, an increase in temperature from 297
K°to 866°K results in a reduction in modulus from 100 down
to 66 GPa.   For the same temperature range, Poisson's ratio
is reduced by about half.

There is very little data presently available regarding the
relationship between compressive strength and temperature.
Figure 2-28 reveals that under static loading, the strength
of Dresser basalt decreases rather dramatically over the
temperature range of 0 to 400°K but then levels off.   The
factor of 2 decrease from room temperature to 400° is of
great importance since the rock in the near vicinity of the
canister would undergo such a change.

Average values of the coefficient of linear thermal expan-
sion for a number of rocks are given in Table 2-30.   This
coefficient, however, has been found for most rocks to

TABLE 2-26 Example of influence of temperature and pressure
on the elastic properties of some basaltic rocks

	Temp. °K	Pressure MPa	Young's Modulus GPa	Poisson's Ratio
Basalt, Hornblende, Chaffee County, Colorado Density = 2,586 kg/m³	298	50	67.5	.246
		500	70.8	.269
	573	50	63.7	.240
		500	69.7	.276
Gabbro, "San Marcos," Escondido, California Density = 2,993 kg/m³	298	50	96.0	.363
		500	99.8	.375
	573	50	88.3	.334
		500	98.3	.370
Gabbro, Bylownite, Duluth, Minnesota Density = 2,585 kg/m³	298	50	90.1	.343
		500	95.3	.362
	573	50	78.1	.303
		500	90.1	.344
Gabbro, Hornblende Location Unknown Density = 2,933 kg/m³	298	50	98.1	.378
		500	105.4	.407
	573	50	87.8	.345
		500	103.7	.403

TABLE 2-27 Experimental values of Young's Modulus and Poisson's
ratio at elevated temperatures in Dresser basalt
Source: (Wingquist, 1969)

Temperature °K	Elastic Modulus GPa	Poisson's Ratio
297	100.7	0.24
395	98.6	0.24
533	95.1	0.12
644	87.6	0.1
755	83.4	0.18
811	79.9	0.16
866	66.5	0.11

TABLE 2-28 Elastic moduli data for Dresser basalt.
Source: (Winquist, 1969)

	24	121	260	371	Temperature, °C 482	538	565.5	593	704	815.5
YOUNG'S MODULUS, GPa										
Sample 1..............	103.4	101.4	97.9	89.0	84.8	-	—	67.0	49.0	48.5
Sample 2..............	99.3	97.2	93.1	86.2	82.1	80.0	—	65.0	44.6	44.9
Sample 3..............	99.3	97.9	94.5	86.9	82.8	80.0	—	67.7	48.3	48.1
Mean..............	100.7	98.6	95.2	87.6	83.4	80.0	—	66.6	47.3	47.2
Standard deviation...	2.41	2.21	2.48	1.45	1.45	0	—	1.38	2.41	1.93
SHEAR MODULUS, GPa										
Sample 1..............	41.7	40.7	40.1	37.2	36.0	-	—	30.4	23.1	22.8
Sample 2..............	40.0	39.1	38.1	36.0	34.8	34.1	—	29.5	20.6	21.6
Sample 3..............	40.5	39.9	38.8	36.6	35.4	34.3	—	30.3	22.9	22.6
Mean..............	40.7	39.9	39.0	36.6	35.4	34.2	—	30.1	22.2	22.3
Standard deviation...	.828	.828	1.03	.621	.621	1.38	—	.483	1.38	.690
POISSON'S RATIO										
Sample 1..............	.24	.25	.22	.19	.18	-	—	.10	.06	.06
Sample 2..............	.24	.24	.22	.20	.18	.17	—	.10	.08	.04
Sample 3..............	.23	.23	.22	.19	.17	.16	—	.12	.06	.06
Mean..............	.24	.24	.22	.19	.18	.16	—	.11	.07	.05
Standard deviation...	.01	.01	.00	.01	.01	.01	—	.01	.01	.01

TABLE 2-29   Properties of Dresser basalt.
(Lehnhoff and Scheller, 1975)

Dresser Basalt

Temperature °C	Young's Modulus E,10^5 MPa	Poisson's Ratio ν	Coeff. of Thermal Expansion α,10^5/° C
24	1.007	0.24	0.290
122	.9860	0.24	0.500
260	.9510	0.22	0.770
371	.8760	0.19	0.940
482	.8340	0.18	1.020
538	.7990	0.16	1.080
593	.6650	0.11	1.160
700	.0010	0.10	1.160
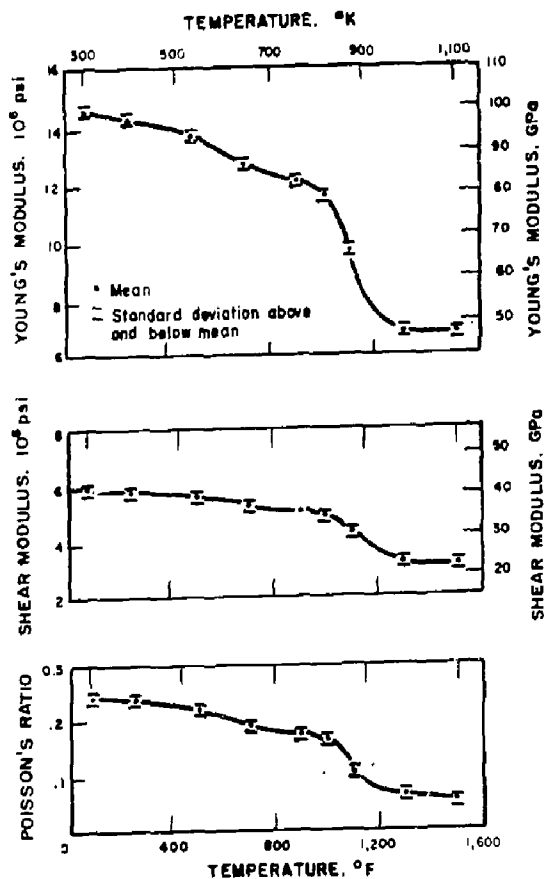
FIGURE 2-27 Elastic moduli and Poisson's Ratio as a functio
of temperature for Dresser basalt.
Source: Wingquist, 1969.
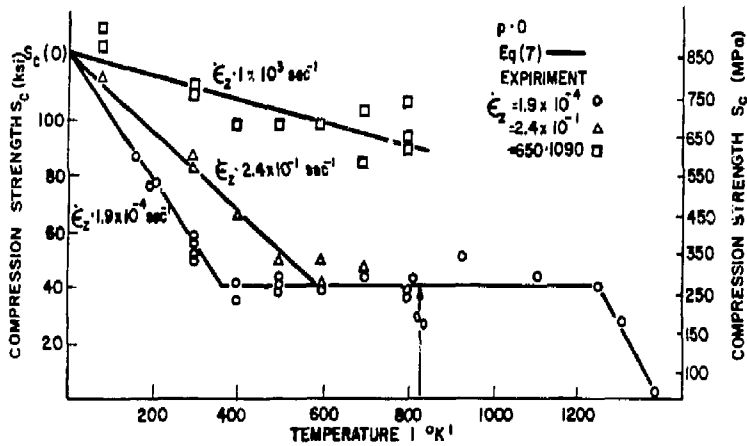
FIGURE 2-28 Influence of temperature and strain rate
            on strength of Dresser basalt
            Source: Krumer, 1968.

TABLE 2-30 Coefficient of linear thermal expansion.

Rock Type	Expansion Coefficient $\times 10^{-6}/°K$	Reference
Basalts, Gabbros, Diabase	5.4	9
Basalt (300°K)	4.3 - 6.5	6
Fairfax Diabase	' 5.9	12
Cape Neddick Gabbro	8.5	12
Dresser Basalt	2.9 - 11.6	13

Agapito et al, 1977

depend on temperature and some typical results for Dresser
basalts are given in Table 2-29. Note that for temperature
of 24° C, the coefficient of the thermal expansion is .29 x 10^{-5}.
At 700° C, the same coefficient is 1.16 x 10^{-5}.

If there is any gap between the canister and the rock (as
will most certainly be the case in any practical situation),
these thermally induced stresses and displacements can cause
the material directly around the canister to degrade or
spall during the heating process. The effects of this
thermal degradation can be evaluated by numerical models.
Such a modeling study was done by Hardy & Hocking. They
examined the influence of changes in basalt thermal conduc-
tivity which result from the failure of the basalt.

The coupling between thermal and mechanical response, which
was used for modeling the effects of borehole decrepitation
was a volumetric strain-dependent thermal conductivity.
They suggest that this type of coupling is supported by
observation since during rock failure, micro-cracks and void
spaces develop and, hence, the volumetric strain increases

The development of such voids in the rock will lead to a
reduced thermal conductivity and thereby restrict the flow
of heat from the canister into the rock. In their analysis,

they assumed the thermal conductivity volumetric strain relationship shown in Figure 2-29. The form shows a reduction in thermal conductivity to one quarter of initial values for large volumetric strains. The expected temperatures for the case with thermomechanical coupling (Figure 2-30) is compared with the case for constant thermal conductivity in Figure 2-31. This shows that for a 1 KW heat source, the reduced thermal conductivity of the rock adjacent to the canister results in an increase of 20% in the canister temperature. This cannot be considered significant. For higher thermal outputs, increased rock failure could produce a more extensive zone of reduced conductivity and, hence, lead to thermal runaway. It is noted that there are no laboratory data available at this point to support such thermal conductivity-volumetric strain curve as shown in Figure 2-29, but the consequences are severe, (breakdown of waste forms, glass for example, greatly reduced canister life, etc.) and, therefore, input data must become available.

A summary of thermomechanical properties for basalt as prepared by Agapito et al is given in Table 2-31.
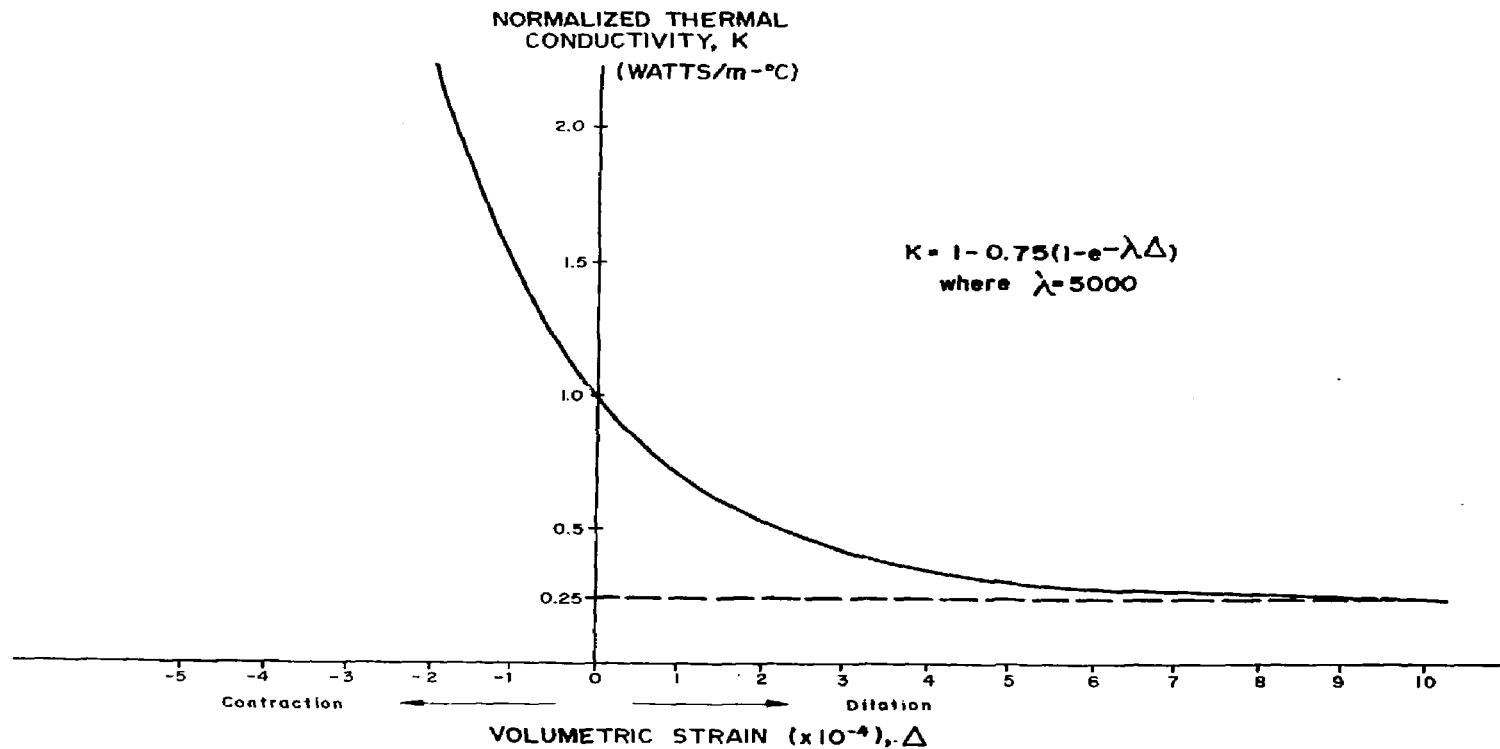
FIGURE 2-29 Form of thermal conductivity - volumetric strain relationship
Source: Hardy and Hocking, 1977.
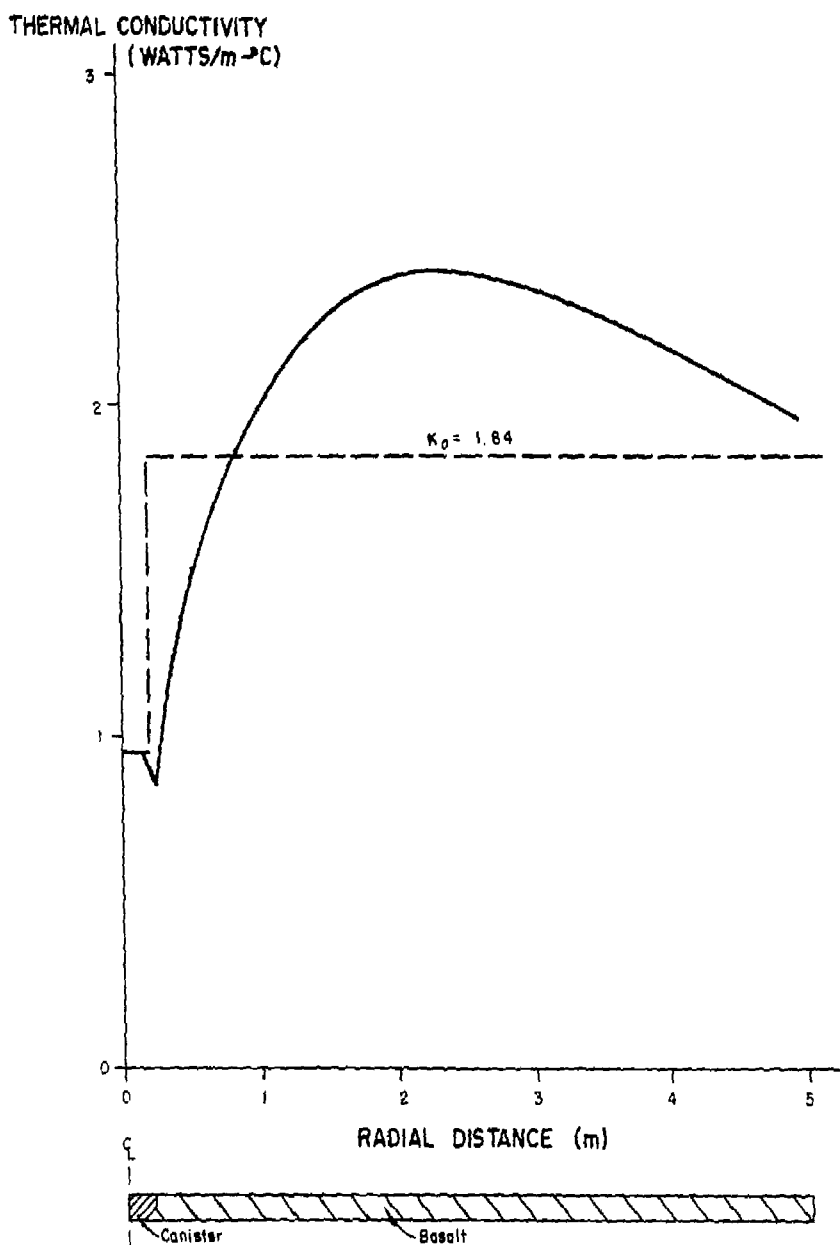
FIGURE 2-30 Conductivity versus radial distance after 28 days
Source: Hardy and Hocking, 1977.
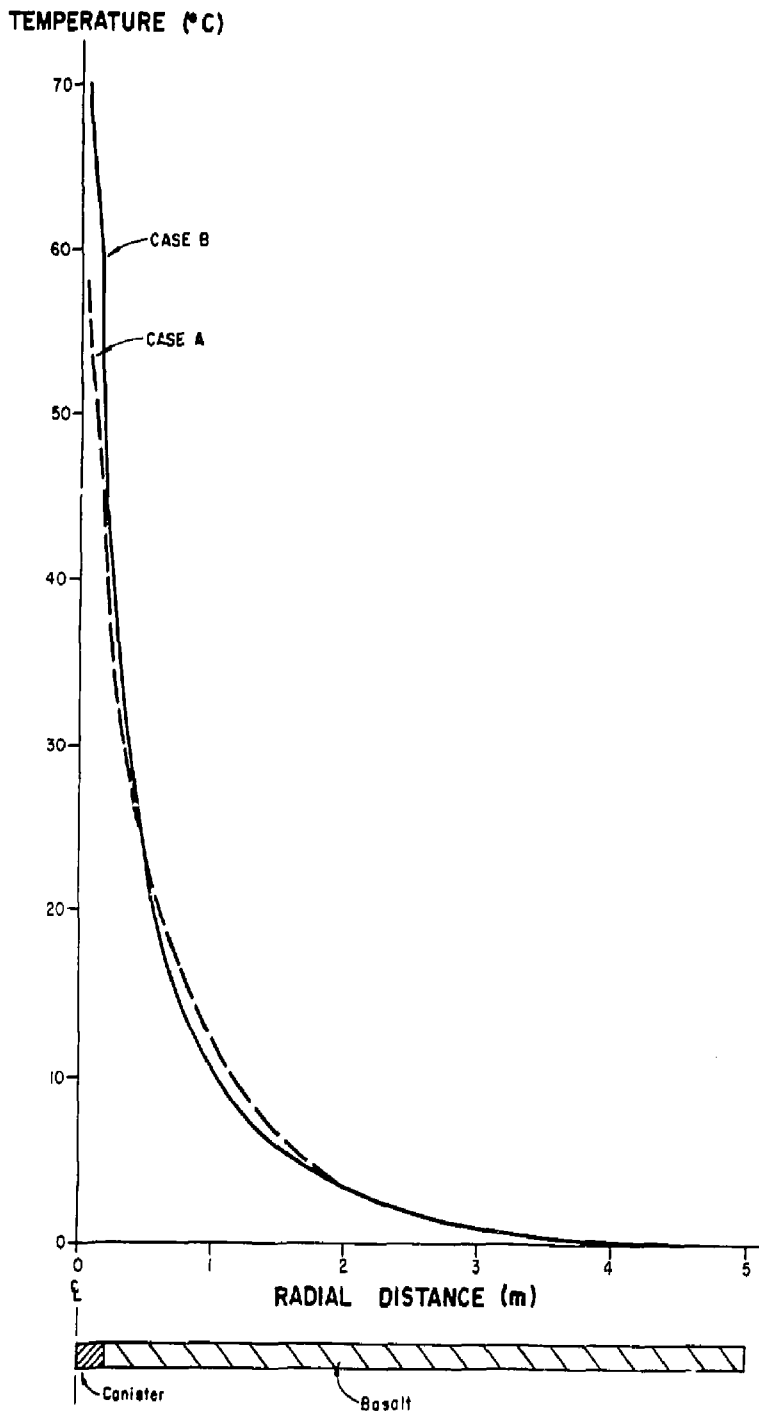
FIGURE 2-31 Comparison of temperatures for uniform conductivity
(case A) and basalt decrepitation (case B)
Source: Hardy and Hocking, 1977.

TABLE 2-31 Summary of thermomechanical basalt properties.

Property	Estimated Value	Range	Units	Major Influence
Density	2.9	2.4-3.1	g/m^3	Porosity
Diffusivity	6.5×10^{-7}	$5.2, 8.0 \times 10^{-7}$	m^2/s	Porosity
Thermal Conductivity	1.5	1.4, 4.28	$w/m°K$	
Specific Heat	1.0	0.95, 1.05	$kJ/kg°K$	
Thermal Expansion Coefficient	5.4×10^{-6}	$2.9, 11.6 \times 10^{-6}$	$/°K$	Temperature
Young's Modulus	70	61, 112	GPa	
Poisson's Ratio	0.26	0.22, 0.28	-	
Uniaxial Compressive Strength	200	0, 400	MPa	Porosity, Jointing
Angle of Internal Friction	55°	45, 60	X°	Jointing
Tensile Strength	14	0, 23.0	MPa	Jointing

SOURCE: Agapito et al, 1977

2.14 OTHER CONSIDERATIONS

Due to the elevated temperatures and the long life of the
repository, the possibility of long-term deformation through
creep must be considered. Unfortunately, the time-dependent
behavior of basalt over the temperature and stress range of
interest for radioactive waste disposal is not well documented.
The compressive strength as a function of creep rate for
Amchitka basalt is shown in Table 2-32. Dense basalts
appear to have a low uniaxial creep rate and exhibit a
minimum average amount of irrecoverable strain. Some creep
curves for basalt as presented by Iida (1960) are shown in
Figure 2-32. All of these tests were performed at approxi-
mately room temperature.

GROUP NO.	LEGEND See Notes	CREEP RATE Microstrains/hr, extrapolated to a time of 200 minutes	IRRECOVERABLE STRAIN Percent, after loading to one-half ultimate strength
		CHITKA POINT FORMATION: HORNBLENDE PYROXENE ANDESITC - Tcp1 - 1	
1	AVG:	1.3	4.7
	MAX:	4.0	10.9
	MIN:	0.1	0.2
	N/S/V:	5/1.4/106	5/4.4/92
		CHITKA POINT FORMATION: DENSE FLOW BRECCIA - Tcp1 - 11	
2	AVG:	1.3	21.2
	MAX:	---	---
	MIN:	---	---
	N/S/V:	1/---/---	1/---/---
		CHITKA POINT FORMATION: HORNBLENDE-ANDESITE BRECCIA - Tcp - 1	
3	N/A	No Date	No Date
		CHITKA POINT FORMATION: TUFF BRECCIAS - Tcp - 1	
4	AVG:	2.8	5.4
	MAX:	3.0	8.9
	MIN:	0.8	1.6
	N/S/V:	3/1.2/56	3/8.6/68
		BANJO POINT FORMATION: BRECCIA - Tcp	
5	AVG:	1.0	4.7
	MAX:	1.8	10.0
	MIN:	0.5	0.4
	N/S/V:	6/0.5/47	6/3.1/67
		DENSE BASALT - Tb	
6	AVG:	1.0	2.7
	MAX:	1.1	4.5
	MIN:	0.9	0.8
	N/S/V:	2/---/---	2/---/---
		AMCHITKA FORMATION: KIRILOF POINT GLASSY BRECCIA - TAKb - 1	
7	AVG:	2.8	9.0
	MAX:	3.0	10.6
	MIN:	2.6	7.3
	N/S/V:	2/---/---	2/---/---
		AMCHITKA FORMATION: KIRILOF POINT PILLOW LAVAS - TAKb - 11	
8	AVG:	0.9	1.7
	MAX:	1.4	2.1
	MIN:	0.4	1.3
	N/S/V:	2/---/---	2/---/---
		AMCHITKA FORMATION: DENSE OLDER BRECCIA - TAb	
9	AVG:	1.7	5.4
	MAX:	2.5	8.2
	MIN:	0.7	2.6
	N/S/V:	4/1.0/58	4/2.5/46
		EAST CAPE QUARTZ DIORITE - Tcp	
10	AVG:	1.5	11.6
	MAX:	3.0	17.1
	MIN:	0.4	4.6
	N/S/V:	5/1.1/71	5/5.7/51

NOTES: Under LEGEND, N = Number of specimens; S = Standard deviation;
        V = Coefficient of variation in percent, respectively.

FIGURE 2-32   Creep curves for basalt
               Source: Iida et al, 1960
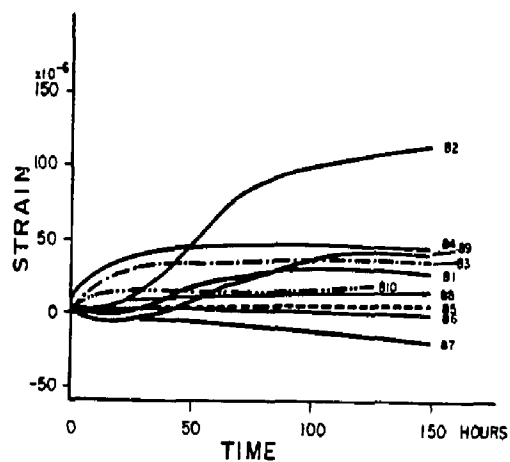
B1: 20.2 kg/cm², 27.5°C.   B2: 32.6 kg/cm², 27.5°C.   B3: 45.6 kg/cm², 28°C.
B4: 58.3 kg/cm², 28°C.   B5: 73.5 kg/cm², 18°C.   B6: 83.4 kg/cm², 28°C.
B7: 92.3 kg/cm², 28°C.   B8: 138.9 kg/cm², 11°C.   B9: 161.7 kg/cm², 27.5°C.
B10: 216.0 kg/cm², 16°C.

2.15   SCALING OF LABORATORY RESULTS

As was indicated in the introduction to this report, basalt can vary considerably in the flows, both horizontally and vertically. One significant structural characteristic of many basalts is their jointing pattern. As previously discussed, these jointing patterns can take many forms. One common form is columnar jointing. It is expected that rock mass properties of the basalt will be considerably different from the intact properties due to the complex interaction of the intact rock, joint system, joint filling, and water effects.

In their report, the Office of Nuclear Waste Isolation, (1978) have presented a discussion of how one might go from intact values to rock mass values. Their discussion is extremely worthwhile to include, as it presents the state of the art regarding this important characterization:

> "The rock-mass properties of a basalt will
> be considerably different from the intact prop-
> erties, due to the complex interaction of the
> rock substance, joint system, joint filling and
> water effects.
>
> For two important design parameters, namely,
> Young's Modulus and Unconfined Compressive
> Strength, the rock-mass values are typically
> much smaller than the intact values. In each
> case the rock-mass value is usually obtained
> from the intact value by multiplying by an
> appropriate reduction factor; i.e.
>
> $$\text{Reduction Factor, } R = \frac{\text{Rock-Mass Value (Strength)}}{\text{Intact Value (Strength)}}$$

Considerable judgment is required in select-
ing a suitable reduction factor. This is because
the reduction factor depends very much on geologi-
cal considerations, such as the joint pattern,
joint spacing and joint filling. Although the
rock-mass properties (and hence, reduction factors)
may be determined directly from large-scale field
tests, these are time-consuming, and expensive;
this largely explains why no large-scale field
tests have been reported in the literature.

Since geological structure plays a very
important role in rock-mass behavior, a descrip-
tion of structures found in a typical basalt is
presented in Table 2-33. These structures have
been taken into account in deriving the rock-mass
properties.

The rock-mass properties of a typical dense
basalt representative of the lower portion of a
thick flow are given in Table 2-34. The moduli
and strength characteristics were determined by
the use of reduction factors applied to the
representative intact data.

It was necessary to use a considerable amount
of judgment in arriving at a reduction factor of
0.18 for Young's modulus. A certain amount of
weight was given to considerations by Panek (1970)
in which the reduction factor is related to the
fracture spacing and the width of the excavation.
Due largely to the relatively close jointing in
basalt, which we have assumed to have an average
spacing of about two feet, a reduction factor of
0.18 was chose. This then gave a Young's modulus
of 12.4GPa for the rock mass.

Although jointing also has a considerable
effect on rock-mass strength it is not considered
to be as significant as with Young's modulus.
Hence, a reduction factor of 0.45 was used which
gives a uniaxial confined compressive strength of
124MPa for the rock mass.

The strength of the rock mass is considerably
reduced at elevated temperatures. This reduction
in strength has been taken into account in the
calculations of tunnel and pillar stability; it is
discussed further in the report on thermal stress
analysis.

TABLE 2-33 Partial description of typical structures in basalt

	SET A	SET B	SET C	SET D
Type of Joint	Joint	Joint	Joint	Joint
Filling	Hematite	Nontronite	Calcite	Clean
Orientation	350/85	100/90	230/80	160/10
Opening Width	Tight	Tight	Tight	Tight
Spacing	> 2 m	0.3-2 m	0.1-2 m	0.1-1 m
Waviness	Planar/Rough	Planar/Rough	Planar/Rough	Planar/Rough
Extents of Joints (Lengths)	∿ 6 m	∿4.5 m	∿ 9 m	∿3 m

Typical RQD: > 95%

Typical Fracture Frequency: Horizontal: 6 to 0.5 per meter
                            Vertical: 3 to 0.3 per meter

The non-linear failure curve that is recom-
mended for a typical basalt at room temperature is
shown in Figure 2-33. It may be described by the
following three parameters:

Unconfined compressive strength σ_c = 124 MPa

Curve fitting parameter,   A = 4.5

Curve fitting parameter,   k = 0.75

A value of 2,880 kg/m^3 was assumed to be the
unit weight of the basalt rock mass. Thermal
properties at depth were assumed to be similar to
the intact properties.

Although isotropic behavior has been assumed
in this general study, anisotropic behavior should
be investigated at the design stage for a specific
repository; for instance, detailed geological
mapping and in situ testing will be required at
the actual site of the underground repository".
(Office of Nuclear Waste Isolation, 1978)

In their approach, rock-mass value is related to the intact

value through a reduction factor "R". As is noted, "it was

necessary to use a considerable amount of judgment is arriving

at a reduction factor of 0.18 for Young's modulus". The same

type of judgment entered into considering a reduction factor

of 0.45 for the uniaxial compressive strength. There is no

justification other than intuitive feeling for the choice of

such reduction factors. Assume for the moment that a strength

reduction function such as

$$\frac{\sigma_1}{\sigma_c} = A \left(\frac{\sigma_3}{\sigma_c}\right)^k + 1$$

does exist for basalt (A = 4.5, k = 0.75, σ_c = 124 MPa).
If one wanted to calculate the rock-mass strength (σ_1) under
a confining stress (σ_3 = 10 MPa), then

$$\sigma_1 = \sigma_c \left\{ A \left(\frac{\sigma_3}{\sigma_c}\right)^k + 1\right\} = 1.68 \; \sigma_c = 208 \text{ MPa}$$

The equation shown in the figure:

$$\frac{\sigma_1}{\sigma_c} = \Delta \left(\frac{\sigma_3}{\sigma_c} \right)^k + 1.0$$
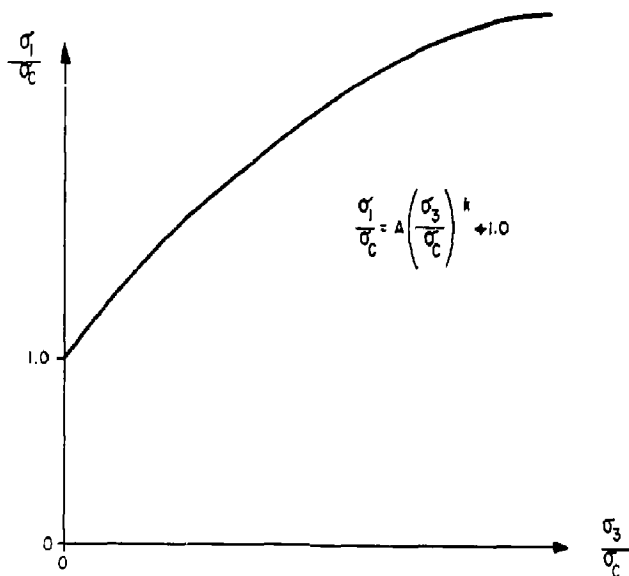
FIGURE 2-33 Non-linear curve of strength for rock mass
Source: Hardy and Hocking, 1977.

The values of A and k are presumably determined from a suite
of tests performed on small samples. Only the value of σ_c
requires scaling from small to large samples and this is
done through the reduction factor R. A great amount of
laboratory and field testing is required before any such
simplified way of inferring from small to large scale
properties for hard rock can be done.

In Table 2-34, in which intact properties are compared to
rock-mass properties for a typical dense basalt, no justi-
fication has been given for the reduction factors other
than for modulus and compressive strength. Thermal expansion,
for example, is indicated to be the same for the intact and
the rock mass. It is believed that this is probably far from
true. The presence of joints in a rock mass influences its
elastic properties, strength, thermal conductivity (Figure 2-34)
and thermal expansion coefficient. The stress across the joint
influences all these properties and as the stress history of
the joints will change during the mining of the repository,
the response of the joints during and after this stress change
is of primary concern.

The behavior can be very non-linear as shown as idealized
curves in Figures 2-34 - 2-36.

TABLE 2-34 Intact properties for a typical dense basalt

TYPE OF PROPERTY	PARAMETER	INTACT VALUE	ROCK MASS VALUE	MKS UNITS
Index	. Density	3.01	2.88	gm/cm^3
	. Natural Moisture Content		--	%
	. Porosity	2.0	0.6	%
Stress-strain	. Young's Modulus	69	12.4	GPa
	. Poisson's Ratio	0.26	0.26	--
Strength	. Strength Parameters			
	A		4.5	
	k		0.75	
	. Uniaxia Compressive Strength	276	124	MPa
	. Tensile Strength	16	0	MPa
Thermal	. Coefficient of Linear Thermal Expansion	1.7×10^{-6}	1.7×10^{-6}	$°C^{-1}$

. Heat Capacity

TEMPERATURE	HEAT CAPACITY	HEAT CAPACITY
0°C	0.71 J/g-°C	0.71 J/g-°C
100°C	0.80	0.80
200°C	0.92	0.92
300°C	0.96	0.96

. Thermal Conductivity

TEMPERATURE	HEAT CAPACITY	THERMAL CONDUCTIVITY
0°C	1.12 w/m°k	1.12 w/m°k
50°C	1.19	1.19
100°C	1.26	1.26
150°C	1.32	1.32
200°C	1.38	1.38
300°C	1.47	1.47
400°C	1.56	1.56
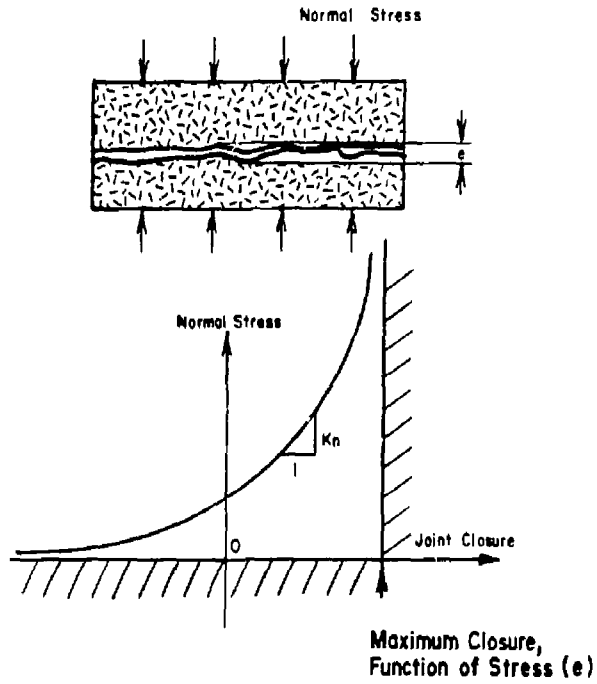
FIGURE 2-34 Influence of normal stress on normal stiffness (K_N) of a joint   Source: Agapito et al, 1977.
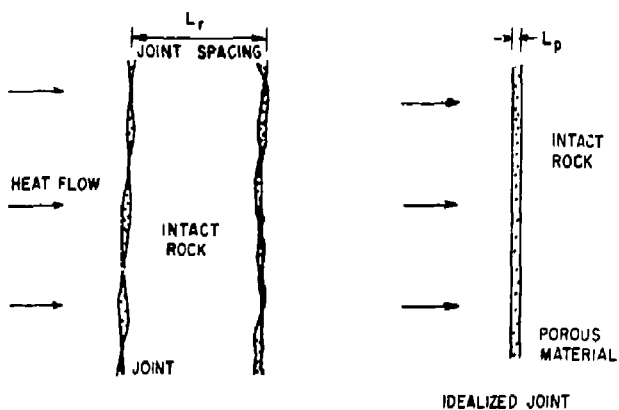
SCHEMATIC IDEALIZATION OF A JOINT FOR ESTIMATION
OF THERMAL CONDUCTIVITY
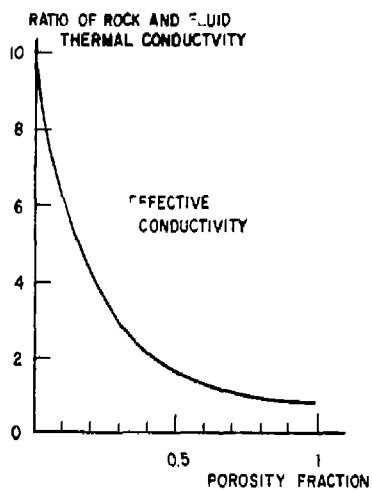
FIGURE 2-35 Thermal conductivity of porous material
Source: Agapito et al, 1977.

Shear Stress

Cohesive Joint
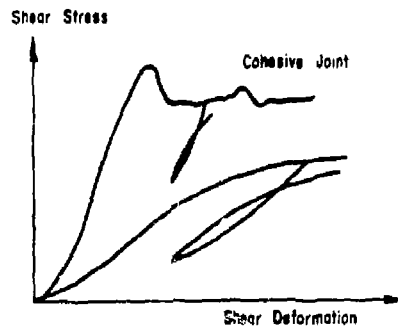
Shear Deformation

ACTUAL EXPERIMENTAL RESPONSE
OF TWO JOINTS

Shear Stress

Peak Strength

Residual Strength

K_s

Stiffness
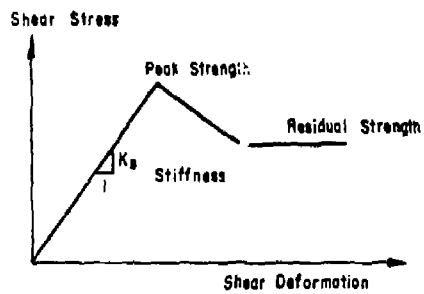
Shear Deformation

IDEALIZED REPRESENTATION OF
JOINT RESPONSE

FIGURE 2-36 Typical shear stress, shear deformation response
of joints Source: Agapito et al, 1977.

No quantitative information was found on joint stiffness,
either shear stiffness (Figure 2-35) or normal stiffness
(Figure 2-36). Coulson (1970) has performed shear strength
testing on artificial surfaces which were cut and sand-
blasted and lapped with various grades of material. The
data shown in Figures 2-37 and 2-38 constitute the data base
for basalt at the present time regarding behavior of the joints.

The mechanical, thermal, and thermal-mechanical properties
of basalt must be determined both in situ and in the labora-
tory under carefully controlled conditions so that the input
data required for scoping studies and for detailed quantita-
tive evaluations can be made. At the present time, it is
felt that the input data required for any significant modeling
does not exist. The modelers, however, should be working in
close cooperation with the experimentalists in helping to
construct the experiments required to provide the input data
(See CHAPTER I - GRANITES for a more comprehensive discussion
of the modelers role.)

FIGURE 2-37   Minimum coefficients of friction versus normal
                pressure for lower granite basalt
                Source: Coulson, 1970

No quantitative information was found on joint stiffness, either shear stiffness (Figure 2-35) or normal stiffness (Figure 2-26). Coulson (1970) has performed shear strength testing on artificial surfaces which were cut and sandblasted and lapped with various grades of material. The data shown in Figures 2-37 and 2-38 constitute the data base for basalt at the present time regarding behavior of the joints.

The mechanical, thermal, and thermal-mechanical properties of basalt must be determined both in situ and in the laboratory under carefully controlled conditions so that the input data required for scoping studies and for detailed quantitative evaluations can be made. At the present time, it is felt that the input data required for any significant modeling does not exist. The modelers, however, should be working in close cooperation with the experimentalists in helping to construct the experiments required to provide the input data (See CHAPTER I - GRANITES for a more comprehensive discussion of the modelers role.)

FIGURE 2-38   Initial residual coefficients of friction versus
normal pressure for lower granite basalt
Source: Coulson, 1970.

2.16 REFERENCES

Agapito, J.F.T., Hardy, M.P. and D.R. St. Laurent, 1977,
    Geo-Engineering review and proposed program outline for
    the structural design of a radioactive waste repository
    in Columbia River Basalt, Rockwell International, RHO-
    ST-6.

Atlantic Richfield Hanford Company, November 1976, Pre-
    liminary feasibility study on storage on radioactive
    wastes in Columbia River Basalts, ARH-ST-137.

Birch, F. and H. Clark, August 1940, The thermal conduc-
    tivity of rocks and its dependence upon temperature and
    composition, "American Journal of Science."

Birch F., Schairer, J.F., and H.C. Spencer, 1942, Handbook
    of Physical Constants, Geological Society of America,
    Memoir 36.

Board, M.P., and J.F. Marron, December 1977, Near surface
    test facility test plan, Unpublished report on contract
    EY-77-C-06-1030.

Bolz, R.E. and G.L. Tuve, 1942, Handbook of Tables for
    Applied Physical Constants, Geological Society of
    America, Memoir 36.

Clark, S.P., 1966, Handbook of Physical Constants, Geolog-
    ical Society of America, Memoir 97.

Coulson, J.H., 1970, The effects of surface roughness on the
    shear strength of joints in rock, Corps of Engineers,
    NTIS AD714244.

Deere, D.U., and R.P. Miller, December 1966, Engineering
    classification and index properties for intact rock,
    Air Force Weapons Lab Tech. Report, AFWL-TR-65-116.

Deju, R.A., November 26, 1976, Feasibility of storing
    radioactive wastes in Columbia River Basalts, ARH-SA-
    281, Atlantic Richfield Hanford Company.

Deju, R.A., Feasibility of Storing Radioactive Wastes in
    Columbia River Basalts, Storage in Excavated Rock
    Caverns (Proceedings of Rock Store 77), Stockholm,
    Sweden, 1977, V. 3.

Deju, R.A., April 1977, A plan to study the environmental
    factors needed to establish the feasibility of storing
    radioactive wastes in Columbia River Basalts, ARH-ST-
    152, Atlantic Richfield Hanford Company, Richland,
    Washington.

Deju, R.A., et al, September 1977, Environmental factors needed to establish the geotechnical feasibility of storing radioactive wastes in Columbia River Basalts, RHO-ST-8.

Deju, R.A., and R.E. Gephart, November 1, 1976, Preliminary feasibility study on storage of radioactive wastes in Columbia River Basalts, ARH-ST-137, V. 1, Atlantic Richfield Hanford Company, Richland, Washington.

Duval, W.I., Miller, R.J., and F.D. Wang, May 1978, Preliminary report on physical and thermal properties of basalt: drill hole DC-10, Pomona Flow-Gable Mountain, RHO-BWI-C-11.

Ekren, E.B., 1968, Geologic Setting of Nevada Test Site and Nellis Air Force Range, in Nevada Test Site, Geological Society of America, Memoir 110.

Griggs, D.T., Turner, F.J., and H.C. Heard, Deformation of rocks at 500 C to 800 C, Rock Deformation, Griggs and Handin, Geological Society of America, Memoir 79.

Hardy, M.P., and G. Hocking, 1977, Numerical Modelling of rock stresses within a basaltic nuclear waste repository: phase II - parametric design studies, reported submitted to Rockwell Hanford Operations, EY-77-C-06-1030.

Hoek, E., and E.T. Brown, Underground Excavation Engineering, The Institution of Mining and Metallurgy, London, In Press.

Iida, K., Wada, T., Aida, Y., and R. Schichi, 1960, Measurements of creep in igneous rocks, "Journal of Earth Sciences," Nagoya University.

Kreck, W.W., Henderson, F.A., and K.E. Jhelmstad, 1974, A standard rock suite for rapid excavation research, U.S. Bureau of Mines, R.I. 7865.

Krupka, M.C., 1974, Selected physico-chemical properties of basaltic rocks, liquids and glasses, LA-5540-MC, Los Alamos Scientific Laboratory, Los Alamos, New Mexico.

Krumer, A., 1968, The Effect of Stress Rate and Temperature on the Strength of Basalt and Granite, Geophysics, 33, (3).

Lee, W.H., and Morris, R.H., 1968, Preliminary Lithologic Log of Drill Hole UAE-1 from 5000 to 7000 feet, Amchitaka Island, Alaska, USGS 474-47, Clearing-house, Springfield, Virginia.

Lehnhoff, T.F., and J.D. Scheller, 1975, The influence of temperature dependent properties on thermal rock fragmentation, IJRM.

Lindholm, U.S., Yeakley, L.M., and Nagy, A., 1974, The dynamic strength and fracture properties of Dresser Basalt, International Journal of Rock Mechanics and Mining Sciences, and Geomechanics Abstracts, V. 11, pp. 181-191.

Lindner, E.N., and J.A. Halpern, 1977, Insitu stress: an analysis, 18th U.S. symposium on rock mechanics.

Lindroth, D.P., and W.G. Krawza, Heat content and specific heat of six rock types at temperature to 1000 C, USBM RI 7503.

Lutton, R.J., 1968, Comparison of Strengths of Dense and Vesicular Types of Basalt. "Bull. Assn. Eng. Geol.," V. 5, No. 1.

Morovelli, R.L., and K.F. Veith, 1965, Thermal conductivity of rock: measured by the transit line source method, U.S. Bureau of Mines, R.I. 6604.

Munjal, P., and I. Fatt, December 24, 1966, Thermal anisotropy in rocks, Nature, V. 212.

Murrell, S.A.F., and S. Chakravarty, 1973, Some new rheological experiments on igneous rocks at temperatures of up to 1120 C, Journale of Geophysical Research, Abstracts, Soc. 34.

Nafe, J.D., and C.L. Drake, 1968, Physical properties of rocks of basaltic composition, Basalts, Hess and Poldervaart.

Nafe, J.E., and C.L. Drake, 1968, Physical properties of rocks of basaltic composition, basalts, The Poldervaart Treatise on Rocks of Basaltic Composition, edited by H.H. Hess and A. Poldervaart, Interscience Publishers, V. 2, pp. 483-502.

Nieble, C., Midea, N.F., Fujimura, F., and S.B. Neto, 1974, Shear strength of typical features of basaltic rock masses - Parana Basin, Brazil, proceedings of the Third International Congress on Rock Mech., Denver, Colorado.

Office of Nuclear Waste Isolation, 1978, Technical support for GEIS: Radioactive waste isolation in geologic formations: V. 7-baseline rock properties (basalt), Y/OWI/TM/-36/7.

Panek, L.A., 1970, Effect of rock fracturing on the modulus as determined by bore hole dilation tests, proceedings of the Second International Congress on Rock Mech., Belgrade.

Parsons, Brinckerhoff, Quade, and Douglas, Inc., April 1978, Technical support for GEIS, radioactive waste isolation in geologic formations, V.14 - repository preconceptual design studies (basalt), Y-OWI-TM-36-14.

Parsons, Brinckerhoff, Quade and Douglas, Inc., September, 1976, Thermal guidelines for a repository in bedrock, Y-OWI-SUB-76-16504.

Richter, D., and G. Simmons, 1974, Thermal expansion behavior of igneous rocks, _International Journal of Rock Mechanics and Mining Sciences, and Geomechanics Abstracts_, V. 11, pp. 403-411.

Rodrigues, F.P., "Anisotropy of Granites", 2nd Int. Congress on Rock Mechanics, Belgrade, 1970

Sandia, 1962, _Project Buckboard, 20-ton adn 1/2-ton High Explosive Cratering Experiments in Basalt Rock_, final report, August 1962, by Sanida Corporation.

Sellers, J.B., January 1970, Rock testing report, teledyne terrametrics.

Sharp, R.R., 1372, _A Geological Engineering Evaluation of an Underground Nuclear Test Site_, PhD. thesis, University of Arizona.

Stowe, R., 1969, _Strength and Deformation Properties of Granite, Basalt, Limestone, and Tuff at Various Loading Rates_, U.S. Army Eng. Waterways Exp. Station, Misc. Paper C-69-1.

Thirumalai, K., 1970, Rock fragmentation by creating a thermal inclusion with dielectric heating, U.S. Bureau of Mines, R.I. 7424.

Wingquist, C.F., 1970, elastic modulii of rock at elevated temperatures, U.S. Bureau of Mines, R.I. 7269.

Wuerker, R.G., 1956, Annotated tables of strength and elastic properties of rock, Trans. SPE (AIME).

Union Carbide Corporation/Office of Waste Isolation, Nuclear Division, April 1978, _Commercial Waste Forms, Packaging and Projections for Preconceptual Repository Design Studies_, Y-OWI-TM-3672, Oak Ridge, Tennessee, Part I.

U.S. Army Corps of Engineers, 1965, _Project Longshot, Amchitka Island_, Alaska, Geologic and hydrologic investigations (Phase I), U.S. Army Eng. District, Anchorage.

U.S. Bureau of Reclamation, January 1976, Construction and foundation materials test data for bacon siphon and tunnel-second unit, DC-7206.

HYDROLOGY OF BASALT

2.17 INTRODUCTION TO HYDROLOGY OF BASALT

Ground water migration through a basalt sequence occurs as it flows
through both porous intergranular and non-porous fractured
media. The mechanics of flow through both of these media
was presented in sections 1.18 through 1.22.
Drawing upon this background, this section presents a summary
of the physical characteristics of basalt flows and discusses
porosity, permeability and ground water flow regimes through
basalt sequences. Special hydrologic features of basalts found
on the Columbia Plateau, Snake River Plain and Modac Plateau
are then discussed.

2.18 PHYSICAL CHARACTERISTICS OF BASALT FLOWS

Lava Forms

The subareal lava flows issuing from fissure eruptions in the
American northwest are predominantly of two types, pahoehoe and
aa. These two forms of lava are distinquished by various flow
features controlled by the viscosity and degree of agitation in
the extruded lava mass. Most flows issue as pahoehoe, and as
viscosity declines downslope change into aa.

Pahoehoe flows are characterized by a rolling, billowy or "ropy"
surface. This feature results from the deformation and folding
of the thin, cooled lava surface by deeper flowing lavas. Vesicles,
resulting from the release of gas by the lava, are abundant in
pahoehoe flows. Spherical or nearly spherical vesicules may
fully permeate thin flows, while in thicker flows vesicles concentrate
near the top of the flow. In some cases, vesicles may also be
found in a chilled layer near the base o   flow.

In contrast to the relatively smooth, undulating surface of a
pahoehoe flow, aa flows are rough, spiny, fragmented, and blocky.
The surface is scoriaceous, the top and margins of the flow being
covered with clinker. Occasionally, a layer of clinker may also
be found on the lower surface of the flow; however, in the Columbia
River and Cascade region, flows generally lack this feature. Aa flows
are generally much less vesicular than pahoehoe flows. Vesicularity

may reach 50% in some flows, however, normally is less than
30% (MacDonald, 1967). Those vesicles present are generally
less than 2 cm. in diameter and nonspherical.

A third type of subareal flow, block lavas, are rarely found
in the northwest. Block flows are generally characteristic
of siliceous lavas rather than lavas of basaltic composition
such as those of the Columbia Plateau region.

Since lavas were extruded in some areas of the northwest
into shallow seas or fresh water lakes, subaqueous flows are
also of some interest. The predominant subaqueous form is
pillow lavas. These flows consist of stacked elipsoidal
bodies of lava generally ranging 10 cm. to 7 m. in diameter.
"Pillows" may be compactly molded together or separated
partly or wholely by detrital materials. Most have glassy
skins and are radially fractured.

Joints And Cooling Features

As a basalt flow cools, shrinkage of the lava causes the
development of vertical tension fractures or joints. In a
massive flow these joints form in regular patterns. Thin
flows are normally characterized by rectangular or irregular
polygonal joint configurations in the horizontal plane.
Thicker flows exhibit more uniform hexagonal systems of
joints in the x-y plane, resulting in the formation of
vertically standing columnar structures. Holmes (1965)
explains the formation of "columnar" joints:

"When a hot homogeneous rock cools uniformly against a
plane surface, the contraction is equally developed in
all directions throughout the surface. This is mechanically
the same as if the contraction acted towards each of a
series of equally spaced centres. Such centres (C. 1,2,
3, etc. in Figure 2-39a) form the corners of equilateral
triangles, and theoretically, this is the only possible
arrangement. At the moment of rupture the distance
between any given centre C and those nearest to it is
such that the contraction along lines such as C-1 is
just sufficient to overcome the tensile strength of the
rock. A tension crack then forms halfway between C and
1 and at right angles to the line C-1. As each centre
is surrounded by six others (1-6 in Figure 2-39a), the
resultant system of cracks is hexagonal. Once a crack
occurs somewhere in the cooling layer the centres are
definitely localized, and a repeated pattern of hexagonal
cracks spreads almost simultaneously throughout the
layer (Figure 2-39b). As cooling proceeds into the sheet
of rock the cracks grow inward at right angles to the
cooling surface and so divide the body into a system of
hexagonal columns."

The description of jointing presented by Holms, although

generally accepted in principle, is somewhat oversimplified.

A diagramatic cross section of the Pomona flow of the Columbia

River Basalt, Figure 2-40, shows jointing to be somewhat more

complex. Ryan (1974) suggests the Pamona flow consists of 7

relatively distinct vertically distributed zones. The

uppermost zone, Zone I, which he identifies as the flow top,

consists of a 20 to 30 cm. layer of weathered scoriaceous

lava and rubble underlain by a 2-3 m. thick zone of high

vesicularity. Vesicles in this zone range from 5 to 25 mm.

in diameter.

Zone II is termed the upper colonnade. This region contains

vertically standing hexagonal columns of 2-3 m. in diameter

with face widths of 1-2 m. and heights of 4-8 m. These

columns, the largest in the flow unit, often bear faces
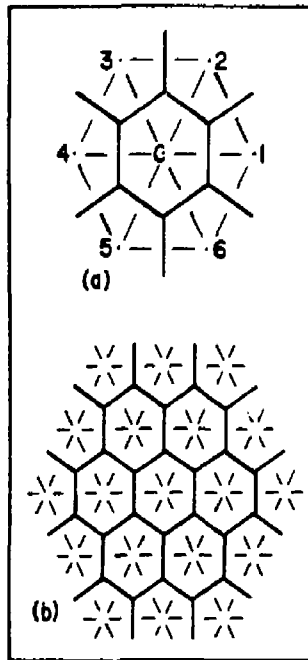
Figure 2-39 Formation of "ideal" hexagonal fracture pattern due
to uniform contraction toward evenly-spaced centers.
Source: Ryan (1974)
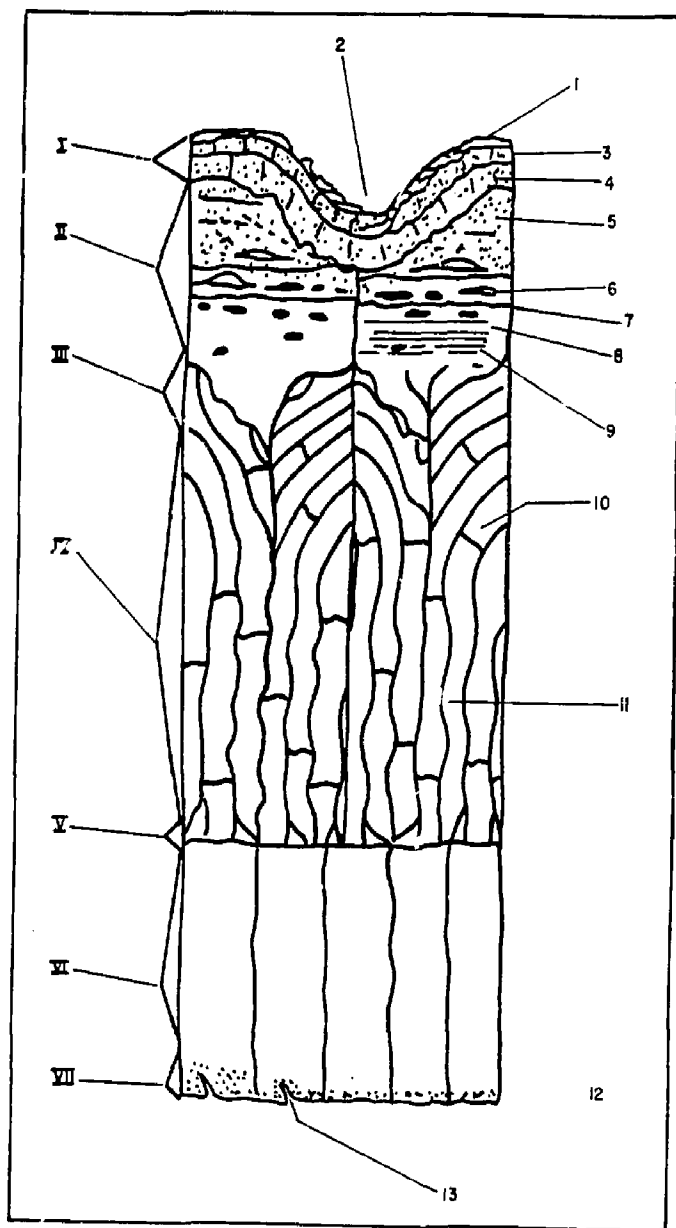
Figure 2-40 Simplified cross section of the Pomona flow unit:
(1) Flow top; (II) Upper colonnade; (III) Upper
transition zone; (IV) Entablature; (V) Lower
transition zone; (VI) Lower colonnade; (VII) Flow
base. Smaller structures are: (1) Pahoehoe or
Ropy lava; (2) Localized sags in the flow top
(not to scale); (3) Blocky Scoria; (4) Small
sub-vertical jointing confined to flow top;
(5) Transition from spherical vessicles to
elongate ones; (6) Large elliptical vessicles;
(7) Cross fractures; (8) Upper colonnade column;
(9) Horizontal ridges; (10) Cross fractures;
(11) Undulating fracture surfaces; (12) Vessicular
zone; (13) Spiracles.
Source: Ryan, 1974

2-132

which are non-planer and appear warped or twisted. Some
cross fracturing is evident in this zone and is often found
to coincide with eliptical vesicles having horizontal major
axis.

Underlying the upper colonnade is an upper transition zone,
Zone III, wherein the size of both column faces and diameters
are rapidly reduced. Within this 3-5 m. thick zone, the
large columns of the upper colonnade are subdivided into
smaller and smaller polygons. The large columns of the
upper colonnade are transformed into bundles of smaller
columns which blend to form the next lower zone known as the
entablature.

The entablature, Zone IV, is characterized by slender,
subparallel columns 15 to 20 m. in height. The joints
bounding the columns of Zone II often extend into the entablature
grouping columns in this unit into "megacolumns". Individual
columns within the megacolumn are often cross fractured,
although fractures among columns are not generally coincident.

Below the entablature is a lower transition zone, Zone V,
about 1 m. in thickness. This zone marks the abrupt boundary
between the entablature and the lower colonnade. The lower
colonnade, Zone VI, consists of columns 6 to 7 m. in length
and 1 to 1.5 m. in diameter. Symmetry among hexagonal
columns is generally most evident in the lower colonnade.

The lowermost zone in the Pamona flow, Zone VII, is identified
by Ryan as the flow base. This region consists of small
vesicles and spiracls which result from gases formed along
the lower contact migrating upward into the lava. The flow
base, where present, is 20 to 30 cm. thick.

Not all lava flows exhibit all classical features associated
with columnar jointing as described by Ryan in the Pamona
flow. However, most are quite similar in general configuration.

Flow Geometrics

Individual flows are topographically controlled. In regions
of low relief, viscous lavas generally fill valleys or flow
onto plains and solidify, leaving a basalt mass with a
roughly convex cross section perpendicular to the direction
of flow. Lavas of lower viscosity or those flowing in areas
with greater topographic relief often result in basaltic
masses with a concave cross section. This feature, results
as cooling, is initiated along the margins of a flow while
the core remains mobile. In many of the larger flows of the
Columbia Plateau, the convex or concave shape is apparent
only in terminating tongues of the flow. Because of the
large quantity of lava extruded and great areas covered, the
central portions of the flow may appear nearly horizontal.

Interbeds

In the deeper parts of the Columbia Plateau there are in
excess of fifty individually identifiable Miocene lava
flows, many in excess of 10 m. in thickness. Between flow
event the surfaces of the exposed flows were exposed to
weathering and erosion. Fluvial silts, sands and gravels,
as well as lacustrine silts and clays were deposited in some
regions forming interbeds between the flows. Strata consisting
of tuff and volcanic ash can also be found interdispersed
with the flows.

Tectonic Features

As volcanism proceeded, tectonic activity caused faulting
and folding of previously deposited sequences. Faults and
structural axis often are found to control ground water flow
through the basaltic aquifer. Also of some importance are
regional joint systems. These regional joint and fracture
systems may be mapped throughout most of the area of deposition
of the northwest basalts; however, their relation to lava
emplacement and later tectonic activity is not well understood

2.19 POROSITY, PERMEABILITY AND GROUND WATER FLOW REGIMES

Variations in permeability and porosity among flows and even
within flows is so great that the assignment of average values
of k and θ for a generic basalt would be both arbitrary and
misleading. However, some generalizations concerning ground
water flow through a basalt may be developed without assigning
definitive or "representative" values for hydrologic parameters.

Permeability of basaltic sequences is highly anisotropic. Horizontal
components of permeability generally greatly exceed vertical
components. In any given flow, permeabilities are generally
much greater near the upper and lower margins of the flow than
in its center. While jointing in the entablature and lower
colonnade does contribute to ground water flow, permeabilities
of Zones I, II, and VII of the flow unit are generally much
higher. Principal flow regimes within a basalt sequence may
be categorized:

1. Interflow regions - interfaces between flows, or
    the interfaces between flows and interbeds, provide
    one of the most permeable regimes for flow within the
    basaltic sequence. Rubble zones, scoria, weathered
    surfaces, fracture-connected vesicles and interflow
    voids in Zones I and II on the upper surface of a
    flow and in Zone VII of an overlying flow often
    provide a highly pervious medium in which ground water
    migration may occur.

2. Interbeds - Interbeds, or sediments deposited between volcanic events, are highly varied in character. Fluvial sands and gravels as well as some sandy lacustrine deposits compose highly permeable zones between lava flows. However, interbeds composed of lacustrine silts and clays bear a much lower permeability and often act as aquitards or aquicludes in the sequence.

3. Joints - Joints observed in flows on the Columbia Plateau range from less than a centimeter to several meters in width. These joints are the principal means of vertical movement of ground water through a basalt sequence and are also often an important means of horizontal flow.

4. Other features - Lava tubes, breccia pipes and fault zones all form localized features which can dominate ground water flow. However, the frequency of occurrence of these features is sufficiently low in the northwest basalts as to minimize their importance when discussing regional flow. A waste repository will probably not be sited in the vicinity of highly permeable ground water conduits such as these.

Ranges of values of hydraulic conductivity measured in various basalts of the northwest United States are summarized on Figure 2-41. Specific permeability data are presented in Sections 2.20 through 2.22 and are summarized in Appendix A.

FIGURE 2-41

HYDRAULIC CONDUCTIVITY DATA FROM BASALTS IN THE NORTHWEST UNITED STATES
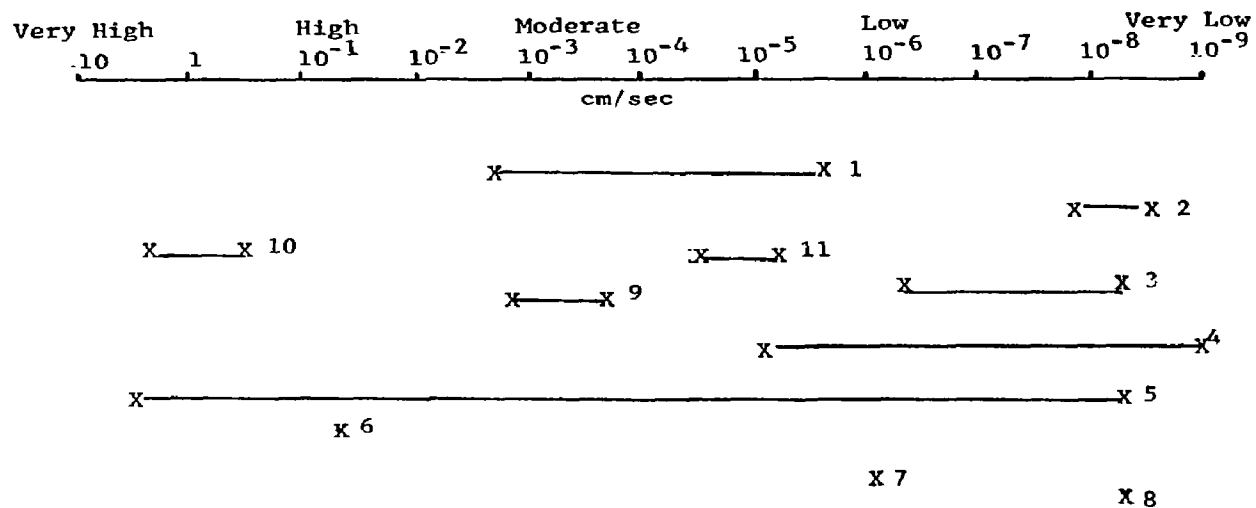
SOURCES OF DATA

	AREA	TYPE & SOURCE
1.	Columbia River Basalt	Field, La Sala & Others, 1970
2.	Columbia River Basalt	La Sala & Others, 1972 (lab data)
3.	Columbia River Basalt	ONWI, 1978 (v7)
4.	Hypothetical Case	ONWI, 1978 (v21)
5.	Snake River Plain	Idealized, Skibitzke and Costa, 1962
6.	Dalles, Oregon	Foxworthy and Bryant, 1967
7.	Columbia River Basalt	Fractured, Hanford, Co., 1976
8.	Columbia River Basalt	Dense, Hanford, Co., 1976
9.	Columbia River Basalt	Eddy, 1969
10.	Columbia River Basalt	Summers & Deju, 1976 (highest values)
11.	Columbia River Basalt	Summers & Deju, 1976 (lowest values)

Figure 2-41 (Con't) Sources

2.20 HYDROLOGIC FEATURES OF THE COLUMBIA RIVER BASALT

Origin

The Columbia River basalt, as located and discussed in Section 2.7, encompasses an area in excess of 150,000 sq. kilometers in southeast Washington, northeast Oregon and western Idaho. During a period extending from the middle to late Miocene, this region was subsiding while fissure eruptions repeatedly poured lava into the developing basin.

By the late Miocene, the basin encompassed an area bounded by Mesozoic granites of the Okanogan highlands on the north, the pre-Cambrian to Mesozoic sequences of the Rocky Mountains to the east and the folded tertiary sediments of the Cascades and Blue Mountains to the west and south (Deju et al, 1977). As volcanism declined in the late tertiary, a series of west to northwest trending anticlinal ridges formed across the subsiding basin. Broad synclines formed between these ridges creating the Umatilla, Pasco, Quincy, and several smaller structural basins.

Stratigraphy of the Pasco Basin

The Pasco basin, located on Figure 2-42, is situated near the depocenter of the regional subsidence. The minimum thickness of the Miocene basalt sequence in the basin is estimated to be 1500 m. (Meyers, 1973)(Meyers and Brown, 1973)(Brown and Ledgewood,1973).
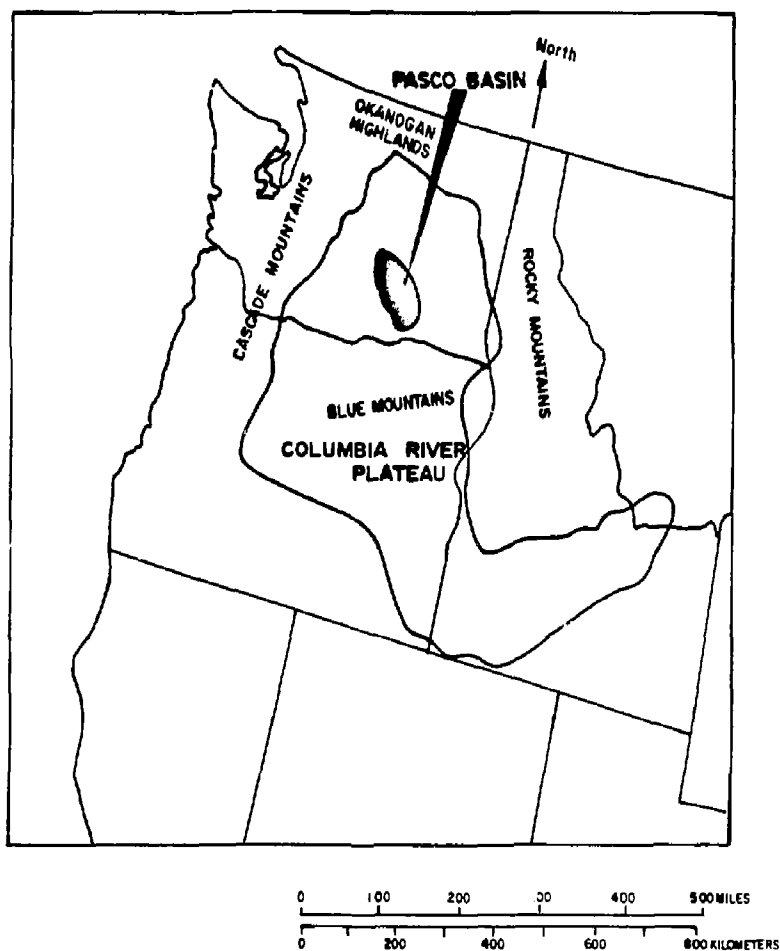
Figure 2-42 The Columbia River Plateau. Source: NWTSP (1976)

The maximum thickness of this sequence is not precisely known; however, where these flows have been penetrated, they are found to overlie older basalts of Oligocene and Eocene age.

There are 5 principal accumulations of flows in the Columbia River Group of the Pasco Basin. The lower two units are the Picture Gorge Basalt and Imnaha Basalt. The upper 3 formations, identified on the stratigraphic column, Figure 2-43, are the Grande Ronde (Lower Yakima), Wanapum (Middle Yakima) and Saddle Mountains (Upper Yakima). Each of these formations contains numerous individual flows, many interbedded with sandstones, siltstones, tuff or diatomite. The geographic relationships of these flows are identified on Figures 2-44 through 2-46. Detailed physical and chemical descriptions of individual flows may be found in a report prepared for the National Waste Terminal Storage Program (1976).

Overlying the upper basalts in the basin is the Ringold formation, a series of early Pleistocene fluvial silts, sands and gravels with interbedded clays in the lower portions cf the formation. The youngest rocks in the basin are late Pleistocene glaciofluvial sediments, ash beds and eolian deposits which overlie the Ringold Formation.

GEOLOGIC TIME SCALE

ERA	PERIOD	EPOCH	RADIOGENIC DATE YEARS B.P	STRATIGRAPHIC UNITS	BED OR FLOW UNIT	LITHOLOGIC CHARACTER	THICKNESS IN METERS
CENOZOIC	QUATERNARY	HOLOCENE		ALLUVIUM, COLLUVIUM & EOLIAN SEDIMENTS		SANDS, SILTS, GRAVELS & CLAYS MODIFIED BY WIND EROSION.	DUNES TO 20
			6,600 / 10,000		MAZAMA ASH	ASH FALL, CRATER LAKE, OREGON.	.2 - .3
			12,500		GLACIER PEAK ASH	ASH FALL, GLACIER PEAK, WASHINGTON	.05
			>12,000 / <18,000		ST. HELENS ASH	ASH FALL, MT. ST. HELENS, WASHINGTON	.05
		PLEISTOCENE		GLACIOFLUVIATILE SANDS & GRAVELS	TOUCHET SILTS	FINE GRAINED FACIES OF THE GLACIOFLUVIATILE DEPOSITS. BEDDED IN QUIET WATER.	0 - 120
			40,000		PASCO GRAVELS *	PREDOMINANTLY COARSE GRAINED GRAVELS, COBBLES & SANDS WITH CUT & FILL STRUCTURE.	
				RINGOLD FORMATION	PALOUSE SOIL	CALCAREOUS SAND, SILT & EOLIAN DEPOSIT. MAINLY DERIVED FROM RINGOLD FORMATION	0 - 25
					(UPPER) RINGOLD	LOCALLY CAPPED BY CALICHE. MOSTLY WELL BEDDED FLUVIAL SILTS & SANDS WITH SOME GRAVELS.	0 - 125
					(MIDDLE) RINGOLD	SANDS & GRAVELS, WELL SORTED, COMPACT BUT VARIABLY CEMENTED.	0 - 120
			1,000,000 / 1,500,000		(LOWER) RINGOLD	SILTS & CLAYS WITH INTERBEDDED GRAVELS & SANDS. CLAY IS CHARACTERISTICALLY BLUE BUT MAY BE GREEN, BROWN OR TAN.	0 - 125
		PLIOCENE	8,000,000	COLUMBIA RIVER BASALT GROUP — UPPER YAKIMA BASALT — YAKIMA BASALT FORMATION (SADDLE MOUNTAINS BASALT FORMATION)	ICE HARBOR MEMBER — ICE HARBOR II	BASALT	0 - 5
					ICE HARBOR I	BASALT	0 - 20
	TERTIARY	MIOCENE		ELEPHANT MOUNTAIN MEMBER — LEVEY *	TUFF & TUFFACEOUS SANDSTONE.	0 - 10
					WARD GAP / ELEPHANT MOUNTAIN	BASALT	0 - 30
					RATTLESNAKE RIDGE	SANDSTONE, TUFFACEOUS.	0 - 15
			10,000,000	POMONA MEMBER	POMONA II * / POMONA I *	BASALT	0 - 75
				GABLE MOUNTAIN (ESQUATZEL ?) MEMBER *	SELAH	SANDSTONE, TUFFACEOUS.	0 - 10
					GABLE MOUNTAIN II *	BASALT	0 - 10
					GABLE MOUNTAIN TUFF *	TUFF-DISCONTINUOUS.	0 - 2
					GABLE MOUNTAIN I *	BASALT	0 - 20
				HUNTZINGER MEMBER	COLD CREEK *	SANDSTONE - WITH TUFF, SAND & GRAVEL	0 - 30
					HUNTZINGER	BASALT	0 - 80
					WAHLUKE * (WARDEN ?)	BASALT	0 - 20
			14,000,000	UMATILLA MEMBER	SILLUSI / UMATILLA	BASALT	0 - 75
				PRIEST RAPIDS MEMBER	MABTON	SANDSTONE WITH SOME GRAVEL	15 - 30
					PRIEST RAPIDS IV / PRIEST RAPIDS III / PRIEST RAPIDS II / PRIEST RAPIDS I	BASALT	0 - 70
			15,000,000	MIDDLE YAKIMA BASALT * — YAKIMA BASALT FORMATION (WANAPUM BASALT FORMATION)	QUINCY	SANDSTONE WITH CLAY & DIATOMACEOUS MATERIAL.	0 - 10
				ROZA MEMBER		BASALT	30 - 50
				FRENCHMAN SPRINGS MEMBER	SQUAW CREEK	DIATOMITE	0 - 10
					SENTINEL GAP / SAND HOLLOW / GINGKO	BASALT	40 - 100
				VANTAGE SANDSTONE FORMATION *		SANDSTONE - WEAKLY CEMENTED.	0 - 10
				LOWER YAKIMA BASALT * — (GRANDE RONDE BASALT FORMATION)	MUSEUM / ROCKY COULEE / HIGH Mg CHEMICAL TYPE * — SEVEN TO THIRTEEN FLOWS	BASALT	250
					LOW Mg-HIGH K CHEMICAL TYPE * — APPROXIMATELY TWENTY FLOWS (INCLUDES UMTANUM)	BASALT	100 - 250

* INFORMALLY USED NAME OR STRATIGRAPHIC RANK

NOTE: THIS STRATIGRAPHIC CHART IS UNDER REVISION

Figure 2-43 Stratigraphy of the Pasco Basin. Source: NWTSP (1976)

2-144

Figure 2-44 Geography of Pasco Basin. Source: NWTSP (1976)

Figure 2-45 Generalized cross section A-A parallel to the same axis of the Pasco Basin. Source: WPPSS (1978)

Figure 2-46 Generalized cross section B-B' normal to axis of Pasco
Basin. Source: WPPSP (1976)

Hydrology of the Pasco Basin Sequence

The Pasco basin has often been suggested as a potential site
for a deep repository because it appears to possess the
smallest quantity of usable ground water per unit surface
area of any of the structural basins (Deju et al, 1977). The
basin has numerous thin beds of clay-rich sediment and
saprolite which were deposited between the outpourage of
Columbia River Basalt. This material has since plugged pore
and fracture spaces, reducing the rate of ground water
movement and hydraulically separating individual interflow
zones. Pumping data from the Columbia River Basalt within
the Pasco Basin show that no large amounts of water have
been obtained. The basalts themselves offer zones as thick
as 200 m. that are fully dry (Deju, 1977).

Since the siting of the Hanford facility in the Pasco basin,
more hydrologic data on deep rock units have been developed
on this area than on most of the remainder of the plateau.
Testing of the deep basalts at Hanford was begun in 1969
with the construction of well ARH-DC-1. Since then, several
more wells have been constructed and additional wells proposed
(Apps et al, 1978. 1979). The results of the tests conducted
on DC-series wells at Hanford comprise a large portion of
the geologic and hydrologic data available on the basin and
the deep basalts of the Plateau in general.

At Hanford an unconfined aquifer overlies the basalts. This
aquifer consists of the basal portions of the glaciofluvial
sediments and extends downward to the clay layers at the
base of the Ringold formation. These layers act as an effective
aquitard, confining waters in lower formations. A large body
of data is available on the shallow sedimentary aquifer. Summaries
of these data are found in the reports of the National Waste
Terminal Storage Program (1976) and the Committee on Radioactive
Waste Management (1978).

Of principal significance to the deep burial of nuclear waste
are the confined aquifers at Hanford. These are composed of
the lowermost portion of the Ringold formation and the
underlying Columbia River Basalt Group. The general hydrologic
characteristics of the stratigraphic sequence at Hanford are sum-
marized in Figure 2-47.

General Characteristics of Ground Water Flow
Within the sequence of Miocene basalt flows the zones of highest
permeability, as determined from packer test of the Hanford
test wells, are the interflow zones separating basalt flows.
These interflow zones consist of rubble and porous sediments
deposited between flow events. The central volume of most
basalt flows is quite dense, having very low permeabilities.
Fractures, originating from the cooling of the initial
molten rock or subsequent structural deformation, control
the hydraulic interconnection between basalt units.

GEOLOGIC TIME SCALE				GEOLOGIC CHARACTERISTICS				HYDROGEOLOGY	
ERA	PERIOD	EPOCH	RADIOGENIC DATE YEARS B P	STRATIGRAPHIC	BED OR FLOW UNIT	LITHOLOGIC CHARACTER	THICKNESS IN METERS	HYDROLOGIC CHARACTER	AQUIFER
CENOZOIC	QUATERNARY	HOLOCENE	8,000 / 10,000 / 12,500 / >12,000 <18,000	ALLUVIUM COLLUVIUM & EOLIAN SEDIMENTS		SANDS SILTS GRAVELS & CLAYS MODIFIED BY WIND EROSION	DUNES TO 20	OCCUR EVERYWHERE ABOVE THE WATER TABLE	DRY
					MAZAMA ASH	ASH FALL CRATER LAKE OREGON	7-3		
					GLACIER PEAK ASH	ASH FALL, GLACIER PEAK WASHINGTON	03		
					ST HELENS ASH	ASH FALL, MT ST HELENS WASHINGTON	03		
		PLEISTOCENE	40,000	GLACIOFLUVIATILE SANDS & GRAVELS	TOUCHET SILTS	FINE GRAINED FACIES OF THE GLACIOFLUVIATILE DEPOSITS BEDDED IN QUIET WATER		OCCUR ABOVE THE WATER TABLE EXCEPT BETWEEN THE HIGH TERRACE PLATEAUS & THE COLUMBIA RIVER HAS VERY HIGH TRANSMISSIVITY & STORAGE	OCCASIONALLY AN UNCONFINED AQUIFER OR DRY
					PASCO GRAVELS	PREDOMINANTLY COARSE GRAINED GRAVELS COBBLES & SANDS WITH CUT & FILL STRUCTURE	0-120		
					PALOUSE SOIL	CALCAREOUS SAND & SILT EOLIAN DEPOSIT. MAINLY DERIVED FROM RINGOLD FM	0-25	OCCUR EVERYWHERE ABOVE THE WATER TABLE	DRY
				RINGOLD FORMATION	UPPER RINGOLD	LOCALLY CAPPED BY CALICHE. MOSTLY WELL-BEDDED FLUVIAL SILTS & SANDS WITH SOME GRAVELS	0-125	SAND & GRAVEL BEDS HAVE VERY HIGH HYDRAULIC CONDUCTIVITY & STORAGE SOME BEDS OF SILTY CLAY OR CLAY ARE ESSENTIALLY IMPERMEABLE	UNCONFINED AQUIFER
			1,000,000 / 1,500,000		MIDDLE RINGOLD	SANDS & GRAVELS WELL SORTED COMPACT BUT VARIABLY CEMENTED	0-12		
					LOWER RINGOLD	SILTS & CLAYS WITH INTERBEDDED GRAVELS & SANDS CLAY IS CHARACTERISTICALLY BLUE BUT MAY BE GREEN BROWN OR TAN	0-125		AQUICLUDE
	TERTIARY	PLIOCENE						FLOWS ARE DENSE VERTICAL HYDRAULIC CONDUCTIVITY IN THE FLOW IS MODERATE DUE TO SHRINKAGE CRACKS HORIZONTAL HYDRAULIC CONDUCTIVITY & TRANSMISSIVITY OF INTERBEDDED SEDIMENTS IS MODERATE	AQUIFER / AQUITARD / AQUIFER / AQUITARD / AQUIFER (CONFINED SYSTEMS)
			11,000,000	COLUMBIA RIVER BASALT GROUP	UPPER AND MIDDLE YAKIMA	BASALT FLOWS AND INTERBEDS TUFF & TUFFACEOUS SANDSTONE	0-700		
		MIOCENE	15,000,000		VANTAGE SANDSTONE	WEAKLY CEMENTED SANDSTONE	0-10		
					LOWER YAKIMA	BASALT FLOWS & INTERBEDS	0-300		

Figure 2-47 Hydrostatigraphic characteristics of the Pasco Basin.
Source: NWTSP (1976)

In many instances, secondary mineralization has effectively
sealed these fractures from further ground water movement.
Fractures also become tighter the greater their depth of
burial. The hydraulic separation of individual water-
bearing strata is apparent when the water levels at the top
and bottom of some basalt flows are compared (Deju et al,
1977). Figure 2-48 illustrates this confinement of individual
zones of higher permeability in the Hanford well ARH-DC-1.

Porosity

The porosity of rocks in the flood-basalt sequence is not well
defined. Porosity within flows is primarily attributable to
fracturing and voids in rubble zones at flow margins. If the
fractured rock is vesicular, effective porosity is increased by
the volume of vesicles that are parted by fractures. For basalt
penetrated by bore hole ARH-DC-1, values of mean porosity were
calculated by a commerical logging firm as follows: (a) dense,
1 percent; (b) vesicular, 5 percent; and (c) zone of close
fractures, 10 percent (Fenix and Scisson, 1969). These estimates
were developed using log interpretation principles designed for
use in sediments with intergranular porosity. They are not deter-
minations of effective porosity and should only be considered order
of magnitude estimates.
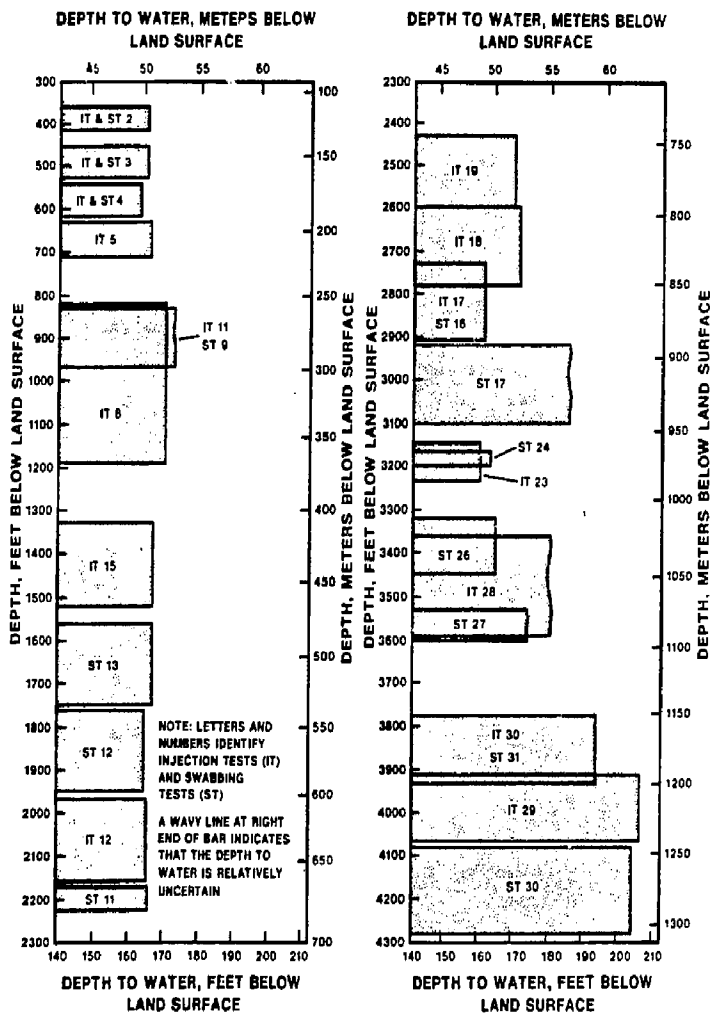
Figure 2-48   Approximate undisturbed ground water head for isolated
water-bearing zones in well ARH-DC-1 (1969).
Source: NWTSP (1976)

2-152

Hydraulic Conductivity

Although there is currently additional well testing work
being carried on (Apps et al, 1978, 1979), the greatest bulk
of published data on the hydraulic conductivity of the
basalt sequences in the Pasco basin is derived from tests of
well ARH-DC-1. This well penetrated the basalts to a depth
of 17^5 m., and in-hole permeability tests were conducted
down to 1305 m. In addition, laboratory permeability tests
were conducted on core samples from specific zones of interest.

Those zones identified in packer tests of well ARH-DC-1
as having the highest hydraulic conductivities are identified
on Table 2-35. These most permeable zones in the well have
hydraulic conductivities ranging from 0.4 to 2.7 m/day.
In the intervening zones, hydraulic conductivities were found
to be much lower. The Committee on Radioactive Waste Manage-
ment (1978), has classified the intervening materials and
assigned representative hydraulic conductivities as follows:

    a)   basalt, dense or with healed joints, about 67 percent
            of aggregate thickness, mean hydraulic conductivity
            about 6×10^{-4} m/day.

    b)   basalt, vesicular, about 7 percent of aggregate
            thickness, mean hydraulic conductivity about 9×10^{-4} m/day.

c) basalt, weathered or jointed, about 17 percent of aggregate thickness, hydraulic conductivity about 3×10^{-3} m/day; and

d) tuff or sand, about 9 percent of aggregate thickness, mean hydraulic conductivity about 6×10^{-2} m/day.

To generalize, all the cited values of conductivity for water-yielding segments are of magnitude 10^{0}; those for the remainder of the confined-water zone grade between magnitudes 10^{-1} and 10^{-4} m/day. Evidently, all the basalt in the confined-water zone of the Hanford Reservation must be considered potentially transmissive, in some degree, for dissolved radioactive waste constituents.

In a report prepared for the National Waste Terminal Storage Program (NWTSP, 1976), ranges are presented for the hydraulic properties of both the uppermost confined aquifer, Table 2-36, and various forms of basalt for the Lower Yakima flows, Table 2-37. In the Lower Yakima basalts, in situ measurements of hydraulic conductivity were found to be as low as 10^{-6} m/day for dense basalt.

Laboratory tests of core taken from well ARH-DC-1 show the hydraulic conductivities to be about 2 orders of magnitude smaller than the average values determined from injection

DEPTH (m)	K m/day	ZONE THICKNESS	DESCRIPTION OF BEDS
147			Sands/Sands & Clay
181			Sands/Sands & Clay
226	0.4 to 1.0	4.6 - 33 m	Sands/Sands & Clay
254			Sands/Sands & Clay
344			Flow Breccia
626	2.7	2m	
803	0.6	3.7m	Sands & Tuff
983	2	3m	Scoria or Breccia
1210	.5	15m	Fractured Basalt

TABLE 2-35 Principal zones of high hydraulic conductivity
Well ARH-DC-1
Source: CRWM (1978)

Well Number	Transmissivity ft^2/day	m^2/day	Hydraulic Conductivity ft/day	m/day	Other Properties
LOWER RINGOLD					
699-84-35P	4	0.4	0.11	0.03	
699-24-1P	90	8.3	5	1.5	
699-S11-E12	40	3.7	0.5	0.15	The porosity for the
699-20-E12P	350	32	7	2.1	uppermost confined aqui-
Mean	120	11	3	0.91	fers ranges between 0.3
Range	4-350	0.4-32	0.11-7	0.03-2.1	and 0.4 (30 to 40%). The vertical hydraulic con-
RATTLESNAKE RIDGE					ductivity in the interbeds ranges between 5 x 10^{-4}
199-B3-2P	3.5	0.3	0.25	0.08	m/day and 20 x 10^{-4} m/day.
199-H4-2	3	0.3	0.3	0.09	The storage coefficient
699-14-E6Q	600	55	30	9.1	approaches the compressi-
Mean	200	18	10	3.0	bility of water.
Range	3-600	0.3-55	0.25-30	0.08-9.1	
MABTON					
DH-8 Range	600-2000	55-180	20-60	5.0-20.0	

Table 2-36   Hydraulic characteristics of the uppermost confined aquifers. Source: NWTSP (1976)

	Hydraulic Conductivity		Transmissivity		Effective Porosity[a]	Storage Coefficient
	ft/day	m/day	ft²/day	m²/day	Dimensionless	Dimensionless
Dense basalt	$1\times10^{-5}-3\times10^{-3}$	$3\times10^{-6}-9\times10^{-4}$	$1\times10^{-4}-3\times10^{-1}$	$9\times10^{-6}-3\times10^{-2}$	0.1-1	$1\times10^{-5}-1\times10^{-6}$
Vesicular basalt	$1\times10^{-3}-1\times10^{-2}$	$3\times10^{-4}-3\times10^{-3}$	$1\times10^{-2}-1$	$9\times10^{-4}-9\times10^{-2}$	5	$<1\times10^{-4}$
Fractured, weathered or brecciated basalt	$3\times10^{-3}-5$	$3\times10^{-4}-1.5$	$1\times10^{-2}-500$	$9\times10^{-4}-46$	10	$<1\times10^{-3}$
Interbed	$3\times10^{-3}-10$	$9\times10^{-4}-3$	$3\times10^{-2}-100$	$3\times10^{-3}-9$	20	$<1\times10^{-2}$

[a]Volume percent.

Table 2-37   Range of Hydrologic properties of lower Yakima Basalt
flows and interbeds.   Source: NWTSP (1976)

tests (Table 2-38). The difference in these measurements is explained by La Sala and Doty (1971):

> "These differences in values of hydraulic conductivity result, because these two types of tests measure different characteristics of the rocks. The field values of hydraulic conductivity were determined on a large volume of in-place rocks. The basalt, as can be seen in outcrops, is cut by shrinkage cracks and other fractures which are capable of transmitting water. The field hydraulic conductivities, therefore, apply not only to the ability of the basalt flows to transmit water through intergranular pore spaces, but also through fractures. The laboratory tests were made on small cylinders of rock that were selected to be free of open fractures and, therefore, indicate the hydraulic conductivity dependent on movement through intergranular pore spaces. The results of the tests indicate that the hydraulic conductivity of basalt flows results mainly from fractures."

Although the bulk of the permeability data currently available on basalts of the Pasco Basin is derived from well ARH-DC-1, some additional data is available. Tests conducted at Hanford on well RSH-1 in 1976 yielded hydraulic conductivity values ranging from 1.5×10^{-2} to 2.5×10^{-5} m/day (Raymond and Tillson, 1968). In tests run in 1978 on well DC-6 at Hanford, hydraulic conductivities ranging from 0.3 to 9.5×10^{-5} m/day were observed (Apps et al, 1979).

Vertical Permeability

Little work has currently been done regarding a determination of the vertical component of permeability in the Columbia basalts. Vertical permeability is difficult to evaluate in situ since deep wells utilized for testing run parallel to vertical joint

TABLE 2-38   SUMMARY OF LABORATORY ANALYSES OF ROCK CORES FROM TEST WELL ARH-DC-1

Core number	Depth (Meters) From	To	Hydraulic conductivity	Porosity (percent)
6--------------- 725.7		726.8	1.12×10^{-5} m/day	9.8
7-------------- 847.0		847.3	1.18×10^{-5} m/day	10.5
8-------------- 898.1		899.2	9.5×10^{-6} m/day	25.4
13-------------- 953.1		953.4	5.79×10^{-6} m/day	2.1
28-------------1306.0		1306.2	1.12×10^{-5} m/day	10.9

Source: NWTSP (1976)

systems. Ledgerwood and Deju (1976), utilizing data developed
by La Sala et al (1973), suggest the vertical components of
permeability to be approximately an order of magnitude lower than
horizontal permeability. Tanaka et al (1974), in a modeling study
of an area north of Hanford, attempted to match hydraulic con-
ductivity to head response in an effort to develop a suitable
valve for vertical conductivity. Tanaka concluded the vertical
component of K should be between $3x10^{-7}$ and $1x10^{-5}$ m/day. Deju et al
(1977), conclude hydraulic conductivities in the central volume
of a dense, thick basalt are usually 2 or 3 orders of magnitude
less than 10^{-9} m/day. An understanding of permeability anisotropies
is critical to effective modeling of a deep repository. Further
work on directional components of permeability needs to be
completed.

Vertical Hydraulic Gradients

In 1972, 5 piezometers were installed in well ARH-DC-1
as depicted in Figure 2-49. These piezometers have been
monitored on a more or less continuous basis since. Data
from these piezometers indicate there is a potential inter-
connection of basalt beds above the 888m level. This is
confirmed by the uniformity of the piezometric surfaces
measured in the injection tests summarized on Figure 2-48.
Data collected from 1972 to 1976 also indicate an inter-
connection of beds in the 970 to 1480 m. interval. Separating
these two apparent flow regimes is the Umtanum flow unit.
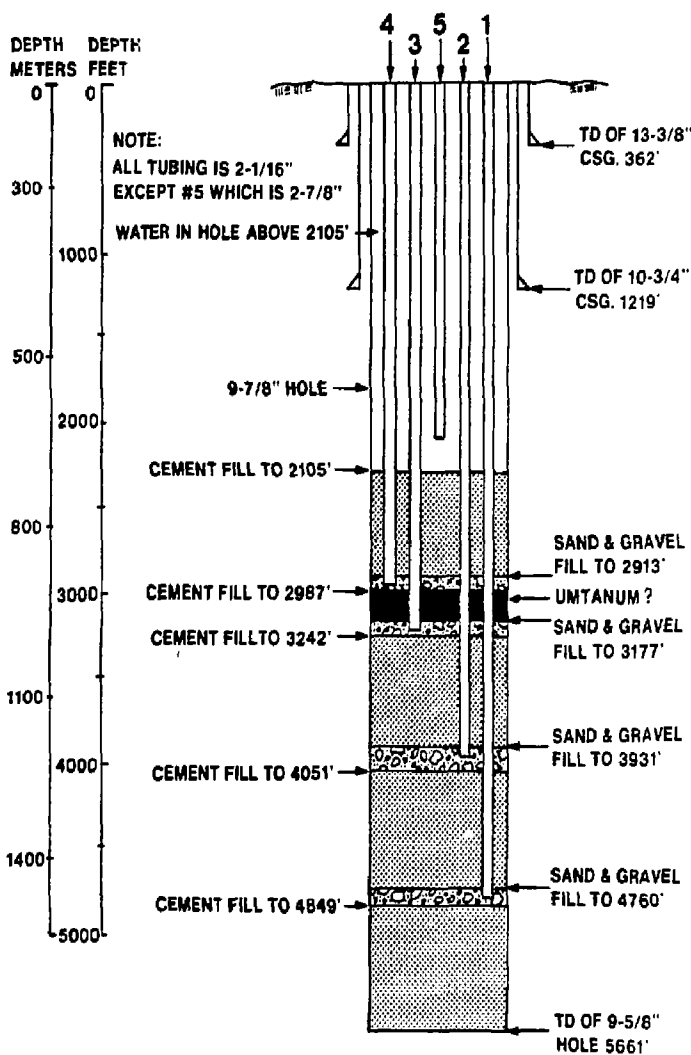
Figure 2-49 Piezometers installed in ARH-DC-1. Source: NWTSP (1976)

During 1978, additional wells in the DC sequence were constructed
as depicted in Figure 2-50. Although work with this series of
wells continues and full data are not yet published, Apps et al
(1979) suggest there are errors in piezometer readings from well
DC-1 created by leakage through cement seals between piezometers
1, 2, and 3. Readings from well DC-1 indicated that units below
the Umtanum flow were hydraulically connected and that there was
an upward gradient across this flow unit. Piezometric readings
made in well DC-2, 40 feet from DC-1, confirm the hydraulic
connection of beds above the Umtanum, but show a sharp down-
ward gradient immediately below this flow followed by a sharp
upward gradient encountered at a point approximately 1000 ft.
below the Umtanum. As illustrated in Figure 2-51, this pattern
of gradient reversals was also confirmed in well DC-6. While
some dense basalts within the Columbia River group are sufficiently
impermeable to allow different heads to be maintained on various
portions of the aquifer, this does not signify there exists an
absolute hydraulic discontinuity between these aquifers. The
head differential between beds continues to drive waters across
the "confining layer" at a rate porportioned to the hydraulic
conductivity of the strata and at a velocity inversely porportional
to its effective porosity.
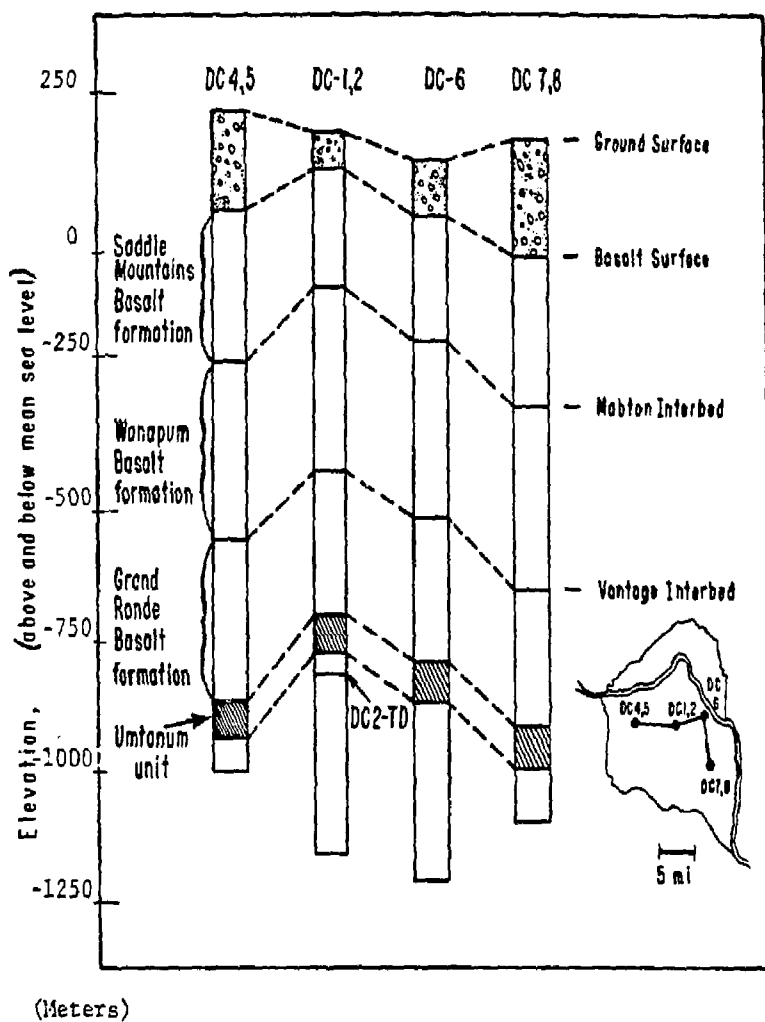
Figure 2-50 Generalized basalt stratigraphy within the Pasco Basin.
Source: Apps et al (1979)
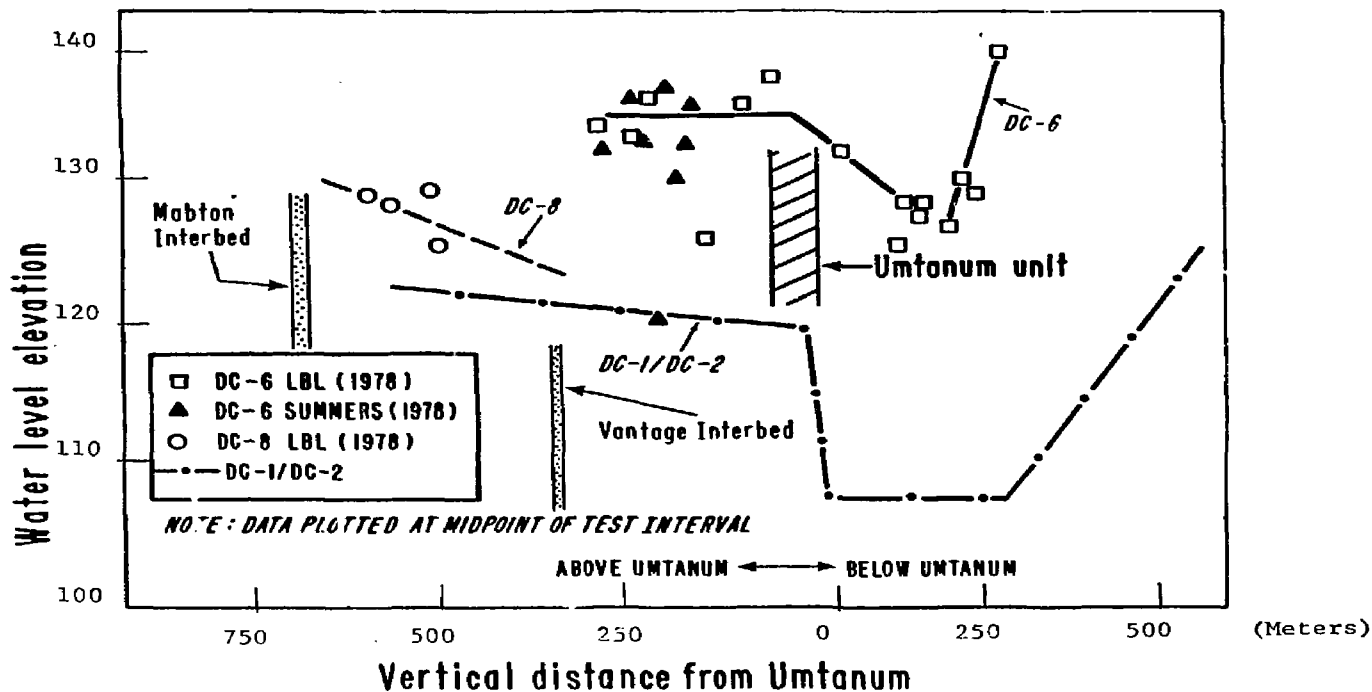
Figure 2-51   Summary of pressure data vs. stratigraphy.
             Source: Apps et al (1979)

Storage Coefficients

Available data on storage coefficients of basalts are minimal. Utilizing well ARH-DC-1, estimates of storage coefficient for the confined basaltic flows were developed. These estimates are summarized on Table 2-39. A range of values of S was observed from 1.8×10^{-3} to 1.4×10^{-6}. However, these results were drawn from analysis of single well tests and are, at best, only order of magnitude estimates.

La Sala and Doty (1971) observe, "the storage coefficients of basaltic rocks should generally be smaller (than those observed in well ARH-DC-1) and, for the most dense, most competent rocks, should approach the value for the compressibility of water."

Average Velocity of Ground Water

Average velocities for ground water in various zones of basalt are suggested by La Sala and Doty (1971) on Table 2-41. They conclude that average velocity ranges from $5 \times 10^{-2} \frac{dh}{dl}$ to $5.0 \frac{dh}{dl}$ m/day, where $\frac{dh}{dl}$ is gradient. Assuming a mean gradient in the confined aquifer at Hanford of .0006 meters per meter (CRWM, 1978), average velocities of ground water would range from 3×10^{-5} to 3×10^{-3} m/day.

The estimates of La Sala and Doty are based upon very minimal porosity data and limited information on hydraulic conductivity. Current programs should help better define average ground water velocities.

TABLE 2-39 STORAGE COEFFICIENTS COMPUTED FROM HYDRAULIC
TEST DATA, WELL ARH-DC-1

Depth Interval (Meters)	Storage Coefficient, S
110.3 - 126.8	0.000066
405.4 - 463.3	[1] .0018
536.4 - 594.4	.00063
958.9 - 986.3	.0000014

[1] This comparatively high-storage coefficient may reflect
largely the characteristics of two sections of sand inter-
layered with the basaltic rocks in this zone.

Source: La Sala and Doty (1971)

Regional Ground Water Systems

Detailed peizometric surface maps indicating direction of ground-water flow have been developed for the unconfined and the shallow confined aquifer in the Pasco basin (Committee on Waste Management, 1978). However, little is known of the direction of migration through deep basalts and interbeds. La Sala and Doty (1971) discuss the effects of ground-water flow through the deep basalts and inter-beds and their potential recharge and discharge areas. Their investigations, however, are based upon meager data and the results remain unsubstantiated (NWTSP, 1976).

2.21 HYDROLOGY OF THE SNAKE RIVER PLAIN

Origin

The Snake River Plain is a structural basin covering an area
of about 31,000 km^2 in southern Idaho. As depicted on
Figure 2-52, the basin is approximately 320 km in length and
50-70 km. in width. Geologic data on the basin are limited
due to the lack of economic mineralization in the basalt
sequence. However, since the siting of the Idaho National
Engineering Laboratory (INEL) on the Snake River Plain in
the early 1950's, sufficient work has been sponsored by the
Department of Energy and the U.S. Geological Survey to
develop a quantitive knowledge of the basin as a whole and a
more specific knowledge of the INEL site in particular.

It is thought that a north-south trending geosyncline lay
across southern Idaho in late Precambrian time. Deposition
of sandstones and shales occurred in this broad depression
through the early Ordovician (Crittenden et al, 1971). As
the Cordilleran geosyncline developed, deposition shifted to
principally carbonate rocks during the later Paleozoic.

Beginning in the Permian and continuing on into the Mesozoic,
tectonic activity increased in the region. The Idaho Batholith
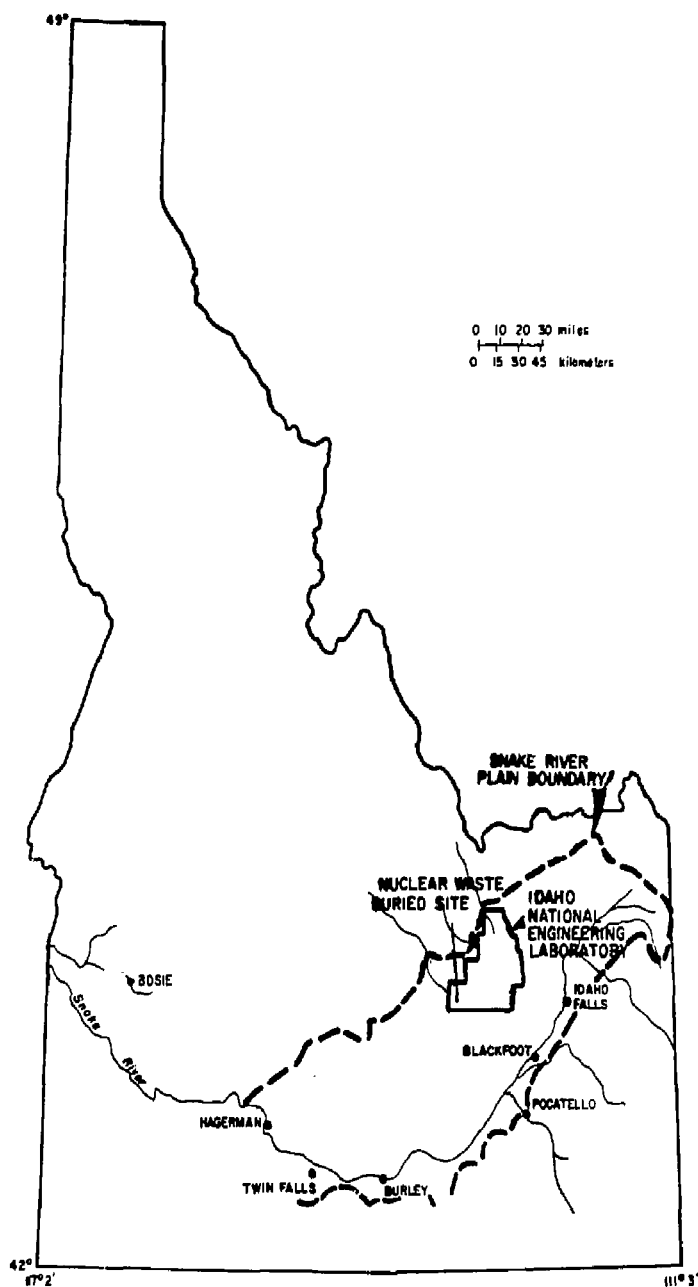
FIGURE 2-52   Location map of Snake River Plain
Source: Robertson et al (1974)

was emplaced to the north and west, and the resulting uplift provided a source of detritus for Mesozoic sedimentation on its flanks. By the middle of the Mesozoic, approximately 15,250 m. of Paleozoic and 10,700 m. of Mesozoic rocks had filled the basin. Uplift and tectonism continued, culminating in the Laramide Orogeny during the late Cretaceous.

By early Cenozoic time, deposition had terminated and erosion of the uplifted sediments had begun. Basin and range faulting during the Miocene created a rugged mountain range in southern Idaho, bounded on the north and west by the Idaho batholith and on the east by large basin and range horsts and grabens. This topography was maintained until the early Pliocene when tectonic events began to create the basin which developed into the Snake River Plain.

A number of theories have been presented for the development of the basin in which the basalts of the Snake River Plain were deposited (Lindgren (1898), Russel (1902), Kirkham (1931), Hamilton (1963)). Currently, the most accepted theory includes the development of a large downfaulted graben inundated by flood basalts. The development of this graben is summarized by Robertson et al, (1974):

> "This hypothesis proposes that in late Miocene the granitic terrain of the Idaho batholith extended southward to the south edge of the present plain where it

either thinned considerably or was displaced westward. Tension during the early Pliocene, probably due to subcrustal forces similar to those envisaged by Hamilton and Myers (1966), produced the present Snake River graben into which the southern tip of the batholith subsided.

Along with subcrustal tension directly reponsible for the grabening, magma developed in the subcrust, perhaps fractionated from a tholeiite into immiscible rhyolite and olivine basalt (Hamilton, 1965), and erupted along tensional openings in the overlying rocks. Sialic volcanism occurred first and covered the floor of the graben as well as much of the surrounding region with tuff and flows (Idavada Volcanics). Effusive removal of subcrustal material from beneath the graben allowed downfaulting to continue and the Snake River Plain crustal block settled into the mantle. By middle Pliocene time all the rhyolite was gone from the magma chamber and eruption of olivine basalt began. Basalt flows were restricted to filling the graben though some flowed short distances up valleys in the adjoining blocks (Crosthwaite and others, 1970). It is the addition of this subcrustal material to the top of the Snake River graben that accounts for the maintenance of isostasy. Figure 2-53 depicts these stages in the hypothetical grabening of the Snake River Plain."

Stratigraphy

The sequence of volcanic rock which fills the graben is thought to range from 300 to over 3000 m. in thickness (Robertson, 1974). Early wells constructed at INEL showed the upper 450 meters of the section to consist of a series of thin basalt flows 3 to 25 m. in thickness, interbedded with fluvial, lacustrine, eolian and pyroclastic sediments. A cross section of the nuclear waste burial ground at INEL, Figure 2-54, identifies the interbedded sediments in the upper portion of the sequence.
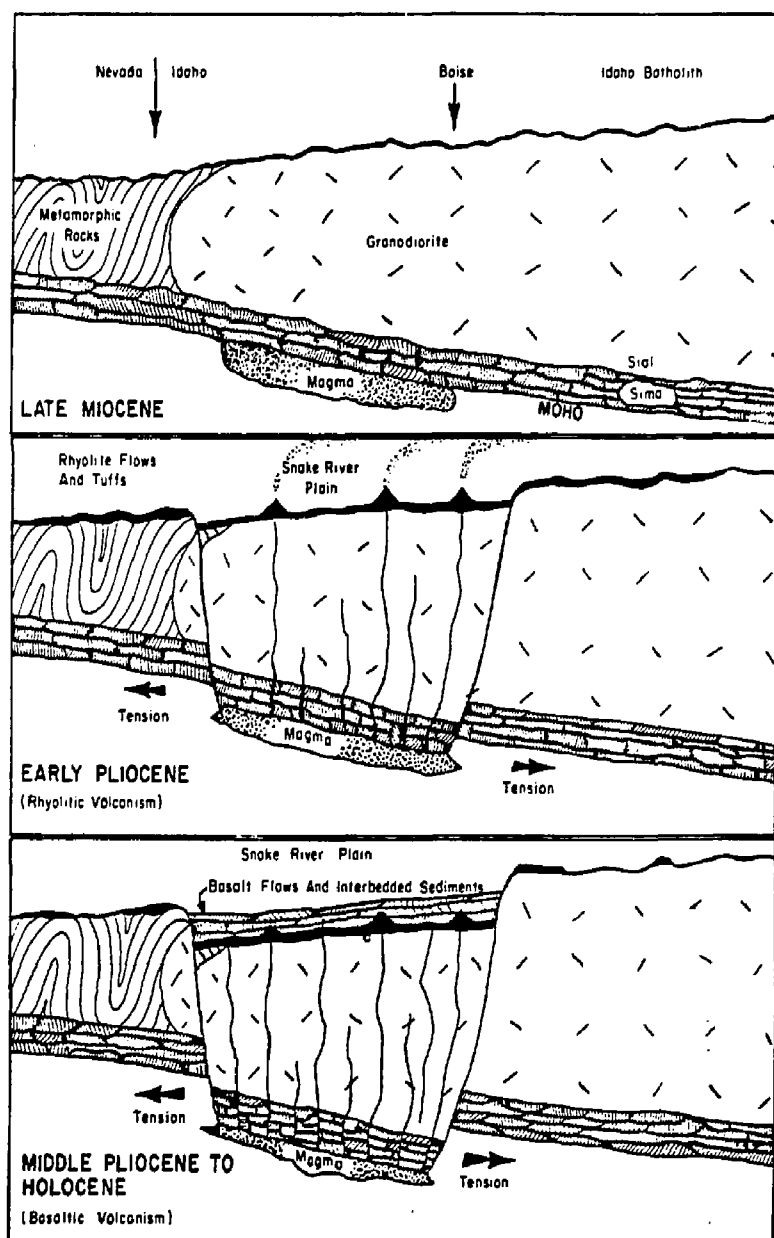
FIGURE 2-53   Cross sections showing hypothetical stages
of grabening during formation of the Snake
River Plain
Source: Robertson et al (1974)
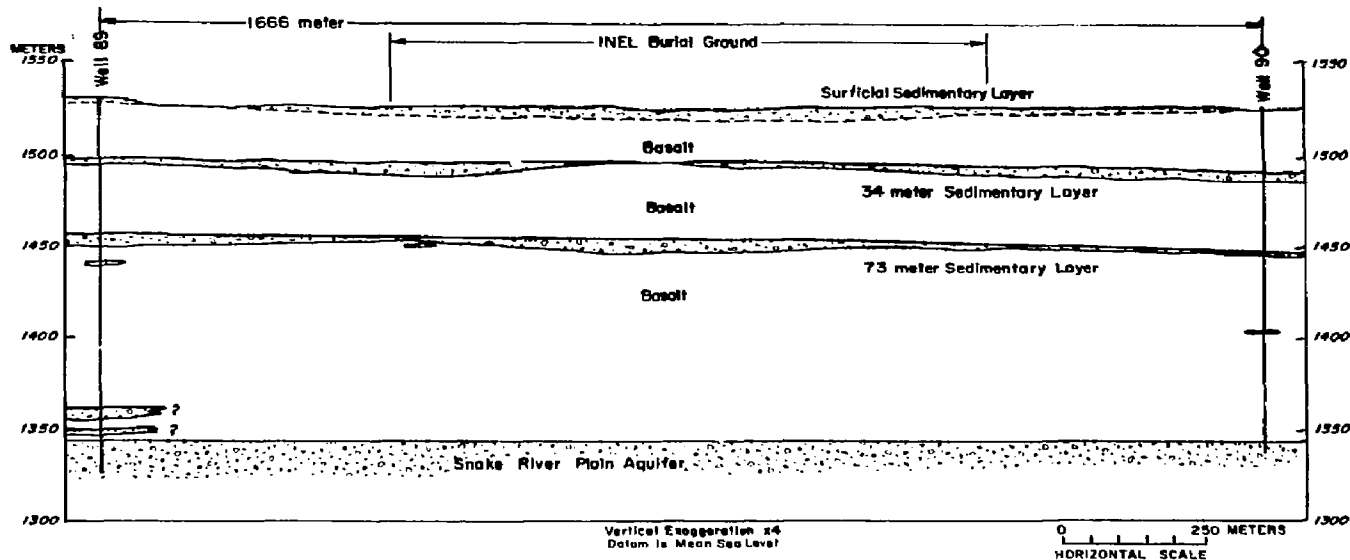
FIGURE 2-54   Cross section of INEL burial ground
Source: Barraclough (1976)

In May 1979, the Department of Energy completed a 3159 m.
geothermal test well at the Idaho National Engineering
Laboratories approximately 30 km. north of the burial site.
The upper 745 m. of this well penetrated basalt flows and
sedimentary interbeds. Below 745 m. a sequence was encountered
which consists of rhyolitic welded ash-flow tuffs, air fall
ash deposits, nonwelded ash-flow tuffs and volcaniclastic
sediments. Doherty et al, (1979) suggests these rocks are
part of an intracaldera fill and that a collapsed caldera
approximately 25 km. in diameter may exist in the region of
well INEL-1.

Characteristics of Ground Water Flow
Ground water flow in the Snake River Plain aquifer occurs
principally along the upper and lower contacts of successive
basaltic flows which have large and irregular fractures,
fissures and other voids (Robertson, 1974). Barraclough et
al, (1976) observed the tops of many flows core-drilled at
INEL to be highly vesicular with numerous intersecting fractures
resulting in high porosity and permeability. The center of
the flows was observed to be relatively dense and of a
significantly lower porosity and permeability. The lowermost
portion of the flow was vesicular and fractured, though to a
lesser degree than the flow top. Consistent with basalts in
other regions, columnar jointing is apparent in the flows of
the Snake River Plain.

Ground water flow paths are not well defined in the rhyolitic
ash flow sequence below 745 m. Doherty et al (1979) notes
that most of the rhyolitic rocks are devitrified and dense.
Nearly all fractures in recovered core are sealed by propylitic
alteration products including calcite, quartz, hematite,
pyrite, a septechlorite mineral, and a variety of clays.
Although most of the fractures, joints and vesicles in the
rhyolite rocks have been filled by products of hydrothermal
alteration, there may be large scale fracture features
condusive to the flow of ground water a: these depths.
Doherty et al (1979) in their study of gecthermal potential
state, "Porous and fractured rocks in ring fracture zones
(around the collapsed caldera) provide channel ways for
circulation and storage of water and, therefore, rocks in
these zones may be likely targets for further geothermal
explorations."

Hydraulic Conductivity
Little reliable hydraulic conductivity data exist for the
Snake River Plain aquifer. Such data as is available is
derived from water well tests and tests at INEL on wells
generally less than 500 m. in depth. Available data suggests
the greatest permeabilities may be found in the upper 200 m.
of the aquifer and permeabilities may significantly decline
from this point downward (Robertson,1974). However, insufficient
deep well data are available to fully confirm this conclusion.

Pumping tests conducted by Norvitch et al (1969), on irrigation
wells penetrating the basalt aquifer showed transmissivities
to range from 1.25×10^4 to 1.25×10^5 m^2/d. and to average
6×10^4 m^2/d. In similar tests at INEL, transmissivities were
observed to range from 3.7×10^2 to 2.2×10^5 m^2/d. and to
average 2.5×10^4 m^2/d. (Robertson, 1974). Barraclough (1976),
in well tests at INEL, found hydraulic conductivity to vary
quite substantially within very short distances. He observed
values of hydraulic conductivity to range from 30 to 3000
m/day. Barraclough further observed that vertical components
of permeability are significantly less than horizontal
components. In tests of a 30 m. thick section of basalt,
King (1968) found horizontal conductivities to average 17
m/day while vertical components averaged 4.5 m/day. At this
test site and depth, the horizontal component of hydraulic
conductivity was found to be 3.7 times that of the vertical
component; however, the data is insufficient to make generalizations
about the rock mass as a whole.

The sedimentary interbeds within the Snake River Plain
aquifer are generally more homogeneous in hydraulic pro, ties
and have a greater porosity, greater capillary pressure and
lower permeability than the basalt.(Barraclough, 1976). Unlike
the Columbia River region, sedimentary interbeds in the
Snake River Plain aquifer are generally barriers to the

downward movement of ground water (Doe, written communication,

1979). Vertical hydraulic conductivities measured from core

of the 34-m. and 73-m. interbeds at the INEL burial ground

are summarized on Table 2-40. The vertical conductivities

of these strata were found to range from 1.67×10^{-7} to 3.0 m/d.

These values are a factor of about 20 less than the above

described permeabilities for in-place basalt.

The basalt-sediment interface is suspected of having vertical

permeabilities even lower than that of the interbeds.

Barraclough (1976) suggests:

> "An additional and even greater constraint occurs at
> the base of each sedimentary layer, at the sediment-
> basalt interface. This is caused by the discontinuity
> of pore spaces from the sediment to the basalt due
> both to the lower porosity of the basalt and to the
> relatively great distances between its fractures. In
> other words, at the interface, perhaps only 10% of the
> basalt surface is composed of permeable openings, and
> these are partially filled by sediment. The other 90%
> is virtually impermeable. This, in effect, provides a
> thin skin that is estimated to have one-tenth or less
> of the permeability of the sediments alone."

In many areas of the Snake River Plain, the vertical permeabilities

of sediments lying above the zone of water saturation are

sufficiently low as to allow perched water tables to exist locally.

Perched waters have been identified on the burial ground

site at INEL. However, leakage of the TRA disposal ponds at

INEL and the subsequent contamination of the Snake River Plain

aquifer indicates that some vertical leakage does occur through

the sediments.

Table 2-49 Vertical Hydraulic Conductivities of
Sedimentary Interbeds - INEL Wells 87-96

Well No.	Depth Zone	Vertical Hydraulic Conductivity M/day
87	C	2.5×10^{-2}
87	C	3.2×10^{-1}
88	C	1.3×10^{-1}
88	C	3.5×10^{-5}
88	C	8×10^{-7}
88	C	3.1×10^{-6}
89	C	1.6×10^{-7}
89	C	6.1×10^{-5}
89	C	5.9×10^{-6}
90	C	2.9×10^{-2}
91	A	1.3×10^{-2}
91	B	3.0
91	C	7.1×10^{-1}
91	C	2.6×10^{-1}
92	A	5.5×10^{-4}
92	C	2.7
92	C	2.7×10^{-2}
92	C	2.1×10^{-6}
93	A	2.6×10^{-4}
93	C	5.5×10^{-2}
94	A	2.7×10^{-4}
94	A	9.6×10^{-6}
94	B	7.6×10^{-1}

Table 2-40 (Cont'd)

Well No.	Depth Zone	Vertical Hydraulic Conductivity M/day)
94	C	1.6×10^{-2}
94	C	2.3×10^{-1}
94	C	7.3×10^{-5}
94	C	5.5×10^{-5}
95	A	7.9×10^{-3}
95	A	5.3×10^{-1}
95	B	1.5×10^{-1}
95	B	3.1×10^{-6}
95	C	2.8×10^{-1}
95	C	9.3×10^{-1}
96	A	5.9×10^{-1}
96	B	6.7×10^{-6}
96	C	1.9×10^{-3}

Depth Zone	Depth
A	0 - 8 meters
B	23-38
C	69-84

Source: Barraclough (1976)

Storage Coefficients

Estimates of storage coefficient for the Snake River Plain aquifer are minimal in the literature. Norvitch et al (1969) determined the average storage coefficient for that portion of the aquifer pentrated by water wells on the plain to range from .001 to 0.2. In later work at INEL, pumping test data on wells less than 500 m. ir depth showed the storage coefficient of the penetrated section to range from .01 to .06.

Average Velocity of Ground Water

With the minimal data available, average flow rates are uifficult to assess. Tracer tests at INEL identified zones with flow rates of 1 to 7 m/d, however, these rates are not necessarily represent-ative of velocities throughout the aquifer. Barraclough et al (1967) suggest the average effectiv? porosity of the upper 610 meters of the aquifer is 5 to 10%. Utilizing Barraclough's conclusions and gradients estimated by Mundorff et al (1964), Robertson et al (1974) estimated the average flow through a one kilometer section of the aquifer on the southern edge of INEL, to be 2 m^3/s. This is equivalent to a flow of .18 m^3 per m^2 normal to the direction of flow, or utilizing an 8% effective porosity, an average flow velocity of 2.4 m/d.

Regional Ground Water System

Data from irrigation wells across the Snake River Plain indicate that water in the upper 500 m. of the aquifer migrates in a generally southwesterly direction as suggested by Mundorff ct al (1964),

Figure 2-55 . Little, if any, work has been done to delineate
the rate and direction of movement of deeper waters. Although
regionally deeper waters probably also migrate southwesterly,
locally the directions of ground water flow may vary substantially.

At INEL, Barraclough, Robertson, and others have studied in detailed
the ground water flow patterns at the burial site and disposal ponds.
These studies, summarized in Barroclough et al (1976), describe
flow in the upper 3 basalt series and the sedimentary interbeds.
It was found in this investigation that while regional water
movement through the area was to the southwest, movement locally
at the burial ground was northeasterly. This was attributed to
recharge from the Big Lost River and its flood diversion areas
to the west.
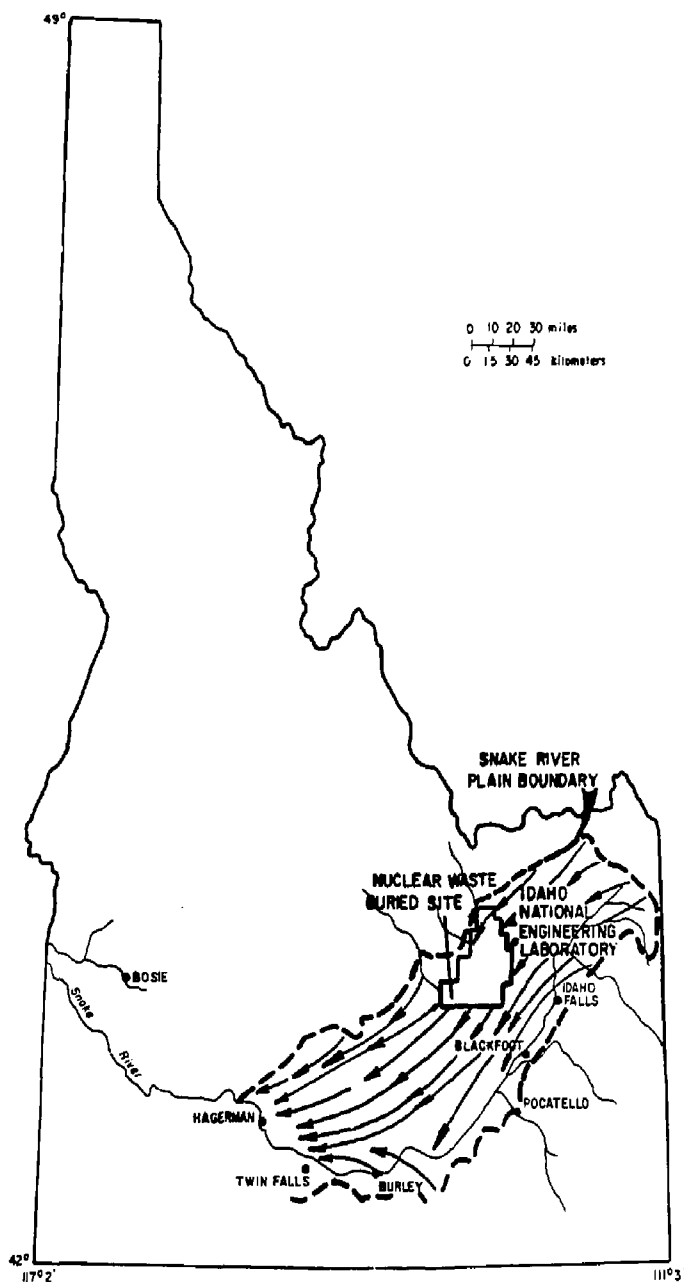
FIGURE 2-55   Regional ground water flow –
                Snake River Plain
                Source: Robertson et al (1974)

2.22   HYDROLOGY OF THE MODOC PLATEAU

Origin

The Modoc plateau lies south of the Columbia River and Snake
River Plain basalts, north of the Sierras and west of the
Cascades and Coastal ranges.   The region consists predominately
of a series of north to northwest trending block-faulted mountain
ranges.   Tectonism culminated in the Miocene or Pliocene on
the plateau; however, faulting has continued into Recent time.
Intervening basins between block-fault ranges have been filled
with a series of basalt flows ranging from Miocene to Recent in
age.   These basalts are often interbedded with lacustrine and
fluvial mudstones, siltstones and sandstones, and volcaniclastic
materials.   Because tectonism has been continuous, many of the
older flows are now faulted and tilted.

Hydrology of Basalt Flows

The intact basalt has a low porosity and permeability.   Most
ground-water flow occurs in breccia layers between flow units,
clinker zones, vesicular zones, joints or lava tunnels (Mack,
1960; Wood, 1960; Brown and Newcomb, 1961; Foxworthy, 1961;
Newcomb, 1961).   Faults in the basalt flows usually form
vertical conduits that enhance permeability rather than form
barriers to horizontal flow.   Interbeds are discontinuous and
generally are only of local significance.

Specific hydrologic data on the aquifer is sparse. Although sustained well yields of 50 to 100 gpm are common, well production is highly variable. Brown and Newcomb (1962) observed transmissivities to range from 1050 to 3720 m^2/day and storage coefficients to range from 1.4×10^{-3} to 2.4×10^{-3}.

Regionally, ground water occurrences in the Modoc Plateau are restricted to many structural basins or grabens between block-fault sequences. These basins are surrounded by crystalline rock of low permeability which provide very little recharge. Most recharge occurs through precipitation or seepage from irrigation facilities or streams.

2.23 REFERENCES

Abegglen, Donn E., Alfred T. Wallace and Roy E. Williams, 1970,
    The Effects of Drain Wells on the Ground-water Quality of
    the Snake River Plain; Idaho Bureau of Mines and Geology
    Pamphlet 148.

Atlantic Richfield Hanford Co., 1976, Preliminary Feasibility
    Study on Storage of Radioactive Wastes in Columbia River
    Basalts; ARH-ST-137.

Barraclough, J. T., 1979, Geohydrology of the Eastern Snake River
    Plain, Idaho, as Shown by a Two-Mile-Deep Well,
    U.S.G.S.

Barraclough, J. T. et al, 1976, Hydrology of the Solid Waste
    Burial Ground, As Related to the Potential Migration of
    Radionuclides, Idaho, National Engineering Laboratory;
    U.S.G.S. Open-File Report 76-471.

Bear, J., 1972, Dynamics of Fluids in Porous Media, American
    Elsevier, New York, pp. 764.

Birch, F., and Clark, H., The Thermal Conductivity of Rocks and Its
Dependence Upon Temperature and Composition, American Journal of
Science, Vol. 238, No. 8, August 1940.

Brown, D.J. and R.K. Ledgerwood, 1973, "Stratigraphy and
    Structure of Yakima Basalt in Pasco Basin, Washington,"
    Geologic Field Trips in Northern Oregon and Southern
    Washington, Oregon Department of Geology and Mineral
    Industries, Bull. 77, 171-181.

Brown, S. G. and R. C. Newcomb, 1962, Ground-water Resources of
    Cow Valley Malheur County, Oregon; U.S.G.S. Water Supply
    Paper 1619-M, 38 p.

Bureau of Reclamation, 1977, Ground Water Manual; A Water Resources
    Technical Publication, U.S. Dept. of Interior.

Committee on Radioactive Waste Management (CRWM), Commission
    on Natural Resources, National Research Council

Crittenden, M.D.,Jr., F.E. Schaeffer, D.E. Trimble, and
    L.A. Woodward, 1971, "Nomenclature and Correlation
    of Some Upper Precambrian and Basal Cambrian Sequences
    in Western Utah and Southeastern Idaho", Geol. Soc.
    America Bull., Vol 82, pp. 581-602.

Crosthwaite, C.A. Thomas, K.L. Dyer, 1970, Water Resources in
    the Big Lost River Basin, South-Central Idaho, U.S. Geol.
    Survey Open-File Report.

Dames and Moore, 1978, Technical Support for GEIS: Radioactive
    Waste Isolation in Geologic Formations, Y/OWI/TM-36/21,
    Vol. 21, Ground Water Movement and Nuclide Transport.

Davis, Stanley N. and Roger J. M. DeWiest, 1966, Hydrogeology,
    N.Y., John Wiley & Sons.

Deju, R. A. et al, 1977, Environmental Factors Needed to Establish
    the Geotechnical Feasibility of Storing Radioactive Waste in
    Columbia River Basalt, RHO-ST-8.

DeWiest, R. J. M., 1970, Geohydrology, New York, J. Wiley &
    Sons, p. 366.

Doherty, David J., Lisa A. McBroome and Mel A. Kuntz, 1979,
    Preliminary Geological Interpretation and Lithologic Log
    of the Exploratory Geothermal Test Well (INEL-1), Idaho
    National Engineering Laboratory, Eastern Snake River Plain,
    Idaho, U.S.G.S. Open-File Report 79-1248.

Eddy, Paul A., 1969, Geohydrology of the Columbia Basin Project
    Area, Washington, abs, in Northwest Science, V 43, n 1,
    p. 35.

Fenix and Scisson, 1969, Exploratory Report, Exploratory
    Hole. ARH-DC-1. Richland, Wash.: Atlantic Richfield
    Hanford Company.

Foxworthy, B. L., 1961, Deformed Basaltic Caprock as an Aquifer
    at Cow Valley, Oregon; U.S.G.S. Prof. Paper 424-C,
    p. C-150 - C-151.

Foxworthy, B. L. and C. T. Bryant, 1967, Artificial Recharge
    Through a Well Tapping Basalt Aquifers at the Dalles,
    Oregon, U.S.G.S. Water Supply Paper 1594-E.

Geohydrological Studies for Nuclear Waste Isolation at the
    Hanford Reservation, Volume II: Final Report

Hamilton, Warren, 1963, "Overlapping of Late Mesozoic Orogens
    in Western Idaho", Geol. Soc. America Bull., Vol 74, pp.
    779-788.
-----1965, Geology and Petrogenesis of the Island Park Caldera
    of Rhyolite and Basalt, Eastern Idaho, U.S. Geol. Survey
    Prof. Paper 504-C.
Hamilton, Warren and W.B. Myers, 1966, "Cenozoic Tectonics of
    the Western United States". Rev. Geophysics, Vol. 4, pp.
    509-549.

Holmes, A., 1965, Principles of Physical Geology, 2nd Ed.
    Ronald Press. New York, 1288 p.

Jones, P. H., 1961, Hydrology of Waste Disposal, National
    Reactor Testing Station, Idaho; U.S.G.S. Open-File Report
    IDO-22042, Issued by U.S. Atomic Energy Comm., Idaho Falls,
    Idaho, 82 p., 70 figs.

King, L.G., 1968, Mathematical Models for Underground Injection
    of Gaseous Wastes into the Vadose Zone: Battelle Memorial
    Institute, BNWL-945.

Kirkham, V.R.D., 1931, Snake River Downwarp: Jour. Geology,
    Vol 39, pp. 456-482.

Konikow, L. F. and J. D. Bredehoeft, 1978, Computer Model of
    Two-Dimensional Solute Transport and Dispersion in Ground
    Water; Techniques of Water-Resources Investigation,
    TWI 7-C2, 90 p.

Lange, N.A., 1956, Lange's Handbook of Chemistry, New York
    McGraw-Hill.

LaSala, A. M. Jr., and G. C. Doty, 1970, Preliminary Evaluation
    of Hydrologic Factors Related to Radioactive Waste Storage
    in Basaltic Rocks at Hanford; U.S.G.S. Admin. Report, in
    Nuclear Science Abstract, V 25, n 21, Art 48606.

LaSala, A. M. Jr., G. C. Doty, and F. J. Pearson, Jr., 1972,
    A Preliminary Evaluation of Regional Ground-water Flow in
    South-Central Washington; U.S.G.S. WRD Admin. Report, 53 p.

Ledgerwood, R.K. and R.A. Deju, 1976, Hydrology of the
    Uppermost Confined Aquifers Underlying the Hanford
    Reservation, US-ERDA Report ARH-SA-253, Atlantic
    Richfield Hanford Company,

Lindgren, Waldemar, 1898, "Geologic Atlas of the United
    States, Boise Folio, Idaho", U.S. Geol. Survey.

Luzier, J. E. and J. A. Skrivan, 1975, Digital Simulation and
    Projection of Water-Level Declines in Basalt Aquifers of the
    Odessa-Lind Area, East-Central Washington; U.S.G.S. Water
    Supply Paper 2036.

MacDonald, G. A., 1966, Geology of the Cascade Range and Modoc
    Plateau; in Geology of Northern California, Bulletin 190,
    California Division of Mines and Geology, San Francisco, 508 p.

Mack, Seymour, 1960, Geology and Ground-water Features of Shasta
    Valley, Siskiyou County, California; U.S.G.S. Water Supply
    Paper 1484, 115 p.

Meinzer, O. E., 1923, The Occurrence of Ground Water in the
    United States, With a Discussion of Principles; U.S.G.S.
    Water Supply Paper 489, 321 p.

Mundorff, M. J., E. G. Crosthwaite and Chabot Kilburn, 1964,
    Ground Water for Irrigation in the Snake River Basin in
    Idaho, U.S.G.S. Water Supply Paper 1654, 224 p.

Myers. C.W.. 1973. Yakima Basalt Flows Near Vantage. and
    from Core Holes in the Pasco Basin, Washington, PHD.
    Dissertation, University of California at Santa Cruz.
    Santa Cruz, California, p.147.

Myers, C.W. and D.J. Brown, 1973,"Stratigraphy of the Yakima
    Basalt in the Pasco Basin, Washington:" (abstract)
    Geol. Soc. of Amer. (Cordilleran Section,) 5(1), 8c

National Waste Terminal Storage Program (NWTSP) of the
    U.S. Energy Research and Development Administration
    by Atlantic Richfield Hanford Company under Contract
    E(45-1)-2130.

Newcomb, R. C., 1961, Ground Water in the Western Part of the
    Cow Creek and Soldier Creek Grazing Units, Malheur County,
    Oregon; U.S.G.S. Water Supply Paper 1475-E, pp. 158-172.

_____ 1969, Effects of Tectonic Structure on the
    Occurrence of Ground Water in the Basalt of the Columbia
    River Group of the Dalles Area, Oregon and Washington;
    U.S.G.S. Prof. Paper 383-C, 105 p.

Norvitch, R.F., C.A. Thomas, and R.G. Maditon, 1969,
    Artificial Recharge to the Snake Plain Aquifer; an
    Evaluation of Potential and Effect: Water Information
    Bulletin No. 12, issued by Idaho Department of Recla-
    mation, Boise, Idaho, 59 pages.

Piper, A. M., 1975, Hypothetical Prototype Sites of Repositories
    for Radioactive Wastes: Flood Basalt; ORNL Subcontract 3745.

Piper, A. M., T. W. Robinson, and C. F. Park, Jr., 1939, Geology
    and Ground-Water Resources of the Harney Basin, Oregon;
    U.S.G.S. Water Supply Paper 841, 189 p.

Raymond, J.R. and D.D. Tillson 1968 , Evaluation of a Thick
    Basalt Sequence in South-Central Washington. BNWL-776.
    Richland, Wash.: Battelle Pacific Northwest Laboratories

Robertson, J. B. and J. T. Barraclough, 1973, Radioactive and
    Chemical Waste Transport in Ground Water at National
    Reactor Testing Station, Idaho; 20-year case history and digital
    model (abs); American Association of Petroleum Geologists
    Bulletin, V 57, n 8, pp. 1603-1604.

Robertson, J. B., Robert Schoen and J. T. Barraclough, 1974,
The Influence of Liquid Waste Disposal on the Geochemistry
of Water at the National Reactor Testing Station, Idaho
1952-1970; U.S.G.S. Report UC-70.

Russell, I.C., 1902, Geology and Water Resources of the Snake
River Plain of Idaho, US Geol. Survey Bull. p. 199.

Scheidegger, A. E., 1961, General Theory of Dispersion in Porous
Media, in Journal of Geophysical Research, V 66, n 10.

Skibitzke, H. E. and J. A. da Costa, 1962, The Ground-Water Flow
System in the Snake River Plain, Idaho - An Idealized
Analysis; U.S.G.S. Water Supply Paper 1536-D, pp. 47-67.

Stearns, H. T., L. Crandall and W. G. Steward, 1938, Geology
and Groundwater Resources of the Snake River Plain in
Southeastern Idaho; U.S.G.S. Water Supply Paper 818.

Tanaka, H. H., A. J. Hansen, Jr., and J. A. Skrivan, 1974,
Digital-Model Study of Ground-Water Hydrology, Columbia
Basin Irrigation Project Area, Washington; Washington State
Dept. of Ecology Water Supply Bull. 40.

Walton, William C., 1970, Ground Water Resource Evaluation,
New York, McGraw-Hill Book Co.

Wood, P. R., 1960, Geology and Ground-Water Features of the Butte
Valley Region Siskiyou County, California; U.S.G.S. Water
Supply Paper 1491, 151 pp.

APPENDICES

APENDIX A

TABLE 2-A.1 Summary of geomechanical properties of granitic rocks

Rock Type & Location	Young's Modulus (GPa)	Density g/cm³	Bulk Modulus (GPa)	Shear Modulus (GPa)	Poisson's Ratio	Uniaxial Compressive Strength (MPa)	Tensile Strength (MPa)	Reference or Source
Granite (coarse-grained) Polehill Power Plant, Loveland, Colorado	26.6 25.4	2.63(0.03,9)				72.1 52.6	2.63(0.03,9) .02(.0002,9)	1
Pegmatite granite Polehill Power Plant, Loveland, Colorado Group A Group B	19.0	2.62(0.09,27)			0.10	42.7(29.2,3) 58.2(.69,2)	..	1
Slightly altered granite Grand Coulee pumping project, Grant County, Washington	7.59				0.13(NR,3)	56.9 26.3		1
Slightly altered granite Grand Coulee pumping project, Grant County, Washington	8.97 8.28	2.61 (0.04,18)			0.126(NR,3)	64.8 33.2		1
Granite Grand Coulee pumping plant, Grant County, Washington	32.6 12.4	2.63(0.07,32)			0.14(NR,3)	148.8		1
Granite Nevada test site of AEC-LRL-Livermore						64.8		2
Granite, no location	31.0-58.6				0.15-0.24		2.9-4.8	10

TABLE 2-A I Summary of geomechanical properties of granitic rocks

	Stress-strain Properties					Strength Properties		
	Young's Modulus (GPa)	Density g/cm³	Bulk Modulus (GPa)	Shear Modulus (GPa)	Poisson's Ratio	Uniaxial Compressive Strength (MPa)	Tensile Strength (MPa)	References or Source
Rock Type or Location								
Granite Valencia County, NM	77.9(NR,2)	3.0				154.5		1
Granite, NM	77.9	2.80		32.3	.27			11
Granite (Gneisses), GA	19.2	2.66		10.3		200.0	2.8	11
Granite Brid Canyon dam site Moh e County, AZ	53.8(NR,5)	2.66(0.06,15)			.08	144.8 (66.2,4)	5.6(1.9,4)	4
Granite Valencia County, NM	7.24(NR,2)	2.59(0.06,2)			.07	(25.5) (9.7,2)		4
Granite, no location given (weathered)		2.74(NR,8)						5
Granite Unsweep granite site Grand Junction, CO	21.9	2.69			.08	164.8	4.17	12
Granite, Vermont	28.9	2.66		15.9				7
Granite, Maryland	54.6	2.65		25.4		251.0		7
Granite, Nevada	51.3	2.63		22.5		273.4		7
Granite, N. Carolina	24.2	2.60		12.3		209.7		7
Granite, no location	43.1(71,65,9)				0.20(.25,23)		6.62(16.6,22)	6
Granite, no location	52.1	2.67			0.16	202.7		9
Guadarrama Granite[a]	24.4					52.8		9

A-3

TABLE 2-A I Summary of geomechanical properties of granitic rocks

Rock Type or Location	Young's Modulus (GPa)	Density g/cm³	Bulk Modulus (GPa)	Shear Modulus (GPa)	Poissons Ratio	Uniaxial Compressive Strength (MPa)	Tensile Strength (MPa)	Reference or Source
Fremont Canyon Granite (coarse-grained)	64.1	2.62			0.14		3.62	9
Salida Granite	70.7	2.64			0.18	324.1		9
Mitidieri Quarry porphyritic granite	69.06	2.74			0.24	91.7		9
Valishos Quarry granite	65.8	2.72			0.18	107.2		9
Cuntareira Quarry granite	64.1	2.81			0.25	111.3		9
Piccicacco Quarry tourmaline granite	75.5	2.65			0.16	127.1		9
Pikes Peak Granite (coarse-grained, weathered)	33.4	2.67			0.37	88.9	3.93	9
Pikes Peak Granite (dense, medium-fine-grained)	70.6	2.67	62.0	27.0	0.31	226.1	11.9	9
Barre Granite (dense, medium-grained)	72.4	2.64	43.1	29.7	0.22	234.5	7.59	9
Silver Plume Granite Straight Creek tunnel site Pilot bore, Colorado	60.4(44.1,40)				0.205(.31,38)	264.9 / 386.2		10
Quartz Monzonite Straight Creek pilot bore, Colorado	52.4	2.67(WR,30)	52.4	19.3	.33			14

TABLE 2-A I Summary of geomechanical properties of granitic rocks

Rock Type or Location	Stress-strain Properties					Strength Properties		Reference of Source
	Young's Modulus (GPa)	Density g/cm³	Bulk Modulus (GPa)	Shear Modulus (GPa)	Poisson's Ratio	Uniaxial Compressive Strength (MPa)	Tensile Strength (MPa)	
Quartz Monzonite Climax stock, Nevada test site	61.4-69.7	2.6-2.66	53.8	20.0	.21-0.22	210.3		14
Monzonite porphyry Grand Coulee pumping plant, Grant County, Washington	41.4(3.4,3)	2.57(0.05,16)			.18(NR,3)	124.8(.08,140)		
Colville Granite (slightly colored)	11.0		6.20	4.82	0.20	64.8	3.24	
Colville Granite (unaltered)	35.9		17.2	15.9	0.15	144.8	7.45	
Monzonite porphyry Grand Coulee pumping plant Grant County, Washington	42.8				0.6	170.6		1
Quartz Monzonite, MT		2.75				112.4		12
Quartz Diorite Bridge Canyon dam site Mohave County, AZ	47.2(NR,2)	2.71(0.15,5)			0.07(NR,2)	118.6 (19.3,2)	8.21	4
Quartz Diorite Garden Valley dam site Boise, ID	25.5 (11.45,3)	1.00(2.5)			0.104(NR,3)	87.4 (9.7,3)		1
Quartz Diorite Gneiss Bridge Canyon dam site Mohave County, Arizona	61.7(NR,4)	2.83(0.09,9)			0.11(NR,4)	81.4 (13.1,3)	13.5 (2.69,3)	4

TABLE 2-A I Summary of geomechanical properties of granitic rocks

Rock Type or Location	Stress-strain Properties					Strength Properties		Reference or Source
	Young's Modulus (GPa)	Density g/cm³	Bulk Modulus (GPa)	Shear Modulus (GPa)	Poisson's Ratio	Uniaxial Compressive Strength (MPa)	Tensile Strength (MPa)	
Diorite Gneiss Sec a, T6S R77W	68.4 (13.4,2)	2.86(0.27,10) 2.87(0.09,3)			.98(NR,2)	64.2(NR,1) 104.4(NR,1)		1
Diorite, no location	69.7,72.4,12)	2.82(0.48,5)						6
Mineralized Diorite Utah	71.7(24.1,5)	2.71(0.08,5)		26.8 (9.17,5)	0.26(08,5)	246.9 (40.0,5)		8
Diorite Michigan	98.6(23.7,5)	2.91(0.20,2)		35.9 (12.6,2)	.29(06,5)	227.6 (.09,2)		12
Diorite (Gneissic-diorite-gabbro) T	71.1(31.6,2)	3.03(0.01,2)		32.5 (9.45,2)		230.0 (87.6,2)		7
Granodiorite Tumut Pond dam site Snowy Mtns. project, Australia	63.1(NR,6)	2.71(0.05,14)			0.16(NR,6)	126.9 (50.3,3)	1.45(.97,3)	4
Pegmatite Morrow Point Dam Montrose, Colorado	18.5-20.6	2.64(NR,4)			0.05-0.07	56.9	6.00	15
St. Cloud Grey Granodiorite (Precambrian)					.25			

TABLE 1-A11 Summary of geomechanical properties of basalts.

| Rock Type & Location | Stress-Strain Properties | | | | | Strength Properties | | Reference |
	Young's Modulus (GPa)	Density g/cm³	Bulk Modulus (GPa)	Shear Modulus (GPa)	Poisson's Ratio	Uniaxial Compressive Strength (MPa)	Tensile Strength (MPa)	or Source
Vesicular basalt South Coulee dam site, Columbia Basin Project, Washington	38.6(NR,5)	2.58(0.4,6)			.14(NR,5)	82.1(37.9,2)		4
Basalt, no location		3.07(2.95-3.15)						5
Basalt, no location	40.4(79.2,9)	2.66(0.65,16)						6
Basalt, Michigan	61.5	2.85		26.8		230.3		7
Basalt, Michigan		2.97		33.9		268.3		7
Basalt, Michigan	70.3	2.91		29.6		338.6		7
Basalt, Michigan						257.9		7
Basalt (altered) Michigan						81.4		7
Heavily altered amygduler Zeolitic basalt, Michigan		2.04			0.04	171.7		8
Heavily altered amygduler Epidotized basalt, Michigan	40.7	2.70		18.5	0.0%	119.3		8

TABLE 2-AI1Summary of geomechanical properties of basalts.

| Rock Type & Location | Stress-Strain Properties | | | | | Strength Properties | | Reference or Source |
	Young's Modulus (GPa)	Density g/cm³	Bulk Modulus (GPa)	Shear Modulus (GPa)	Poisson's Ratio	Uniaxial Compressive Strength (MPa)	Tensile Strength (MPa)	
Basalt Sec 32, T3S5 R4E, Medford, Oregon	62.3(32.4,6)	2.72(0.11,14) 2.74(0.09,13)			0.234 31.850(16.780,3)	168.6(68.1,3)		1
Basalt Nevada test site AEC-LRL-Livermore	34.9	2.676			0.32	148.0	13.1	1
Basalt Columbia Plateau	70.3(60.7-111.7)	2.9(2.4-3.1)			0.26(0.27-0.28)	200(0- 4,000)	14(0-23)	3
Vesicular basalt Kayna dam site, Bombay, India	36.2(NR,3)	2.56(0.5,4)			.15(NR,3)	68(60,3)3)	2.2(2.8,6)	4
Glassy basalt Black Canyon dam site, Boise, Idaho	32.2(NR,6)	2.62(0.16,10)			.10(NR,6)	60(39.3,3)	1.1(.49,2)	4
Basalt South Coulee dam site, Columbia Basin Project, Washington	50.7(NR,3)	2.8(0.13,5)			.18(NR,3)	171.7(NR,1)		4
Vesicular basalt South Coulee dam site, Columbia Basin Project, Washington	54.3(NR,6)	2.62(0.04,10)			.21(NR,6)	95.9(44.1,3)		4
Vesicular basalt South Coulee dam site, Columbia Basin Project, Washington	42.1(NR,5)	2.47(0.24,12)			.19(NR,6)	61.4(7.03,3)		4

TABLE1-AII Summary of geomechanical properties of basalts.

| Rock Type & Location | Strain-Strain Properties | | | | | Strength Properties | | Reference or Source |
	Young's Modulus (GPa)	Density g/cm³	Bulk Modulus (GPa)	Shear Modulus (GPa)	Poisson's Ratio	Uniaxial Compressive Strength (MPa)	Tensile Strength (MPa)	
Heavily altered amygdular Calcitized basalt, Michigan	60.0	2.80			0.15	342.1		8
Jupia Dam basalt (dense)	73.1	3.00			0.21	104.8		9
Barra Bonita Dam basalt (dense)	61.0	2.97			0.19	137.4		9
Juramirin Dam basalt (dense)	42.8	2.71			0.16	133.0		9
Nussa Quarry basalt (dense)	44.0	2.68			0.19	126.8		9
AEC Nevada test site basalt (dense, fine-grained, unweathered)	34.9	2.83			0.32	148.0	13.9	9
Howard Prarie Dam basalt (very dense, fine-grained)	61.8	2.73			0.23	194.1		9
Lower Granite basalt (massive, compact)	50.2	2.73			0.24	228.1	26.3	9
Little Goose basalt (massive, compact)	77.2				0.27	196.1	11.1	9

TABLE2-AII Summary of geomechanical properties of basalts.

Rock Type & Location	Stress-Strain Properties					Strength Properties		
	Young's Modulus (GPa)	Density g/cm³	Bulk Modulus (GPa)	Shear Modulus (GPa)	Poisson's Ratio	Uniaxial Compressive Strength (MPa)	Tensile Strength (MPa)	Reference or Source
John Day basalt (compact to vesicular)	83.4				0.29	355.1	14.5	9
Basalt	18.7	2.06			0.16	146.1		9
Dresser basalt	93.1			41.5		440.7	22.1	9
Amchitka Island basalt (dense)	61.1		31.8	25.7		249.9	13.5	9

TABLE 2- A III Summary table of hydraulic and thermal properties

Rock Type & Location	Hydraulic Properties		Thermal Properties		Reference or Source
	Porosity %	Hydraulic Conductivity m/day	Thermal Conductivity w/m°K	Heat Capacity J/g°C	
Stripa Granite (F)		1.7×10^{-6} to 34×10^{-6}			16
Metasediments – Straight Creek Tunnel (F)		2.1×10^{-3}			13
Granites (L)		7.4×10^{-8} to 3.3×10^{-4}			13
Metamorphics (L)		4.4×10^{-7} to 8.3×10^{-5}			18
White Lake Gneiss (L)		7.5×10^{-10} to 7.5×10^{-9}			18
Fractured Metamorphics (F) Colorado Front Range		4.1 to 8.3×10^{-3}			18
Crystalline Rocks – Dansites (F) in Western U.S.		0.4 to 4.9			18
Laramie Granite (F)		8.3×10^{-4} to 4.2×10^{-3}			18
Crystalline basement rocks (F) Aiken, S.C.		8.3×10^{-7} to 8.3×10^{-2}			18
Stripa Granite (F)		8.3×10^{-7} to 1.7×10^{-5}			18
Granites & Gneisses (F) Sweden		8.3×10^{-7} to 0.4			18

TABLE 2-A III Summary table of hydraulic and thermal properties

Rock Type & Location	Hydraulic Properties		Thermal Properties		Reference or Source
	Porosity %	Hydraulic Conductivity m/day	Thermal Conductivity w/m^0K	Heat Capacity J/g^0C	
Barre Granite (dense, medium-grained)	0.4	L.T.8x10^{-2}	2.37	.92	9
Silver Plume Granite Straight Creek Tunnel site, Pilot bore, Colo.	1.19(2.5,25)				13
Quartz Monzonite Climax stock, Nevada test site	0.7-1.1		3.		14
Monzonite prophyry Grand Coulee pumping plant, Grant County, Washington	2.32(2.44,16)				1
Quartz Diorite Garden Valley dam site, Boise, Idaho	2.7(0.1)				1
Diorite Gneiss Sec. 1, T6S,R77W Montezuma Quad, Colo.	0.49(1.07,10) 0.22(0.10,3)				1
Diorite, no given location	1.7(8.1,12)				6
Mineralized Diorite,Utah	0.94(1.65,5)				8
Diorite (Gneissic-diorite-gabbro) New York	0.8(.4,2)				7
Pagmatite Morrow Point Dam Montrose, Colorado	0.93(NB,4)				15

TABLE 2- A111 Summary table of hydraulic and thermal properties

Rock Type & Location	Hydraulic Properties		Thermal Properties		Reference or Source
	Porosity %	Hydraulic Conductivity a/day	Thermal Conductivity w/m°K	Heat Capacity J/g°C	
Granite, Maryland	0.08				7
Granite, Nevada	0.09				7
Granite, North Carolina	0.07				7
Granite, no location	1.6(11.1, 146)	1(1,41)			6
Granite, no location	1.6				9
Guadarrama Granite					9
Fremont Canyon Granite (coarse-grained)	0.8				9
Salida Granite					9
Mitidieri Quarry porhyritic Granite	3.6				9
Valinhos Quarry Granite	3.2				9
Cantareira Quarry Granite	2.1				9
Piccicacco Quarry Tourmaline Granite	2.8				9

TABLE 2-4 III Summary table of hydraulic and thermal properties

Granite	Hydraulic Properties		Thermal Properties		
Rock Type & Location	Porosity %	Hydraulic Conductivity m/day	Thermal Conductivity w/m°K	Heat Capacity J/g°C	Reference or Source
Granite (coarse-grained) Polehill Power Plant, Loveland, Colorado	1.0(1.4,27)				1
Pegmatite granite Polehill Power Plant, Loveland, Colorado	1.0				
Slightly altered granite Grand Coulee pumping project, Grant County, Washington	2.61(1.01,18)				1
Granite Grand Coulee pumping plant, Grant County, Washington	1.59(1.48,32)				1
Granite Unaweep granite site Grand Junction, Colorado	0.6				12
Granite, Vermont	0.9				7

TABLE 2-A IV Summary table of hydraulic and thermal properties

Basalts Rock Type & Location	Hydraulic Properties		Thermal Properties		Reference or Source
	Porosity %	Hydraulic Conductivity m/day	Thermal Conductivity $w/m^{\circ}K$	Heat Capacity $J/g^{\circ}C$	
Lac Du Bonnet Batholith (P) Manitoba		4.2×10^{-6} to 4			18
Granodiorite - Los Alamos New Mexico (F)		5.8×10^{-6} to 6.6×10^{-2}			18
Crystalline basement (P) Rocky Mountain Arsenal		4.9×10^{-1} to 6.6×10^{-1}			18
Climax Stock - Colorado (F)		2.5×10^{-1} to 7.5×10^{-1}			: .
Howard Prarie Dam basalt (very dense, fine-grained)	3.1				9
Basalt	10.2				9
Dresser basalt	.264		1.3	.962	9
Amchitka Island basalt (dense)	2.8				

TABLE 2-A IV Summary table of hydraulic and thermal properties

Basalts Rock Type & Location	Hydraulic Properties		Thermal Properties		Reference or Source
	Porosity %	Hydraulic Conductivity m/day	Thermal Conductivity w/m°K	Heat Capacity J/g°C	
Yakima Basalt (upper) a. Interbeds		.08–20			23
Yakima Basalt (lower) a. Dense	(0.1–1)	$(3x10^{-6}-9x10^{-4})$			23
b. Vesicular	5	$(3x10^{-4}-3x10^{-3})$			23
c. Fractured,	10	$(3x10^{-4}-1.5)$			23
weathered or brecciated					
d. Interbed	20	$(9x10^{-4}-3)$			23
Generic Basalt	$(5x10^{-4}-0.35)$	$(4x10^{-5}-4)$			24
Snake River Basalt		$(10^{-5}-10^{-6})$	•		25
Snake River Basalt	8 (5–10)				26
Yakima Basalt		$(10^{-4}-1)$			27
Yakima Basalt a. Laboratory		$(5x10^{-6}-10^{-5})$			28
b. In Situ		(10^{-4})			28
Yakima River		$(4x10^{-1}-1.7)$			30
Snake River		$(2.6x10^{-6}-2)$			31

A-16

TABLE 2-A IV Summary table of hydraulic and thermal properties

Basalts Rock Type & Location	Hydraulic Properties		Thermal Properties		Reference or Source
	Porosity %	Hydraulic Conductivity m/day	Thermal Conductivity w/m°K	Heat Capacity J/g°C	
Cavernous and fractured		10^3 (10-10^5)			19
Basalt		(10^{-5}-10)			19
Snake River Plain	10				20
Columbia River					
a. Sedimentary Interbeds	0.1(0.01-0.25)	10^{-1}(10^{-2}-10)			21
b. Upper Interflow Zones	0.1(0.01-0.25)	10^{-3}(10^{-6}-1)			21
c. Deep Interflow Zones	0.1(0.01-0.25)	10^{-4}(10^{-5}-10^{-2})			21
d. Central basalt Portion	0.001(0.0001-0.1)	10^{-5}(10^{-6}-10^{-4})			21
Flood Basalt					
a. Dense, Depth 1,000 ft.		10^{-2}			22
b. Dense or with healed joints, depth 71,000 ft.		(4.8×10^{-4}-8.6×10^{-4})			22
c. Vesicular		(4.8×10^{-4}-3.62×10^{-3})			22
d. Fractured, weathered or brecciated		(4.8×10^{-4}-2.0)			22
e. Interbeds; sand, clay and turf		(10^{-3}-1)			22
f. Zone of close fractures	10				22
g. Vesicular	5				22
h. Dense	1				22
i. Interbed, sandy	20				22

A-17

EXPLANATION OF NOTATION - APPENDIX A

All values given are presented in the Form

A (B,C)

where:

A is the average value of a set of determinations

B is the range of values observed

C is the number of samples tested

A may be specified as a range A_1-A_2 if values of B and C are unknown. A may also represent the value of a single determination.

B may be specified as a single value, B, or a true range B_1-B_2. If given as a single number, range represents the difference between the maximum and minimum values observed. The expression of range as a single value is common practice in many publications of the U.S. Bureau of Reclamation.

SOURCES FOR APPENDIX A

1. U.S. Bureau of Reclamation, Physical properties of some
       typical foundation rocks Concrete Laboratory Report
       #SP-39.

2. Kunar, A., 1968, The effect of stress rate and temperature
       on the strength of basalt and granite. Geophysics
       Vol. 33, No. 3, pp. 501-510.

3. Deju, R.A. et al, 1978, Structural Considerations in the
       Design of a Repository to Store Radioactive Waste
       in Basalt Formation.

4. Brandon, J.R., 1976, Rock Mechanics Properties of typical
       Foundation Rock Types Engineering & Research Center,
       Bureau of Reclamation REC-ERC-74-10.

5. Morris, D.A. and A.I. Johnson, 1948-60. Summary of Hydrologic
       & Physical Properties of Rock and Soil Materials as
       Analyzed by the Hydrologic Laboratory of the USGS.

6. Judd, W.R., Strain Distribution around Underground Openings;
       Statistical Methods to Compile and Correlate Rocks.
       Properties, and preliminary results, Purdue University,
       Technical Report 2.

7. Windes, S.L., 1949, Physical Properties of Mine Rock Part I.
       Report of Investigation, R.I. 4459
8. -----, Physical Properties of Mine Rock, Part II.

9. Kulhany, Fred H., Stress Deformation Properties of Rock
       and Rock Discontinuities.

10. Richey, J.E., 1968, Granite, Water Power.

11. Blair, B.E., 1955, Physical Properties of Mine Rock Part III,
       Bureau of Mines - Report of Investigation 5130.
12. -----, 1956, Physical Properties of Mine Rock Part IV, Bureau
       of Mines - Report of Investigation 5244.

13. Engineering Geologic, Geophysical, Hydrologic & Rock Mechanics
       Investigations of the Straight Creek Tunnel Site and Pilot
       Bore Colorado. Geologic Survey Professional Paper 815.

14. Carroll, Roderick D. et al, Elastic Module of Granite Rock from
       In situ Measurements of Seismic Velocity, USGS Prof. Paper
       550-C.

15. Dodd, J., 1967, Morror Point Dam and Powerplant Foundations
       Investigations, Bureau of Reclamation Colorado River Storage
       Project, Colorado.

16. Lundstrom and Stille, 1978, Large Scale Permeability Test of the Granite in the Stripa Mine and Thermal Conductivity Test, Lawrence Berkley Laboratory, LBL-7052.

17. Bureau of Reclamation, 1977, Ground Water Manual; A Water Resources Technical Publication, U.S. Dept. of Interior.

18. Brace, W.F., 1979, Permeability of Crystalline and Argillaceous Rocks, Preprint Submitted to Int. Jour. of Rock Mech. and Mine Science.

19. Schneider, K.J., and A. M. Platt, 1974, High-level Radioactive Waste Management Alternatives, Battelle Pacific Northwest Laboratories, Richland, Wash., Rept. BNWL-1900.

20. Robertson, J.B. and J. T. Barraclough, 1973, Radioactive and Chemical Waste Transport in Ground Water at National Reactor Testing Station, Idaho; 20-year case history and digital model (abs); American Association of Petroleum Geologists Bulletin, V 57, n 8, pp. 1603-1604.

21. Deju, R.A., et al, 1977, Environmental Factors Needed to Establish the Geotechnical Feasibility of Storing Radioactive Waste in Columbia River Basalt, RHO-ST-8.

22. Piper, A.M., 1975, Hypothetical Prototype Sites of Repositories for Radioactive Wastes: Flood Basalt; ORNL Subcontract 3745.

23. National Waste Terminal Storage Program Preliminary Feasibility Study of Storage of Radioactive Waste in Columbia River Basalts for U.S. Energy Research and Development Administration 1976.

24. Dames and Moore, 1978, Technical Support for GEIS: Radioactive Waste Isolation in Geologic Formations, Y/OWI/TM-36/21. Vol. 21, Ground Water Movement and Nuclide Transport.

25. Barraclough, J. T., et al, 1976, Hydrology of the Solid Waste Burial Ground, As Related to the Potential Migration of Radionuclides, Idaho, National Engineering Laboratory; U.S.G.S. Open-File Report 76-471.

26. Robertson, J.B., Robert Schoen and J.T. Barraclough, 1976, The Influence of Liquid Waste Disposal on the Geochemistry of Water at the National reactor Testing Station, Idaho 1952-1970; U.S.G.S. Report UC-70.

27. LaSala, A.M. Jr., and G.C. Doty, 1979, Preliminary Evaluation of Hydrologic Factors Related to Radioactive Waste Storage in Basaltic Rocks at Hanford; U.S.G.S. Open-File Report.

28. LaSala, A.M. Jr., G.C. Doty, and F.J. Person, Jr., 1972, A Preliminary Evaluation of Regional Ground-water Flow in South-Central Washington; U.S.G.S. WRD Admin. Report, 53 p.

29. Foxworthy, B.L. and C.T. Bryant, 1967, Artificial Recharge Through a Well Tapping Basalt Aquifers at the Dalles, Oregon, U.S.G.S. Water Supply Paper 1594-E.

30. Eddy, Paul A., 1969, Geohydrology of the Columbia Basin Project Area, Washington, abs, in Nrothwest Science, V 43, n 1. p. 35.

31. Skibitzke, H.E. and J.A. da Costa, 1962, The Ground-Water Flow System in the Snake River Plain, Idaho - An Idealized Analysis; U.S.G.S. Water Supply Paper 1536-D, pp. 47-67.

APPENDIX B

APPENDIX B

GLOSSARY

Bulk Modulus, Modulus of
Compression

The ratio of the change in av-
erage stress to the change in
unit volume.

Hydraulic Conductivity

If a porous medium is isotropic
and the fluid is homogeneous, the
hydraulic conductivity of the
medium is the volume of water at
the existing kinematic viscosity
that will move in unit time under
a unit hydraulic gradient through
a unit area measured at right
angles to the direction of flow.

Hydraulic Gradient
(Dimensionless)

Is the change in static head per
unit of distance in a given direc-
tion. If not specified, the
direction generally is understood
to be that of the maximum rate of
decrease in head. The gradient of
the head is a mathematical term
which refers to the vector denoted
by Δh or grad h, whose magnitude
dh/dl is equal to the maximum rate
of change in head and whose direction
is that in which the maximum rate of
increase occurs. The hydraulic
gradient and the gradient of the
head are equal but of opposite sign.

Modulus of Elasticity
(Modulus of Deformation)

The ratio of normal stress to
normal strain for a material
under given loading conditions;
numerically equal to the slope
of the tangent (hence 'tangent
modulus') or the secant (hence
'secant modulus') of a stress-
strain curve. The use of the
term Modulus of Elasticity is
recommended for materials that
deform in accordance with
Hooke's Law, the term Modulus
of Deformation for materials
that deform otherwise.

Permeability (Intrinsic)   A measure of the relative ease with
                            which a porous medium can transmit
                            a liquid under a potential gradient.
                            It is a property of the medium alone
                            and is independent of the nature of
                            the liquid and of the force field
                            causing movement. It is a property
                            of the medium that is dependent
                            upon the shape and size of the pores.

Poisson's Ratio   The ratio of the transverse
                            normal strain to the longi-
                            tudinal normal strain of a
                            body under uniaxial stress.

Porosity (Effective)   The amount of interconnected pore
                            space available for fluid trans-
                            mission. It is expressed as a
                            percentage of the total volume
                            occupied by the interconnecting
                            interstices. Although effective
                            porosity has been used to mean about
                            the same thing as specific yield,
                            such use is discouraged.

Shear Failure   Failure resulting from shear
                            stresses.

Specific Heat

Specific heat of a substance at temperature v is defined as:

$$v = \frac{dQ}{dv}$$

Where dQ is the quantity of heat necessary to raise the temperature of a unit mass of the substance through the small temperature range from v to v+dv. It depends on both the temperature and the assumed mode of heating. It is expressed in:

$$\frac{calories}{gm - {}^{0}C}$$

The specific heat of water at 15^{0}C is 1 cal/gm-^{0}C. Some authors regard the above definition as that of heat capacity or heat capacity per unit map of the substance, and define the specific heat of a substance as the ratio of its heat capacity per unit map to that of water.

Storage Coefficient

The storage coefficient is the volume of water an aquifer releases from or takes into storage per unit surface area of the aquifer per unit change in head. In a confined water body the water derived from storage with decline in head comes from expansion of the water and compression of the aquifer; similarly, water added to storage with a rise in head is accommodated partly by compression of the water and partly by expansion of the aquifer. In an unconfined water body, the amount of water derived from or added to the aquifer by these processes generally is negligible compared to that involved in gravity drainage or filling or pores; hence, in an unconfined water body the storage coefficient is virtually equal to the specific yield.

Strain

Deformation per unit of
length. Normal Strain is the
deformation per unit of length
in the direction of the defor-
mation. Shear Strain is the
deformation per unit of
length at right angles to the
deformation or more commonly
the relative change in the
angle defining the sides of
an infinitesimal element.

Strength

The maximum stress that a body
can withstand without failing
by rupture or continuous de-
formation. Rupture strength
or breaking strength refers to
the stress at the time of rup-
ture. If a body deforms,
after a certain stress has
been reached, continuously
without any increase in
stress, this is also called
strength. By common
usage, it can be described as
the greatest stress that a
substance can withstand under
normal short-time experiments,
or the highest point on a
stress-strain curve.

Stress   The force per unit area, when
                                the area approaches zero, act-
                                ing within a body. Biaxial
                                Stress: The state of stress
                                where either the intermediate
                                or the minor principal stress
                                equals zero. Effective Stress
                                (Effective Pressure) (Inter-
                                granular Pressure)   :
                                The average normal force per
                                unit area transmitted from
                                grain to grain in a granular
                                mass. It is the stress that
                                is effective in mobilizing
                                internal friction. Field
                                Stress: The stress existing
                                in a rock mass independent of
                                any man-made works. Residual
                                Stress: Stress that exists
                                in a formation owing to pre-
                                viously applied forces or
                                deformations. Triaxial Stress:
                                A state of stress where the
                                three principal stresses have
                                finite magnitudes, or simply
                                a three-dimensional state of
                                stress. Neutral Stress (Pore
                                Pressure) (Pore Water Pressure)
                                         : Stress transmitted
                                through the pore water (water
                                filling the voids of the mass).
                                Normal Stress   : The
                                stress component normal to a
                                given plane. Principal Stress,
                                            : Stresses
                                acting normal to three mutu-
                                ally perpendicular planes
                                intersecting at a point in a
                                body, on which the shear
                                stresses are zero. Major
                                Principal Stress   :
                                The largest (with regard to
                                sign) principal stress.

Thermal Conductivity

Thermal Conductivity is a material defined as:

$$K = \frac{Qd}{(V_0 - V_1)\, St}$$

Where Q is the quantity of heat which flows through a plate of the substance having a thickness d, cross-sectional area S, temperatures at the upper and lower surfaces of V_0 and V_1, over the time t.

The conductivity is generally not constant for the same substance but depends upon the temperature. For non-homogeneous solids, the conductivity varies from point-to-point as well as in direction at each point.
are:

Thermal Diffusivity

Thermal diffusivity measures the change of temperature which would be produced in a unit volume o the substance by the quantity of heat which flows in unit time through a unit area of a layer of the substance of u..it thickness with unit difference of temperature between its faces. It is defined in terms of the thermal conductivity (K), density (p), and specific heat (c) as:

$$k = \frac{K}{pc}$$

Conduction of Heat in Solids, H.S. Carslaw and J.C. Jaeger Oxford Univ. Press, 1959, 2nd Edition.

Transmissivity

The rate at which water of the
prevailing kinematic viscosity is
transmitted through a unit width
of the aquifer under a unit
hydraulic gradient. Though spoken
of as a property of the aquifer, it
embodies also the saturated thick-
ness of the aquifer (b) and the
properties of the contained liquid.
It is equal to an integration of
the hydraulic conductivities across
the saturated part of the aquifer
perpendicular to the flow paths.

Uniaxial Stress

A state of stress where the
minor and intermediate prin-
cipal stresses are zero.